

Studies on FKBP ligands and inhibitors for GS-like enzymes



TECHNISCHE
UNIVERSITÄT
DARMSTADT

„Studies on FKBP ligands and inhibitors for GS-like enzymes“

**Vom Fachbereich Chemie
der Technischen Universität Darmstadt**

zur Erlangung des Grades

Doctor rerum naturalium
(Dr. rer. nat.)

**Dissertation
von Patrick Purder**

Erstgutachter: Prof. Dr. Felix Hausch
Zweitgutachter: Prof. Dr. Michael Reggelin

Darmstadt 2022

Patrick Purder: Studies on FKBP ligands and inhibitors for GS-like enzymes

Darmstadt, Technische Universität Darmstadt

Jahr der Veröffentlichung der Dissertation auf TUprints: 2023

URN: urn:nbn:de:tuda-tuprints-228759

Tag der mündlichen Prüfung: 07.11.2022

Veröffentlicht unter CC BY-SA 4.0 International

<https://creativecommons.org/licenses/>

Tag der Einreichung: 19. September 2022

Tag der mündlichen Prüfung: 07. November 2022

Teile dieser Arbeit sind bereits publiziert in:

Purder *et al.*, *ChemBioChem*, **2022**, e202200312.

Erklärung laut Promotionsordnung

§8 Abs. 1 lit. c PromO

Ich versichere hiermit, dass die elektronische Version meiner Dissertation mit der schriftlichen Version übereinstimmt und für die Durchführung des Promotionsverfahrens vorliegt.

§8 Abs. 1 lit. d PromO

Ich versichere hiermit, dass zu einem vorherigen Zeitpunkt noch keine Promotion versucht wurde und zu keinem früheren Zeitpunkt an einer in- oder ausländischen Hochschule eingereicht wurde. In diesem Fall sind nähere Angaben über Zeitpunkt, Hochschule, Dissertationsthema und Ergebnis dieses Versuchs mitzuteilen.

§9 Abs. 1 PromO

Ich versichere hiermit, dass die Vorliegende Dissertation selbstständig und nur unter der Verwendung der angegebenen Quellen verfasst wurde.

§9 Abs. 2 PromO

Die Arbeit hat bisher noch nicht zu Prüfungszwecken gedient.

Darmstadt,

(Unterschrift)

Contributions

The work presented in this dissertation has in some parts been performed by colleagues and collaboration partners. While it is mentioned where the results are presented, I give here an overview of which work has been contributed by someone other than me.

The synthesis of *C*-substituted MSO analogs **105d** and **105f** was performed by Jonathan Funk during his bachelor thesis under my supervision.

FKBP protein expression and purification was done by Stephanie Merz, Thomas Geiger and Christian Meyners.

FP assays were performed by Wisely Oki Sugiarto, Stephanie Merz as well as myself.

HTRF assays were performed by Thomas Geiger and Wisely Oki Sugiarto.

NanoBRET assays were performed by Thomas Geiger.

Crystallization and analysis of the cocrystals was performed by Christian Meyners.

GS activity assays were performed by Christian Meyners.

Macrophage infectivity potentiator proteins LpMip, TcMip and BpMip were provided by Benedikt Goretzki and Ute Hellmich from the Friedrich Schiller University Jena.

Cytotoxicity, MIC and HLTE assays with *Legionella pneumophila* were performed by Safa Karagöz from the Technical University Braunschweig.

S. coelicolor growth assays and GlnA4 expression and purification were performed by Sergii Krysenko from the Eberhard Karl University Tübingen.

Acknowledgements

First and foremost, I want to thank Felix Hausch for supporting me as his doctoral student. You provided me with more than one interesting research topic and a lab filled with enough space and equipment to excellently pursue my research. You taught me how to approach scientific problems and many skills inside and outside of the lab.

I am grateful to have had such a great team of co-workers over the years. I thank my former colleagues Jürgen, Michael B., Andreas, Stephanie and Tianqi who were always ready to give synthetic and analytical advice. I especially thank Jürgen for the close collaboration on bicycles and Stephanie for teaching me how to do FP-assays with our pipetting robot. My colleagues Fabian, Michael W., Asat, Robin, Christian M. and Tim have accompanied me throughout my whole doctoral studies and I could not imagine my everyday lab work without you. I thank Oki for relieving me of my duty to measure FP-assays, and for then measuring countless assays for me. My bicycle team with Robin, Patryk, Yuxin, Johannes and Michael W. had an excellent cooperation regarding expertise and intermediates. The SAFit team with Fabian, Vanessa, Christian B., Moritz and Carlo were always farther away but close at heart. With our PROTAC successor Min, I shared only a few months in the lab but I appreciate that time with you. I am glad that we had a huge team of synthetic chemists and biochemists working so closely together. Thereby I always had an expert at hand whenever I had a biochemical question or needed a compound analyzed. Many thanks to our biochemists Christian M., Oki, Asat, Anna, Sarah, Thomas, Monika, Steffen, Max, Sabine and Martha! Every colleague contributed to the great working atmosphere, which made the workplace really pleasant. I enjoyed all non-work-related activities we shared, like playing Skat during the lunch break and in regular tournaments, going running, celebrating the summer and Christmas parties, going for some Laternchen, making Christmas movies and hiking in the Kleinwalsertal. I appreciate your patience when all of you spent hours and days watching me eat salad in the mensa and I challenge anyone who comes after me to eat more than two and a quarter Giant Burger's.

I will always remember the end-of-the-week tradition with the timeless artists G. M. and H. E.

I thank Barbara, Conny and Petra for all their support during my years in the group.

I am glad that the students I supervised over the years, Lukas, Jonathan and Arkadiy, were so easy to work with. I am grateful for your contributions to my research and wish you all the best for your own work.

Extensive research cannot be done alone and I am thankful for the collaboration partners in the GPS-TBT and the Mip teams. I enjoyed the many meetings and discussions that we shared online and in person.

I thank our NMR department at the TU Darmstadt, Reinhard Meusinger, Jörg Fohrer and Christina Spanheimer and our MS department, Alexander Schießler, Christiane Rudolph and Gül Sahinalp for countless measurements that helped me to characterize my intended and unintended synthetic products.

I am very thankful for all friends I have made in the chemistry department at the TU Darmstadt. Without you, all these years of studying would not have been as exciting. It cannot be taken for granted that we still meet regularly even after we all have gone separate ways. Thank you Lotti, Moritz, Patrick, Severine, Sebastian, Torben, Torsten and Ursula for building a friendship that exceeds the shared lab time.

Of course, I am likewise grateful for all my friends outside the chemistry department with whom I could share many concerts, game nights, sport events, travels and conversations. Thank you for keeping me in touch with the real world. Special gratitude goes to Julia for sharing so much with me and opening my eyes in many ways during the past years.

When I think back to the start of my interest in chemistry, I still feel indebted to the great teaching skills of Viktor Neufeld.

Finally, I want to thank my family who have continuously supported my studies long before I started my doctoral research or joined the university. I know I can always count on you and would certainly not have accomplished this much without you.

Table of Contents

Contributions	vii
Acknowledgements	ix
Table of Contents	xi
1. Abstract	1
1. Zusammenfassung	3
2. Introduction	5
2.1. FKBP	5
2.2. FKBP ligands	8
2.3. GS and GS-like enzymes	14
2.4. Inhibitors of GS and GS-like enzymes	16
3. Results and Discussion	19
3.1. A [4.2.1]-bicyclic FKBP ligand negative control substance	19
3.2. Synthesis and properties of (<i>S</i>)-2-(2-oxo-3,10-diazabicyclo[4.3.1]decan-3-yl)propanoic acids as FKBP ligands	22
3.3. (1 <i>S</i> ,5 <i>S</i> ,6 <i>R</i>)-10-benzylsulfonyl-3,10-diazabicyclo[4.3.1]decan-2-ones as FKBP ligands	25
3.4. Ultra-high affinity FKBP12 ligands	29
3.5. Introducing sulfonimidamides to bicyclic FKBP ligands	45
3.6. Miscellaneous FKBP ligands	61
3.7. 3,10-Diazabicyclo[4.3.1]decan-2-ones as Mip ligands	65
3.8. MSO-derivatives as GlnA3- and GlnA4-inhibitors	69
3.9. Synthesis of Homocysteine sulfonimidamide	77
4. Conclusion and Outlook	87
5. Experimental Part	89
5.1. General Methods	89
5.2. Synthetic Procedures	96
5.2.1. Compound 4	96
5.2.2. Compound 5	97
5.2.3. Compound 2	98
5.2.4. Compound 10	99
5.2.5. Compound 11	100

5.2.6.	Compound 12	101
5.2.7.	Compound 13	102
5.2.8.	Compound 14	103
5.2.9.	Compound 15	104
5.2.10.	Compound 16	105
5.2.11.	Compound 17	106
5.2.12.	Compound 8	107
5.2.13.	Compound 19	108
5.2.14.	Compound 18	109
5.2.15.	Compound 20	110
5.2.16.	Compound 22	111
5.2.17.	Compound 23	112
5.2.18.	Compound 24	113
5.2.19.	Compound 29	114
5.2.20.	Compound 31	115
5.2.21.	Compound 32	117
5.2.22.	Compound 33	118
5.2.23.	Compound 38	120
5.2.24.	Compound 34	121
5.2.25.	Compound 39	122
5.2.26.	Compound 35	123
5.2.27.	Compound 36	124
5.2.28.	Compound 37	125
5.2.29.	Compound 43	126
5.2.30.	Compound 40	127
5.2.31.	Compound 41	128
5.2.32.	Compound 46	129
5.2.33.	Compound 47	130
5.2.34.	Compound 50	131
5.2.35.	Compound 53	132
5.2.36.	Compound 56	133

5.2.37. Compound 48.....	134
5.2.38. Compound 51.....	135
5.2.39. Compound 57.....	136
5.2.40. Compound 49.....	138
5.2.41. Compound 52.....	139
5.2.42. Compound 55.....	140
5.2.43. Compound 58.....	141
5.2.44. Compound 59.....	142
5.2.45. Compound 60.....	143
5.2.46. Compound 65.....	144
5.2.47. Compound 66.....	145
5.2.48. Compound 67.....	146
5.2.49. Compound 68.....	147
5.2.50. Compound 70.....	148
5.2.51. Compound 71.....	149
5.2.52. Compound 72.....	150
5.2.53. Compound 75.....	151
5.2.54. Compound 76a and 76b.....	152
5.2.55. Compound 77a and 77b.....	154
5.2.56. Compound 78a.....	156
5.2.57. Compound 78b.....	157
5.2.58. Compound 79a.....	158
5.2.59. Compound 79b.....	159
5.2.60. Compound 80a.....	160
5.2.61. Compound 80b.....	161
5.2.62. Compound 81a.....	162
5.2.63. Compound 81b.....	163
5.2.64. Compound 1.....	164
5.2.65. Compound 82.....	165
5.2.66. Compound 83.....	166
5.2.67. Compound 85.....	167

5.2.68. Compound 86	168
5.2.69. Compound 87	169
5.2.70. Compound 88	170
5.2.71. Compound 90	171
5.2.72. Compound 91	172
5.2.73. Compound 92	173
5.2.74. Compound 93	174
5.2.75. Compound 94	175
5.2.76. Compound 112	176
5.2.77. Compound 113	177
5.2.78. Compound 101	178
5.2.79. Compound 116	179
5.2.80. Compound 117	180
5.2.81. Compound 115a.....	181
5.2.82. Compound 118a.....	182
5.2.83. Compound 169	183
5.2.84. Compound 114b.....	184
5.2.85. Compound 115b.....	185
5.2.86. Compound 118b.....	186
5.2.87. Compound 169c.....	187
5.2.88. Compound 114c.....	188
5.2.89. Compound 115c.....	189
5.2.90. Compound 118c.....	190
5.2.91. Compound 107	191
5.2.92. Compound 170a.....	192
5.2.93. Compound 108a.....	193
5.2.94. Compound 109a.....	194
5.2.95. Compound 110a.....	195
5.2.96. Compound 171a.....	196
5.2.97. Compound 105a.....	197
5.2.98. Compound 109b.....	198

5.2.99. Compound 110b	199
5.2.100. Compound 171b	200
5.2.101. Compound 105b	201
5.2.102. Compound 170c	202
5.2.103. Compound 108c	203
5.2.104. Compound 109c	204
5.2.105. Compound 110c	205
5.2.106. Compound 171c	206
5.2.107. Compound 105c	207
5.2.108. Compound 109d	208
5.2.109. Compound 110d	209
5.2.110. Compound 172d	210
5.2.111. Compound 105d	211
5.2.112. Compound 108e	212
5.2.113. Compound 109e	213
5.2.114. Compound 110e	214
5.2.115. Compound 172e	215
5.2.116. Compound 105e	216
5.2.117. Compound 109f	217
5.2.118. Compound 110f	218
5.2.119. Compound 172f	219
5.2.120. Compound 105f	220
5.2.121. Compound 141	221
5.2.122. Compound 153	222
5.2.123. Compound 154	223
5.2.124. Compound 155	224
5.2.125. Compound 156	225
5.2.126. Compound 157	226
5.2.127. Compound 158	227
5.2.128. Compound 159	228
5.2.129. Compound 160	229

5.2.130. Compound 161	230
6. Appendix	231
6.1. List of abbreviations	231
6.2. List of Figures.....	234
6.3. List of Tables.....	237
6.4. List of Schemes	239
7. References.....	243

1. Abstract

The first half of this dissertation is dedicated to the development of novel FKBP ligands, aiming to improve binding affinity, selectivity between selected members of the FKBP family, and metabolic stability. The basis of this project is the molecular 3,10-diazabicyclo[4.3.1]decan-2-one scaffold, which proved to be privileged for FKBP binding. Three attachment points were found to allow beneficial derivatization of this scaffold, which are atoms 3, 5 and 10 (Figure 1a).

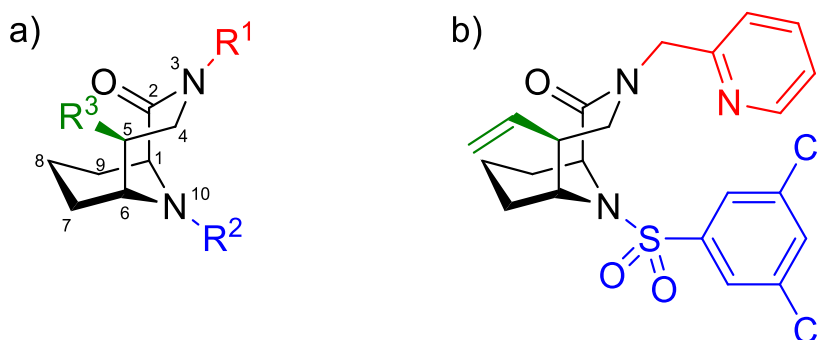


Figure 1. 3,10-Diazabicyclo[4.3.1]decan-2-ones, a) scaffold (black) with substitutions at positions 3 (R1, red), 5 (R3, green) and 10 (R2, blue); b) reference ligand for this scaffold with standard substitutions R1 = pyridine-2-ylmethyl, R2 = (3,5-dichlorophenyl)sulfonyl, R3 = vinyl.

In this work, a structurally similar but non-binding negative control was developed to be used in biochemical and biological experiments with FKBP ligands. Next, FKBP ligands with a carboxylic acid in the R1 position and hydroxy groups in the R3 position were synthesized with the purpose of creating more water-soluble ligands for biochemical experiments. These compounds also presented an increased metabolic stability. Furthermore, the typically used phenyl sulfonamides in the R2 position were substituted with benzyl sulfonamides, a moiety that was reported to show good binding in other pipercolate-based scaffolds. However, benzyl sulfonamides are not suited in the 3,10-diazabicyclo[4.3.1]decan-2-one scaffold. As an extension of my master thesis, the R2 residue was extended in the para position. One motif was found to show a strong enhancement in FKBP12 binding and selectivity, which was further analyzed and optimized. Furthermore, the influence of the highly conserved sulfonamide in R2 was addressed. Analogous sulfenamide, sulfinamides and sulfonimidamides were synthesized to gain structure-affinity relationship information. The sulfonimidamide handle was used to expand the ligand, and this ligand series indicated a novel FKBP12 binding mode. Finally, all synthesized FKBP ligands were tested for Mip binding and selected compounds showed *in vitro* activity against *Legionella pneumophila*.

The second half of this dissertation describes the design and synthesis of methionine sulfoximine analogs (Figure 2). The recently characterized glutamine synthetase-like enzyme GlnA4 could be targeted and the best inhibitor showed *in vitro* inhibition of GlnA4 in *Streptomyces coelicolor*. Lastly, the synthesis of homocysteine sulfonimidamide is described, which aimed to improve glutamine synthetase binding compared to the gold standard inhibitor MSO. Unfortunately, it showed no improved GS inhibition.

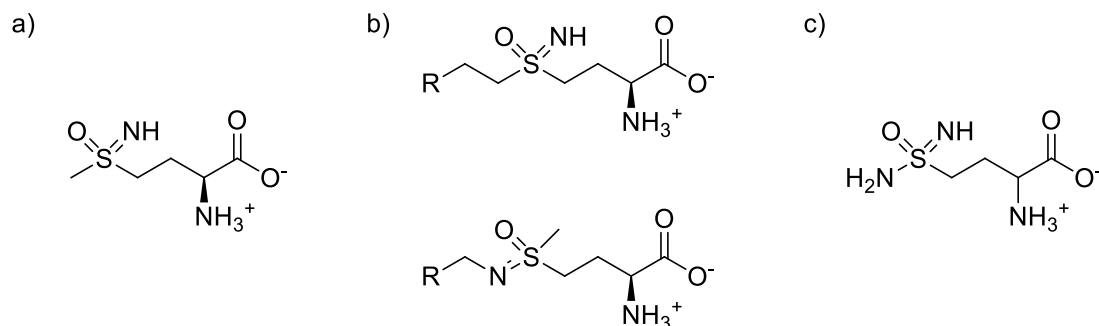


Figure 2. a) Methionine sulfoximine, b) MSO-derivatives as novel GlnA3 and GlnA4 inhibitors, c) Homocysteine sulfonimidamide.

1. Zusammenfassung

Die erste Hälfte dieser Dissertation beschäftigt sich mit der Entwicklung neuer FKBP Liganden, mit dem Ziel deren Bindungsaffinität, die Selektivität zwischen ausgewählten Mitgliedern der FKBP Familie sowie die metabolische Stabilität zu erhöhen. Die Basis dieses Projekts ist das 3,10-diazabicyclo[4.3.1]decan-2-on-Gerüst, das sich als besonders geeignet für FKBP Liganden herausstellte. Drei Anknüpfungspunkte wurden gefunden, die eine verbessernde Derivatisierung des Gerüsts erlauben. Dies sind die Atome 3, 5 und 10 (Abbildung 1a).

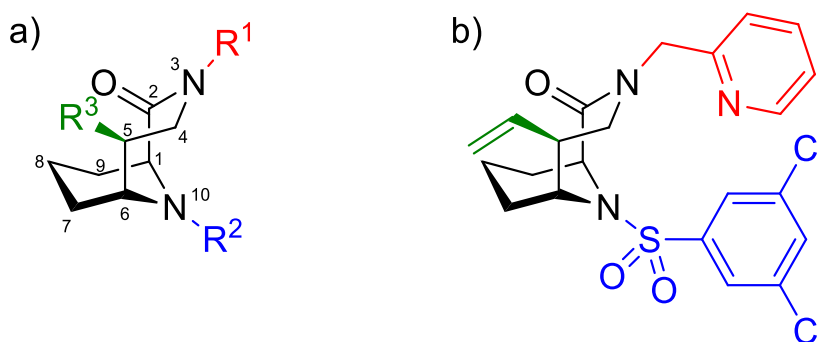


Abbildung 1. 3,10-Diazabicyclo[4.3.1]decan-2-one, a) Gerüst (schwarz) mit Substitutionen in den Positionen 3 (R1, rot), 5 (R3, grün) und 10 (R2, blau); b) Referenzligand dieses Gerüsts mit den Standard Substituenten R1 = pyridin-2-ylmethyl, R2 = (3,5-dichlorophenyl)sulfonyl, R3 = vinyl.

In dieser Arbeit wurde eine strukturell ähnliche aber nicht bindende Negativkontrolle entwickelt, die in biochemischen und biologischen Experimenten mit FKBP Liganden eingesetzt wird. Anschließend wurden FKBP Liganden mit Carbonsäuren in der R1 Position und Hydroxygruppen in der R3 Position synthetisiert mit der Absicht wasserlöslichere FKBP Liganden für biochemische Experimente bereit zu stellen. Diese Verbindungen zeigten außerdem eine erhöhte metabolische Stabilität. Ferner wurde das oft genutzte Phenylsulfonamid in der R2 Position durch ein Benzylsulfonamid ersetzt, für das im Kontext von anderen Pipecolat-basierten Gerüsten gute Bindung gezeigt wurde. Im 3,10-diazabicyclo[4.3.1]decan-2-on-Gerüst jedoch waren Benzylsulfonamide ungeeignet. Als Fortführung meiner Masterarbeit wurde die para-Position des R2 Rests expandiert. Ein Motiv zeigte eine starke Verbesserung der FKBP12 Bindung und Selektivität, was tiefergehend analysiert und optimiert wurde. Dann wurde der Einfluss des konservierten Sulfonamids in R2 Position adressiert. Analoge Sulfenamid, Sulfinamide und Sulfonimidamide wurde synthetisiert um Struktur-Affinitätsbeziehungen aufzuklären. Das Sulfonimidamid Motiv wurde benutzt um den Liganden zu erweitern. Diese Ligandenserie deutete auf einen neuen FKBP12 Bindungsmodus hin. Zuletzt wurden alle synthetisierten FKBP Liganden auf

Mip Bindung getestet und ausgewählte Verbindungen zeigten *in vitro* Aktivität gegen *Legionella pneumophila*.

Die zweite Hälfte dieser Dissertation beschreibt das Design und die Synthese neuer Methioninsulfoximin-Analoga (Abbildung 2). Das kürzlich charakterisierte Glutaminsynthetase-ähnliche Enzym GlnA4 konnte inhibiert werden und der beste Inhibitor zeigte *in vitro* Inhibition des GlnA4 in *Streptomyces coelicolor*. Schlussendlich wurde Homocysteinsulfonimidamid synthetisiert, was eine verbesserte Glutaminsynthetase Inhibition gegenüber MSO bringen sollte. Leider zeigte diese Verbindung jedoch keine stärkere GS Inhibition.

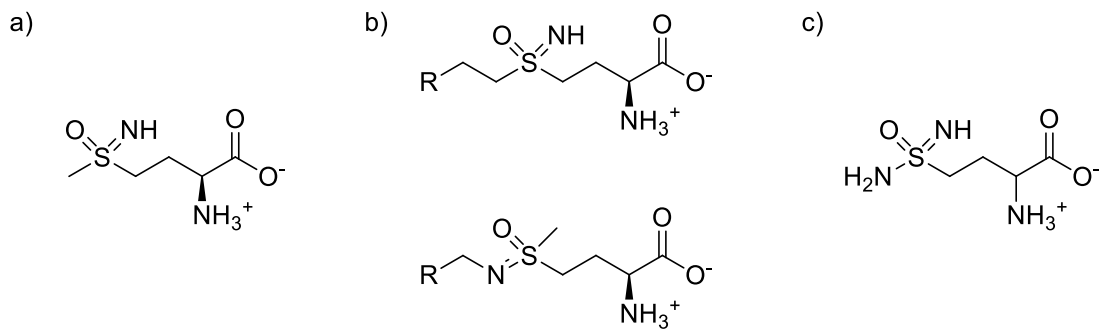


Abbildung 2. a) Methioninsulfoximin, b) MSO-Derivate als neue GlnA3- und GlnA4-Inhibitoren, c) Homocysteinsulfonimidamid.

2. Introduction

2.1. FKBP

FK506-binding proteins (FKBPs) were identified as the binding partners of the natural products and immunosuppressants FK506 and rapamycin. Their clinical use in allograft transplant patients sparked interest in the field in the last decade of the 20th century.^[1] The small molecules bind the archetypal 12 kDa member of the FKBP family, FKBP12, which allows the formation of a ternary complex with calcineurin (with FK506) or mTOR (with rapamycin),^[2] thereby altering the cellular immune response.^[3] FKBP12 was first isolated in 1989 and characterized as a peptidyl-prolyl cis-trans isomerase (PPIase).^[4] After the identification of FKBP12, many other members of the human FKBP family were identified and characterized (Table 1).^[5]

Table 1. Members of the mammalian FKBP, with gene name and classification.

FKBP	Refseq ID	Class
FKBP12	FKBP1	Cytoplasmic
FKBP12.6	FKBP1B	Cytoplasmic
FKBP25	FKBP3	Nuclear
FKBP135	KIAA0674	Nuclear
FKBP36	FKBP6	TPR-containing
FKBP37	AIP	TPR-containing
FKBP38	FKBP8	TPR-containing
FKBP51	FKBP5	TPR-containing
FKBP52	FKBP4	TPR-containing
FKBP13	FKBP2	Secretory pathway
FKBP19	FKBP11	Secretory pathway
FKBP22	FKBP14	Secretory pathway
FKBP23	FKBP7	Secretory pathway
FKBP60	FKBP9	Secretory pathway
FKBP65	FKBP10	Secretory pathway

All FKBP family members consist of at least one FKBP domain which bears high similarity to FKBP12 and might have PPIase activity. Some family members have an additional FKBP domain without PPIase activity and/or a tetratricopeptide repeat (TPR) domain.^[5]

Among the mammalian FKBP family members, the smallest FKBP12 is the best characterized one. A natural function of FKBP12 is the stabilization of the ryanodine receptor (RyR), which regulates the intracellular calcium release.^[6] In this context, FKBP12 and the closely related FKBP12.6 have different functions on the cardiac RyR2 and the skeletal muscle RyR1.^[7] The disruption of this function was suggested to result in endothelial dysfunction and hypertension as side effects of FK506 or rapamycin treatment.^[8] A high expression of FKBP12 after nerve damage and elevated levels in brain neurons situated in areas of degeneration links this protein to regulatory processes in neurons.^[9] Non-immunosuppressant FKBP12 ligands were claimed to enhance neurite outgrowth *in vitro* and *in vivo* in rats^[10] and reverse the abnormalities of 6-hydroxydopamine (6-OHDA) lesioned rats.^[11]

The larger FKBP38 has a FKBP domain, a TPR domain and a leucine-zipper repeat.^[12] It cannot bind FK506 but was claimed to still bind to calcineurin and mTOR in a binary complex.^[13] FKBP38 resides in the mitochondrial membrane and Ca²⁺- and calmodulin dependently binds to Bcl-2, thereby promoting apoptosis.^[14] HSP90 can bind the TPR domain of FKBP38 when it is Ca²⁺/calmodulin activated, which blocks the active site of FKBP38 and prevents interaction with Bcl-2.^[15]

Another interesting and therapeutically highly relevant member of the FKBP family is FKBP51, which will be discussed together with its closest homolog FKBP52. FKBP51 and FKBP52 both consist of one FKBP domain with PPIase activity (Fk1), one FKBP domain without PPIase activity (Fk2) and one TPR domain.^[16] FKBP51 and FKBP52 both competitively bind to HSP90 and form complexes with the glucocorticoid receptor (GR).^[17] FKBP52 potentiates the GR activity whereas FKBP51 blocks it.^[18] Besides the GR, FKBP52 can also HSP90-dependently bind the androgen receptor (AR), in which context FKBP52 plays a relevant role in reproductive organ development.^[19] FKBP51 on the other side proved to be rather dispensable under basal conditions,^[20] but emerged as a promising target in stress response,^[21] mood- and sleep-disorders,^[22] obesity and diabetes^[23] and chronic pain.^[24]

FKBP65 is overexpressed in glioma and involved in proliferation of glioma cells by interacting with HSP47.^[25]

Next to humans and mammals, many other organisms like bacteria, plasmodia, yeast, plants and archaea also possess FKBP-like proteins, which vary only little in their respective binding sites.^[26]

Therapeutical interest in the bacterial FKBP-like macrophage infectivity potentiators (Mips) was initiated in 1989 when a surface protein of *Legionella pneumophila*, the causative agent of legionnaires' disease, was identified to be important for its infectivity.^[27] The protein consists of a FKBP domain with PPIase activity and a long N-terminal α -helix for dimerization.^[28] LpMip was shown to contribute to bacterial

dissemination within lung tissue and spreading to the spleen. It enables transmigration through the barrier of lung epithelial cells, however this effect can be blocked by FK506 or rapamycin.^[29] LpMip acts synergistically with another PPIase of *L. pneumophila*, PpiB, to get a better temperature tolerance and infectivity.^[30] Another Mip was later found in *Trypanosoma cruzi*, the Chagas disease causing parasite, which is important for cell invasion.^[31] Like LpMip, TcMip also possesses a FKBP domain with PPIase activity and a N-terminal α -helix, however TcMip has an additional shorter C-terminal α -helix. Loss of TcMip is accompanied by a loss in infectivity, but its infectivity can be restored by introducing LpMip.^[32] *Burkholderia pseudomallei* is another bacterium which possesses a Mip consisting of only a FKBP domain with PPIase activity.^[33] Without BpMip the bacterium shows a significantly lowered virulence.^[34]

2.2. FKBP ligands

The pharmacological targeting of FKBP started when the atomic structure of their complex with the natural ligands FK506 and rapamycin was elucidated.^[35-37] It became clear that one part of these molecules (binding domain) was relevant for binding of FKBP12 while the other part (effector domain) causes the immunosuppressant effect by recruiting either calcineurin (for FK506) or mTOR (for rapamycin), see Figure 3. The binding affinities of these two natural ligands were determined to be $K_D = 0.2$ nM for rapamycin and $K_D = 0.4$ nM for FK506.^[38]

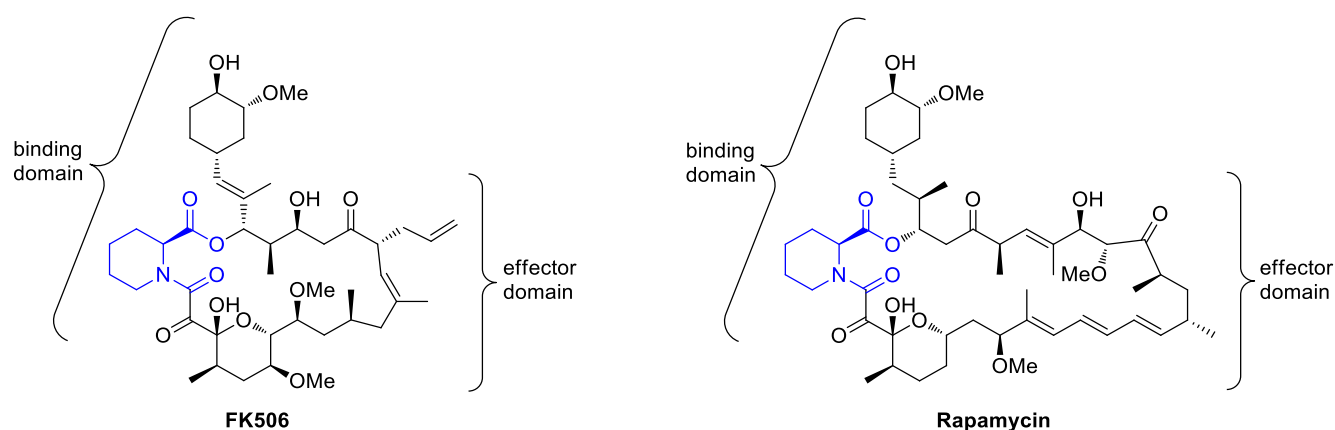


Figure 3. Structures of natural FKBP ligands FK506 and rapamycin. Pipercolate motif highlighted in blue.

Changes in their respective effector domains had a significant impact on their immunosuppressive function while FKBP12 binding was mostly unaffected.^[39] A comparison of the binding domains of FK506 and rapamycin revealed a minimal binding domain necessary for FKBP12 binding and allowed the synthesis of smaller non-immunosuppressive FKBP ligands.^[40] The core of these ligands is the pipercolate motif which is conserved in most FKBP ligands until today. Derivatization of the pipercolate core allowed a first structure-activity relationship analysis and provided FKBP-ligands with binding affinities comparable with FK506 (Figure 4a,b).^[41,42] Guilford Pharmaceuticals further developed a FKBP ligand, GPI-1046 (Figure 4c), which was claimed to present neuroprotective and neuroregenerative properties in pM concentrations.^[10]

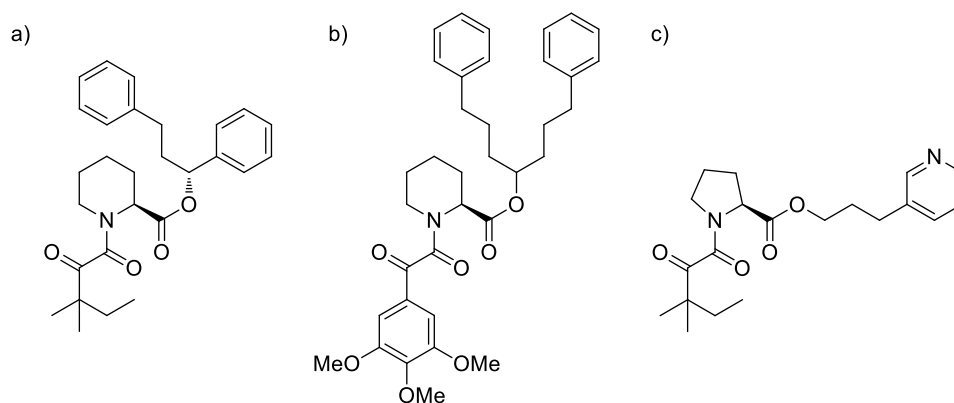


Figure 4. FKBP12 ligands developed by a) SmithKline Beecham Pharmaceuticals,^[42] $K_D = 2$ nM and b) Vertex Pharmaceuticals,^[41] $K_D = 1$ nM, c) Guilford Pharmaceuticals.^[10]

To investigate the protein-ligand interactions, ARIAD Gene Therapeutics performed a bump-and-hole approach, where a mutated FKBP12-F36V had an artificially created hole in the surface and specially designed ligands filled this pocket. These ligands bound FKBP12-F36V with IC_{50} -values in the low nM range (Figure 5a).^[43] Bifunctional molecules (Figure 5b) were able to dimerize FKBP12-F36V and were shown to bind the mutated FKBP12-F36V with an IC_{50} of 5 nM, while their binding to wild type FKBP12 was negligible.^[44]

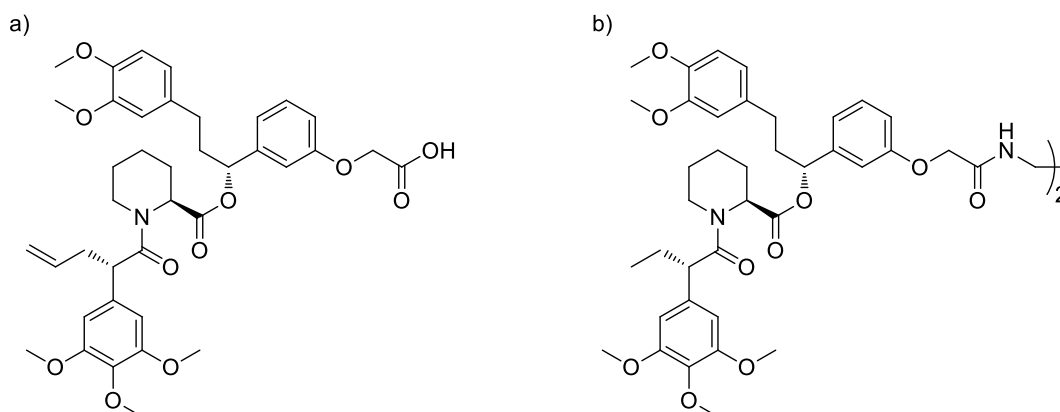


Figure 5. „Bumped“ FKBP12 ligands with specific binding to the mutated FKBP12-F36V. a) $IC_{50} = 1.5$ nM,^[43] b) $IC_{50} = 5$ nM.^[44]

The development of a fluorescent FKBP ligand (Figure 6) allowed a competitive fluorescence polarization assay in a high-throughput format. This way also the larger homologs FKBP12.6, FKBP51 and FKBP52 could be addressed.^[45]

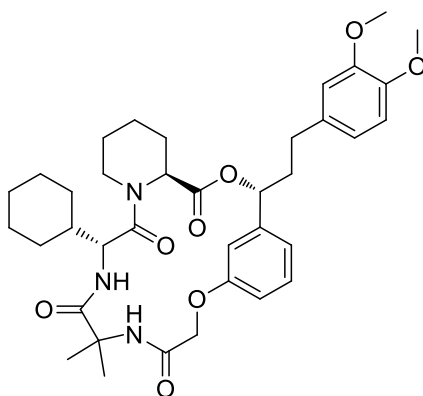


Figure 8. Macrocyclic SAFit-analog with FKBP51 selectivity over FKBP12, 12.6 and 52.^[48]

In a different ligand development direction, the carboxamide bottom group of pipicolate-based ligands was replaced by a sulfonamide. In one series, substituted phenylsulfonamides were shown to bind FKBP12 in a high nM range and FKBP51 and 52 in a medium μM range.^[49] In another series, substituted benzylsulfonamides were synthesized which were reported to bind LpMip in a good nM and BpMip in a low μM range (Figure 9).^[50]

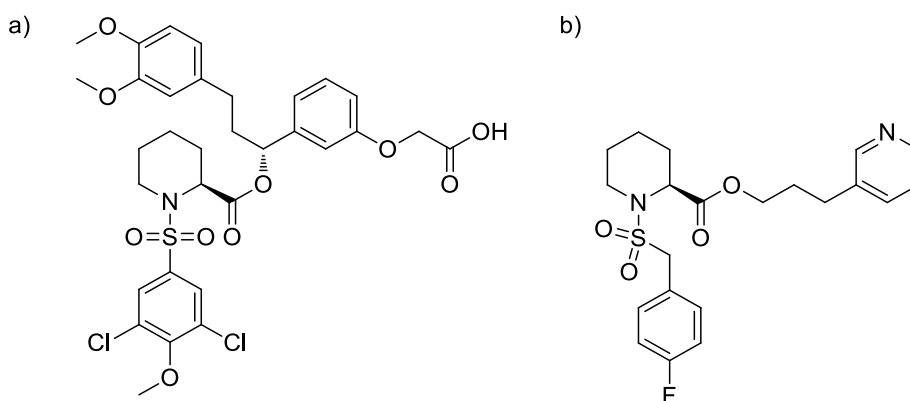


Figure 9. FKBP ligands bearing pipicolate sulfonamides, a) $\text{IC}_{50} = 0.23 \mu\text{M}$ for FKBP12, $\text{IC}_{50} = 16 \mu\text{M}$ for FKBP51, $\text{IC}_{50} = 18 \mu\text{M}$ for FKBP52 ; b) $\text{IC}_{50} = 72 \text{ nM}$ for BpMip, $\text{IC}_{50} = 5.7 \text{ nM}$ for LpMip.

One immense leap in ligand development was the fixation of the FKBP ligand core's active conformation. Cocrystal structures of pipicolate-based FKBP ligands showed that the pipicolate core binds the protein in an axial conformation, which is energetically unfavoured. The rigidification of the core removed the energetically elaborate pre-organisation and increased the binding affinity. This approach was pursued early by Agouron Pharmaceuticals,^[51] Guilford Pharmaceuticals^[52] and Pfizer^[53] and provided nM FKBP12 ligands (Figure 10).

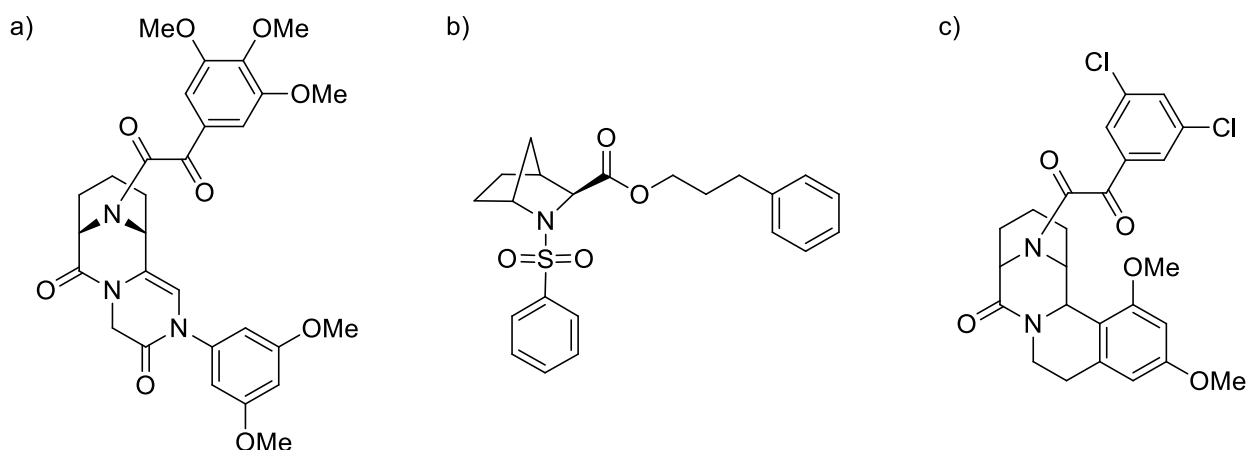


Figure 10. Bicyclic FKBP ligands by a) Agouron Pharmaceuticals, $K_i = 54$ nM for FKBP12;^[51] b) Guilford Pharmaceuticals, $IC_{50} = 650$ nM for FKBP12;^[52] c) Pfizer, $K_i = 34$ nM for FKBP12.^[53]

In these approaches, [3.3.1] and [2.2.1] bicyclic cores were used. However, WANG *et al.* later developed a synthesis for [4.3.1] bicyclic pipercolates as 3,10-diazabicyclo[4.3.1]decan-2-ones.^[54] In this new scaffold, the C5-position was found to offer an additional, beneficial attachment point for molecular expansion (Figure 11).^[55]

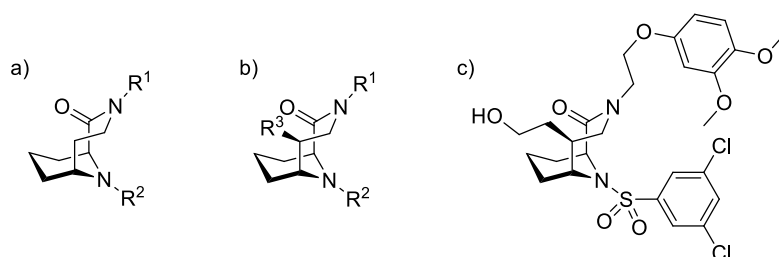


Figure 11. 3,10-Diazabicyclo[4.3.1]decan-2-ones as FKBP ligands. a) First developed scaffold;^[54] b) Improvement by C5-attachment;^[55] c) exemplary ligand with the new scaffold, $K_i = 0.2$ nM for FKBP12, $K_i = 21$ nM for FKBP51.^[56]

The synthetic route presented by POMPLUN *et al.*^[56] easily allowed late stage derivatization and facilitated the synthesis of a large library of 3,10-diazabicyclo[4.3.1]decan-2-one FKBP ligands, as well as a new fluorescently labeled tracer molecule for fluorescence polarization assays. A screening of multiple FKBP and FKBP-like proteins revealed that ligands of this scaffold can bind different human FKBP and bacterial Mips, with K_i -values ranging up to 0.2 nM for FKBP12. Furthermore, the best ligands of this screening showed promising antimalarial, antilegionellal and antichlamydial properties in cellular models of infectivity, suggesting that these ligands could present a novel class of anti-infectives.^[57] One further rational design to improve binding affinity of 3,10-diazabicyclo[4.3.1]decan-2-ones to FKBP was the introduction of one sophisticatedly placed methyl group in the R1 residue, which replaces a

conserved, energetically unfavoured water molecule at the binding site (Figure 12). This effect is generally more pronounced in the larger FKBP51, but still improves binding to FKBP12 significantly.

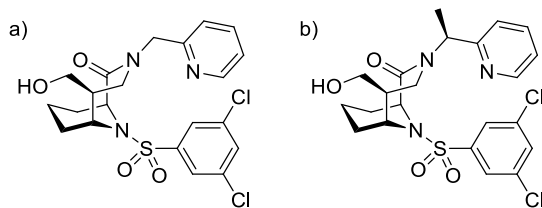
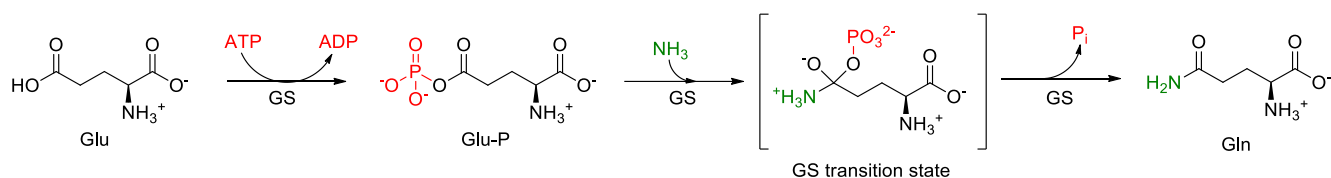


Figure 12. Introduction of an α -methyl group in R1 improves binding affinity: a) $K_D = 0.52$ nM for FKBP12, $K_D = 33$ nM for FKBP51; b) $K_D = 0.29$ nM for FKBP12, $K_D = 2.9$ nM for FKBP51.

2.3. GS and GS-like enzymes

Glutamine synthetase (GS) is a highly conserved enzyme in all branches of life that catalyzes the ATP-dependent conversion of glutamate and ammonia to glutamine (Scheme 1).



Scheme 1. Enzymatic mechanism of glutamine synthetase.

Glutamine synthetase thereby increases the glutamine level but also decreases the glutamate and ammonia levels. This regulation is highly important in the brain, where glutamate acts as a neurotransmitter and increased ammonia concentrations are toxic.^[58] Decreased GS activity in the brain leads to convulsive seizures and memory-related impairments in mice.^[59,60] Glutamine synthetase is also a relevant factor in adipogenesis and could offer a potential therapeutic strategy to treat obesity.^[61] Furthermore, GS was discussed as a possible target in cancer.^[62] Bacteria are as dependent on GS as mammals, which is why GS was intensively studied as a possible target in bacterial infections. For example in *Mycobacterium tuberculosis*, large amounts of GS are secreted and extracellularly aid the formation of the pathogen's poly-L-glutamine/glutamate barrier.^[63,64] The crystal structure has been solved for GS from bacteria, plants and mammals.^[65,66] Typical bacterial GS consists of 12 subunits, which form two rings that face each other. The active sites are located at the interface of each subunit in one ring (Figure 13).

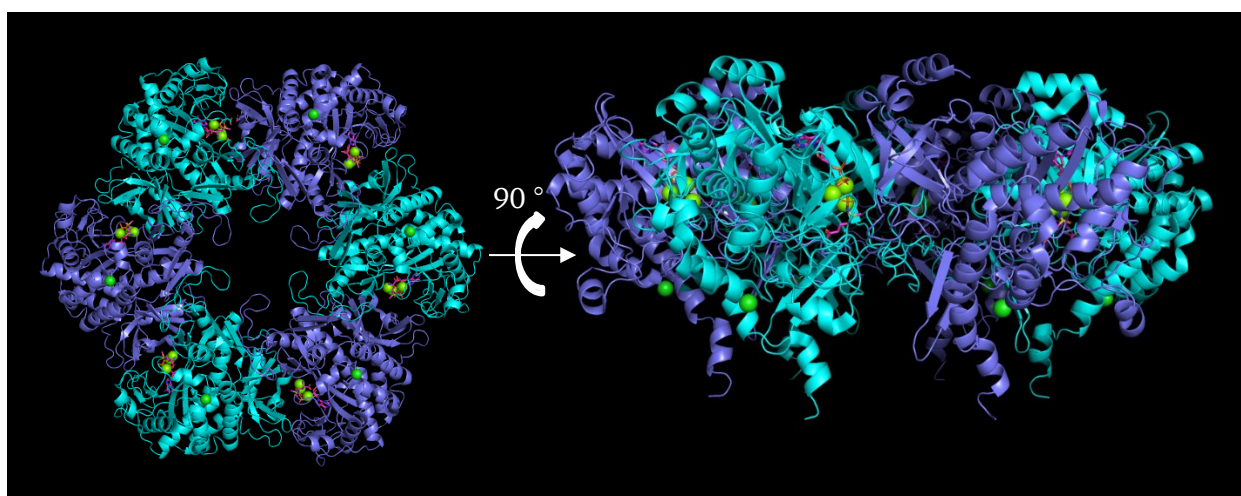


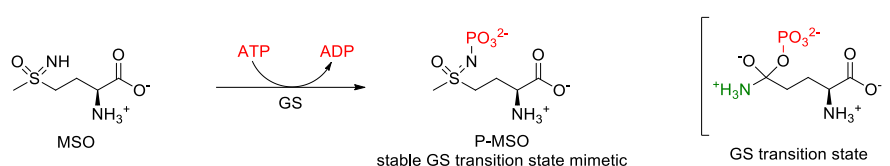
Figure 13. Cocystal structure of MtGS with phosphorylated MSO, ADP, Mg²⁺ and Cl⁻ (PDB: 2BVC). The subunits are alternately colored in light and dark blue. The cocystal structure shows 6 subunits forming one ring.

Eukaryotes typically have a smaller form of GS, which consists of two five-membered rings.^[67] The active site of GS consists of an ATP binding site and a glutamate binding site and requires Mg^{2+}/Mn^{2+} ions. The glutamate binding site is highly conserved among bacterial and eukaryotic GS, whereas the ATP binding site varies much more between bacterial and mammalian GS. The differences between the ATP binding sites of mammalian and plant GS are more subtle.^[65] Another difference between bacterial and eukaryotic GS is their regulation. The activity of bacterial GS is regulated by adenylation via adenylation transferases and feedback inhibition. In contrast, eukaryotic GS is regulated by expression, metal ion concentration (higher affinity for Mn^{2+} but higher activity with Mg^{2+}) and end-product feedback (not brain GS).^[68,69] The catalytic mechanism of GS is well characterized and conserved. The enzyme activates its substrates NH_4^+ by deprotonation and glutamate by phosphorylation using ATP. Quantum mechanism/molecular mechanics calculations suggest these two reactions are spontaneous and essentially barrierless.^[70] Then ammonia attacks the γ -glutamylphosphate to form a tetrahedral transition state, from which PO_4^{3-} and a proton of the former ammonia leave simultaneously as HPO_4^{2-} and the product glutamine remains.^[68,70]

Glutamine synthetase is part of a family of γ -glutamylating enzymes and some organisms have additional GS-like enzymes. *Mycobacterium tuberculosis* has three additional GS-like enzymes (GlnA2_{Mt}, GlnA3_{Mt}, GlnA4_{Mt}), though only the glutamine synthetase GlnA1_{Mt} is essential.^[71] *Streptomyces coelicolor* likewise contains three GS-like enzymes (GlnA2_{Sc}, GlnA3_{Sc}, GlnA4_{Sc}),^[72] *Pseudomonas aeruginosa* has seven (PauA1-7)^[73] and the halophilic archaea *Haloferax mediterranei* has two (GlnA2_{Hm}, GlnA3_{Hm}).^[74] GlnA2_{Sc}, GlnA3_{Sc} and GlnA2_{Hm} were shown to be putative glutamate polyamine ligases. ^[72,74,75] GlnA4_{Sc} was characterized to glutamylate ethanolamine, enabling the ethanolamine utilization as carbon and nitrogen source.^[76] Another important γ -glutamylating enzyme is glutamate cysteine ligase, which catalyzes the first step of the glutathione synthesis.^[77]

2.4. Inhibitors of GS and GS-like enzymes

The long-term gold standard inhibitor of glutamine synthetase is methionine sulfoximine (MSO). MSO was first found as a toxic by-product of ‘agenized’ (NCl_3 treated) zein, which produced convulsive fits in rabbits.^[78] It was later found to have this effect by inhibiting GS and thereby disturbing the glutamate and ammonia balance in the brain.^[60,79] The binding affinity of MSO itself is comparable to that of glutamate, but MSO is phosphorylated by GS to form P-MSO, which then binds GS quasi irreversibly as a stable transition state mimetic (Scheme 2).^[80]



Scheme 2. Inhibitory mechanism of MSO.

Of the four MSO diastereomers, the L-methionine-S-sulfoximine is the most active one, with the R-sulfoximine still showing 10 % of its epimer's potency.^[81,82] The affinity of MSO for GS varies between species. The K_i value for sheep brain GS is $100 \mu\text{M}$ while MSO inhibits MtGS and *E. coli* GS with an K_i of $1 \mu\text{M}$.^[64] The physiological effect also varies among mammals. For example, dogs are unusually sensitive to MSO and easily develop convulsive seizures, whereas humans are rather insensitive.^[83] MSO has been intensively studied as a potential treatment against the pathogen *Mycobacterium tuberculosis*.

The growth of *M. tb* can be inhibited by MSO and this effect can be countered with excess glutamine. Interestingly, MSO affects only pathogenic bacteria which export GS but does not affect e.g. *M. smegmatis* or *L. pneumophila*.^[64] In *M. tb*, which exports about 33 % of its GS, only the extracellular enzyme is inhibited while the activity of cell-associated GS is only minimally decreased.^[63,64] By inhibiting the extracellular GS, MSO decreases the amount of poly-glutamate/glutamine in the *M. tb* cell wall. This gives MSO a synergistic effect with other conventional *M. tb* antibiotics.^[64] However, although MSO could counter disease symptoms and infection of tuberculosis in a guinea pig model, it was never considered a drug candidate. Besides being epileptogenic, MSO inhibits glutamate cysteine ligase and therefore the glutathione synthesis. This effect can be partly compensated by administration of ascorbate, but MSO is also metabolised to a ketoacid, which leads to potentially toxic methane sulfinimide and vinylglyoxate.^[84]

Another established GS inhibitor is phosphinothricin (PPT), which was first isolated as a tripeptide from *Streptomyces viridochromogenes*. PPT is widely used as a herbicide under the name glufosinate.^[85] Although different synthetic programs aimed to improve MSO or PPT, no drug could yet be generated.^[86] A different way to inhibit GS would be to target its ATP binding pocket. Many HTS approaches aimed to find ATP competitive GS inhibitors and various compounds, based on different scaffolds, were found to be active up to a low nM range.^[87,88,89] Some of these scaffolds presented promising inhibition of *M. tuberculosis*^[88] while others failed to transfer a strong MtGS binding to a whole cell activity against *M. tb.*^[87]

3. Results and Discussion

3.1. A [4.2.1]-bicyclic FKBP ligand negative control substance

A good pharmacological negative control substance should show a high structural resemblance to the compound or compound class of interest but is ideally inactive against the biological target. The direct comparison of active compound and inactive negative control substance gives a strong indication for on-target vs. off-target effects.

To design a negative control for FKBP ligands of the 3,10-diazabicyclo[4.3.1]decan-2-one scaffold, the piperolate core is modified. The 6-membered ring is contracted to a 5-membered ring which results in a 3,9-diazabicyclo[4.2.1]nonan-2-one core motif (Figure 14).

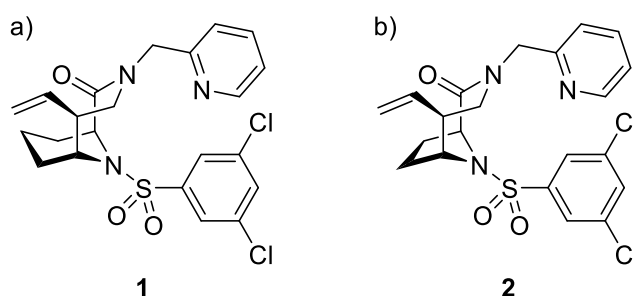
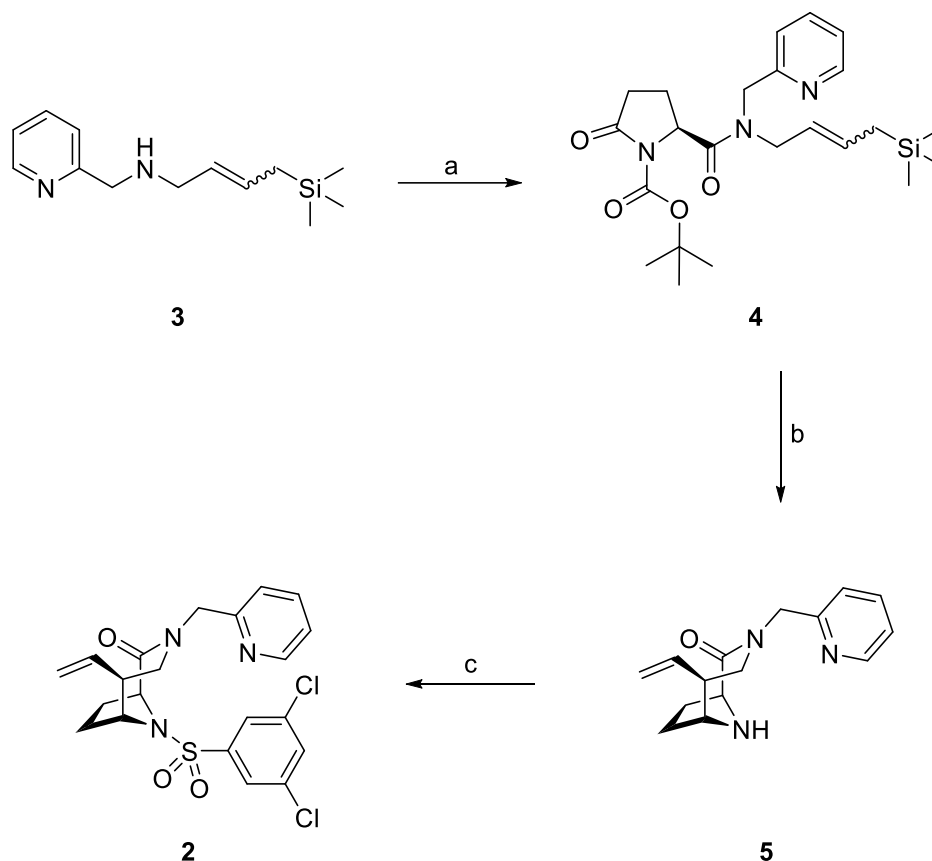


Figure 14. a) Well-characterized [4.3.1]-bicyclic FKBP-ligand **1**, b) analogous [4.2.1]-bicyclic compound **2**.

The synthesis route of **2** was planned similar to the synthesis of **1**, except instead of 6-oxopipercolic acid, 5-oxoproline was used (Scheme 3).



Scheme 3. Reagents and conditions: a) L-Pyroglutamic acid **6**, EDC, HOBT, DMF, 0 °C – rt, 17 h, then Boc₂O, DIPEA, DMAP, DCM, rt, 15 h, 57 % over two steps; b) DIBAH, THF, -98 °C, 5 min, then HF-pyridine, -84 °C – 0 °C, 3 h, 40 % over two steps; c) 3,5-Dichlorobenzesulfonyl chloride **7**, DIPEA, MeCN, rt, 18 h, 80 %.

The synthesis of compound **2** starts with the common precursor **3**, which is coupled to 5-oxoproline (L-pyroglutamic acid) **6** and subsequently Boc-protected to form **4**. The key step in this synthesis is the cyclization reaction, which forms the [4.2.1]bicyclodecan-core **5** upon DIBAH reduction and treatment with hydrofluoric acid. Coupling of sulfonyl chloride **7** to **5** gives the final FKBP-ligand **2**.

The biochemical evaluation of **2** for binding to different FKBP_s was performed in a fluorescence polarization assay by Wisely Oki Sugiarto to determine the binding affinities for FKBP₅₁, **52**, **12** and **12.6** (Table 2).

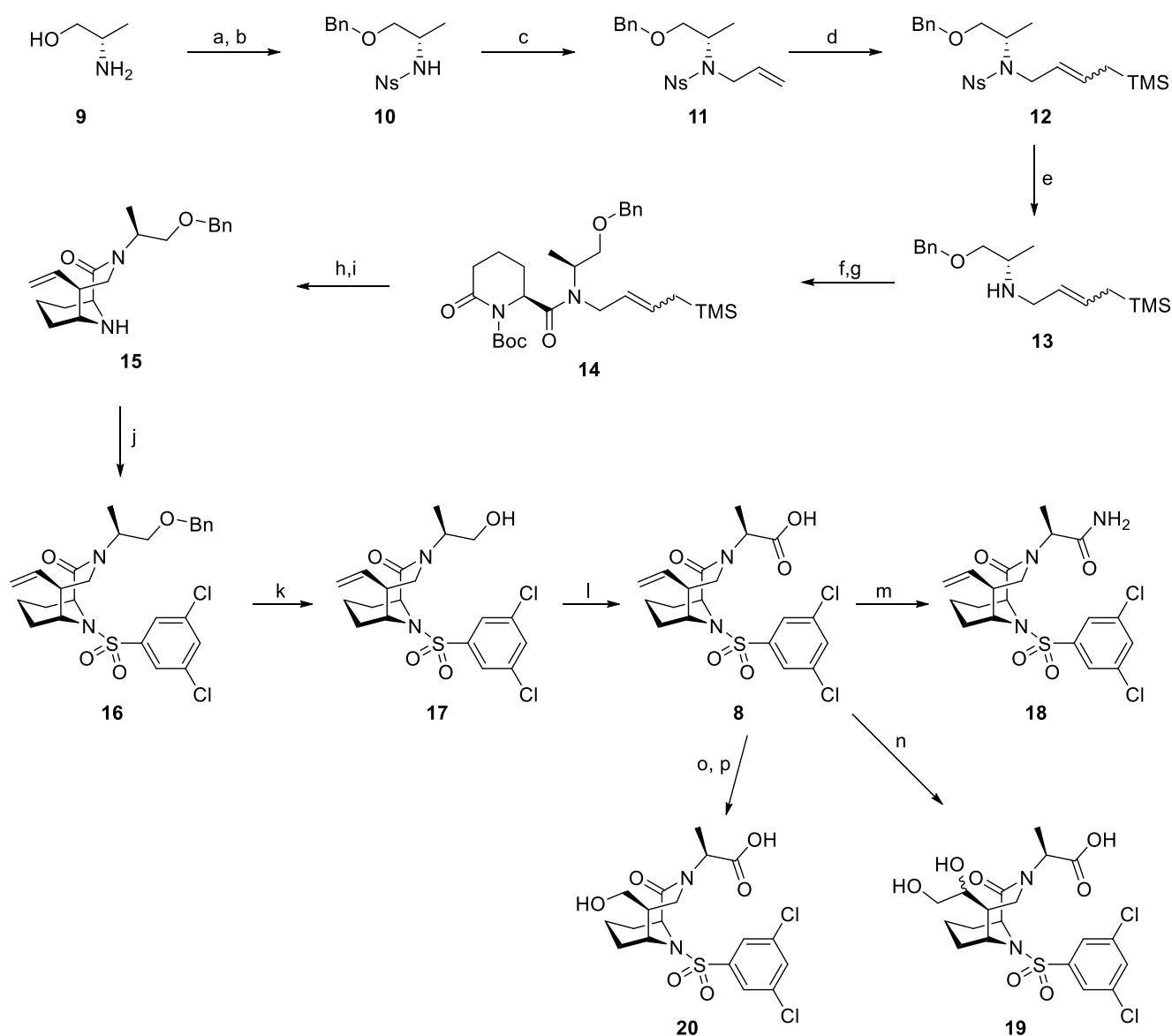
Table 2. Binding affinities of compound **1** and **2** against different FKBP. All K_D values were measured in the same assay.

Compound	K_D for FKBP51 in nM	K_D for FKBP52 in nM	K_D for FKBP12 in nM	K_D for FKBP12.6 in nM
1	146 ± 7	101 ± 10	2.4 ± 0.3	7.8 ± 1.2
2	>10,000	>10,000	658 ± 39	5,940 ±1,210

Compound **2** did not show any binding affinity to FKBP51 and FKBP52. The compound precipitates at concentrations above 10 μ M in this assay. Therefore the binding affinity can only be determined as greater than 10 μ M. For FKBP12 and FKBP12.6 some affinity remains, however it drops more than 100-fold compared to the [4.3.1]-bicyclic analog **1**. These two compounds differ only in one methylene group, making **2** an excellent negative control substance for biochemical and biological assays with FKBP-ligands of the 3,10-diazabicyclo[4.3.1]decan-2-one type.

3.2. Synthesis and properties of (S)-2-(2-oxo-3,10-diazabicyclo[4.3.1]decan-3-yl)propanoic acids as FKBP ligands

Carboxylic acids and amides are known R1-substituents for 3,10-diazabicyclo[4.3.1]decan-2-ones as FKBP ligands with good binding affinities.^[57,90] An α -methyl group to the carboxylic acid can further boost the ligand's binding affinity.^[90] The synthesis of compound **8** was performed as described in KOLOS & POMPLUN *et al.*^[90] (Scheme 4). Further late-stage derivatization was performed to access the respective carboxylic amide and to introduce hydroxy groups in R3 to increase the aqueous solubility.



Scheme 4. Reagents and conditions: a) NaH, BnCl, THF, reflux, 1 h; b) DIPEA, NsCl, MeCN, rt, 1 h, 58 % (over 2 steps); c) K₂CO₃, allyl bromide, DMF, 60 °C, 5 h, 92 %; d) p-benzoquinone, Grubbs cat. 2nd gen., allyltrimethylsilane, DCM, reflux, 6 h, 73 %; e) K₂CO₃, thiophenol, DMF, rt, 16 h, 93 %; f) S-6-Oxo-2-piperidinecarboxylic acid, HATU, DIPEA, DMF, rt, 19 h; g) Boc₂O, DIPEA, DMAP, rt, 15 h, 91 % (over 2 steps); h) DIBAH, THF, -98 °C, 5 min; i) HF-pyridine, DCM, -84 – 0 °C, 3 h, 48 % (over 2 steps); j) 3,5-Dichlorobenzenesulfonyl chloride **7**,

DIPEA, MeCN, rt, 15 h, 63 %; k) BCl₃-SMe₂, DCM, 5 h, 86 %; l) Jones reagent, acetone, 0 °C – rt, 4 h, 96 %; m) CDI, THF, rt, 3 h, then aq. NH₃, rt, 2 h, 82 % ; n) 2,6-Lutidine, NMO, OsO₄, acetone/water (9:1), rt, 25 h, 59 %; o) 2,6-Lutidine, OsO₄, NaIO₄, dioxan/water (3:1), rt, 18 h; p) NaBH₄, THF, 0 °C – rt, 21 h, 26 % (over 2 steps).

The carboxylic acid **8** could be converted to the amide **18** in good yield using CDI/NH₃. A Lemieux-Johnson oxidation of **8** followed by NaBH₄ reduction of the intermediary aldehyde gave the alcohol **20**. The dihydroxylated compound **19** was synthesized with OsO₄ oxidation of **8**, and was isolated as a mixture of diastereomers. The synthesis of **19** could be repeated on a relatively large scale and yielded 324 mg product in a resynthesis. All final compounds from this series were analyzed for their binding affinity in a FP-Assay for FKBP12, FKBP12.6, FKBP51 and FKBP52 (Table 3). As references, the carboxylic acid and amide without the α -methyl group (Figure 15) are shown in the same table. Their binding affinities for the human FKBP are taken from POMPLUN *et al.*^[57]

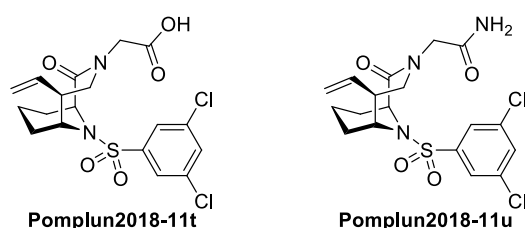


Figure 15. Structures of carboxylic acid and amide without α -methyl group in the R1 position.

Table 3. Binding affinities of (*S*)-2-(2-oxo-3,10-diazabicyclo[4.3.1]decan-3-yl)propanoic acids for FKBP12, 12.6, 51 and 52. ^aValues taken from POMPLUN *et al.*^[57] ^{b-d}Values taken from the same assay, respectively.

Compound	K _D for FKBP12 in nM	K _D for FKBP12.6 in nM	K _D for FKBP51 in nM	K _D for FKBP52 in nM
Pomplun2018-11t	20 ^a ± 1	51 ^a ± 3	213 ^a ± 48	640 ^a ± 111
Pomplun2018-11u	6.8 ^a ± 1.3	22 ^a ± 4	160 ^a ± 29	135 ^a ± 23
8	3.3 ^b ± 0.4	13 ^b ± 2	36 ^b ± 5	66 ^b ± 5
18	3.1 ^c ± 0.4	13 ^c ± 2	41 ^c ± 4	49 ^c ± 4
19	1.7 ^b ± 0.2	5.3 ^b ± 1.9	32 ^b ± 5	38 ^b ± 4
20	2.7 ^d ± 0.3	8.7 ^d ± 0.8	8.0 ^d ± 1.2	19 ^d ± 2

The effect of the α -methyl group can be seen in the direct comparison between **Pomplun2018-11t** and **8** and between **Pomplun2018-11u** and **18**. With the carboxy group in the R1 position, the α -methyl group boosts the binding affinity by a factor 3.9-9.6 for the tested FKBP. With the amide, this effect is

less pronounced, with a boost in binding affinity by a factor 1.7-3.9 for all tested FKBP. The difference between the carboxy group and the respective amide, with and without the α -methyl group, is rather small. With few exceptions, their binding affinities differ by a factor 0.8-1.8. The hydroxylation (**20**) and dihydroxylation (**19**) slightly improve the binding affinity for all tested FKBP. Based on the strong *in vitro* binding affinity of **19** for FKBP12, the cellular activity of **19** was examined in a nanoBRET™ assay. However, the binding curve could not be fitted properly but an IC₅₀ in the μ M range can be estimated from the data. This low cellular activity may reflect a poor membrane permeability, likely due to the high polarity of the compound. The strong protein binding but poor membrane permeability makes compound **19** an excellent control compound to differentiate between intra- and extracellular effects. Compounds **8**, **18** and **19** were subjected to a metabolic stability assay with mouse liver microsomes. Therein amide **18** was poorly stable with an intrinsic clearance of $CL_{int} = 1400 \mu\text{L}/\text{min}/\text{mg}$. Carboxylic acid **8** on the other hand showed a better stability with 71 % compound remaining after 60 min with mouse liver microsomes. Dihydroxylated carboxylic acid **19** was even more stable with 96 % compound remaining after 60 min, or a $CL_{int} = 2.8 \mu\text{L}/\text{min}/\text{mg}$. This presents a first lead on metabolically stable 3,10-diazabicyclo[4.3.1]decan-2-ones, however the structure-stability relationship remains to be elucidated.

3.3. (1*S*,5*S*,6*R*)-10-benzylsulfonyl-3,10-diazabicyclo[4.3.1]decan-2-ones as FKBP ligands

So far, all FKBP-inhibitors of the 3,10-diazabicyclo[4.3.1]decan-2-one scaffold have always been bearing an aryl substituent on the sulfonamide in R2.^[54–57,90] This motif provided many strongly binding FKBP inhibitors (Figure 16a). Other pipercolate-derived scaffolds, however, show FKBP12 or Mip-binding with benzyl-sulfonamides in what correlates to the R2 position in 3,10-diazabicyclo[4.3.1]decan-2-one (Figure 16b and c).^[50,52] Therefore, (1*S*,5*S*,6*R*)-10-benzylsulfonyl-3,10-diazabicyclo[4.3.1]decan-2-ones were synthesized and their FKBP binding was analyzed.

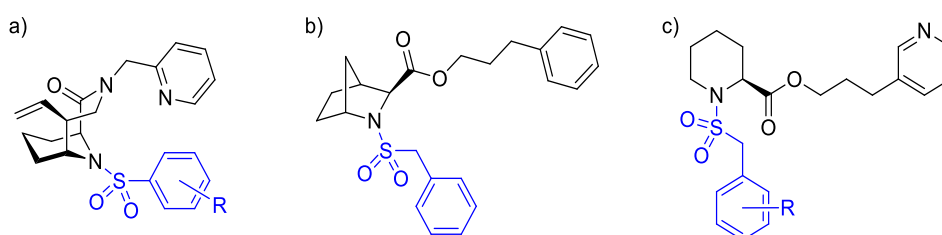
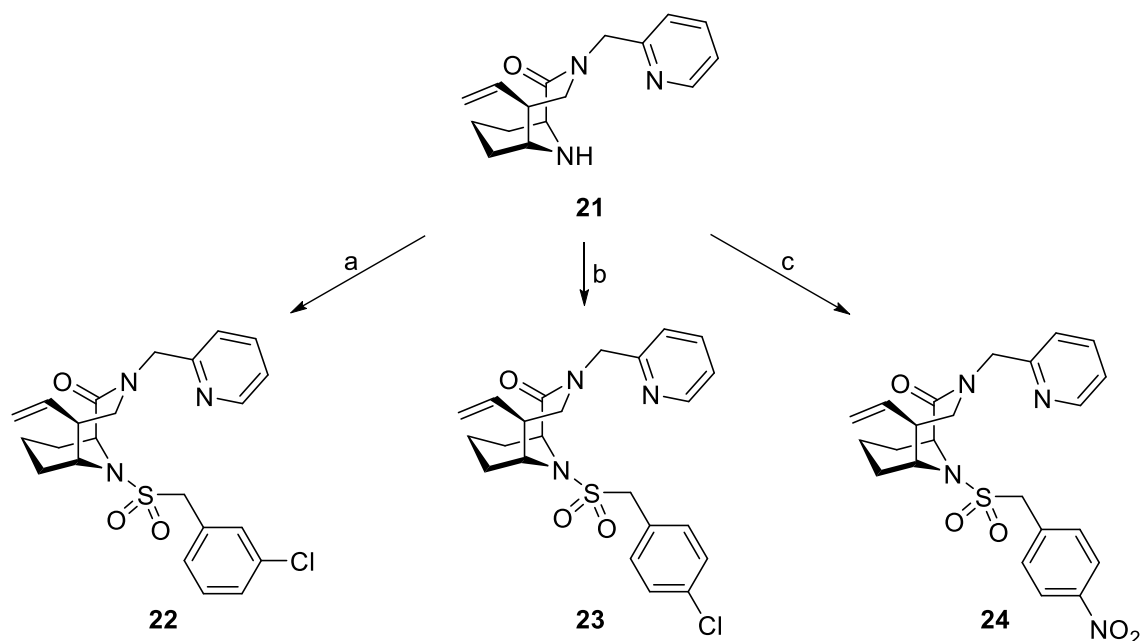


Figure 16. a) FKBP-inhibitor developed by the HAUSCH lab,^[57] with the arylsulfonamide highlighted in blue, **Pomplun2018-15e** R = 3-Cl, K_D = 8.8 nM against FKBP12. b) FKBP12-inhibitor developed by Guilford Pharmaceuticals,^[52] with the benzylsulfonamide highlighted in blue, IC_{50} = 1300 nM against FKBP12. c) LpMip and BpMip-inhibitor developed by the HOLZGRABE lab,^[50] with the benzylsulfonamide highlighted in blue, **Seufert2016-5n** R = 3-Cl, IC_{50} = 230 nM against BpMip.

The target molecules were chosen based on the structure-activity relationship of the BpMip-ligands published by SEUFERT *et al.*,^[50] and the synthesis was performed by coupling the bicyclic core **21** with the respective sulfonyl chlorides (Scheme 5). Binding affinities towards FKBP51, 52, 12 and 12.6 were measured in a fluorescence polarization assay by Wisely Oki Sugiarto (Table 4). Binding of Mips is discussed in Chapter 3.7.



Scheme 5. Reagents and conditions: a) *meta*-chlorobenzylsulfonyl chloride **25**, DMAP, MeCN, 0 °C – rt, 30 h, 84 %; b) *para*-chlorobenzylsulfonyl chloride **26**, DMAP, MeCN, 0 °C – rt, 45 h, 71 %; c) *para*-nitrobenzylsulfonyl chloride **27**, DMAP, MeCN, 0 °C – rt, 45 h, 82 %.

Table 4. Binding affinities of (1*S*,5*S*,6*R*)-10-benzylsulfonyl-3,10-diazabicyclo[4.3.1]decan-2-ones **22**, **23** and **24**, and reference 3-chlorobenzenesulfonamide **Pomplun2018-15e** for FKBP. ^a Values taken from Pomplun *et al.*^[57] Values for all other compounds are taken from the same assay.

Compound	K _D for FKBP51 in nM	K _D for FKBP52 in nM	K _D for FKBP12 in nM	K _D for FKBP12.6 in nM
22	>80,000	>80,000	1,120 ±59	1,420 ±131
23	19,000 ±8,000	43,000 ±6,000	363 ±27	625 ±72
24	>80,000	35,000 ±11,000	988 ±114	1,560 ±200
Pomplun2018-15e	298 ^a ±51	344 ^a ±28	8.8 ^a ±1.1	6.1 ^a ±1.1

The benzyl sulfonamide is clearly not suited for the R2 position of 3,10-diazabicyclo[4.3.1]decan-2-ones as FKBP-ligands. Some residual binding can still be observed with FKBP12 and FKBP12.6, however the

binding affinity is drastically lower compared to analogous phenyl-substituted sulfonamides, e.g. 3-chlorophenylsulfonamide in **Pomplun2018-15e**.^[57] To better understand this structure-activity relationship, the cocrystal structures of phenyl sulfonamide **1** with FKBP12 (discussed in more detail in Chapter 3.5) and of benzyl sulfonamide **SF354** with BpMip (PDB: 5VT8) were superimposed (Figure 18A). **1** is also modeled in PyMol to bear a benzyl sulfonamide instead of its 3,5-dichlorobenzenesulfonamide residue, which is also superimposed with **SF354** (Figure 18B). Chemical structures of all three compounds are shown in Figure 17.

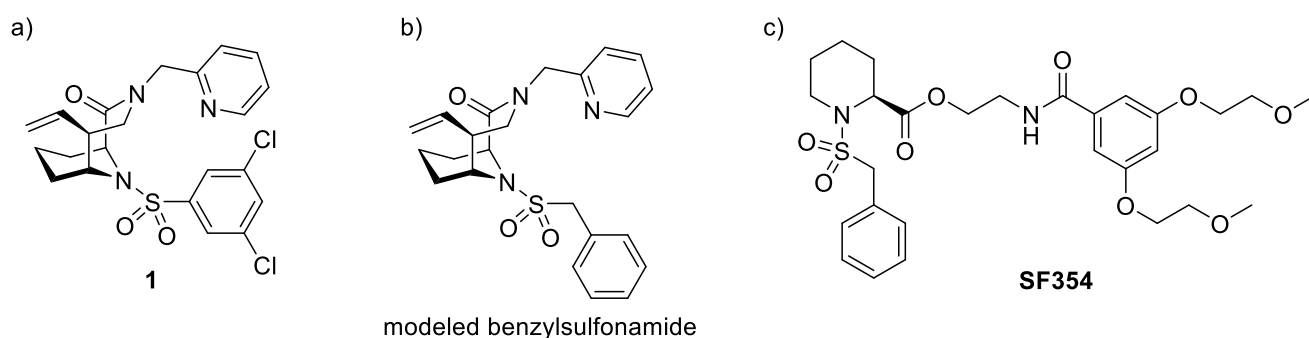


Figure 17. Chemical structures of a) Phenylsulfonamide **1**, b) modeled bicyclic benzylsulfonamide and b) benzylsulfonamide **SF354**.

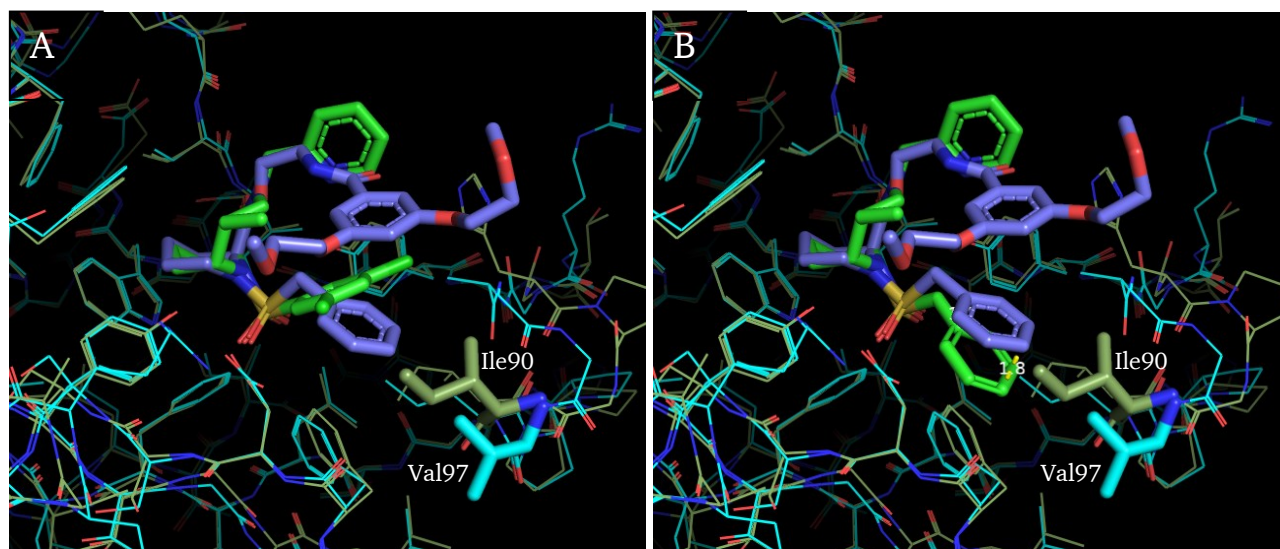


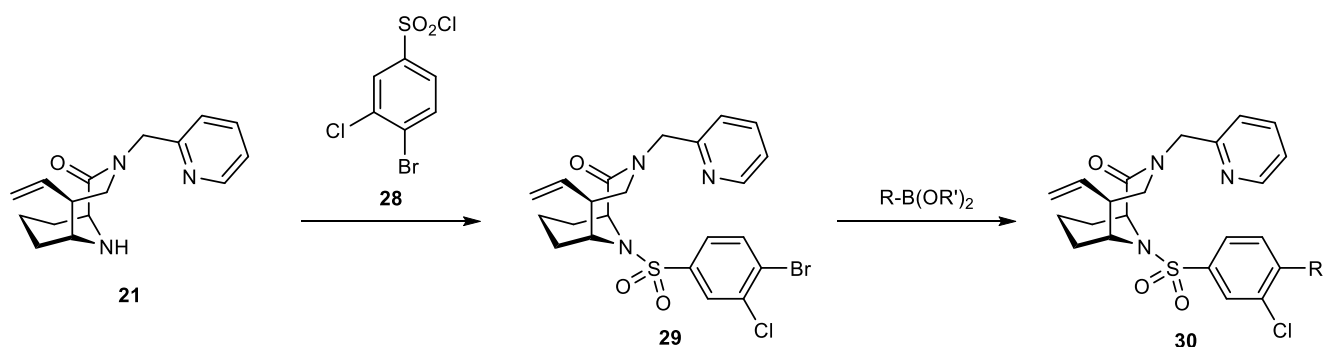
Figure 18. A) Cocrystal structures of **1** (green) with FKBP12 (olive) and of **SF354** (purple) with BpMip (blue) (PDB:5V8T); B) Cocrystal structure of benzyl sulfonamide modeled from **1** (green) with FKBP12 (olive) and of **SF354** (purple) with BpMip (blue) (PDB:5V8T).

The active sites of both proteins are mostly identical, with differences presenting in the loop around the compound's R2 position. The pipecolate cores of both ligands occupy the same space in their respective protein, however it can clearly be seen that the angle of the sulfonamide is different in both ligands. While the extended length of the benzyl moiety, compared to a phenyl, can be compensated by a

widening of the surrounding loop, like the side chain of Val97 does in BpMip compared to Ile90 in FKBP12, the modeled benzyl group of the bicyclic ligand is positioned 1.1-1.8 Å lower than the benzyl group of **SF354**. This likely causes a clash with the protein, which can hardly be compensated and results in the observed low binding affinities for FKBP12. Binding affinities for BpMip were not determined, but a one-point screening at 10 μM compound concentration showed low binding (<10 % tracer replacement) for all three benzylsulfonamides (**22**, **23** and **24**).

3.4. Ultra-high affinity FKBP12 ligands

During my master thesis, a small library of FKBP ligands based on the 3,10-diazabicyclo[4.3.1]decan-2-one scaffold was synthesized to explore the structure-affinity relationship of an expanded R2 residue. In that project, an aryl sulfonamide bearing a bromide was introduced in the R2 position, which was then derivatized in a series of Suzuki reactions (Scheme 6).

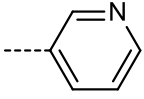
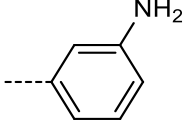
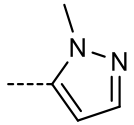
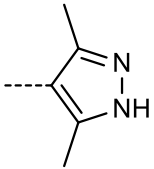
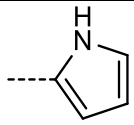
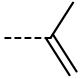
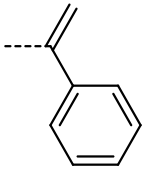
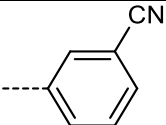
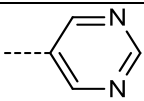


Scheme 6. Synthesis of a FKBP ligand library with different R2-para substituents.

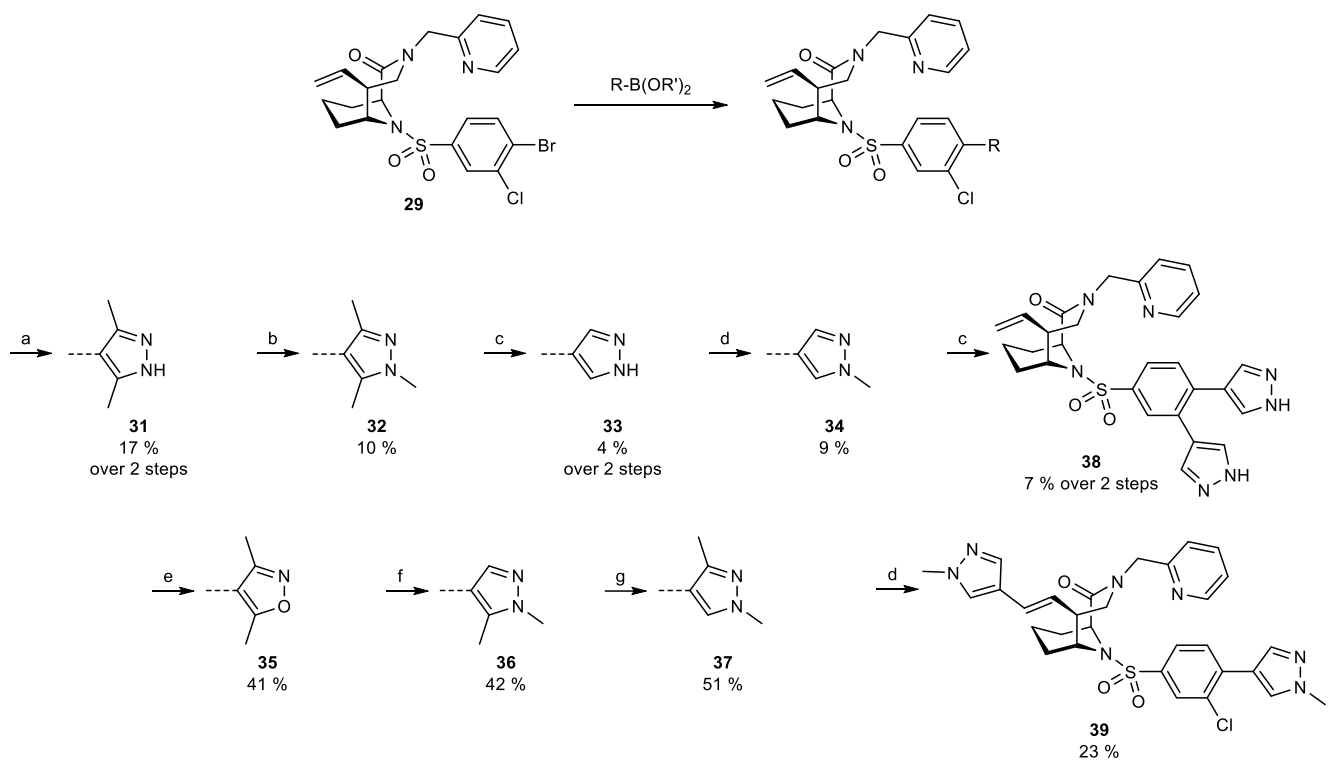
At the time of my master thesis, the synthesis of the **30**-series was completed but the determination of the novel ligands' binding affinities was missing. The necessary fluorescence polarization assays were later added by Stephanie Merz during my doctoral research (Table 5). **Pomplun2018-15e** is listed as a reference compound with R = H.

Table 5. Binding affinities of compounds **30a**-**l** for FKBP12, 51 and 52. ^aValues taken from Pomplun *et al.*^[57] Values for all other compounds are taken from the same assay.

Compound	Structure R =	K _D for FKBP12 in nM	K _D for FKBP51 in nM	K _D for FKBP52 in nM
Pomplun2018-15e	---H	8.8 ^a ± 1.1	298 ^a ± 51	344 ^a ± 29
30a		48 ± 5	2,180 ± 1,320	882 ± 475
30b		31 ± 5	3,920 ± 2,890	717 ± 339
30c		18 ± 3	395 ± 132	172 ± 83

30d		2.9 ± 0.5	323 ± 79	173 ± 62
30e		21 ± 3	417 ± 127	226 ± 76
30f		2.3 ± 0.4	166 ± 63	148 ± 42
30g		0.6 ± 0.1	411 ± 105	291 ± 129
30h		7.3 ± 1.9	15 ± 6	17 ± 11
30i		28 ± 4	$1,520 \pm 750$	$2,180 \pm 1,140$
30j		84 ± 27	$1,690 \pm 990$	$1,170 \pm 670$
30k		19 ± 3	759 ± 305	451 ± 178
30l		11 ± 2	407 ± 108	889 ± 443

Most compounds show poor binding affinities for FKBP51 and 52 and moderate binding affinities for FKBP12. One intriguing observation could be made with ligand **30g**, which was measured to bind FKBP12 with a K_D -value of 0.6 nM. K_D -values below 1 nM cannot be precisely determined in this FP-assay, however it is clear that the binding of **30g** is much stronger than that of any other compound in this series. To confirm and to further investigate this strong binding, **30g** was resynthesized (**31**) together with close analogs with the same pyrazole or a similar isoxazole motif (Scheme 7). Different methylation patterns were tested to answer the question whether the sterically hindered rotation of the pyrazole ring or the H-bond donor is responsible for the compounds' strong binding affinity.

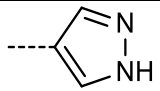
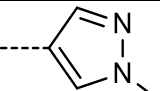
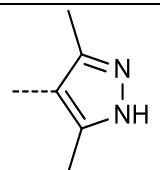
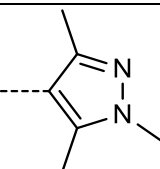
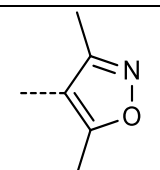
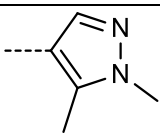
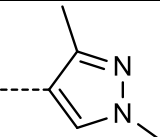


Scheme 7. Reagents and conditions: Suzuki reactions for a,b,c,d) Pd(OAc)₂, XPhos, K₃PO₄, respective boronic acid or ester, THF, reflux, 2-5 d, 10 % **32**, 9 % **34**; Boc-cleavage for a,c) TFA, DCM, rt, 65 h, yields over two steps: 17 % **31**, 4 % **33**, 7 % **38**; Suzuki reactions for e,f,g) Pd(dppf)Cl₂, K₂CO₃, respective boronic acid or ester, dioxane/water, 80 °C, 2-17 h, 41 % **35**, 42 % **36**, 51 % **37**.

Suzuki reactions to form **31**, **32**, **33** and **34** gave poor yields (4-17 %). This required a change in reaction conditions. Therefore, for the subsequent Suzuki reactions the solvent was changed from THF to dioxane/water, the solvent was later degassed with argon to remove any oxygen, the catalyst was changed from Pd(OAc)₂/Xphos to Pd(dppf)Cl₂ and the base was changed from K₃PO₄ to K₂CO₃. The new reaction conditions gave much better yields (41-51 %) for **35**, **36** and **37**. Compounds **31** and **33** were synthesized over two steps. The pyrazole amine of the respective boronic acid or ester was bearing a protective Boc-group, which needed to be removed under acidic conditions after the Suzuki coupling. Furthermore two side products were isolated, one each from the reactions of **33** and **34**. In the case of **33**, the boronic acid reacted not only with the aryl bromide but additionally with the aryl chloride, which yielded side product **38** after acidic Boc-deprotection. In the synthesis of **34**, the boronic ester also underwent an oxidative Heck coupling with the terminal double bond in R3, yielding **39**.

The binding affinities of all **30g** analogs were determined in a FP-assay, with the help of Wisely Oki Sugiarto. When the K_D-values for FKBP12 and 12.6 were in the sub-nanomolar range, a more sensitive Homogenous Time Resolved Fluorescence (HTRF) assay was performed by Thomas Geiger to generate more precise data (Table 6). Previously published compound **Pomplun2018-15e** is shown as a reference.^[57]

Table 6. K_D -values of **30g** analogs for FKBP12, 12.6, 51 and 52 by FP assay. * K_D -values determined in HTRF assay. ^a Values taken from POMPLUN *et al.*^[57] ^{b-f} Values taken from the same assay, respectively.

Compound	Structure R =	K_D for FKBP12 in nM	K_D for FKBP12.6 in nM	K_D for FKBP51 in nM	K_D for FKBP52 in nM
Pomplun2018-15e	---H	$8.9^a \pm 1.1$	$6.1^a \pm 1.1$	$298^a \pm 51$	$344^a \pm 28$
33		$2.0^b \pm 0.2$	$1.7^b \pm 0.2$	$100^b \pm 10$	$73^b \pm 8$
34		$1.3^b \pm 0.2$	$1.0^b \pm 0.1$	$185^b \pm 17$	$170^b \pm 17$
31		$0.381^{*d} \pm 0.028$	$0.177^{*e} \pm 0.015$	$360^b \pm 35$	$201^b \pm 21$
32		$0.115^{*f} \pm 0.025$	$0.022^{*f} \pm 0.003$	$451^b \pm 48$	$368^b \pm 46$
35		$0.222^{*f} \pm 0.019$	$0.057^{*f} \pm 0.012$	$440^c \pm 58$	$470^c \pm 60$
36		$0.235^{*f} \pm 0.033$	$0.065^{*f} \pm 0.007$	$220^c \pm 22$	$250^c \pm 23$
37		$0.209^{*f} \pm 0.011$	$0.104^{*f} \pm 0.005$	$230^c \pm 30$	$190^c \pm 20$
38		$21^b \pm 2$	$71^b \pm 17$	$494^b \pm 53$	$332^b \pm 36$
39		$0.056^{*f} \pm 0.002$	$0.045^{*f} \pm 0.003$	$15^b \pm 2$	$11^b \pm 2$

Comparison of **33** and **34** shows that the methylation of the H-bond donor in the pyrazole ring barely makes a difference for the binding affinities (factor 1.5 for FKBP12). The difference between **31** and **32** is only slightly greater (factor 3.3 for FKBP12), with the analogous isoxazole **35** having an affinity between the free and the methylated amine. This allows the conclusion that the H-bond donor is not

important for the binding affinity of this pyrazole motif. A stronger effect is observed when comparing the methylation in the 3- and 5-position of these pyrazoles/isoxazoles. The binding affinity increases from **33** to **31** by a factor 5.2 and from **34** to **32** by 11.3. Moreover, the presence of only one methyl group, no matter if in 3- or 5-position (**36** and **37**) has the same increase in binding affinity for FKBP12 as the dimethyl variant **32**. Differences in the 3- or 5- mono- and dimethylated pyrazoles/isoxazoles become clear when the binding affinities for FKBP51 and 52 are taken into consideration. The non-methylated compounds **33** and **34** have a selectivity of ~ 50 and ~ 140 , respectively, for FKBP12 over 51 and 52. Surprisingly, the monomethyl compounds **36** and **37** have a $\sim 1,000$ fold higher binding affinity for FKBP12 than for 51 and 52. Dimethylated **32** and **35** have a similar K_D -value for FKBP12 as the monomethyl analogs, but the additional methyl group increases the K_D -value for FKBP51 and 52, resulting in a $\sim 2,000$ fold selectivity for FKBP12 over 51 and 52. With its slightly increased K_D -value for FKBP12, the selectivity of **31** is a little lower (~ 500 - $1,000$) than its related 3,5-dimethyl variants. In comparison with the unsubstituted ligand **Pomplun2018-15e**, the pyrazole substituent in **31** boosts the binding affinity for FKBP12 by a factor of 23 and reduces affinity for FKBP51 by a factor of 1.2. The barrier in rotational freedom at the pyrazole/isoxazole in para-R2 seems to play an important role in the binding affinity for FKBP12. The two side products **38** and **39** give additional structure-affinity information. **38** has two pyrazoles attached to R2 and has a much lower binding affinity to FKBP12 and 12.6, its binding affinity for FKBP51 and 52 on the other hand is not as much decreased. Compound **39** shows a surprisingly strong binding to all FKBP. In comparison with its non-Heck parent compound **34**, the pyrazole in R3 seems to increase binding to FKBP12 and 12.6 by a factor 20, and to FKBP51 and 52 by a factor 12.

To better understand the molecular binding mode of the pyrazole moiety in R2, compound **31** was cocrystallized with FKBP12 by Christian Meyners (Figure 19). The cocrystal structure could be resolved at 1.0 Å resolution.

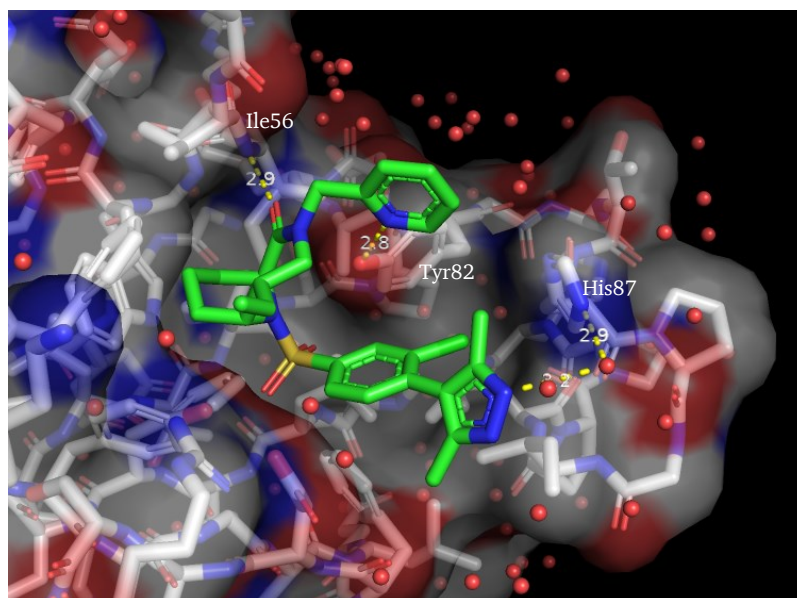


Figure 19. Cocrystal structure of **31** with FKBP12. Sticks and transparent surface shown, important ligand-protein-interactions indicated by yellow dotted lines. Distances are given in Å.

The position of the bicyclic core in the active site of FKBP12 is conserved in the **31**-FKBP12 complex and the most important interactions are still present (H-bonds to Ile56, Tyr82, halogen- π -interaction to His87). Additionally, a water-mediated H-bond can be observed between one pyrazole nitrogen atom and His87. This cocrystal structure might also help to explain the strong selectivity over FKBP51. Figure 20 shows the cocrystal structure of **31** with FKBP12 overlaid with FKBP51FK1 from a cocrystal structure with a similar ligand (PDB: 5OBK). Two major differences might explain the strong differences in binding affinities: (i) His87 from FKBP12 is not present in FKBP51, instead Ser118 takes its place. While Ser118 in FKBP51 can form the halogen- π -interaction with the ligand, it cannot form a water-mediated hydrogen bond with the ligand's pyrazole at the same time. (ii) Ile90 from FKBP12 leaves a cavity next to it (Figure 20A), which is occupied by one methyl group of the pyrazole of **31**. This cavity is blocked by Lys121 in FKBP51 (Figure 20B), causing the methyl group to clash with the protein. Taken together, these effects could explain the high selectivity towards FKBP12 over FKBP51.

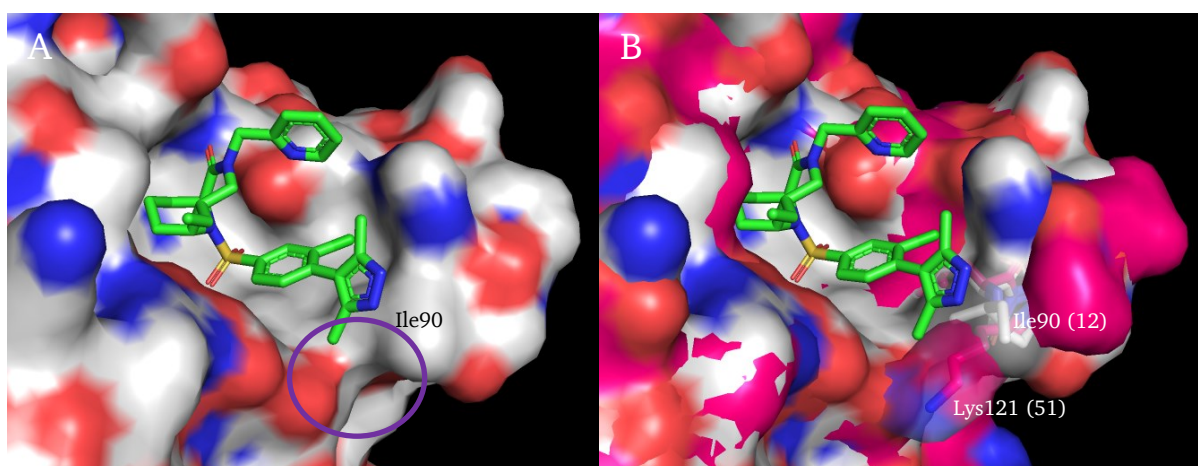
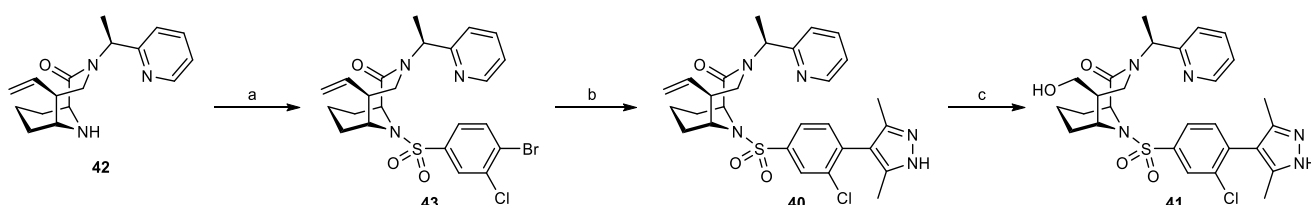


Figure 20. A) Cocrystal structure of **31** (green sticks) with FKBP12 (white surface), cavity next to Ile90 highlighted in purple, B) Same cocrystal structure superimposed with FKBP51FK1 (pink, PDB: 5OBK), cocrystalized with a similar ligand (not shown).

The novel pyrazole motif in R2 position was combined with optimized R1 and R3 residues to create an ultra-high affinity FKBP12 ligand (Scheme 8). This optimization effort was performed before the screening shown in Table 6 was finished, which is why the initial R2 residue of **31** was used instead of the slightly stronger binding residue of **32** or **35**. The binding affinities of **40** and **41** were again determined by FP- and HTRF-assay, performed by Wisely Oki Sugiarto and Thomas Geiger, respectively (Table 7). As reference compounds, the closest literature-known compounds **Kolos2021-16**^{(S)-Me} and **Kolos2021-18**^{(S)-Me} (Figure 21) are listed.^[90]



Scheme 8. Reagents and conditions: a) 4-bromo-3-chlorobenzene-1-sulfonyl chloride **28**, DIPEA, MeCN, rt, 3 d, 18 %; b) *tert*-butyl 3,5-dimethyl-4-(4,4,5,5-tetramethyl-1,3,2-dioxaborolan-2-yl)-1*H*-pyrazole-1-carboxylate **44**, Pd(OAc)₂, XPhos, K₂CO₃, THF/water 9:1, reflux, 6 h, then TFA, DCM, rt, 19 h, 40 % over two steps; c) NaIO₄, 2,6-lutidine, OsO₄, dioxane/water 3:1, rt, 23 h, then NaBH₄, EtOH, 0 °C – rt, 1 h, 25 % over two steps.

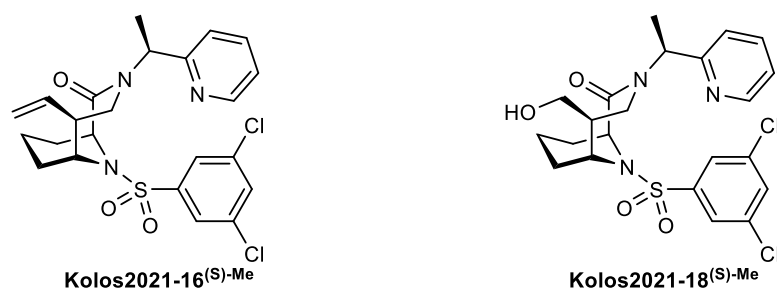


Figure 21. Structures of reference compounds **Kolos2021-16^(S)-Me** and **Kolos2021-18^(S)-Me**.

Table 7. Binding affinities of optimized FKBP12 ligands **40** and **41**. * K_D -values determined in HTRF-assay. ^aValues taken from Kolos *et al.*^[90]
^{b-f}Values taken from the same assay, respectively.

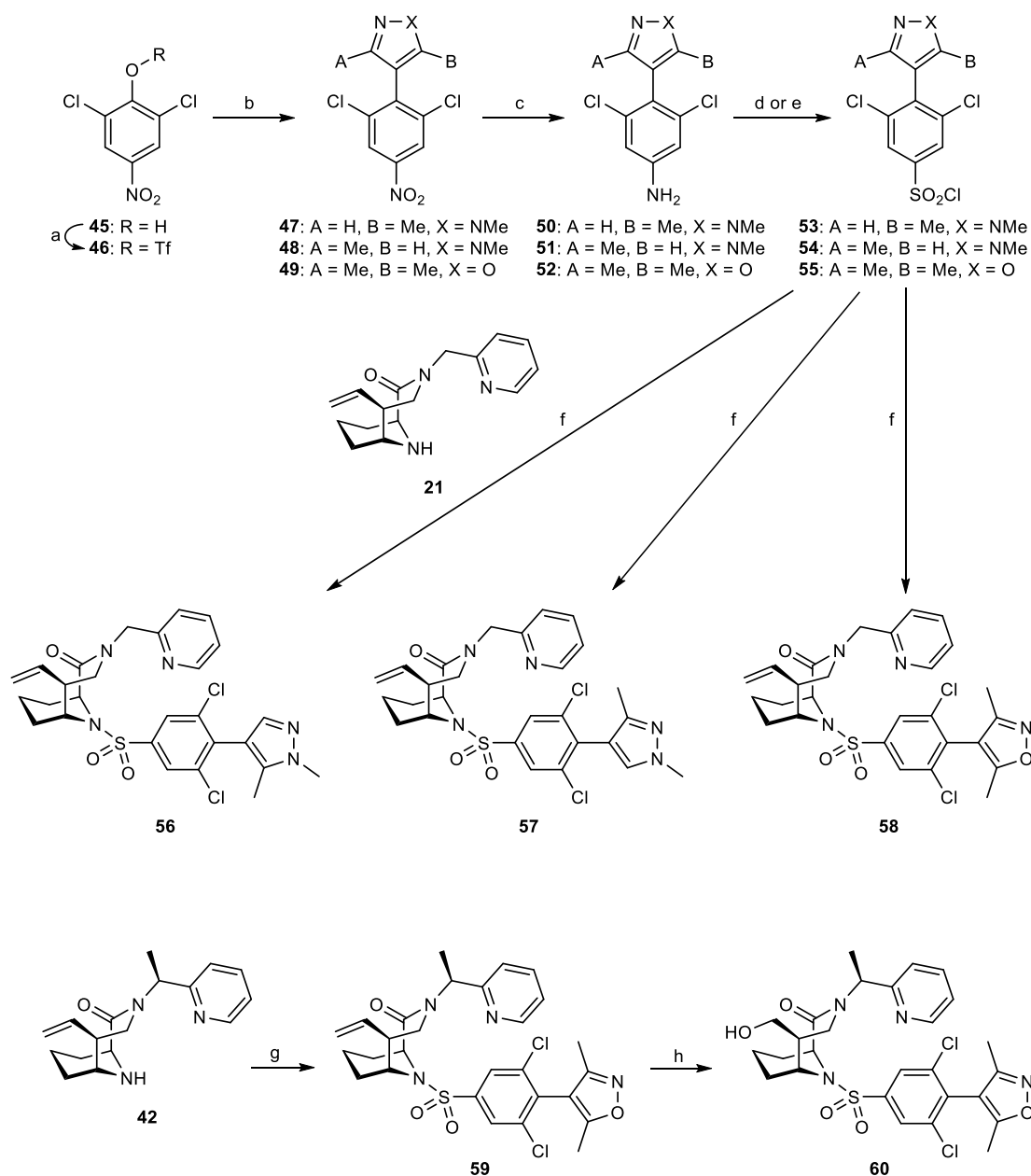
Compound	K_D for FKBP12 in nM	K_D for FKBP12.6 in nM	K_D for FKBP51 in nM	K_D for FKBP52 in nM
Kolos2021-16^(S)-Me	0.72 ^a	-	2.6 ^a	2.2 ^a
40	0.113 ^{*e} ±0.058	0.084 ^{*d} ±0.008	33 ^b ±4	22 ^b ±3
Kolos2021-18^(S)-Me	0.29 ^a	-	2.6 ^a	3.6 ^a
41	0.023 ^{*f} ±0.004	0.014 ^{*d} ±0.002	10 ^c ±1	8.9 ^c ±0.8

The α -methyl group in R1 boosts the binding affinity for FKBP12 by a factor 3.4 and for FKBP51 by a factor 10.9 (**31** to **40**). Additionally converting the vinyl group in R3 to a hydroxymethyl group (**40** to **41**) gives a further boost of a factor 3.8 for FKBP12 and 3.3 for FKBP51. These enhancements are known and described in literature^[90] and result in **41**. Compound **41** binds to FKBP12 with an affinity of 23 pM, representing the strongest FKBP12 ligand known to date. The closest reference compounds of **40** and **41** are the previously published ligands **Kolos2021-16^(S)-Me** and **Kolos2021-18^(S)-Me**, respectively. The reference compounds bear a second meta-chloro atom in R2 instead of the para-pyrazole. The para-pyrazole substituted ligands give a 6-12 fold stronger affinity for FKBP12 and a 4-12 fold weaker affinity for FKBP51 than their respective meta-chloro analogs. This results in a 50-80 fold higher selectivity for FKBP12 over FKBP51 with **40** and **41** compared with **Kolos2021-16^(S)-Me** and **Kolos2021-18^(S)-Me**, respectively.

41 was subjected to a nanoBRETTM assay to test intracellular activity. Ligand **41** showed intracellular FKBP12 binding, with an IC_{50} of 2.3 nM. This value is two orders of magnitude lower than the K_D -value from the HTRF assay. However, this difference might be due to the detection limit of the nanoBRETTM

assay. The cells still produce endogenous FKBP12 and also other FKBP12s that compete with the exogenously expressed FKBP12-NLuc used for detection of ligand binding. The endogenous FKBP12s may act as an intramolecular trap that sequesters low concentrations of ligand and precludes binding for FKBP12-NLuc unless all endogenous FKBP12s are saturated.

For reasons of synthetic simplicity, the **30** series and the just described **30g** analogs had only one chlorine atom in meta-position of the R2 residue. The standard R2 residue however is 3,5-dichlorobenzenesulfonyl, which binds 3.7x stronger to FKBP12 than the related 3-chlorobenzenesulfonyl (see **1** (3,5-dichloro): 2.4 nM vs. **Pomplun2018-15e** (3-chloro): 8.9 nM). To further increase the binding affinity of the **30g** analogs, another series was synthesized with an additional chlorine atom in R2-meta position (Scheme 9). In this series, only the two monomethylated pyrazoles and the isoxazole, representing the dimethylated pyrazoles/isoxazoles, were synthesized.

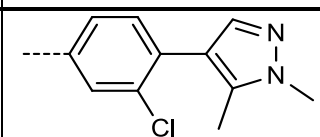
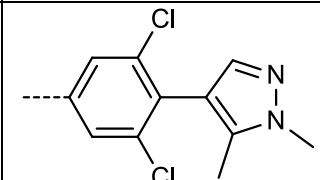
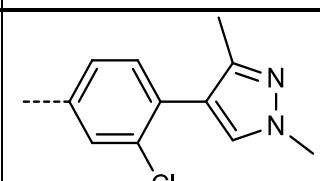
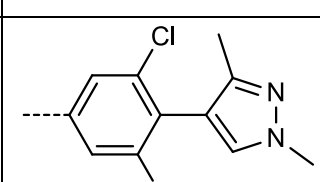


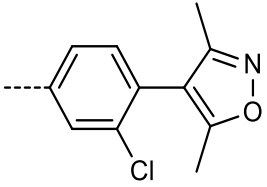
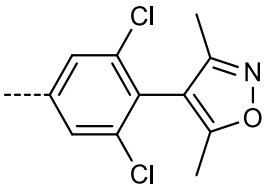
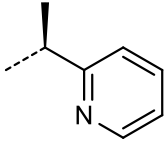
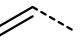
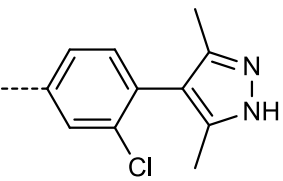
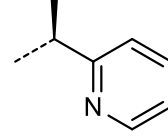
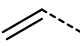
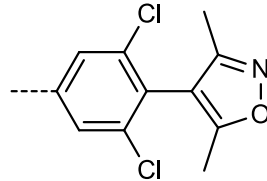
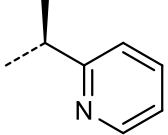
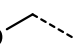
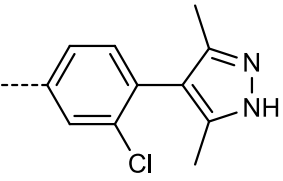
Scheme 9. Reagents and conditions: a) Tf₂O, pyridine, DCM, 0 °C – rt, 18 h, 93 %; b) boronic acid or ester **61**, **62** or **63**, Pd(dppf)Cl₂, K₂CO₃, dioxane/water 20:1, 80 °C, 5-19 h, 39 % **47**, 56 % **48**, 30 % **49**; c) Zn-powder, NH₄Cl, EtOH, reflux, 1-5 h, impure **50**, impure **51**, 94 % **52**; d) NaNO₂, HCl, MeCN/H₂O, 10 min, rt, then SOCl₂/H₂O/CuCl, 0 °C – rt, 1 h, then POCl₃, dry MeCN, 55 °C, 23 h, 21 % **53** over three steps, **54** used in the next reaction without complete purification; e) NaNO₂, HCl, MeCN/H₂O, 10 min, rt, then SOCl₂/H₂O/CuCl, 0 °C – rt, 3 h, 47 % **55**; f) **21**, DIPEA, dry MeCN, rt, 17-21 h, 14 % **56**, 2 % **57** over four steps, 42 % **58**; g) **55**, DIPEA, dry MeCN, rt, 66 h, 16 %; h) 2,6-lutidine, NaIO₄, OsO₄, dioxane/water 3:1, 0 °C – rt, 20 h, then NaBH₄, EtOH, 0 °C – rt, 50 min, 47 % over two steps.

In this series, the sulfonyl chlorides were synthesized as complete building blocks before coupling to the ligand core. 2,6-Dichloro-4-nitrophenol **45** was converted to the respective triflate, which was then subjected to Suzuki reactions with previously used boronic acids or esters **61**, **62** and **63**. The nitro groups of the intermediates **47**, **48** and **49** were reduced to the respective amines, which were in one

case isolated in high yield, and in two cases obtained in impure form but used in the next reaction without further purification. The anilines **50**, **51** and **52** were transformed to sulfonyl chlorides in a Sandmeyer reaction, however the sulfonyl chlorides from **50** and **51** hydrolyzed during their purification to the respective sulfonic acids. These sulfonic acids could be transformed to the sulfonyl chlorides again using POCl₃, and the sulfonyl chloride **53** could be isolated. The sulfonyl chloride **54** was less stable and was therefore directly used in the next reaction with **21**, which then gave **57** in poor yield. Isolated sulfonyl chlorides **53** and **55** were coupled to **21** to give final products **56** and **58**. The isoxazole building block **55** was further coupled to **42** to combine this R2 residue with an optimized R1 residue. After a Lemieux-Johnson oxidation of the R3 vinyl group to an aldehyde and reduction to a hydroxy group, the optimized ligand **60** was obtained. Binding affinities of this new series were determined in FP- and HTRF-assays, performed by Wisely Oki Sugiarto and Thomas Geiger, respectively (Table 8). Some K_D-values for FKBP12.6 are below 1 nM, which is below the detection range of the FP-assay. For these compounds the HTRF-assay should be performed.

Table 8. Binding affinities of the **30g**-analogous 3,5-dichloro variants and respective reference compounds. *K_D-values determined by HTRF assay. ^{a-f}Values taken from the same assay, respectively.

Compound	Structure R2	K _D for FKBP12 in nM	K _D for FKBP12.6 in nM	K _D for FKBP51 in nM	K _D for FKBP52 in nM
36		0.235 ^{*a} ±0.033	0.065 ^{*a} ±0.007	220 ^b ±22	250 ^b ±23
56		0.162 ^{*d} ±0.023	0.2 ^c ±0.1	246 ^c ±31	166 ^c ±17
37		0.209 ^{*a} ±0.011	0.104 ^{*a} ±0.005	230 ^b ±30	190 ^b ±20
57		3.0 ^c ±0.8	3.6 ^c ±0.9	367 ^c ±53	230 ^c ±28

35		0.222^{*a} ± 0.019	0.057^{*a} ± 0.012	$440^b \pm 58$	$470^b \pm 60$
58		$2.5^c \pm 0.3$	$1.5^c \pm 0.4$	$1,750^c$ ± 150	$892^c \pm 81$
40	<p>R1 = </p> <p>R3 = </p> 	0.113^{*e} ± 0.058	0.084^{*f} ± 0.008	$33^g \pm 4$	$22^g \pm 3$
59	<p>R1 = </p> <p>R3 = </p> 	0.107^{*d} ± 0.019	$0.2^c \pm 0.1$	$115^c \pm 14$	$71^c \pm 8$
41	<p>R1 = </p> <p>R3 = </p> 	0.023^{*h} ± 0.004	0.014^{*f} ± 0.002	$10^i \pm 1$	$8.9^i \pm 0.8$

60	<p>R1 = </p> <p>R3 = HO-CH₂-</p>	0.076 ^{*h} ±0.009	0.1 ⁱ ±0.01	29 ⁱ ±26	27 ⁱ ±37
----	---	-------------------------------	------------------------	---------------------	---------------------

The binding affinities of **57** and **58** for FKBP12 are one order of magnitude lower compared to the respective mono-chloro variants (**37** and **35**). Only **56** showed an improved binding compared to its analog **36** (Factor 1.5, 235 pM to 162 pM for FKBP12).

This change might be explained when the biaryl dihedral angle is considered in the cocrystal structure of **31** with FKBP12 (Figure 22A). In this monochloro ligand, the dihedral angle between the benzene and pyrazole ring is 57°, which allows the pyrazole ring to lie on the side chain of Ile90 (highlighted in magenta) and one of its methyl groups to fill the cavity next to Ile90 (see Figure 20A) while the halogen- π -interaction to His87 is intact. The 3,5-dichlorobenzene ring will fix the attached pyrazole or isoxazole in a larger dihedral angle, pushing it towards 90°. [91] This fixed conformation for the compounds **57**, **56** and **58** can be modeled in the cocrystal structure of **31** with FKBP12 (Figure 22B-D).

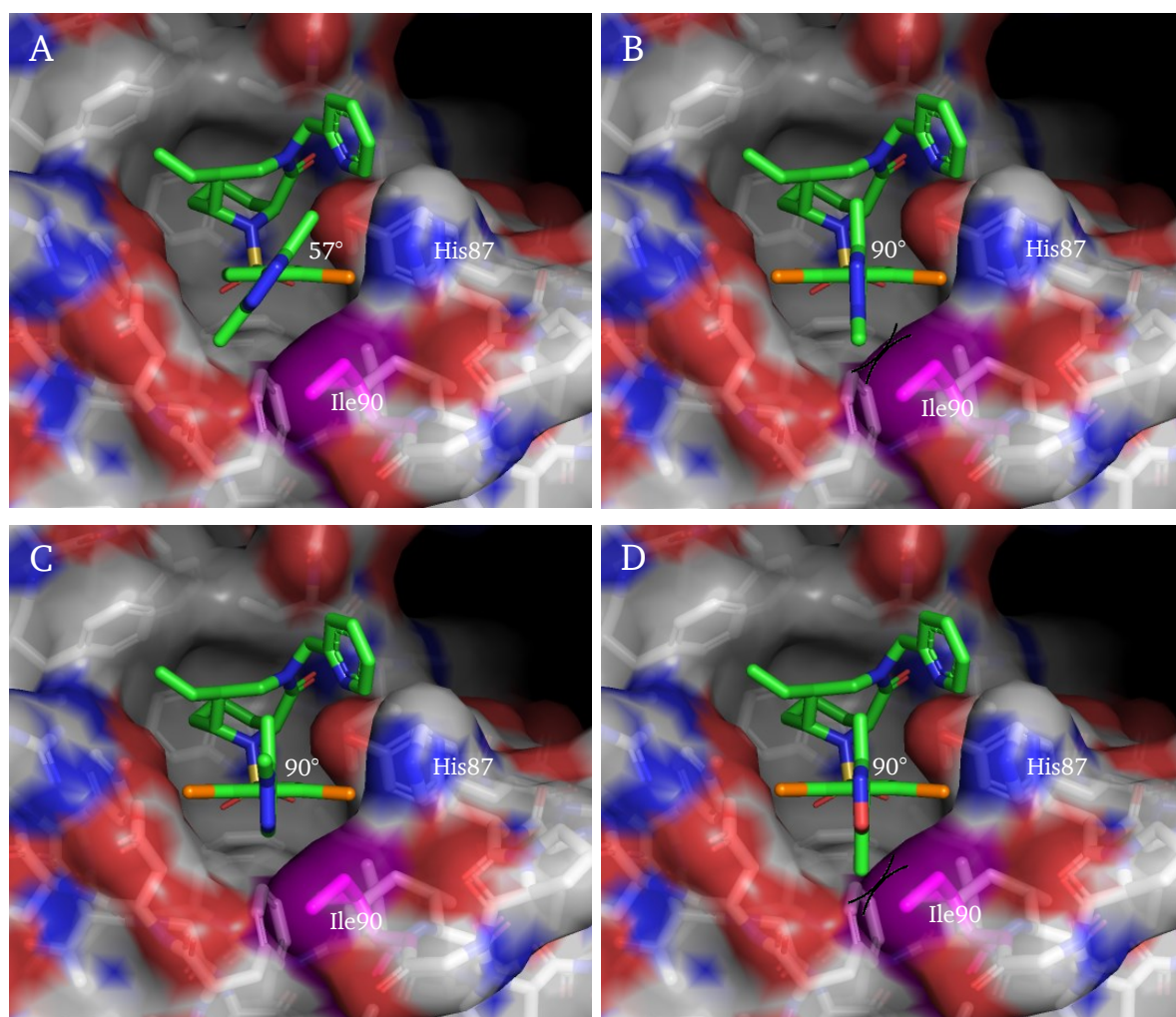
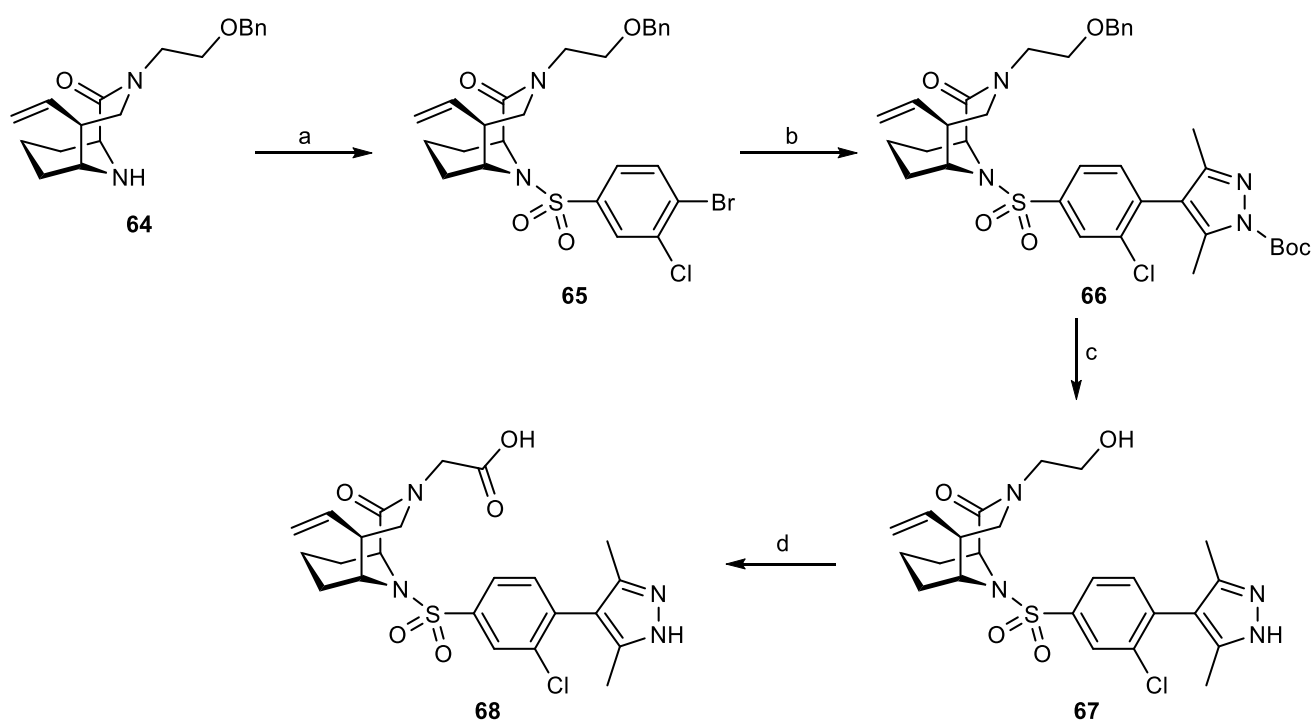


Figure 22. Crystal structure of FKBP12, cocrystallized with **31**. Ile90 highlighted in magenta, ligand's chlorine atoms highlighted in orange. A) Original crystal structure of **31**, B) **57** modeled, C) **56** modeled, D) **58** modeled. Biaryl dihedral angle measured as 57° for **31** (A), modeled as 90° for 3,5-dichloro analogs (B-D).

In these models, one methyl group of **57** (Figure 22B) and **58** (Figure 22D) would clash with the side chain of Ile90, assuming the conformation of the 3,5-dichlorobenzene ring remains unchanged to preserve the halogen- π -interaction with His87. The adaption of the protein to the ligand's conformation seems to be energetically unfavorable, which results in a loss of binding affinity. Compound **56** (Figure 22C) has both pyrazole methyl groups on one side of the ring, allowing it to face both methyl groups away from the protein and thereby avoiding a clash without a conformational change on the protein's side. In this scenario, the additional chlorine atom increases the ligand's binding affinity as planned, although the effect is smaller compared to the reference ligand without a R2-para substituent (Factor 3.7 from **Pomplun2018-15e** to **1**, factor 1.5 from **36** to **56**). In analogy to the monochloro series, the combination with known affinity-boosting R1- and R3-residues increases the binding affinity of these dichloro compounds as well. The introduction of the methyl group in R1 boosts the K_D -value for FKBP12

by a factor 23 (2.5 nM for **58** vs. 107 pM for **59**) and for FKBP51 by a factor 15 (1,750 nM for **58** vs. 115 nM for **59**). This α -methyl effect is much stronger than in the monochloro reference compound **40** (**31** to **40**: factor 3.4 for FKBP12, factor 13 for FKBP51), however the absolute binding affinities of **59** and the monochloro ligand **40** for FKBP12 are almost the same (107 pM vs. 113 pM, respectively). The hydroxy group in R3 of the dichloro compound **60** gives only a slight improvement in binding affinity (**59** to **60**: factor 1.4 for FKBP12, factor 4.0 for FKBP51), whereas the effect of the hydroxy group in R3 is greater for the monochloro ligand **41** (**40** to **41**: factor 3.8 for FKBP12, factor 4.5 for FKBP51). Nevertheless, the α -methyl group in R1 and the hydroxymethyl group in R3 show an improved binding affinity for all FKBP, no matter which R2 residue they were combined with.

The ultra-high affinity R2 residue of **31** was combined with a carboxy group in R1, an often used moiety in 3,10-diazabicyclo[4.3.1]decan-2-one FKBP ligands (Scheme 10).



Scheme 10. Reagents and conditions: a) 4-Bromo-3-chlorobenzenesulfonyl chloride **28**, DIPEA, MeCN, rt, 18 h, 59 %; b) *tert*-butyl 3,5-dimethyl-4-(4,4,5,5-tetramethyl-1,3,2-dioxaborolan-2-yl)-1*H*-pyrazole-1-carboxylate **44**, Pd(OAc)₂, XPhos, THF/water 9:1, reflux, 18 h, 75 %; c) BCl₃-SMe₂, DCM, rt, 3 d, 52 %; d) Jones reagent, acetone, 0 °C – rt, 17 h, 21 %.

The known precursor **64**^[92] was coupled with 4-bromo-3-chlorobenzenesulfonyl chloride **28** to get intermediate **65**. Then, the Boc-protected pyrazole was introduced in a Suzuki reaction to form **66**. Benzyl and Boc protective groups were simultaneously cleaved using BCl₃-SMe₂ and finally product **68** was obtained after a Jones oxidation. The binding affinities of the final product and previous

intermediates were analyzed in a FP assay (Table 9). Compound **31**, bearing the same R2 residue and a pyridine group in R1, is listed as a reference compound.

Table 9. Binding affinities of compound **68** and previous intermediates. *K_D-values determined by HTRF-assay. ^{a-c}Values taken from the same assay, respectively.

Compound	K _D for FKBP12 in nM	K _D for FKBP12.6 in nM	K _D for FKBP51 in nM	K _D for FKBP52 in nM
31	0.381 ^{*a} ±0.028	0.177 ^{*b} ±0.015	360 ^c ±35	201 ^c ±21
66	79 ^c ±17	64 ^c ±8	>30,000 ^c	>30,000 ^c
67	4.9 ^c ±0.4	3.2 ^c ±0.2	2,600 ^c ±840	1,500 ^c ±350
68	5.2 ^c ±0.7	5.5 ^c ±0.5	1,600 ^c ±320	1,500 ^c ±270

The binding affinities of **68** are surprisingly lower than the R1 = CH₂-pyridine variant **31** (5.2 nM (**68**) vs. 0.381 nM (**31**) for FKBP12, 1,600 nM (**68**) vs. 360 nM (**31**) for FKBP51). While the binding affinities for each protein decreased with the R1 = CH₂COOH substituent, the selectivity for FKBP12 and 12.6 over FKBP51 and 52 remains high (270-300x). The reduced intermediate **67** with only a R1 = CH₂CH₂OH group has very similar K_D-values to the carboxylic acid **68** for all four FKBP. Only the benzyl and Boc protected intermediate **66** has a significantly lower binding affinity for FKBP12 and 12.6 (79 and 64 nM, respectively), but is still highly selective over FKBP51 and 52 (>380x).

Compound **68** was analyzed for intracellular activity in a nanoBRET™ assay. Therein, it showed an IC₅₀ of 181 nM for binding intracellular FKBP12-NLuc, which reflects a hindered membrane permeability. This likely results from the highly polar moieties in the molecule. Interestingly, ligand **68** still has a significantly lower intracellular IC₅₀ value than another tested R1 = CH₂COOH ligand, **19** (see Chapter 3.2), by at least one order of magnitude.

3.5. Introducing sulfonimidamides to bicyclic FKBP ligands

Since the rigidification of the 3,10-diazabicyclo[4.3.1]decan-2-one core,^[54] the R2-substituent always consisted of a sulfonamide. In this study, the sulfonamide was systematically exchanged for a sulfenamide, a sulfinamide and a sulfonimidamide with different substituents on the sulfonimidamide.

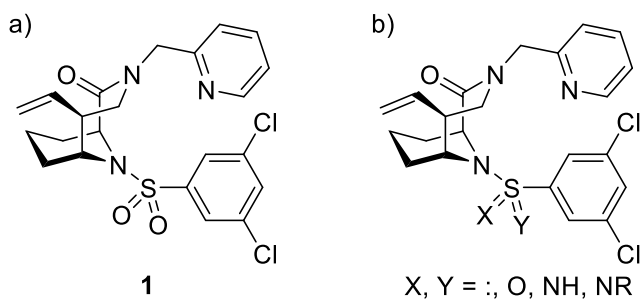


Figure 23. a) Sulfonamide **1** and b) analogous sulfenamide, sulfinamide, sulfonimidamide.

The initial goal of this compound series was the investigation of ligand-protein interactions at a sulfonamide motif. FKBP's present an excellent model system for this kind of study because the sulfonamide of 3,10-diazabicyclo[4.3.1]decan-2-ones forms multiple attractive S=O...HC interactions. To the best of my knowledge, this is the first systematic study to address the significance on single oxygen atoms in sulfonamide-protein interactions. The second part of this ligand series, the sulfonimidamides, allow an analysis of their protein interactions in a direct comparison with their respective sulfonamide analog. Only one cocrystal structure of a protein with a sulfonimidamide ligand is published to date (PDB: 7JTC). The FKBP12 cocrystal structures presented in this study are a valuable addition to the understanding of sulfonimidamides as ligands. Lastly, the alkylation of these novel sulfonimidamide ligands aimed to mimic the binding mode of the FKBP51-selective SAFit2. That selectivity is achieved by the cyclohexyl moiety on the bottom group of the SAFit molecule (Figure 24a, cyclohexyl moiety highlighted in blue).^[46] Replacing the sulfonamide with a sulfonimidamide could offer an attachment point for the selectivity-bearing cyclohexyl group in a similar geometry to SAFit (Figure 24b). This FKBP51-selectivity was not achieved, but the substituted sulfonimidamides suggested a novel FKBP12 binding mode.

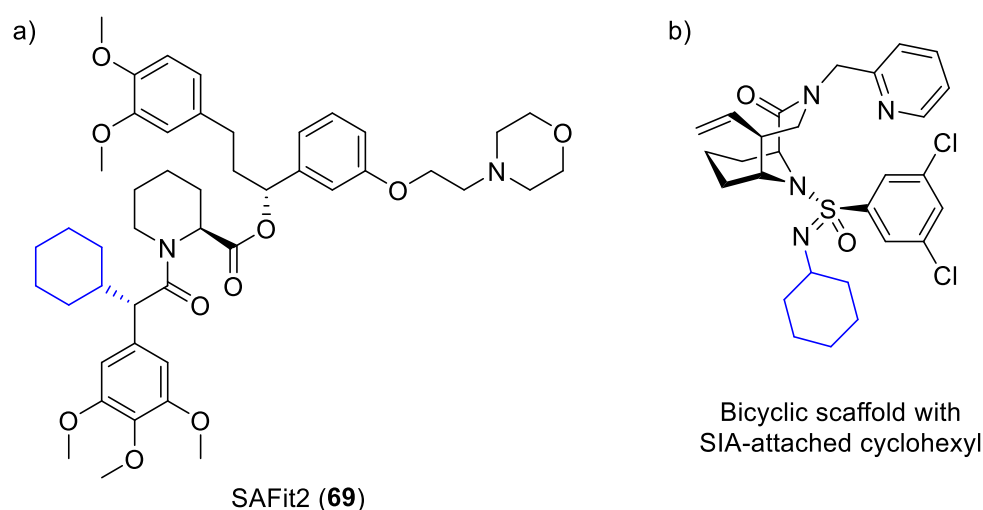
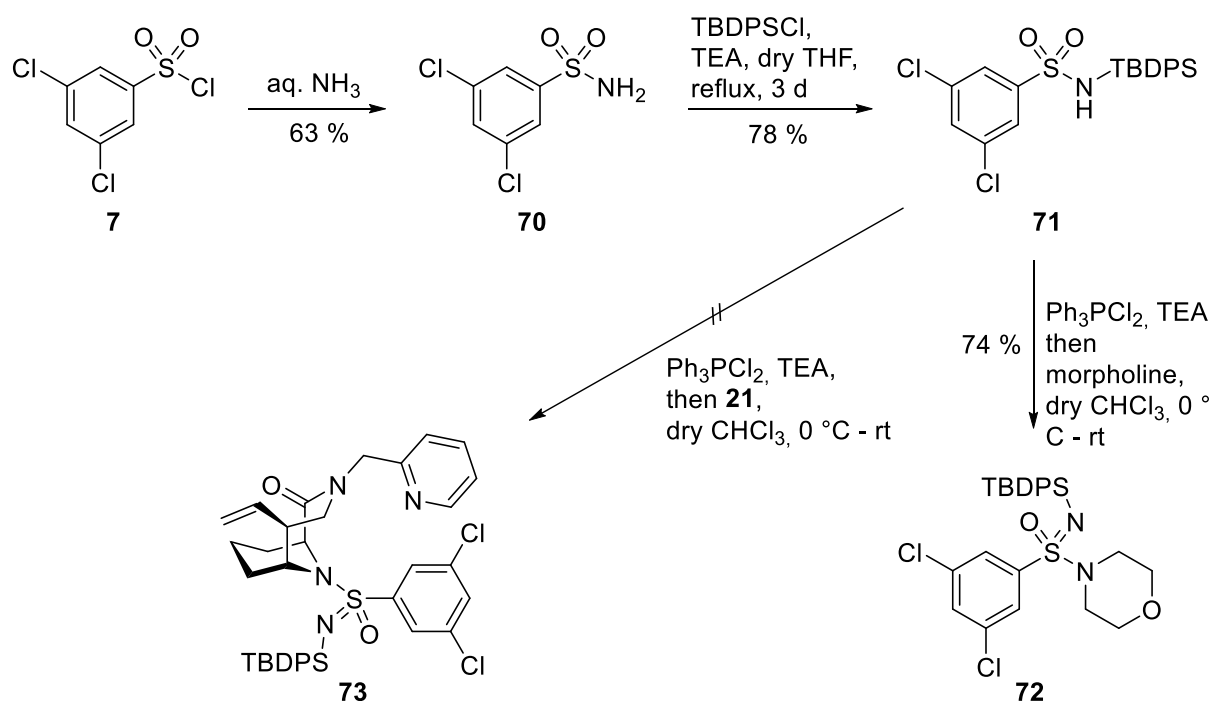


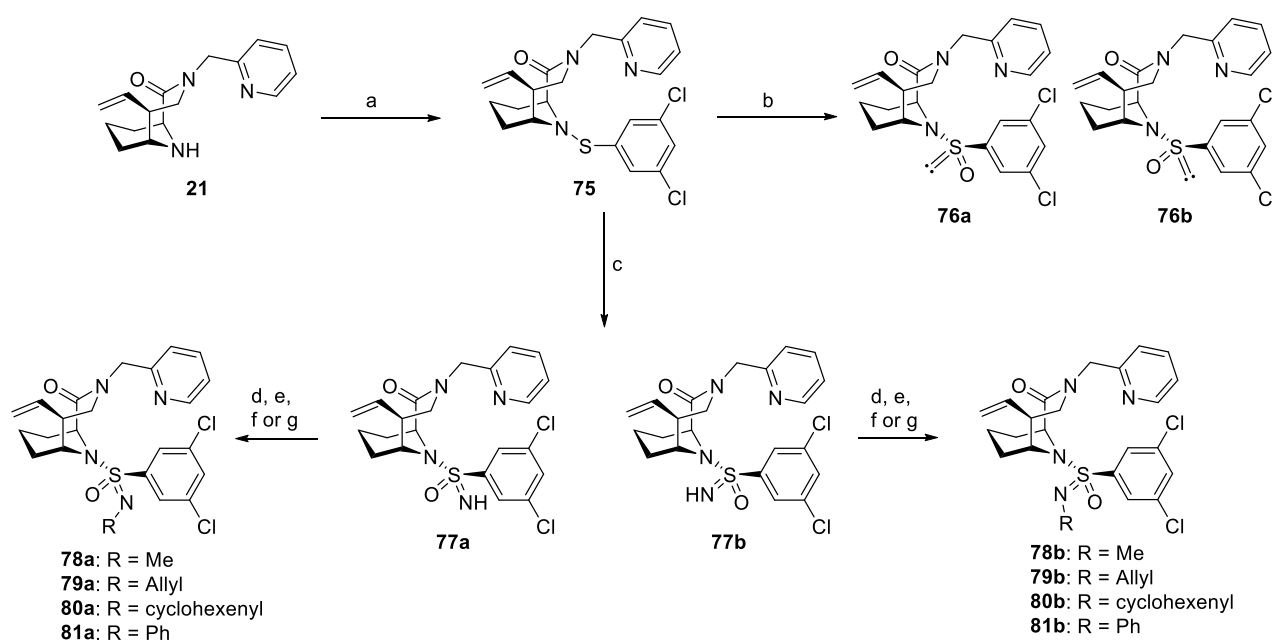
Figure 24. a) Structure of FKBP51-selective SAFit2 (**69**), b) Structure of a bicyclic FKBP-ligand-scaffold with a cyclohexyl attached via a sulfonimidamide.

The rising popularity of sulfonimidamides provided new procedures to form this structural motif in the past decade.^[93] The most straight-forward route would be the formation of a *N*-protected sulfonimidoyl chloride, analogously to the sulfonyl chloride, which can be coupled to an amine and subsequently deprotected. This synthesis plan was followed in the first attempt to create bicyclic sulfonimidamide FKBP-ligands (Scheme 11).



Scheme 11. Synthetic attempt to form bicyclic sulfonimidamide FKBP-ligands.

The formation of a test sulfonimidamide **72** from a TBDPS-protected sulfonamide **71** was successfully performed, following a literature procedure.^[94] Coupling the intermediate sulfonimidoyl chloride to the bicyclic amine **21**, however, yielded no product (**73**). Assuming the protection group was too sterically demanding, an alternative synthetic route was evaluated to form the free sulfonimidamide without any protection group. This was achieved by coupling the bicyclic amine **21** to a sulfonyl chloride, which was freshly prepared from thiol **74** (Scheme 12).



Scheme 12. Reagents and conditions: a) 3,5-dichlorobenzenethiol **74**, HOAc, SO₂Cl₂, -40 °C → rt, then **21**, DIPEA, MeCN, rt, 55 %; b) KF, mCPBA, MeCN/H₂O 5:1, 30 min, 0 °C, then **75**, 5 h, 0 °C, 5 % **76b** and 7 % **76a** (separated diastereomers); c) PIDA, AcONH₄, MeOH, rt, 26 % **77a** and 35 % **77b** (separated diastereomers); d) NaH, MeI, THF, 0 °C → rt, 82 % **78a**, 64 % **78b**; e) NaH, allyl bromide, THF, 0 °C → rt, 100 % **79a**, 81 % **79b**; f) NaH, 3-bromocyclohexene, 0 °C → rt, 66 % **80a**, 85 % **80b**; g) PhB(OH)₂, Cu(OAc)₂, TEA, MeCN, rt, 100 % **81a**, 87 % **81b**.

The activation of thiol **74** was performed with sulfonyl chloride and acetic acid, as described by MARTZEL *et al.*,^[95] and aimed to form the respective sulfonyl chloride and with **21** the respective sulfenamide. Surprisingly, the only product found in this reaction was sulfenamide **75**. The sulfenamide **75** was oxidized to the sulfinamides **76a** and **76b**. To prevent overoxidation, KF/mCPBA was used as oxidizing agent, as described by DATTA *et al.*^[96] However in the synthesis of **76a** and **76b**, the formation of sulfonamide was still observed. The sulfinamides were difficult to separate but were finally obtained in a low yield, with the most part still being a mixture of diastereomers. Oxidative imination of sulfenamide **75** following the approach of ZENZOLA *et al.*^[97] provided sulfonimidamides **77a** and **77b**, which were separable by silica gel column chromatography. The isolated sulfonimidamides were then alkylated with methyl iodide (**78a** and **78b**), allyl bromide (**79a** and **79b**) and 3-bromocyclohexene

(**80a** and **80b**). A Chan-Lam reaction with phenylboronic acid, as described by BATTULA *et al.*,^[98] yielded products **81a** and **81b**. Compounds **80a** and **80b** were synthesized as respective mixtures of cyclohexenyl-C1-epimers, which were not preparatively separated. Analytical HPLC revealed a ratio of 56/44 for the diastereomers in **80b**, but could not show any analytical separation for **80a**. A reduction of the cyclohexenyl double-bond was attempted with Pd/C and H₂, however these conditions not only reduced the cyclohexenyl and C5-vinyl double-bonds, but also reduced the pyridine ring to a piperazine, excluding these compounds from this substance series.

The configuration of the sulfur atom in the sulfinamides **76a** and **76b**, as well as in the free sulfonimidamides **77a** and **77b** was found to be stable but could not be determined via 2D-NMR spectroscopy. NOESY-NMR experiments of the alkylated sulfonimidamides **78a-81b** revealed their respective configurations (exemplarily shown for **78a** and **78b** in Figure 25-27), from which the configuration of **77a** and **77b** could be deduced. A cocrystal structure of **78a** with FKBP12 (Figure 31c, later) confirmed the structure. After determining the configurations of the free sulfonimidamides **77a** and **77b**, the assignment of the sulfinamides **76a** and **76b** was easily available (Figure 28).

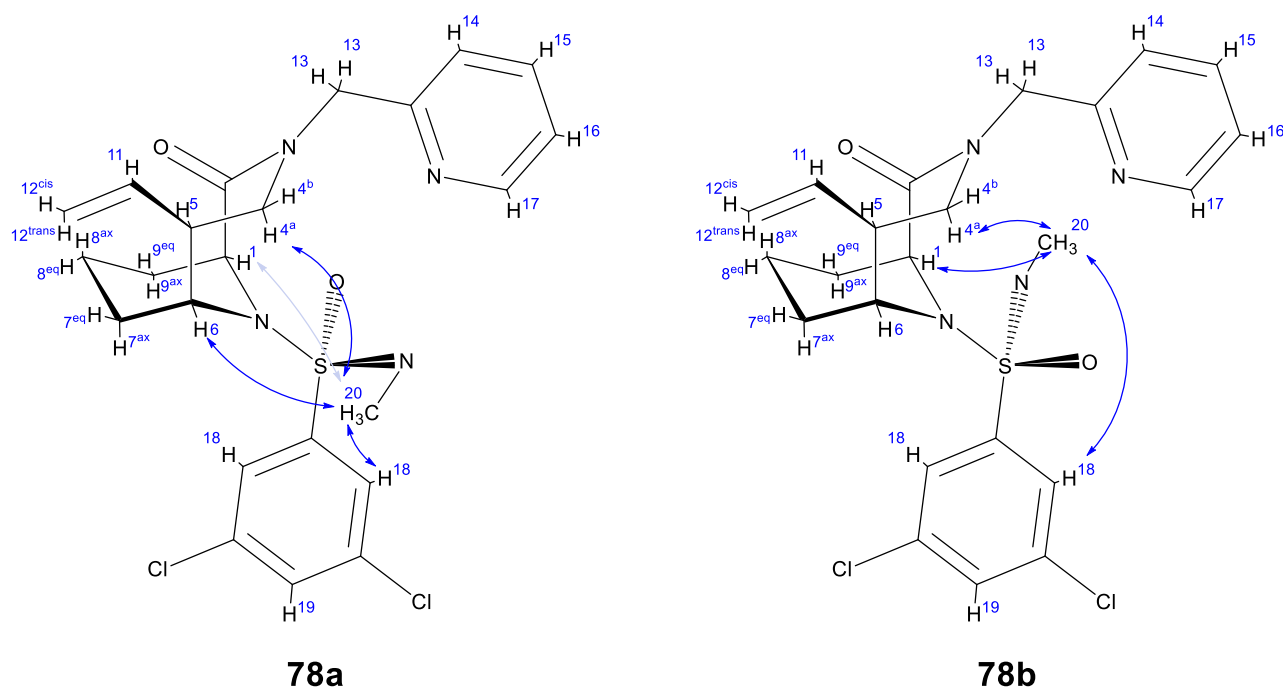


Figure 25. ¹H-¹H coupling of H²⁰ visible in the NOESY-spectra of **78a** and **78b**.

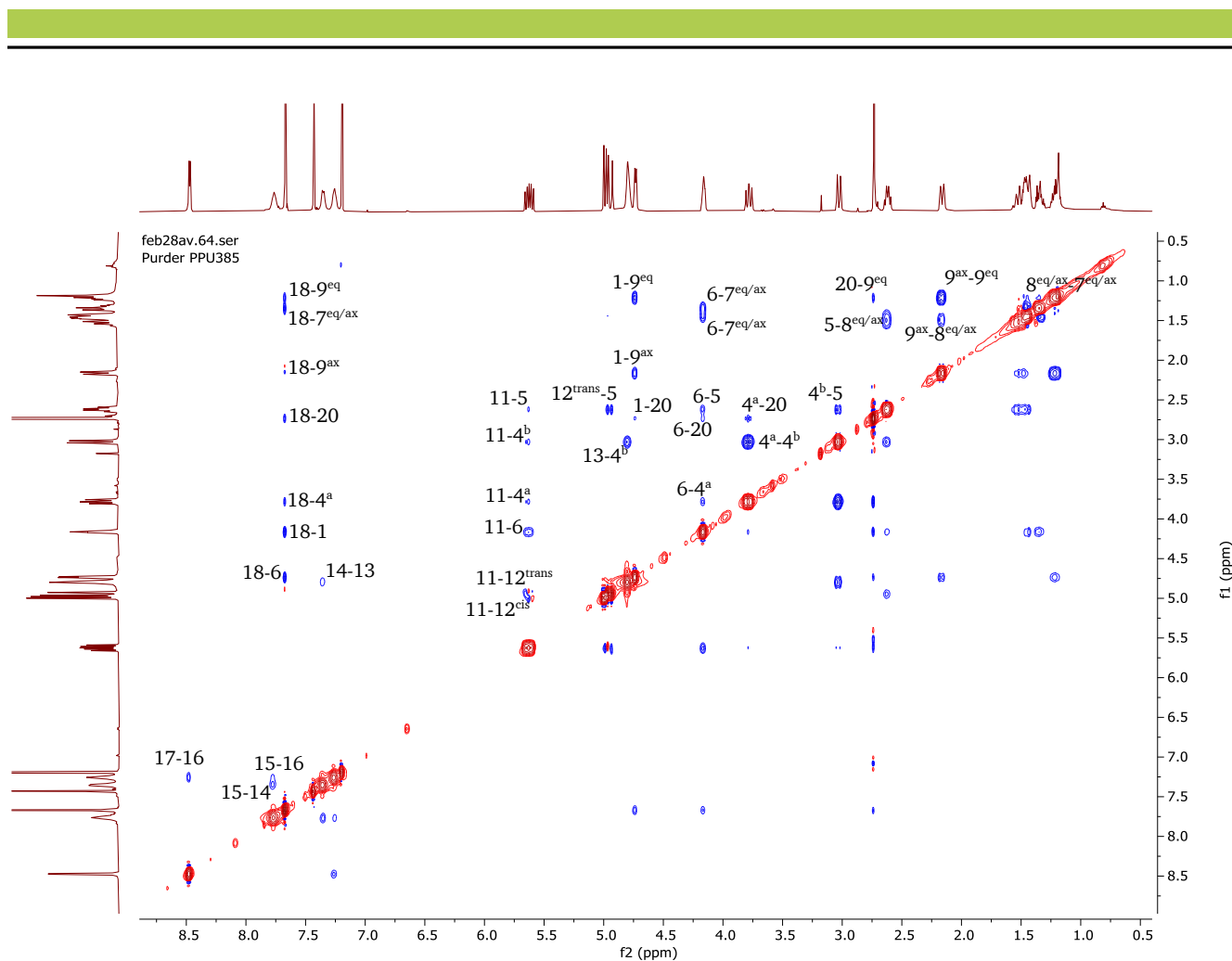


Figure 26. NOESY spectrum of compound **78a**, assignment of ^1H - ^1H -coupling in reference to the compound structure in Figure 25.

In the NMR spectra of **78a** most peaks can be assigned to a specific proton. The two protons H^{13} are chemically different and while they give two distinct signals in other compounds of this class, in **78a** they show only one signal at 4.87 ppm with a relative intensity of 2. Of the six protons at the piperolate methylene groups, only $\text{H}^{9\text{ax}}$ and $\text{H}^{9\text{eq}}$ can be differentiated since $\text{H}^{9\text{ax}}$ is found at a chemical shift of 2.23 ppm, outside the aliphatic bundle (1.2-1.7 ppm). The axial and equatorial protons of H^7 and H^8 overlap and cannot be distinguished in the NOESY spectrum.

Besides the obvious coupling of vicinal protons, the first important spatial coupling is between H^{18} and H^7 , H^9 , H^1 and H^6 . This shows that in solution the phenyl group of the sulfonimidamide is positioned underneath the piperolate core. A weak coupling between H^{18} and $\text{H}^{4\text{a}}$ shows that a conformation where the phenyl group is turned away from the piperolate core is slightly populated as well. The configuration of the sulfonimidamide is revealed by the coupling of H^{20} . A strong signal can be seen between H^{20} and H^{18} , as well as $\text{H}^{4\text{a}}$. The crucial information however is a weak coupling to H^1 and a stronger one to H^6 . This suggests that the coupling of H^{18} to H^6 correlates to the conformation in which the phenyl is

positioned underneath the pipecolate, which makes the H^{18} - H^6 coupling possible only with a *S*-configured sulfur atom.

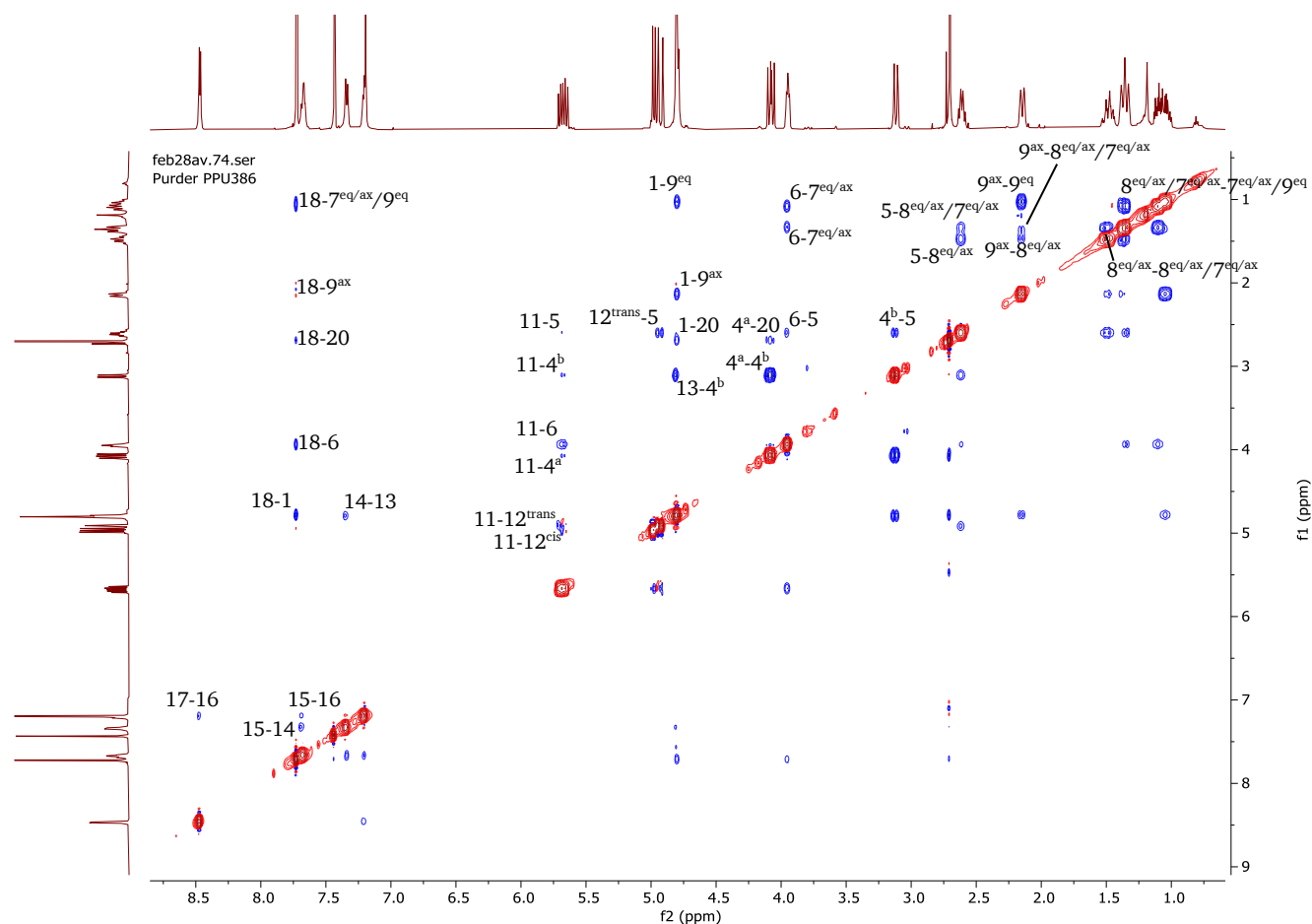


Figure 27. NOESY spectrum of compound **78b**, assignment of 1H - 1H -coupling in reference to the compound structure in Figure 25.

In the NMR spectra of **78b** the two protons H^{13} are again coincidentally isochronic. Furthermore, only C^{9ax} of the six pipecolate methylene groups can be assigned to a single signal.

Most couplings are identical to the NOESY spectrum of **78a**, however in **78b** no coupling between H^{18} and H^{4a} is visible, which means that the phenyl group is positioned underneath the pipecolate core and a configuration in which the phenyl group is turned away from the pipecolate is not detectably populated. H^{20} couples again with H^{18} and H^{4a} , but in contrast to **78a** only a H^{20} - H^1 coupling can be seen and no H^{20} - H^6 coupling. With the phenyl group positioned underneath the pipecolate, a H^{20} - H^1 coupling is possible only with a *R*-configured sulfur atom.

The stereoinformation of alkylated and arylated sulfonimidamides **78a-81b** allows a direct deduction of their respective free sulfonimidamide's stereoconfiguration. The configuration of the sulfonamides **76a** and **76b** could then be determined indirectly. The addition of a nitrene to a sulfonamide proceeds under retention of the configuration at the sulfur atom.^[99] Therefore, sulfonamides **76a** and **76b** were imitated

via a nitrene under conditions known to literature^[97] and their reaction products were each compared with the diastereomerically pure sulfonimidamides **77a** and **77b**, which are separable in a LC-MS analysis. The reaction products were taken directly from the reaction mixtures without purification and were co-injected with the reference sulfonimidamides. To allow an easier evaluation of the experiment, single ion monitoring (SIM) mass spectrometry was performed on LC-MS, analyzing only the mass of the sulfonimidamide product (Figure 28).

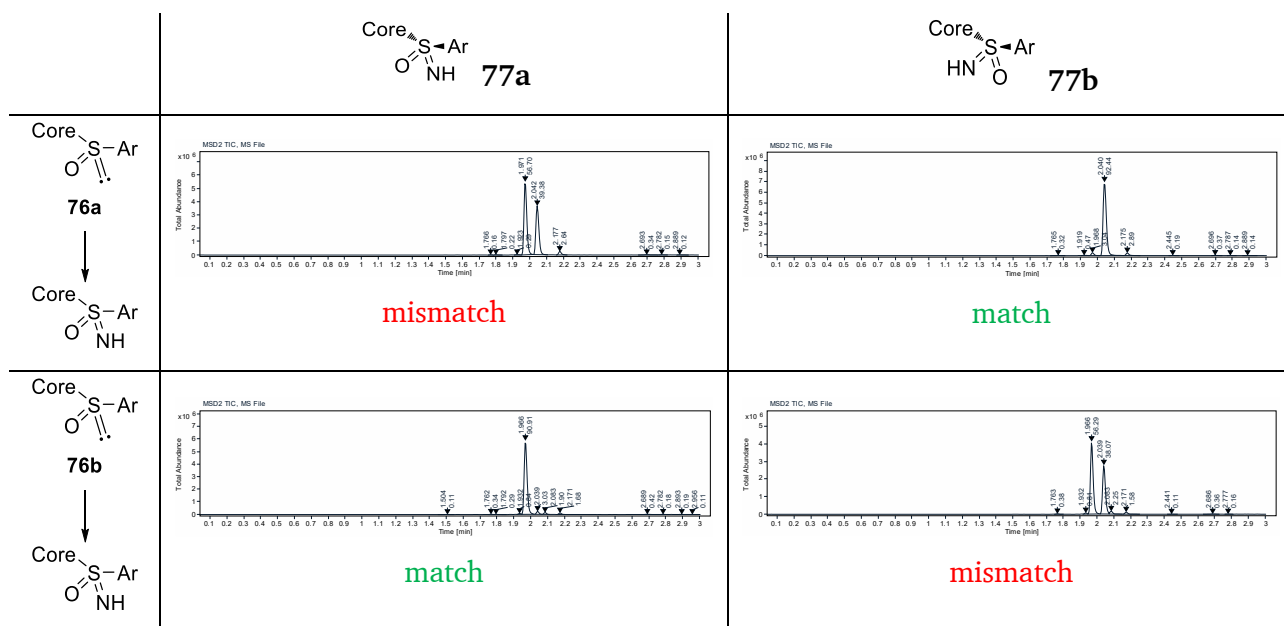


Figure 28. SIM LC-MS analysis of the iminiation reactions of sulfinamides **76a** and **76b**, co-injected with diastereomerically pure sulfonimidamides **77a** and **77b**.

The sulfonimidamide formed from sulfinamide **76a** matches with the reference sulfonimidamide **77b**, and the sulfonimidamide of **76b** matches with **77a**. Under retention of the configuration of the sulfur atom, the sulfinamide **76a** must be in *S*-configuration and **76b** in *R*-configuration (Figure 29).

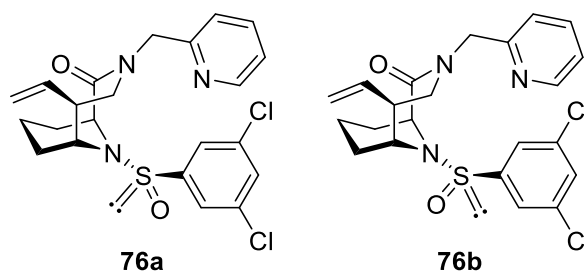


Figure 29. Stereoconfiguration of sulfinamides **76a** and **76b**.

The binding affinities of this series of sulfenamide, sulfinamide and sulfonimidamide FKBP-ligands were measured in a fluorescence polarization assay by Wisely Oki Sugiarto, using sulfonamide **1** as a reference (Table 10).

Table 10. Binding affinities of SIA-FKBP-ligands for FKBP51, 52, 12 and 12.6. Core = (1*S*,5*S*,6*R*)-2-oxo-3-(pyrin-2-ylmethyl)-5-vinyl-3,10-diazabicyclo[4.3.1]decan-10-yl, Ar = 3,5-dichlorophenyl. *Cocrystal structure with FKBP12 solved. ^{a-c}Values taken from the same assay, respectively. ^cValues measured in real triplicates instead of pseudoduplicates.

Compound	Structure	K _D for FKBP51 in nM	K _D for FKBP52 in nM	K _D for FKBP12 in nM	K _D for FKBP12.6 in nM
1*		97 ^a ± 6	92 ^a ± 9	2.6 ^c ± 0.2	6.9 ^a ± 0.6
75		>40,000 ^b	>40,000 ^b	509 ^c ± 152	1,360 ^b ± 520
76a		4,780 ^b ± 900	5,210 ^b ± 1,200	129 ^c ± 19	394 ^b ± 68
76b		2,240 ^b ± 330	3,980 ^b ± 1,260	67 ^c ± 5	211 ^b ± 32
77a		12,600 ^b ± 3,700	20,000 ^b ± 3,000	360 ^c ± 27	857 ^b ± 188
77b*		11,800 ^b ± 3,000	12,000 ^b ± 2,400	283 ^c ± 24	608 ^b ± 128
78a*		>40,000 ^a	>40,000 ^a	1,390 ^c ± 190	3,650 ^a ± 230
78b		>40,000 ^a	>40,000 ^a	1,160 ^c ± 120	4,380 ^a ± 260
79a		>40,000 ^a	>40,000 ^a	1,570 ^c ± 180	7,700 ^a ± 830
79b		>40,000 ^a	>40,000 ^a	912 ^c ± 108	4,580 ^a ± 260

80a		>40,000 ^b	>40,000 ^b	490 ^c ± 57	3,990 ^b ± 870
80b		>40,000 ^b	>40,000 ^b	577 ^c ± 85	4,030 ^b ± 950
81a		>40,000 ^b	>40,000 ^b	658 ^c ± 160	4,380 ^b ± 900
81b		>40,000 ^b	>40,000 ^b	>40,000 ^c	>40,000 ^b

The situations for FKBP51 and FKBP52 look very similar: Sulfonamide **1** binds strongly (97 nM and 92 nM, respectively), the sulfinamides (**76a**, **76b**) and free sulfonimidamides (**77a**, **77b**) still bind weakly (ca. 2-20 μ M) while the sulfenamide **75** and all *N*-substituted sulfonimidamides (**78a-81b**) do not show any binding affinity anymore. Unfortunately, the idea of adding a FKBP51-selectivity inducing moiety to the bicyclic scaffold via a sulfonimidamide handle did not work. Most likely this conformational change in the protein is sensible to the precise geometry of the ligand and these bicyclic ligands do not fit well enough into the transient F67-out binding pocket of FKBP51.

The affinities for FKBP12 and FKBP12.6 are generally higher than for FKBP51 and FKBP52, as usual for 3,10-diazabicyclo[4.3.1]decan-2-one-type FKBP ligands. The strongest binder is again the reference sulfonamide **1** with 2.6 nM and 6.9 nM for FKBP12 and FKBP12.6, respectively, followed by the sulfinamides (**76a**, **76b**) and free sulfonimidamides (**77a**, **77b**) with K_D -values between 67 nM and 360 nM for FKBP12 and between 211 nM and 857 nM for FKBP12.6. The sulfenamide **75** still shows a better binding affinity than most *N*-substituted sulfonimidamides, with 509 nM and 1360 nM, respectively. With the sulfenamide, sulfonamide and both sulfinamides measured, the energetic contribution of each oxygen atom can be calculated from equation (1).^[100]

$$\Delta\Delta G = \Delta G_2 - \Delta G_1 = -RT \ln\left(\frac{c^\circ}{K_{D2}}\right) + RT \ln\left(\frac{c^\circ}{K_{D1}}\right) = RT \ln\left(\frac{K_{D2}}{K_{D1}}\right) \quad (1)$$

$\Delta\Delta G$ is the difference in the molar Gibbs free energies of the binding of two ligands ΔG_1 and ΔG_2 . R is the molar gas constant (8.314 J mol⁻¹ K⁻¹) and T the temperature, which is approximated to be 298 K.

K_{D1} and K_{D2} are the binding affinities of the two ligands. The calculated Gibbs free energies are shown in Figure 30.

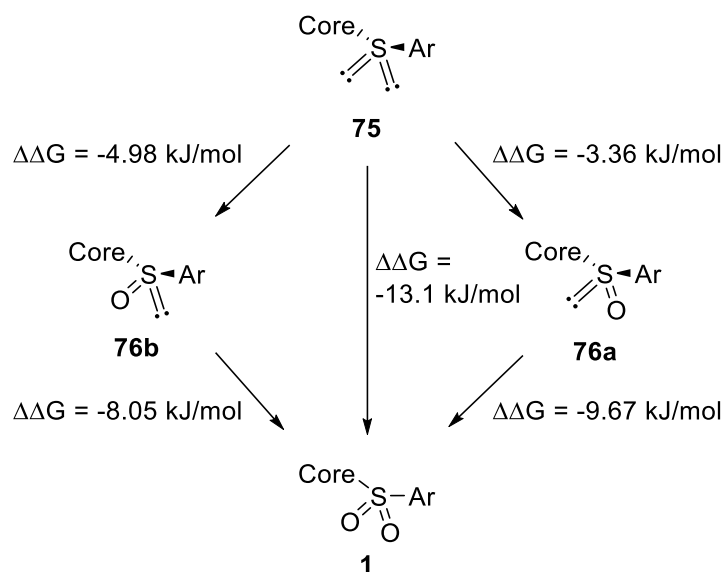


Figure 30. Calculated Gibbs free energy differences between sulfenamide **75**, sulfinamides **76a** and **76b**, and sulfonamide **1**.

The first oxygen atom gives a -3.36 kJ/mol or -4.98 kJ/mol stronger binding, with a slight preference for the *R*-configured sulfinamide. The second oxygen atom further increases binding by -9.67 kJ/mol or -8.05 kJ/mol, resulting in a Gibbs free energy of -13.1 kJ/mol for both oxygen atoms combined. All compounds of this series were attempted to be co-crystallized with FKBP12 by Christian Meyners. Thus far, three co-crystal structures could be solved: **1** at 1.4 Å resolution, **77b** at 1.7 Å resolution and **78a** at 1.7 Å resolution (Figure 31).



Figure 31. Cocystal structures of FKBP12 with compounds A) FK506 (PDB: 1FKJ), B) **1**, C) **77b** and D) **78a**. All protein complexes per asymmetric unit of each cocystal structure are overlaid. Hydrogen bonds are shown in blue, CH...O interactions are shown in yellow. Distances of dashed lines are given in Å.

Figure 31A shows a cocystal structure of FKBP12 with the natural ligand FK506 as reference (PDB: 1FKJ). The ketoamide motif forms a hydrogen bond to Tyr82 and an unusual network of CH...O interactions to Tyr26, Phe36 and Phe99.^[35,36] The cocystal structures of **1**, **77b** and **78a** revealed 2, 4 and 2 proteins in one unit cell, respectively. It becomes clear that the pipecolate core motif is positioned the same way in all structures. In the two complexes per asymmetric unit (Figure 31B), the two ligand molecules of sulfonamide **1** show no significant differences to each other and represent the conserved binding mode of these bicyclic ligands. A detailed analysis of the interaction network of **1** is shown in Figure 32.

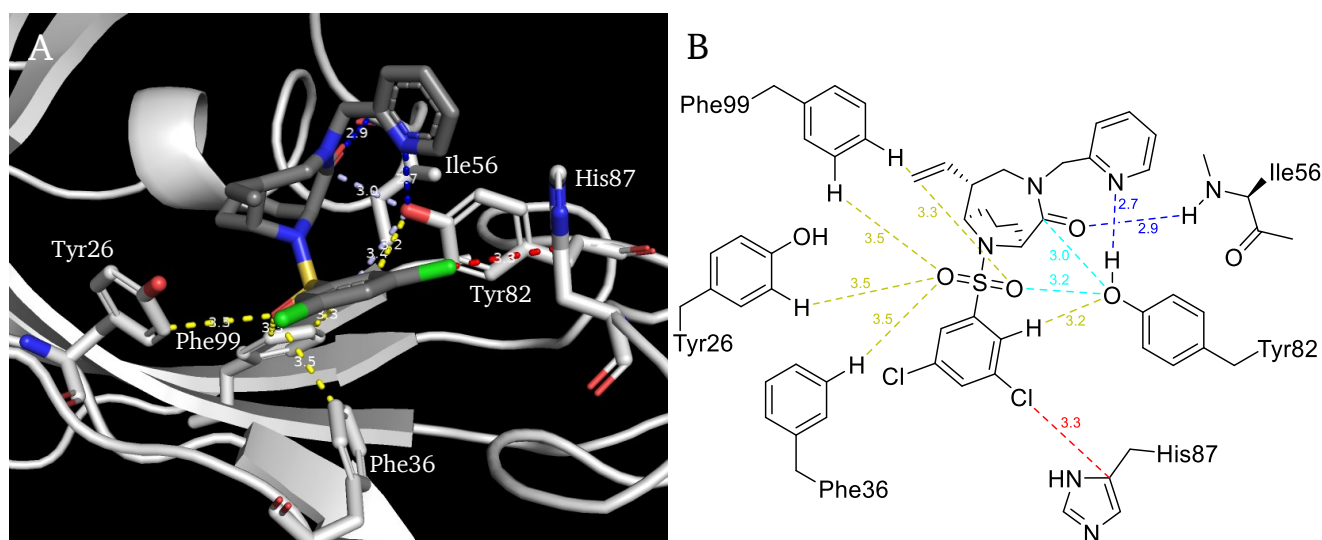


Figure 32. One (Chain A) of the two protein complexes per asymmetric unit of the **1**-FKBP12 cocrystal structure. A) 3D- and B) 2D-Interaction network of **1** with FKBP12. Hydrogen bonds are shown in blue, halogen- π -interactions are shown in red, CH...O interactions are shown in yellow, other polar contacts are shown in light blue. Distances of dashed lines are given in Å.

Suggested strong interactions of **1** and FKBP12 are hydrogen bonds from the ligand's amide carbonyl oxygen to Ile56 and from the ligand's pyridine nitrogen to Tyr82, as well as a halogen- π -interaction to His87. Tyr82 furthermore has polar contacts to the ligand's carbonyl carbon atom and one sulfonamide oxygen, in addition to a CH...O interaction to one ortho hydrogen atom of the ligand's phenyl ring. Similar to the CH...O interactions of the ketone in the FK506 cocrystal structure (see Figure 31A), **1** has CH...O interactions between its sulfonamide oxygen atoms and Tyr26, Phe36 and Phe99.

Compound **77b** crystallized in a structure with four protein complexes per asymmetric unit (Figure 31C). The difference to **1** is the exchange of one sulfonamide O to NH. The sulfonimidamide and the attached dichlorophenyl ring show interesting movements between the different structures. The two structures which are the farthest apart are shown in Figure 33, overlaid with **1** to illustrate their respective differences.

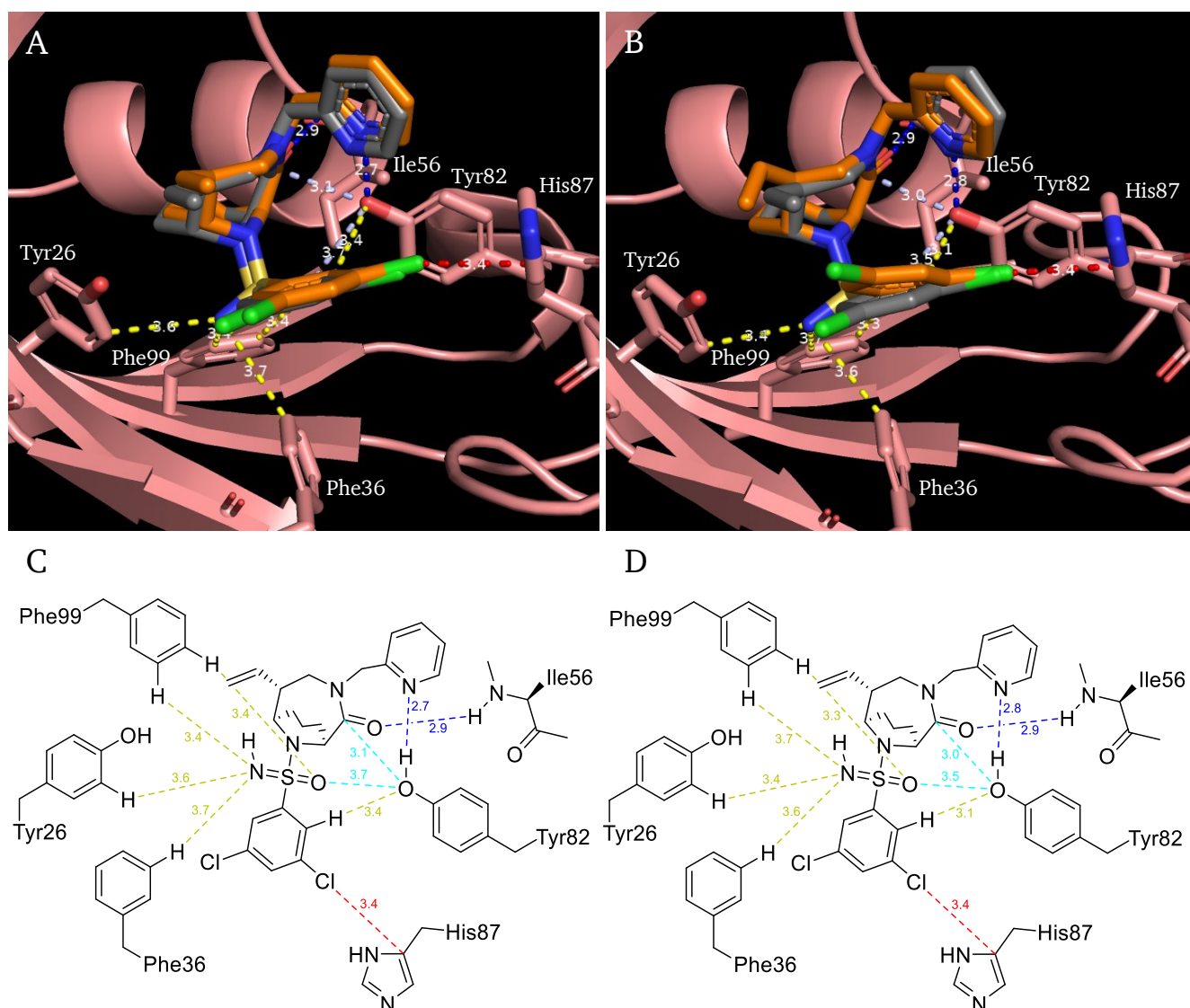


Figure 33. Two (Chain D and C) of the four protein complexes per asymmetric unit of the **77b**-FKBP12 cocrystal structure. A+B) 3D- and C+D) 2D-Interaction network of **77b** with FKBP12, A+B overlaid with **1**. Hydrogen bonds are shown in blue, halogen- π -interactions are shown in red, CH...O interactions are shown in yellow, other polar contacts are shown in light blue. Distances of dashed lines are given in Å.

It can be seen in both structures that the conserved hydrogen bonds to Ile56 and Tyr82 and the halogen- π -interaction to His87 are comparable to sulfonamide **1**. The distances to Tyr26, Phe36 and Phe99 however, are slightly changed compared to **1**. Also, the distances of the sulfonimidamide oxygen to Tyr82 are increased. The lower binding affinity of **77b** compared to the sulfonamide **1** suggests that the imino nitrogen of **77b** creates an energetic penalty when it is placed into the binding site of FKBP12, compared to the sulfonamide of **1**. This likely results from two factors: (i) the imino nitrogen is stronger solvated in solution and therefore needs to invest a higher desolvation energy to bind to FKBP12 and (ii) the nitrogen atom in this position cannot form the same attractive CH...NH interactions as the CH...O

interactions of the sulfonamide. The conserved interactions of the scaffold seem to be strong enough to force the sulfonimidamide into this sulfonamide-like binding mode. **77b** shows a small movement to escape this energetically unfavoured position. However, there is not much flexibility for the molecule. The sulfonimidamide and the attached phenyl ring can move slightly outwards, but it can be seen clearly that one side of the phenyl ring is fixed by its halogen- π -interaction to His87 and allows only the other side to move upwards. Taken together, sulfonimidamide **77b** has little option but to take the conserved binding mode and accept the energetic penalty upon binding. A more detailed analysis of the hydrogen atoms of the free sulfonimidamide would give more information about the putative CH...NH interactions.

Compound **78a** crystallized with two protein complexes per asymmetric unit (Figure 31D). Sulfonimidamide **78a** has the substituted nitrogen on the other side compared to **77b** and in addition has a methyl substitution on that nitrogen atom. The consequences of this O to NMe exchange from **1** can be explained in Figure 34.

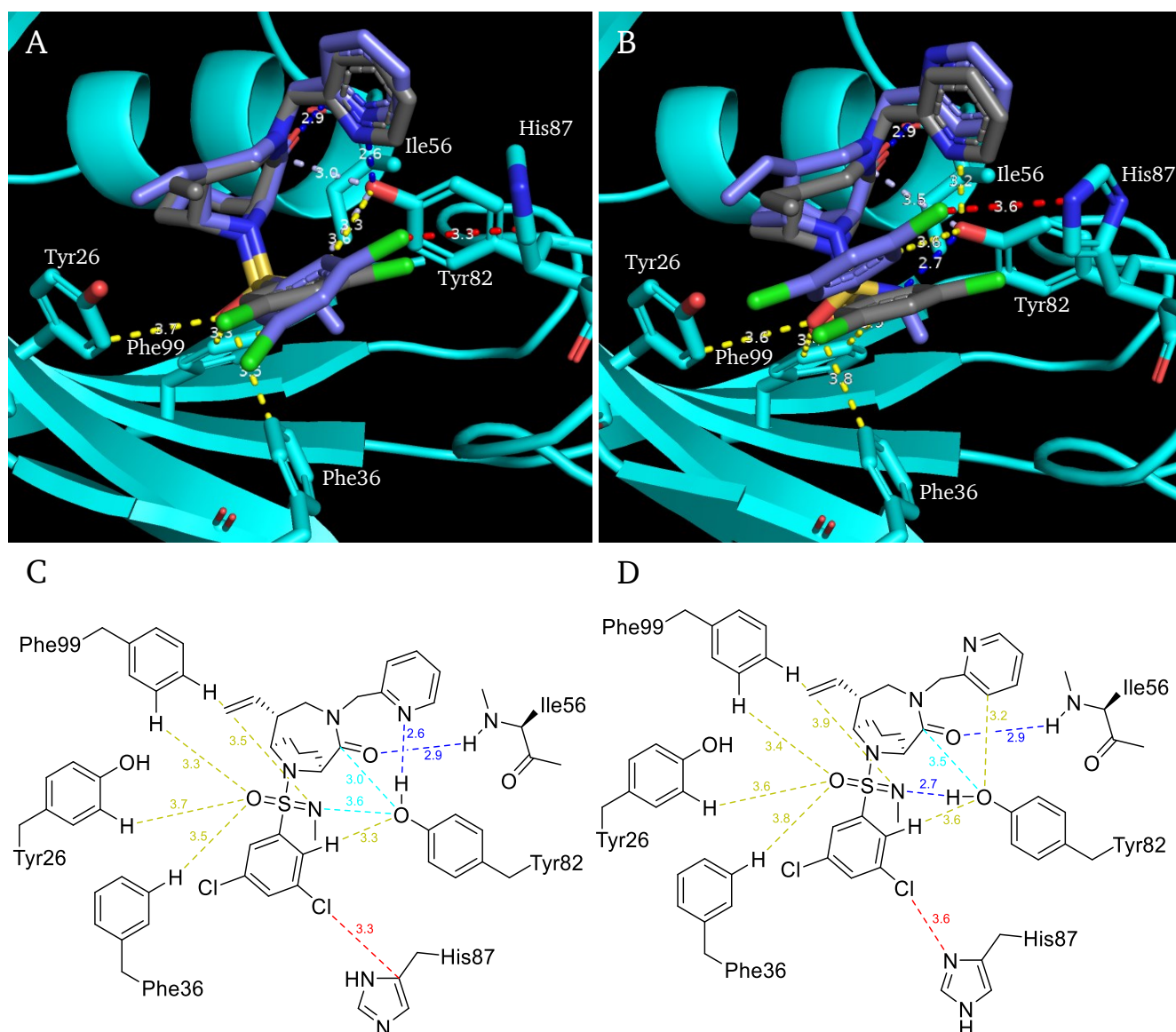


Figure 34. Both (Chain B and A) of the two protein complexes per asymmetric unit of the **78a**-FKBP12 cocrystal structure. A+B) 3D- and C+D) 2D-Interaction network of **78a** with FKBP12, A+B overlaid with **1**. Hydrogen bonds are shown in blue, halogen- π -interactions are shown in red, CH...O interactions are shown in yellow, other polar contacts are shown in light blue. Distances of dashed lines are given in Å.

The binding mode of **78a** shown in Figure 34A and C is very similar to that of **1**. All previously mentioned interactions are still present. The only noteworthy effect of the methylated sulfonimidamide is a twist of the dichlorophenyl ring of the ligand. This twist is likely necessary to make space for the newly introduced methyl group. In this position, similarly to **77b**, the sulfonimidamide is forced to take its energetically unfavoured place by the strong conserved interactions of the bicyclic scaffold. Figure 34B and D shows an interesting new binding mode of sulfonimidamide **78a**. The hydrogen bond to Ile56 and the CH...O interactions of the sulfonimidamide oxygen seem intact. The sulfonimidamide nitrogen atom,

however, is close enough to Tyr82 to form a hydrogen bond. This newly formed hydrogen bond disrupts the polar contact of Tyr82 to the ligand's carbonyl carbon atom and the hydrogen bond to the pyridine nitrogen atom. The pyridine ring is likely rotated by 180° and only forms a CH...O interaction to Tyr82, at best. This change in the interaction network around Tyr82 causes the ligand's phenyl ring to move upwards, compared to sulfonamide **1**. This move increases the distance of the halogen- π -interaction to His87. In this situation, the sulfonimidamide can form an attractive interaction inside the binding pocket. However, this new hydrogen bond can only be formed at the cost of multiple other attractive interactions, causing again an energetic penalty and decreased binding affinity.

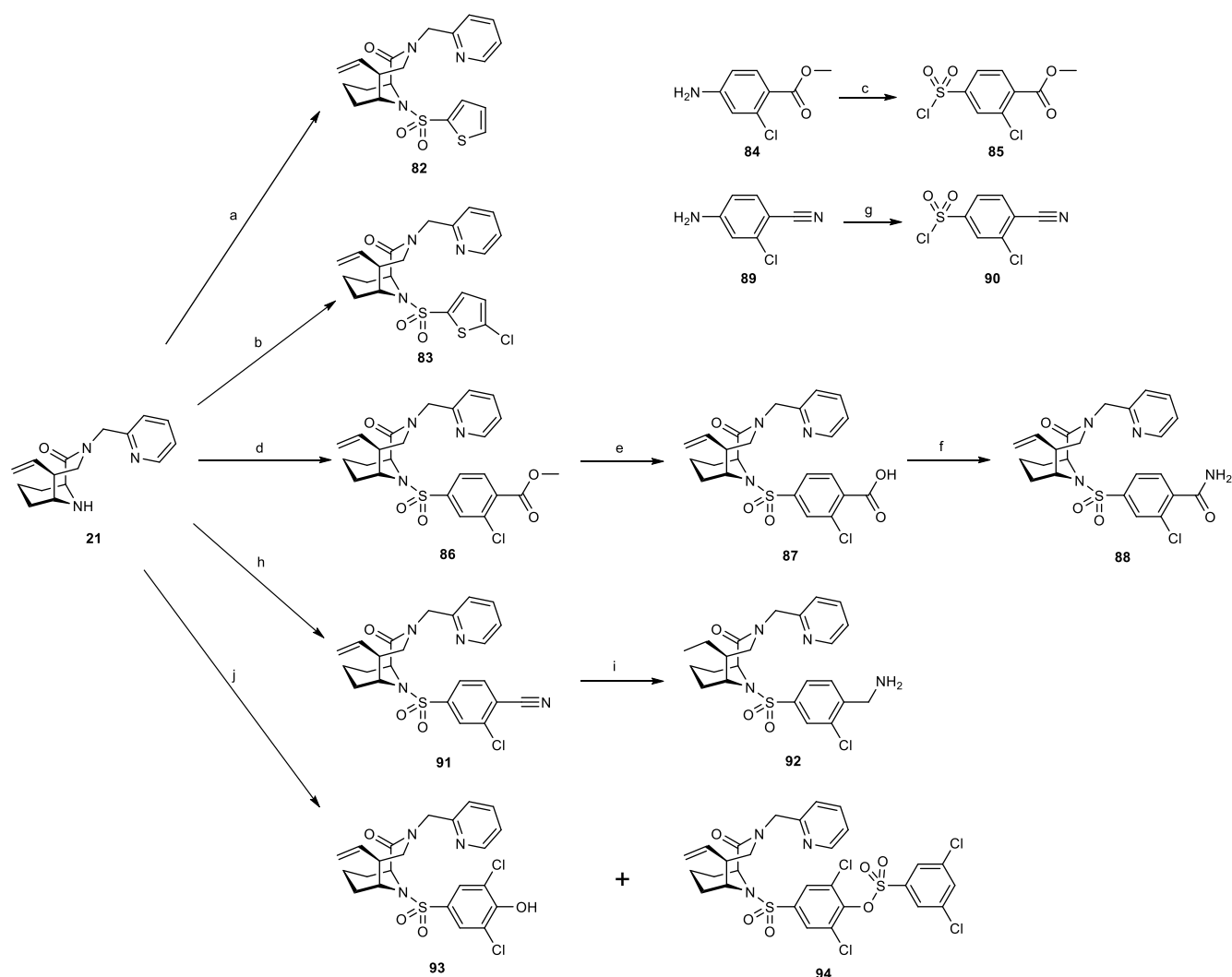
Interestingly, the two binding modes of **78a** were observed clearly distinguishable from each other and no intermediary form was observed.

This study is – to my knowledge – the first example for molecular interactions that the sulfonimidamide motif can form with a protein's binding pocket.

Comparing the binding affinities of the alkylated sulfonimidamides for FKBP12, an interesting trend is revealed: Smaller substituents like methyl (**78a** and **78b**) and allyl (**79a** and **79b**) show a decreasing affinity with a bulkier substituent, as one would expect since the *N*-substituent would reach into the protein surface and clash if the binding mode of the complex remains the same. Also, the *R*-configured phenyl-substituted sulfonimidamide **81b** loses all binding affinity for FKBP12 and FKBP12.6. However for the other three compounds with just as bulky substituents, e.g. cyclohexenyl and phenyl in **80a**, **80b** and **81a**, the binding affinity increases again. This suggests either of two possibilities: (i) the compounds **80a**, **80b** and **81a** bind FKBP12 in a mode completely different than all other 3,10-diazabicyclo[4.3.1]decan-2-one ligands, so their substituents do not clash with the protein, or (ii) the protein adapts its conformation and makes space for the bulky substituents, revealing a novel transient binding pocket. In the latter case, methyl and allyl substituents might not be big enough to efficiently stabilize this transient pocket in FKBP12.

3.6. Miscellaneous FKBP ligands

To further explore the chemical space in the R2 position of 3,10-diazabicyclo[4.3.1]decan-2-ones, a small series with different sulfonamides was synthesized (Scheme 13) and tested for their binding affinities for FKBP12, 12.6, 51 and 52 in a fluorescence polarization assay (Table 11).

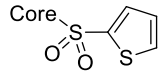
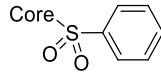
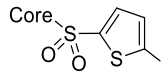
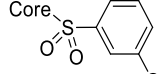
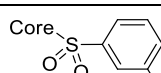
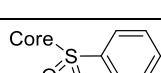
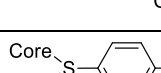


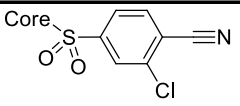
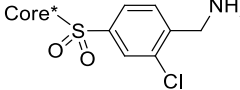
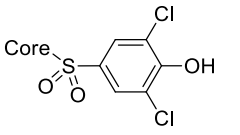
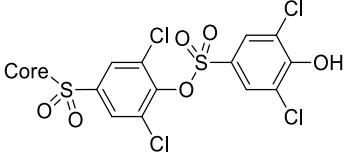
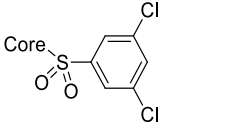
Scheme 13. Reagents and conditions: a) Thiophene-2-sulfonyl chloride **95**, DIPEA, dry MeCN, rt, 17 h, 46 %; b) 5-Chlorothiophene-2-sulfonyl chloride **96**, DIPEA, dry MeCN, rt, 17 h, 41 %; c) NaNO₂, HCl, MeCN, rt, 10 min, then SO₂/HCl/CuCl₂, 0 °C – rt, 3 h, 48 %; d) **85**, DIPEA, dry MeCN, rt, 17 h, 63 %; e) LiOH, THF/H₂O (1:1), rt, 2 h, quant.; f) CDI, aq. NH₃, THF, rt, 15 h, 56 %; g) NaNO₂, HCl, MeCN, rt, 10 min, then SO₂/HCl/CuCl₂, 0 °C – rt, 3 h, 21 %; h) **90**, DIPEA, dry MeCN, rt, 17 h, 53 %; i) CoCl₂, NaBH₄, dry MeOH, 0 °C – rt, 4 h, 31 %; j) 3,5-Dichloro-4-hydroxybenzene-1-sulfonyl chloride **97**, DIPEA, dry MeCN, rt, 18 h, 12% **93**, 31 % **94**.

The bicyclic precursor **21** was coupled with different sulfonyl chlorides to expand the scope of different R2 substitution patterns. Thiophenesulfonyl chlorides **95** and **96** were commercially available and yielded the corresponding sulfonamides **82** and **83** in acceptable yields. Sulfonyl chlorides **85** and **90** were synthesized in a Sandmeyer reaction from the respective anilines. The corresponding sulfonamides **86** and **91** were isolated in yields around 60 %, which is typical for the coupling of **21** with aromatic sulfonyl chlorides. Methyl ester **86** was hydrolysed to afford the free carboxylic acid **87** in quantitative yield, which was then converted to the amide **88**. Nitrile **91** was reduced to the primary amine **92** using CoCl_2 and NaBH_4 , which expectedly reduced the vinyl group at C5 to an ethyl group as well. The coupling of **21** with commercially available 3,5-dichloro-4-hydroxybenzenesulfonyl chloride **97** yielded the desired **93** in a poor yield, and the twice coupled side product **94** as the main product. Binding affinities of all newly synthesized FKBP ligands were measured by Wisely Oki Sugiarto and are shown in Table 11. Compound **1** was used as a reference compound in the same assay. Additionally, reference compounds **Pomplun2018-15b** and **Pomplun2018-15e** are listed with binding affinities from literature.^[57]

Table 11. Binding affinities of miscellaneous bicycles **82-94** for FKBP12, 12.6, 51 and 52. Core* = ethyl group in R3 instead of vinyl group.

^a Values taken from POMPLUN *et al.*^[57] ^{b-c} Values taken from the same assay, respectively.

Compound	Structure	K_D vs. FKBP51 in nM	K_D vs. FKBP52 in nM	K_D vs. FKBP12 in nM	K_D vs. FKBP12.6 in nM
82		1,000 ^b ±130	1,860 ^b ±250	85 ^b ±6	120 ^b ±22
Pomplun2018-15b		1480 ^a ±120	1450 ^a ±300	35 ^a ±1	33 ^a ±4
83		341 ^b ±55	726 ^b ±69	22 ^b ±3	21 ^b ±3
Pomplun2018-15e		298 ^a ±51	344 ^a ±28	8.9 ^a ±1.1	6.1 ^a ±1.1
86		163 ^b ±20	248 ^b ±26	3.9 ^b ±0.5	5.1 ^b ±1.7
87		341 ^b ±36	1,110 ^b ±130	184 ^b ±24	119 ^b ±47
88		326 ^b ±29	523 ^b ±60	23 ^b ±2	14 ^b ±2

91		137 ^b ± 15	187 ^b ± 20	3.3 ^b ± 0.3	4.0 ^b ± 1.2
92		1,500 ^c ± 170	1,200 ^c ± 340	27 ^c ± 4	25 ^c ± 3
93		225 ^c ± 38	331 ^c ± 114	95 ^c ± 30	188 ^c ± 68
94		158 ^c ± 28	123 ^c ± 19	6.2 ^c ± 1.8	5.0 ^c ± 1.2
1		86 ^c ± 6	63 ^c ± 13	1.9 ^c ± 0.4	4.0 ^c ± 0.3

Thiophenes are often considered bioisosters of benzene rings.^[101] Comparison of thiophene **82** with benzene **Pomplun2018-15b** and 5-chlorothiophene **83** with 3-chlorobenzene **Pomplun2018-15e** shows that the binding affinities of thiophenes and benzenes are very similar for FKBP51 and 52. Comparing their affinities for FKBP12 and 12.6, however, the benzenes bind 2-3x stronger than the corresponding thiophenes. In the binding sites of FKBP12 and 12.6 the small differences between thiophene and benzene seem to make a significant difference. Considering these thiophenes (**82** and **83**) it also becomes clear that the chloro atom increases the binding affinity by a factor 2-3 for FKBP51 and 52 and by 4-6 for FKBP12 and 12.6. This effect is comparable to the benzene pair **Pomplun2018-15b** and **Pomplun2018-15e**.

Compound **86** with a methyl ester in para position of R2 shows a strong binding affinity for FKBP12 and 12.6 (3.9 and 5.1 nM) and medium affinity for FKBP51 and 52 (163 and 248 nM), which makes it a slightly stronger ligand than the para-unsubstituted **Pomplun2018-15e**. Changing the ester to the free carboxylic acid in **87** decreases the binding affinity for FKBP12 and 12.6 drastically (184 and 119 nM, factor 47 and 23), the affinity for FKBP51 and 52 on the other hand is only slightly decreased (341 and 1,110 nM, factor 2 and 4). The corresponding amide **88** shows again a stronger binding affinity for FKBP12 and 12.6 (23 and 14 nM, 8 and 9x stronger than **87**) and a similar affinity for FKBP51 and 52 (326 and 523 nM, 1 and 2x stronger than **87**). This structure-activity relationship might be better understood when the differences in the proteins around the compound's R2 residue are considered. For this purpose, the binding pose of **1** with FKBP12 and of **Pomplun2018-16h** with FKBP51Fk1(PDB: 5OBK) were modeled in PyMol to display a carboxylic acid instead of a hydrogen atom in the R2-para position (Figure 35).

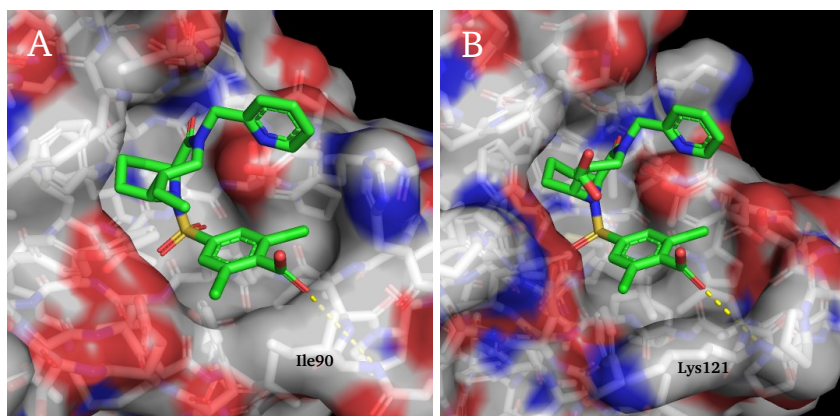


Figure 35. A) R2-para carboxylic acid modelled into the cocrystal structure of **1** and FKBP12; B) R2-para carboxylic acid modelled into the cocrystal structure of **Pomplun2018-16h** and FKBP51Fk1 (PDB: 5OBK). Distances of the carboxylic acid to the Ile90 (A) and Lys121 (B) backbone nitrogen are indicated as yellow dotted lines.

In these models, the binding site around the ligand's R2-para position shows more space available for FKBP51Fk1 than for FKBP12. However, the observation that both the amide and methyl ester bind significantly stronger than the carboxylic acid suggests that the reason behind these affinities is rather electronic than steric. The only electronic difference in the two protein's surfaces that comes into question is the backbone amide of Lys121 in FKBP51Fk1 and Ile90 in FKBP12. While the backbone amide of Lys121 in FKBP51Fk1 is 3.8 Å away from the carboxylic acid in this model, the backbone amide of Ile90 in FKBP12 is at a 5.3 Å distance to the carboxylic acid. Therefore, a polar interaction at the ligand's R2-para position might be easier formed in FKBP51 than FKBP12.

The nitrile **91** shows a slightly higher affinity for all four FKBP's compared to the R2-para unsubstituted **Pomplun2018-15e** (factor 1.5-2.7). The primary amine **92** on the other hand has a ca. 6-11x lower affinity than nitrile **91** for all four FKBP's. This loss of activity most likely results from the amine in R2 since the ethyl group in R3 displays a binding affinity similar to the vinyl group.^[57]

In contrast to the other ligands from this series, the para-hydroxy group in **93** was introduced with the 3,5-dichloro scaffold instead of the 3-chloro scaffold and will therefore be compared to compound **1**. The para-hydroxy group decreases the binding affinity for FKBP51 and 52 by a factor 3 and 5, and for FKBP12 and 12.6 by a striking factor 50 and 47. This again shows that FKBP12 is much more sensitive to the polarity in the R2-para position than FKBP51. The double sulfonylated **94** can rescue the binding affinity for all four FKBP's again to a factor 1.3-3.3 lower affinity than the R2-para unsubstituted **1**. However, the R2-C4 position in **94** seems highly activated for a nucleophilic attack, estimated between a tosyl and nosyl substitution, which makes its chemical stability and usability in a biochemical or biological context questionable.

3.7. 3,10-Diazabicyclo[4.3.1]decan-2-ones as Mip ligands

In a large screening effort, the internal FKBP-ligand library of the Hausch research group was tested for binding to the FKBP-like macrophage infectivity potentiators from *Legionella pneumophila*, *Trypanosoma cruzi* and *Burkholderia pseudomallei*. In the case of LpMip, only the PPIase domain was used, which contains the FKBP-like active site. The proteins were provided by Ute Hellmich from the Friedrich Schiller University Jena. The binding affinity was measured in analogy to the human FKBP in a competitive fluorescence polarization assay with the same fluorescent tracer and was performed by Wisely Oki Sugiarto. The Hausch library contained over 1,000 compounds at the time of the screening, which is why a one-point pre-screening was performed to quickly exclude non-binders. The initial screening was performed at a compound concentration of 10 μ M and the compounds were ranked according to their normalized residual tracer binding. Then, the cut-off was made at 45 % residual tracer binding for TcMip, which left 162 compounds of which K_D values were determined from dose-response curves against all three Mips (Table 12 and Figure 36).

Table 12. K_D values for newly synthesised bicyclic FKBP ligands for LpMip, TcMip, BpMip and FKBP12, sorted by affinity for each protein. **1** highlighted in blue as reference. *No binding was observed at 10 μ M, no dose-response curves were measured. ** K_D value determined in a HTRF assay. ^{a-p}Values taken from the same assay, respectively.

Compound	K_D for LpMip in nM	Compound	K_D for TcMip in nM	Compound	K_D for BpMip in nM	Compound	K_D for FKBP12 in nM
41	7.9 ^a \pm 1.5	19	10 ^b \pm 2	19	0.2 ^b \pm 0.08	41	0.02 ^{**h} \pm 0.004
19	12 ^b \pm 2	20	14 ^c \pm 2	41	0.4 ^a \pm 0.1	40	0.1 ^{**i} \pm 0.06
40	16 ^c \pm 1	41	16 ^a \pm 3	40	1.1 ^c \pm 0.1	39	0.1 ^{**j} \pm 0.002
20	44 ^c \pm 3	18	21 ^c \pm 4	18	2.3 ^c \pm 0.2	32	0.1 ^{**j} \pm 0.03
8	99 ^b \pm 27	8	24 ^b \pm 1	20	2.9 ^c \pm 0.3	17	1.1 ^k \pm 0.2

32	108 ^b ±42	40	32 ^c ±3	39	2.9 ^b ±0.5	34	1.3 ^l ±0.02
18	123 ^c ±15	39	49 ^b ±3	8	5.6 ^b ±0.7	19	1.7 ^m ±0.2
68	184 ^c ±57	17	66 ^f ±3	17	6.5 ^g ±0.4	33	2.0 ^l ±0.2
17	196 ^e ±33	32	84 ^b ±7	32	10 ^b ±2	1	2.4 ⁿ ±0.3
67	364 ^c ±73	38	121 ^b ±21	68	11 ^c ±1	20	2.7 ^o ±0.3
39	372 ^b ±184	1	188 ^d ±40	34	16 ^b ±2	18	3.1 ^l ±0.4
38	483 ^b ±888	68	194 ^c ±52	1	17 ^d ±2	8	3.3 ^m ±0.4
34	766 ^b ±393	34	211 ^b ±15	67	26 ^c ±2	67	4.9 ^o ±0.4
33	1,300 ^b ±740	67	260 ^c ±50	33	37 ^b ±6	68	5.2 ^o ±0.7
1	1,600 ^d ±310	33	430 ^b ±30	38	69 ^b ±14	38	21 ^l ±2
2	>10,000 _e	24	>10,000 _f	2	3,030 ^g ±1,510	23	363 ^p ±27
22	n.b.*	2	>30,000 _f	22	n.b.*	2	658 ⁿ ±39
23	n.b.*	22	>30,000 _f	23	n.b.*	24	988 ^p ±114

24	n.b.*	23	>30,000 _f	24	n.b.*	22	1,120 ^P ±59
----	-------	----	----------------------	----	-------	----	---------------------------

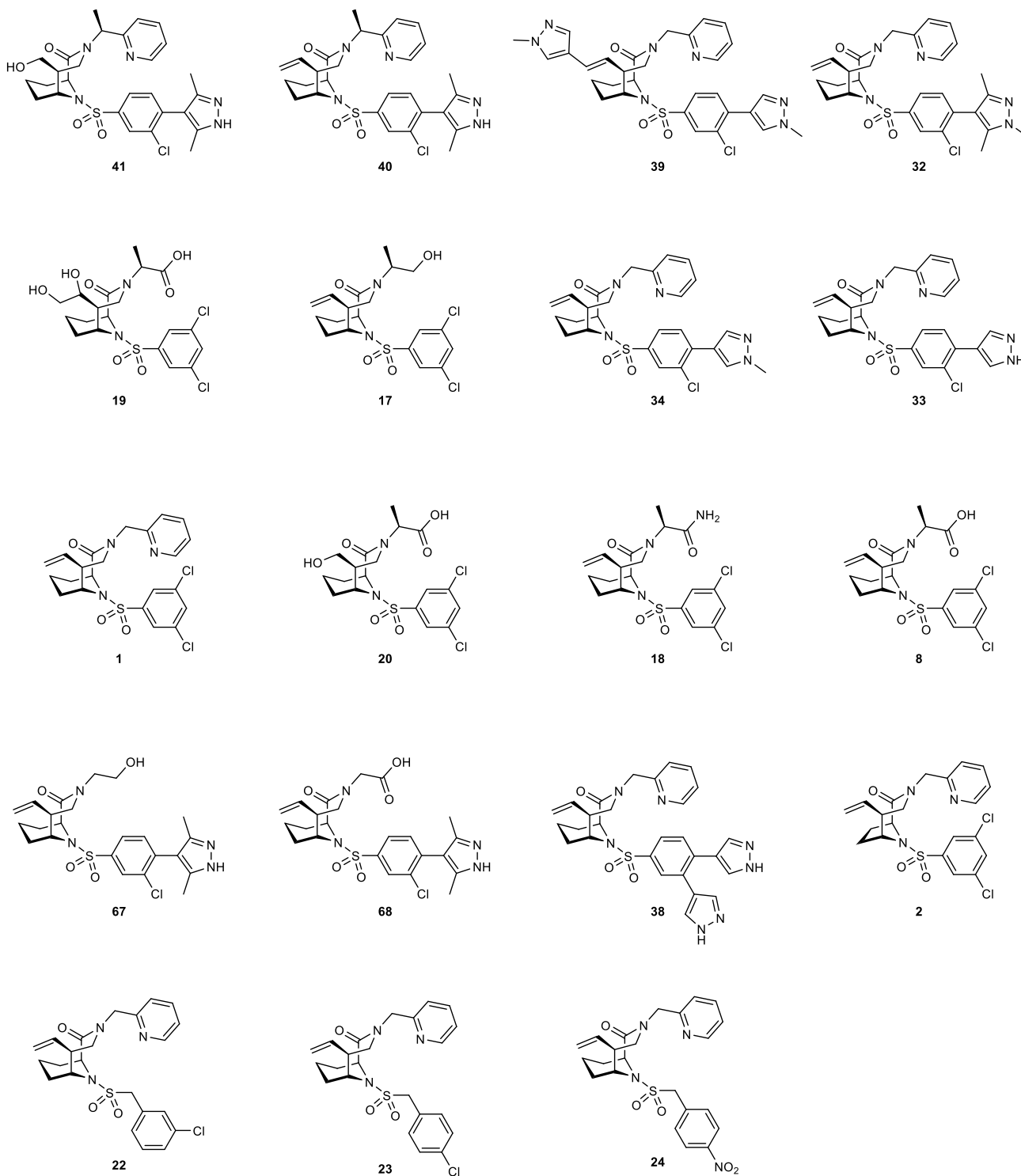


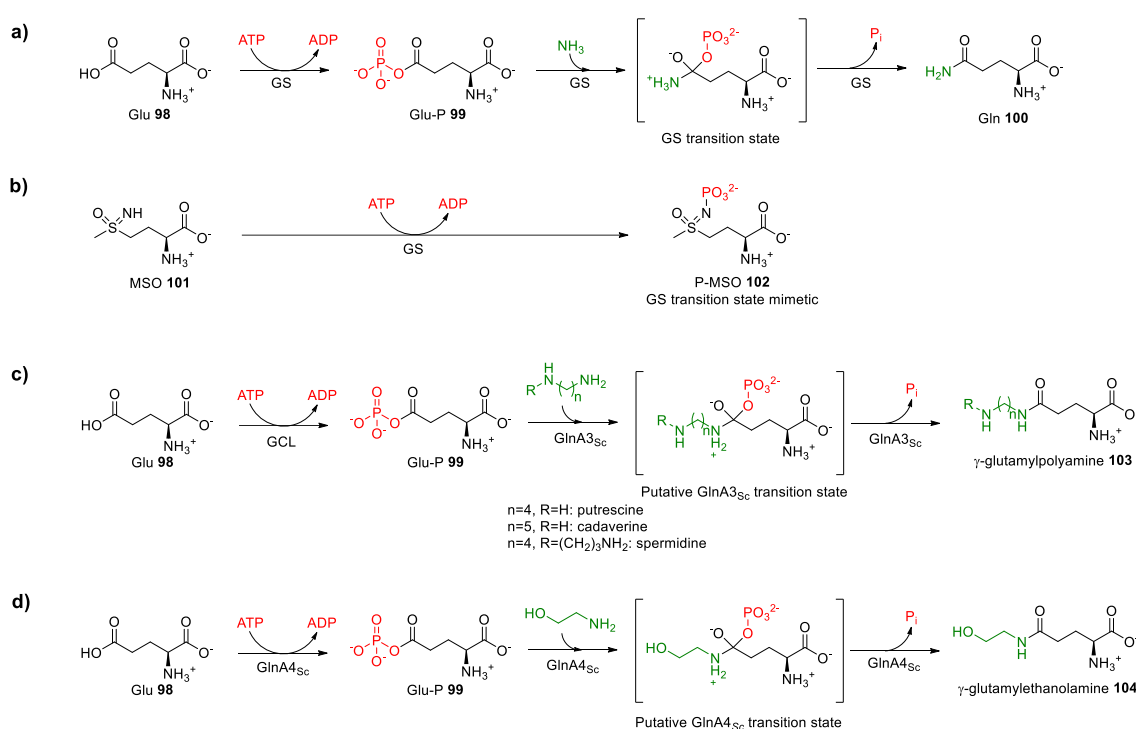
Figure 36. Structures of FKBP ligands with binding affinities measured for LpMip, TcMip and BpMip.

Compound **2** was included as a negative control and in fact it showed, if any, only a very low binding affinity towards these three Mips. Benzylsulfonamides **22**, **23** and **24** were included since their design was inspired by other Mip-ligands (see Chapter 3.3). However, combining the benzyl sulfonamide with the 3,10-diazabicyclo[4.3.1]decan-2-one scaffold did not yield any useful Mip ligands. Similar to their drastically decreased FKBP12 binding affinities, **22**, **23** and **24** have Mip binding affinities above their aqueous solubility. Comparing the other compounds, a general trend among the binding affinities for the four proteins becomes clear. The mean K_D -values for the 14 ligands which show binding affinity increase from FKBP12 (3.3 nM) to BpMip (14 nM) to TcMip (109 nM) to LpMip (290 nM). The same trend was observed when all compounds from the large Mip screening were taken into consideration. Compound **41**, which was optimized for FKBP12 binding, is among the strongest binders also for the Mips. A significant difference between the human and bacterial proteins are the relative affinities for carboxylic acids or amides in the R1 position. For FKBP12, the highest-ranking compounds contain a pyridine group in R1, while those with carboxylic acids or amides are listed lower. For all three Mips, there is no general preference for a pyridine group in R1 observed, with **19** (R1 = CH((S)-Me)COOH) even leading the ranking for TcMip and BpMip. Among the listed compounds are **34**, **33** and **32**, which all bear a pyrazole motif in the R2-para position. These compounds present the same trend for the Mips that was earlier described for FKBP12, as the 3,5-dimethylation of the pyrazole motif gives a greater boost in binding affinity than the N-methylation.

For three of these compounds, further studies with LpMip were performed by Safa Karagöz from the Technical University Braunschweig. **1**, **19** and **2** were tested for their growth inhibition against *Legionella pneumophila* in a Minimal Inhibitory Concentration (MIC) assay. Assays against *Burkholderia* or *Trypanosoma* were not available at the time and will be conducted later. **1** inhibited *Legionella pneumophila* proliferation with an EC_{50} of 28 μ M, while **19** and **2** showed no growth inhibition at concentrations up to 100 μ M. To exclude an unspecific effect, cytotoxicity was measured with A549 cells (adenocarcinomic human alveolar basal epithelial cells) and THP-1 cells (human monocytic cell line derived from acute monocytic leukemia). None of the three compounds showed a significant cytotoxicity up to 100 μ M against A549, and only **1** showed a cytotoxic effect against THP-1 at 100 μ M. In an intracellular replication assay of *Legionella pneumophila*-infected human lung tissue explants, again only **1** showed an inhibitory effect while the data for **19** and **2** were the same as without an inhibitor. These results show that LpMip ligands can be used as antibacterial agents against *Legionella pneumophila*. Compound **2** has no biological effect, which supports an FKBP-related mechanism since its *in vitro* binding of LpMip is non-measurably low. Compound **19** binds isolated LpMip strongly. However, due to its low membrane permeability it cannot bind to intracellular FKBP/Mips. This strongly suggests that the relevant inhibitory effect takes place inside the bacterial cells.

3.8. MSO-derivatives as GlnA3- and GlnA4-inhibitors

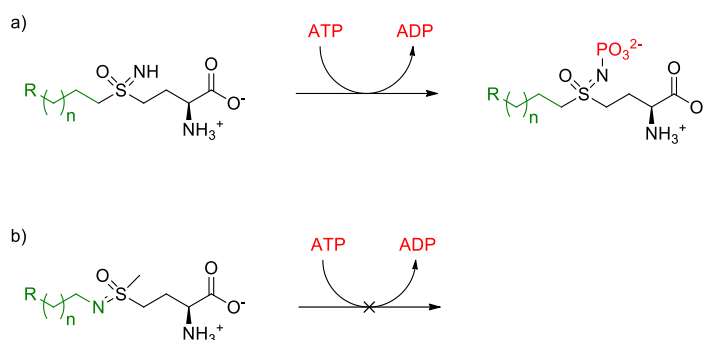
The GS-like enzymes GlnA3_{Sc} and GlnA4_{Sc} have a known ATP-dependency as well as a high sequence homology to GlnA1_{Sc}. *In silico* studies showed that their respective binding sites for ATP and glutamate are very similar but they differ in their amine binding sub-pocket. This suggests that the enzymatic mechanism of GlnA3_{Sc} and GlnA4_{Sc} is similar to the well-studied enzymatic mechanism of glutamine synthetase. The only difference appears to be the amine substrate and consequently the γ -glutamylated product, which was shown by KRYSENKO *et al.* [72,76] While GlnA1_{Sc} produces glutamate, GlnA3_{Sc} produces γ -glutamylated polyamines and GlnA4_{Sc} produces γ -glutamylethanolamine (Scheme 14).



Scheme 14. a) Mechanism of GS-catalyzed conversion of glutamate **98** to glutamine **100**. b) Mechanism of GS inhibition by MSO **101**. c) Putative mechanism of GlnA3_{Sc}-catalyzed conversion of polyamine to γ -glutamylpolyamine **103**. d) Putative mechanism of GlnA4_{Sc}-catalyzed conversion of ethanolamine to γ -glutamylethanolamine **104**.

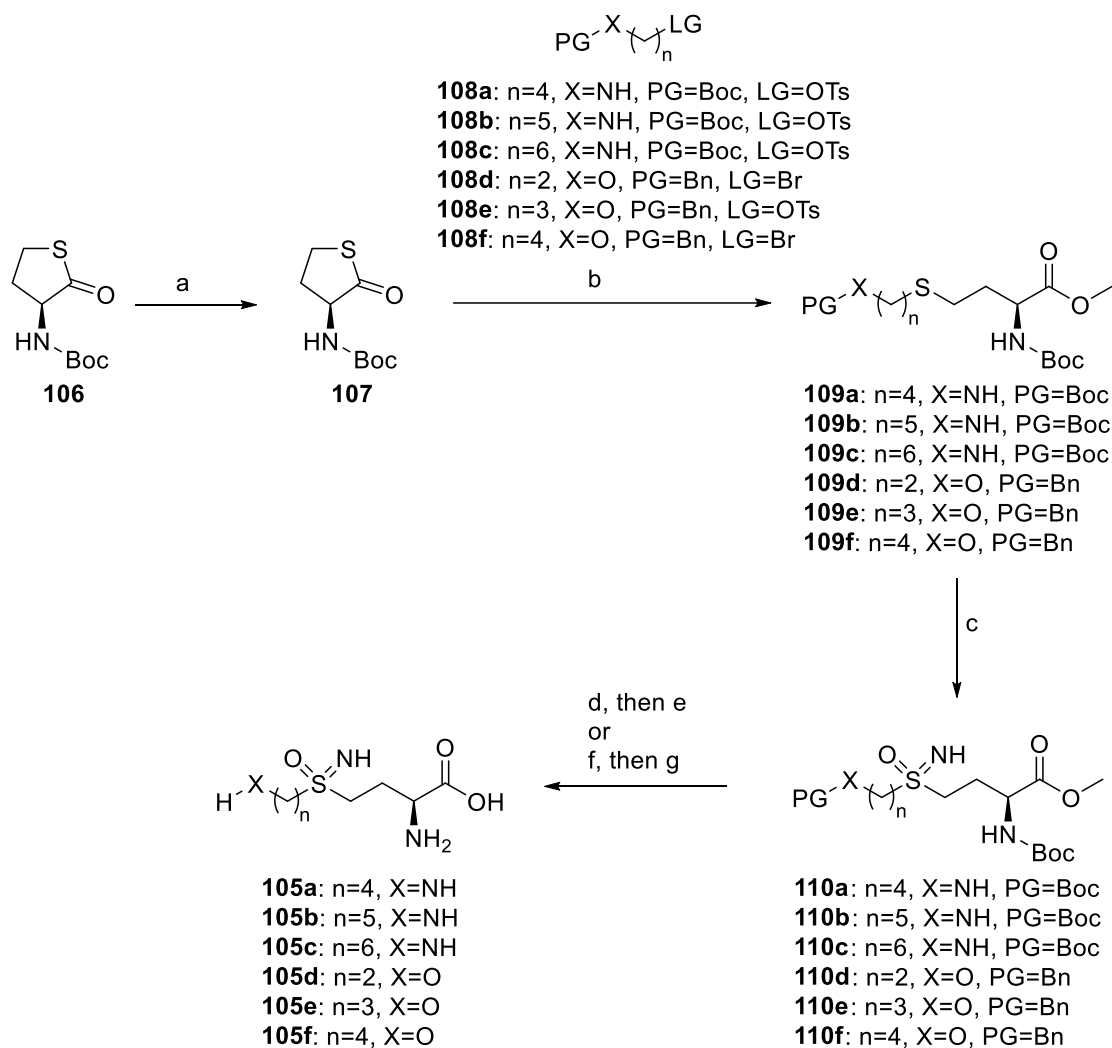
The inhibitor design for GS-like enzymes was inspired by the gold standard GS inhibitor MSO. Since the glutamate- and ATP-binding site in GlnA3_{Sc} and GlnA4_{Sc} is very similar to GS, MSO is a suitable scaffold to address the same pockets in GS-like enzymes. To achieve selectivity for a particular GS-like enzyme their respective amine binding site should be addressed as well. Therefore, the MSO scaffold needs to be extended by a moiety that mimics the respective amine substrate of the GS-like enzyme. MSO presents two possible attachment points for this elongation: (i) the terminal methyl group (Scheme 15a) or (ii)

the sulfoximine nitrogen (Scheme 15b). The first option leaves the molecule with a free imino group that could still be a substrate for phosphorylation. While the second variant cannot be phosphorylated *in situ*, it has a higher resemblance to the natural amine substrate.



Scheme 15. Possible MSO substitutions to achieve GS-like selectivity: a) elongating the terminal methyl group, b) elongating the sulfoximine nitrogen.

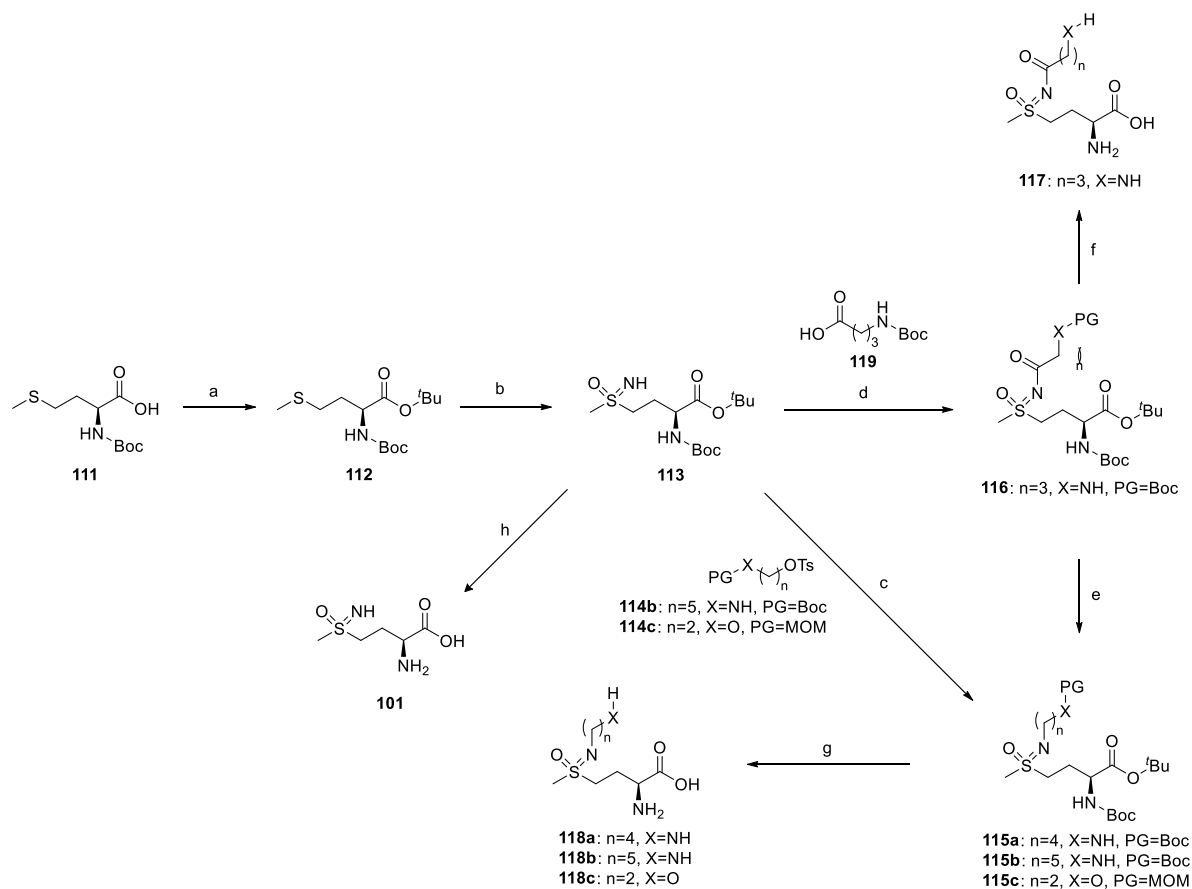
Since there was no clear preference for one of the two options for GS-like inhibition, both options were experimentally tested. For inhibition of GlnA4_{Sc}, 2-hydroxyethyl was selected as the ethanolamine mimicking moiety. To map the ethanolamine sub-pocket, the chain length was varied and hydroxymethyl and 3-hydroxypropyl were also attached to the terminal methyl group. For GlnA3_{Sc}, a few derivatives of different carbon chain lengths with terminal amino groups were chosen, since GlnA3_{Sc} supposedly accepts different polyamines like putrescine and cadaverine. The synthesis of **105d** and **105f** was performed by Jonathan Funk. The synthesis of the C-substituted MSO series starts with a Boc-protection of L-homocysteine thiolactone **106** (Scheme 16). **107** was then opened with NaOMe and the released thiolate was *in situ* alkylated with reagents **108a-f**. Imination and oxidation of thioethers **109a-f** were performed according to ZENZOLA *et al.*^[97] to give sulfoximines **110a-f**. The stereochemistry of the sulfoximine formation was not controlled and gave **110a-f** as mixtures of diastereomers which were each not separated throughout the synthesis. Deprotection of sulfoximines **110d-f** was performed by removal of the benzyl group, followed by basic and then acidic cleavage of the methyl ester and the Boc-group, respectively. The esters of sulfoximines **110a-c** were hydrolyzed under basic conditions, followed by Boc-deprotection under acidic conditions. Final products **105a-f** were purified by cation exchange solid phase extraction.



Scheme 16. Synthesis of C-substituted MSO analogs. Reagents and conditions: (a) Boc_2O , NaHCO_3 , $\text{THF}/\text{H}_2\text{O}$ (1:1), rt, 40 h, 29 %; (b) NaOMe , MeOH , rt, then **108a, b, c, d, e** or **f**, rt, 16-24 h, 59-79 %; (c) PIDA , MeCOONH_4 , MeOH , rt, 16-18 h; (d) LiOH , $\text{THF}/\text{H}_2\text{O}$ (1:1), rt, 3-5 h, 16-62 % over two steps, (e) TFA , DCM , rt, 15-17 h, 82-92 %; (f) Pd/C , H_2 , EtOH , rt, 1-15 h, 8-44 % over two steps; (g) LiOH , $\text{THF}/\text{H}_2\text{O}$ (1:1), rt, 3-18 h then HCl , 40-85 %.

Synthesis of the N-substituted MSO variant started with an esterification between Boc-protected L-methionine **111** and *tert*-butanol (Scheme 17). Fully protected methionine **112** was iminated and oxidized according to the procedure of ZENZOLA *et al.*^[97] to give sulfoximine **113**, again as a mixture of diastereomers with different configurations at the sulfur atom. Direct alkylation with tosylates **114b** and **114c** gave N-substituted sulfoximines **115b** and **115c**. This reaction did not yield any product **115a** with the analogous C4-building block. Therefore, **115a** was synthesized *via* the N-acyl sulfoximine **116**, followed by a borane reduction of the carbonyl group. In addition, part of **116** was deprotected under acidic conditions to give the sulfoximine-N-acylated MSO derivative **117**. Likewise, the protection groups

of compounds **115a-c** were removed under acidic conditions to give *N*-alkylated MSO derivatives **118a-c**. As a reference compound, MSO **101** was synthesised by deprotection of intermediate **113**.



Scheme 17. Synthesis of *N*-substituted MSO. Reagents and conditions: (a) DCC, *tert*-Butanol, DMAP, 0 °C - rt, 18 h, 85 %; (b) PIDA, MeCOONH₄, MeOH, rt, 22 h, 87 %; (c) **114b**, NaHCO₃ or **114c**, K₂CO₃, MeCN, reflux, 2-6 d, 14-56 %; (d) Boc-GABA, HATU, DIPEA, DMF, rt, 3 d, quant.; (e) BH₃-SMe₂, DCM, 0 °C - rt, 17 %; (f) TFA, DCM, rt, 17 h, quant.; (g) TFA, DCM, rt - 90 °C, 17-40 h, 65-80 %; (h) 1 M HCl, 90 °C, 16 h, 69 %.

An overview of all synthesized MSO-derivatives is shown in Figure 37.

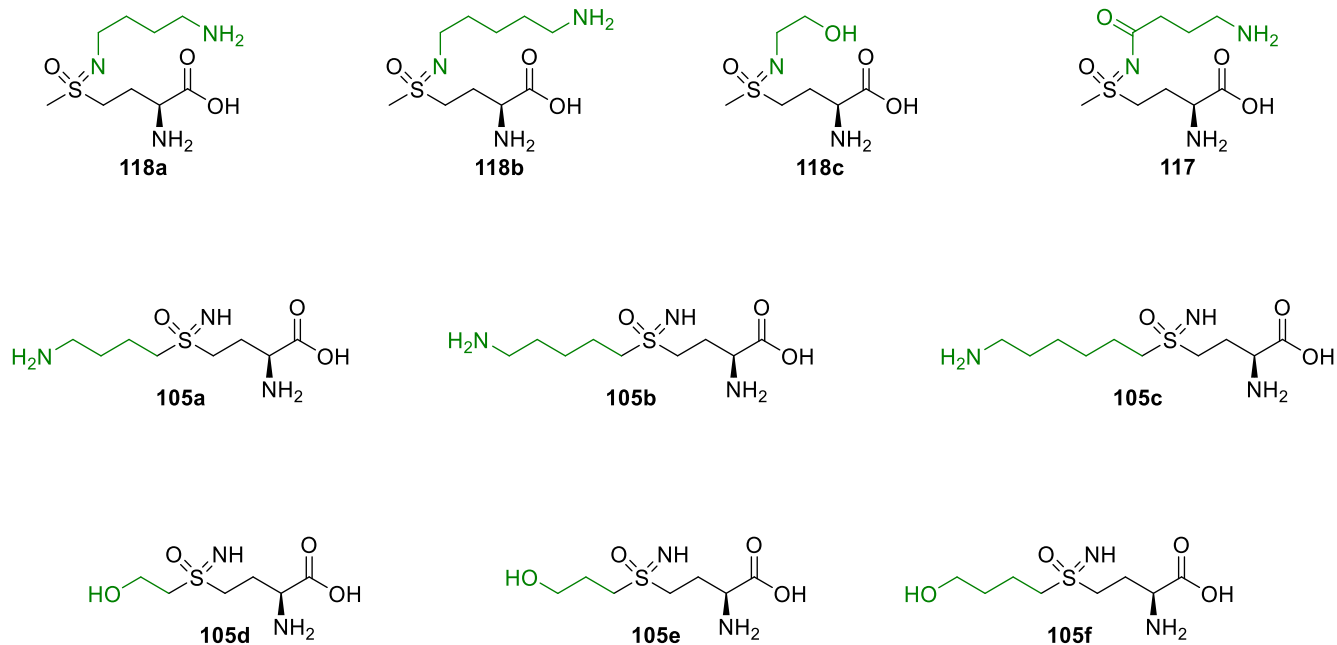


Figure 37. Synthesized GlnA3_{Sc} and GlnA4_{Sc} inhibitors. Amine-mimicking moiety shown in green.

The ability of these novel MSO-derivatives to inhibit MtGS, GlnA3_{Mt} and GlnA4_{Sc} was tested by Christian Meyners in a colorimetric assay, in which the amount of released phosphate is detected as an indicator of enzyme activity (Figure 38).^[76] Self-made MSO **101** and commercially available MSO **101'** were used as references. Compounds **105d** and **f** were not synthesized at the time of the assay and are therefore missing from this data.

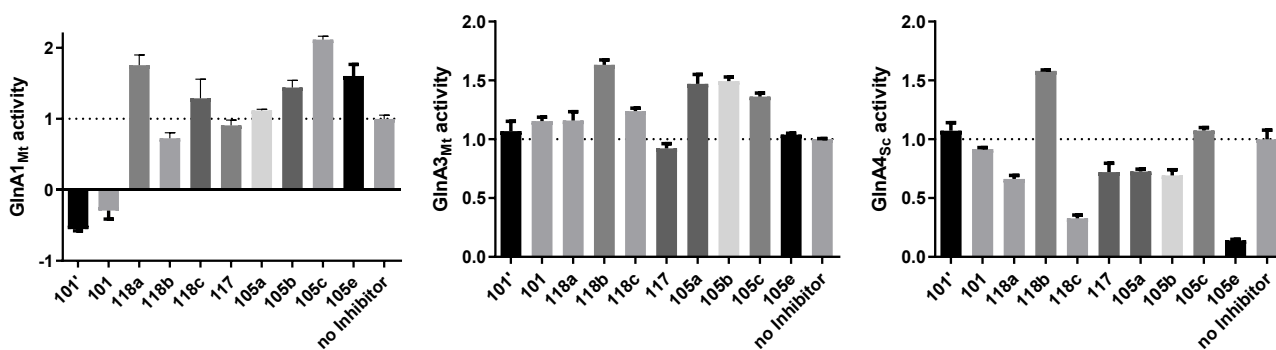


Figure 38. Enzyme activity assays with GlnA1, GlnA3 and GlnA4, normalized to the activity without inhibitor. 5 mM inhibitor, 2.5 mM ATP, 25 mM glutamate, a) 50 mM NH₄Cl, 40 nM GlnA1_{Mt}; b) 50 mM cadaverine, 2.8 μM GlnA3_{Mt}; c) 50 mM ethanolamine, 2 μM GlnA4_{Sc}.

While the activity of MtGS (GlnA1_{Mt}) is completely suppressed by MSO (**101'** and **101**), none of the derivatives show any inhibition for MtGS. This was expected since the amine sub-pocket of MtGS naturally recognizes ammonia and does not provide space for bulkier amines.

GlnA3_{Mt} is also not inhibited by any of the MSO-derivatives, but also MSO shows no effect on GlnA3_{Mt}-activity. The lack of effect was expected for MSO, since it likely cannot address the polyamine-recognizing sub-pocket of GlnA3_{Mt}. Unfortunately, the MSO-derivatives also seem to fail to address this sub-pocket. Perhaps the mechanism of GlnA3_{Mt} is different, despite its close relation to GS, in such a way that the MSO scaffold is not suited to bind to the glutamate-recognizing sub-pocket. Also, this activity assay lacks a positive control. Therefore, it cannot be ruled out that the used GlnA3_{Mt} might be inactive and the measured amount of phosphate is rather the background of slowly hydrolyzed ATP.

The results from the GlnA4_{Sc} activity assay on the other hand were quite satisfying. This enzyme can be inhibited by some of the derivatives. The strongest effect is observed for **118c** and **105e**, the 2-hydroxyethyl substituted MSO variants. It is clear that the C-substituted derivative is much more potent than the N-substituted one. Therefore, the two analogs of **105e** with different carbon chain lengths (**105d** and **105f**) were synthesized to get a better understanding of the ethanolamine sub-pocket. To better quantify inhibitory activity, the GlnA4_{Sc} activity was measured again by Christian Meyners in a dose-responsive way with the inhibitors **118c** and **105d-f** (Figure 39).

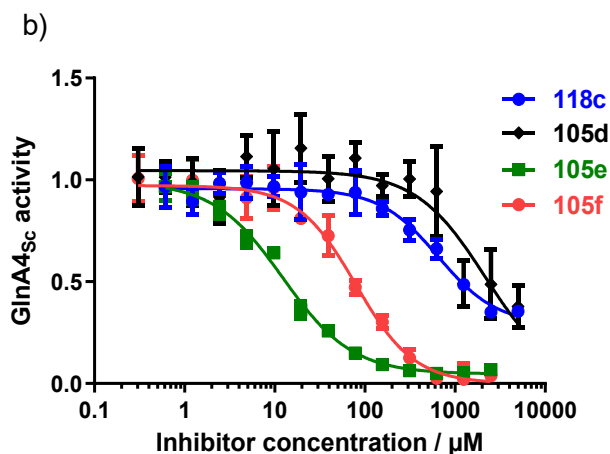
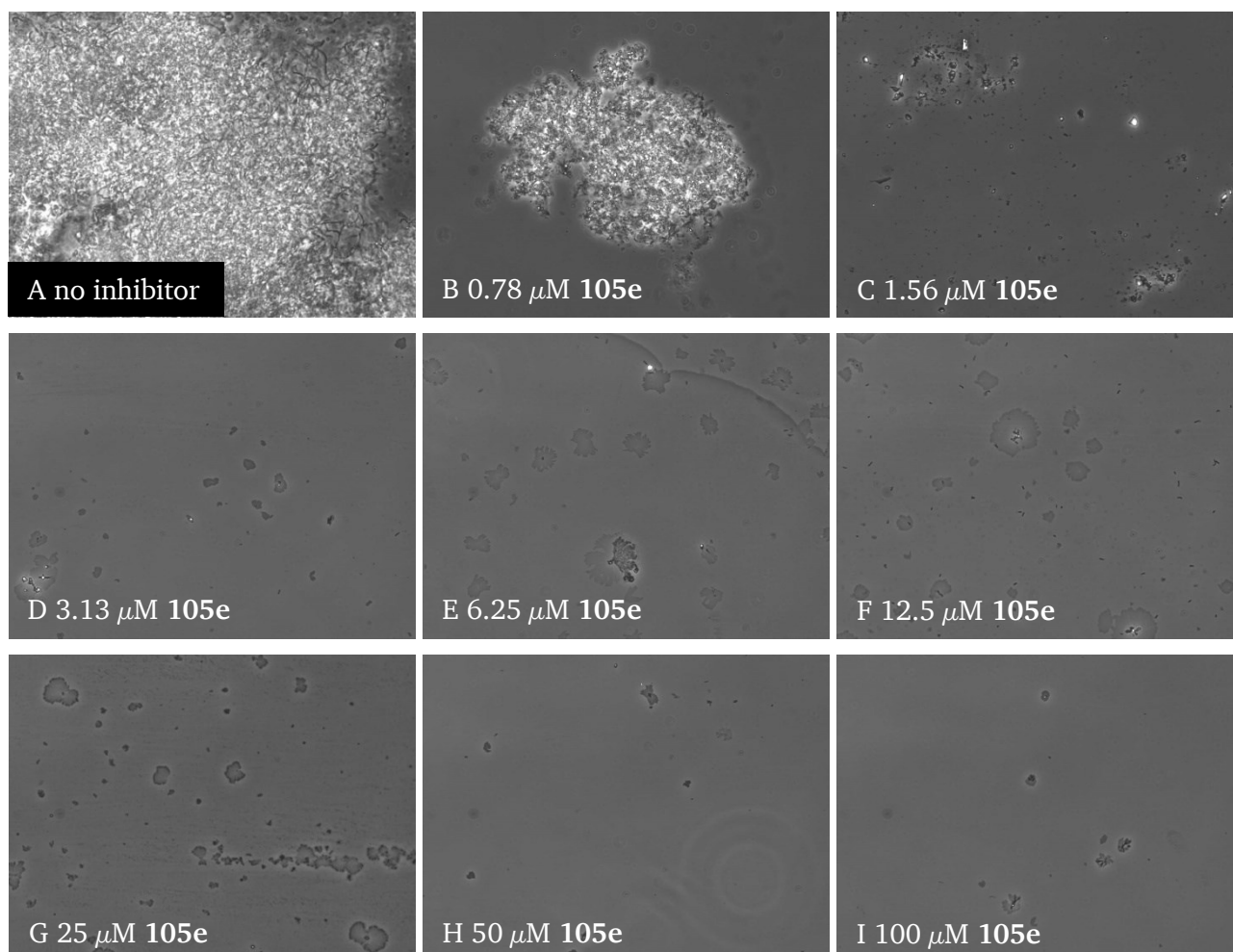


Figure 39. GlnA4_{Sc} activity at different concentrations of inhibitors **118c** and **105d-f**.

The direct comparison of **118c** and **105e** shows that a C-substituted attachment of the ethanolamine mimetic is much better suited for GlnA4_{Sc} inhibition than a N-substitution (IC₅₀ of 12.3 ± 0.9 μM for **105e** vs. 649 ± 133 μM for **118c**, **105d-f** show IC₅₀ values of 2166 ± 390, 12.3 ± 0.9 and 79.3 ± 8.0 μM, respectively). This strongly suggests the generation of an intermediate with a phosphorylated sulfoximine nitrogen atom for **105e**, similar to the binding mode of MSO. This postulated

phosphorylated sulfoximine species seems to act as a transition state mimetic and in turn seems to inhibit much stronger than the more product-like **118c**, which contains a more authentic ethanolamine moiety. Among the three *C*-substituted MSO analogs, **105e** is the best inhibitor, where the three-carbon chain corresponds to the three-atom distance between the hydroxy group and Cy in the product γ -glutamylethanolamine. A longer chain as in **105f** is also tolerated ($IC_{50} = 79.3 \pm 8.0 \mu M$) but a shortening to a two-carbon linker as in **105d** reduced inhibitory activity substantially ($IC_{50} = 2166 \pm 390 \mu M$). The structure-activity relationship is thus consistent with the recognition pattern of the authentic substrate ethanolamine.

The antibacterial activity of compound **105e** against *S. coelicolor* was measured by Sergii Krysenko from the Eberhard Karl University Tübingen in a growth assay on defined Evans medium with ethanolamine as sole nitrogen source. Under these conditions, *S. coelicolor* expresses GlnA4 and depends on it to utilize ethanolamine.^[76] The inhibitory effect of **105e** was visualized using phase-contrast microscopy (Figure 40).



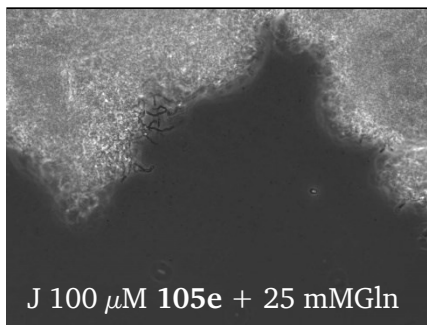


Figure 40. *S. Coelicolor* growth with different concentrations of inhibitor **105e** using ethanolamine as a nitrogen source.

Addition of **105e** reduced the size of the mycelial agglomerates already at the lowest tested concentration (0.78 μ M, Figure 40B). Higher concentrations dramatically blocked the growth of *S. coelicolor* and above 3.1 μ M almost no bacterial growth can be observed. The growth inhibition was clearly GlnA4-dependent, since additional glutamine (25 mM) as an alternative nitrogen source suppresses this effect, rescuing the growth of *S. coelicolor* at 100 μ M **105e** (Figure 40J). This control experiment also excludes any non-specific toxic effects of compound **105e** even at 100 μ M.

3.9. Synthesis of Homocysteine sulfonimidamide

The gold standard inhibitor for glutamine synthetase is, and has been for a very long time, methionine sulfoximine (MSO **101**). The only other repeatedly described GS inhibitor is phosphinothricin (PPT). While many MSO or PPT analogs exist,^[102] none was able to outperform MSO as GS inhibitor. When looking at the structure of P-MSO **102** in comparison to the transition state of the natural substrate of GS (Figure 41a and b) it becomes clear that the terminal methyl group of MSO is positioned where naturally the protonated amino group would be. Replacing that methyl group with an amine could result in a sulfonimidamide group and lead to (phosphorylated **120**) homocysteine sulfonimidamide **121** (P-HCysSIA, Figure 41c).

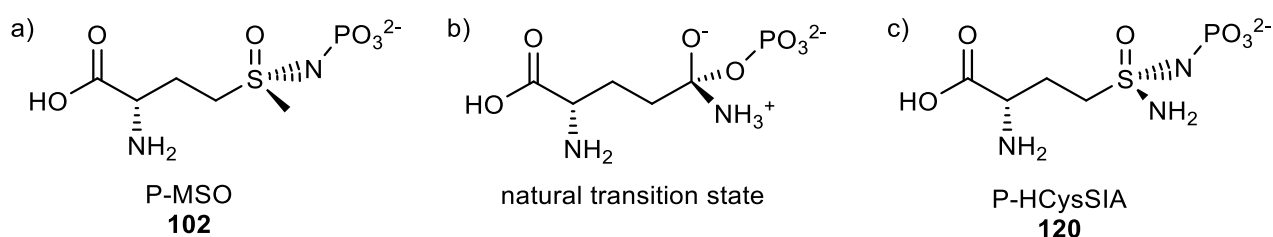


Figure 41. Structures of a) P-MSO, b) the natural transition state of the GS-catalysed Gln formation and c) P-HCysSIA.

Though its amide nitrogen atom would likely not be protonated in aqueous solution, it could act as a hydrogen bond donor. HCysSIA **121** could therefore be a closer homolog to the natural transition state and might have a stronger binding affinity to GS and be a stronger inhibitor than MSO. The possible interactions with the binding pocket are visible in the cocrystal structure of MSO with GS (Figure 42, PDB: 2BVC), where the terminal methyl group of MSO is surrounded by three carboxylic acids (Glu219 (Chain B), Glu335 (Chain B), Asp54 (Chain A)).

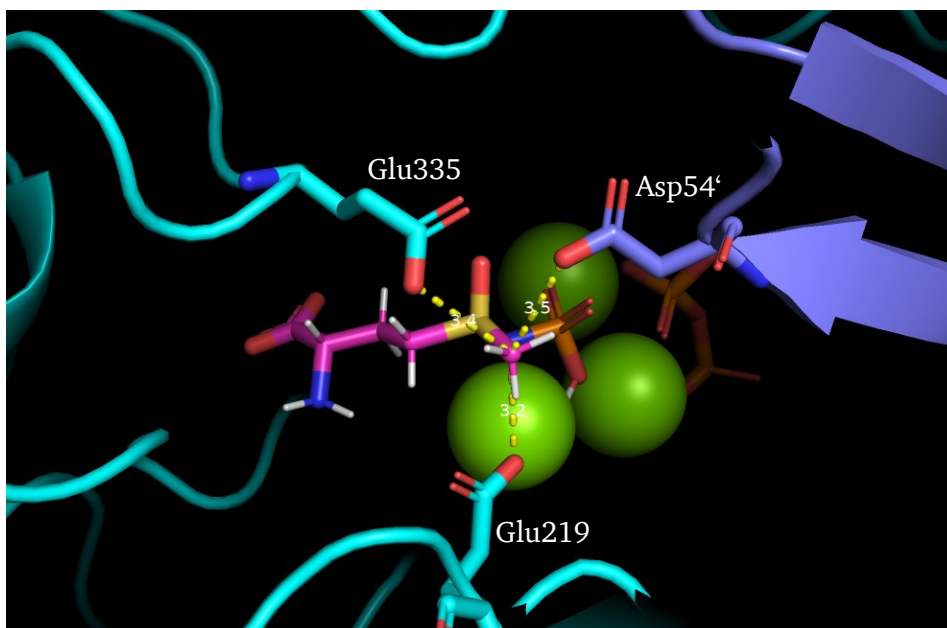
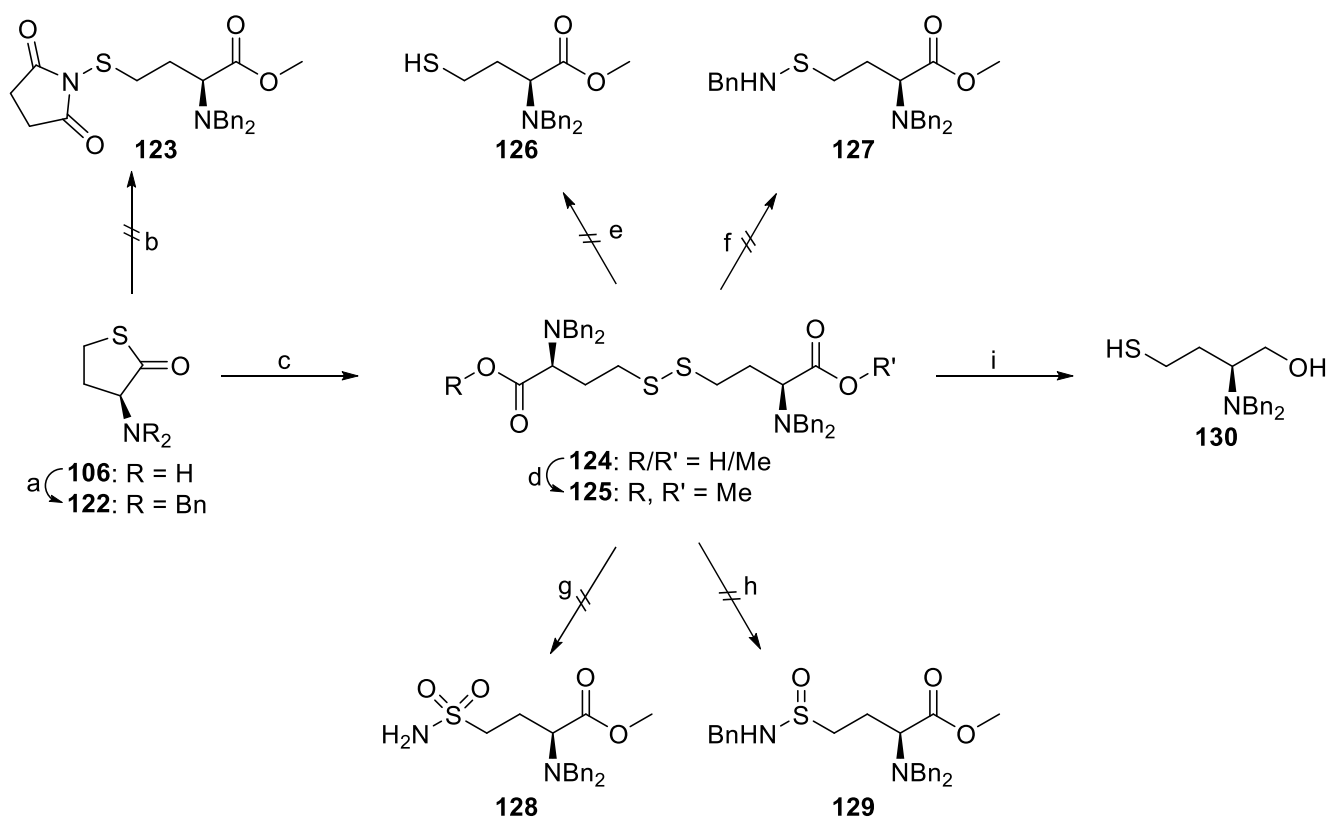


Figure 42. Cocrystal structure of P-MSO **102** and MtGS (PDB: 2BVC). Distances of the terminal methyl group to surrounding carboxylic acids are shown as dashed yellow lines and given in Å.

To see whether HCysSIA **121** can act as a GS inhibitor, I had to synthesize it to allow testing in a GS activity assay.

The synthesis of HCysSIA **121** was initially attempted in analogy to the MSO-derivatives from Chapter 3.8, starting from homocysteine thiolactone **106** (Scheme 18).

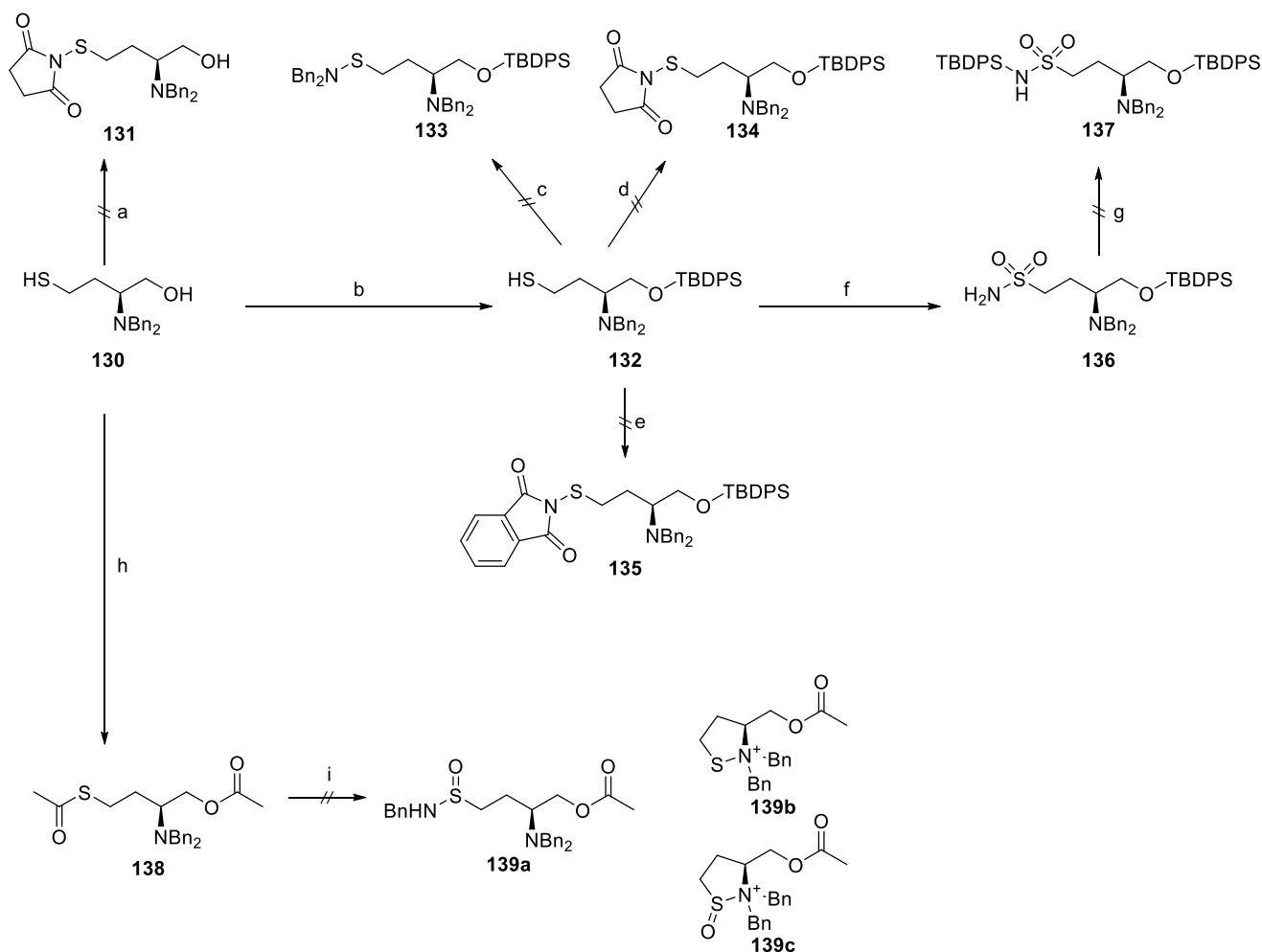


Scheme 18. Synthesis attempts towards HCysSIA **121**, part 1. Reagents and conditions: a) BnBr, TBAI, K₂CO₃, dry MeCN, 0-50 °C, 4 d; b) NaOMe, NCS, dry MeOH, rt, 16 h; c) NaOMe, dry MeOH, rt – 75 °C, 2 d; d) DMAP, DCC, MeOH, DCM, rt, 5 d; e) DTT, H₂O, rt, 21 h; f) SO₂Cl₂, DCM, -15 °C – rt, 7 h, then add benzylamine, DIPEA, rt, 18 h; g) TMSCl, H₂O₂, MeCN, rt, 90 min; h) AcOH, SO₂Cl₂, -40 °C – rt, 1 h, then add benzylamine, DIPEA, MeCN, rt, 17 h; i) LAH, dry THF, -84 °C – rt, 30 min.

Instead of alkylating the thiol group, in this case it was attempted to be coupled with a protected amine so form a sulfenamide, which would then be transformed to the sulfonimidamide in analogy to the sulfenamide from Chapter 3.5, Scheme 12. For this purpose, the amine group of **106** was protected with two benzyl groups to yield **122**, to ensure that it cannot form a stable intramolecular sulfenamide. The reaction of NCS with thiols is known to form sulfenamides.^[103] In this case, however, the addition of NCS to a mixture of **122** and NaOMe in MeOH did not show any trace of the desired product **123** by LC-MS analysis of the reaction mixture. Instead, mostly starting material **122** could be detected. Surprisingly, it was not the opened thiolactone that was observed in this reaction. The next attempt was to isolate the free thiol and form the sulfenamide in a separate reaction. The ring opening of **122** with NaOMe in MeOH proceeded as usual, though it was not the free thiol that was isolated but the respective disulfide as a mixture of carboxylic acids and methyl esters (**124**). This mixture was then reacted with DCC and MeOH to convert the free carboxylic acids to methyl esters completely, which yielded **125** as a homogeneous product. Treatment with dithiothreitol could not cleave the disulfide bond of **125** to

compound **126**. Direct conversion of a disulfide to a sulfenyl chloride using sulfuryl chloride, and in situ coupling with an amine to a sulfenamide is known in the literature,^[104] but could not convert disulfide **125** to sulfenamide **127**. The only signal of a LC-MS analysis of the reaction mixture, which could be assigned to a product, would fit the twice oxidised starting material, being either symmetrically oxidised once on each sulfur, or asymmetrically oxidised twice on one sulfur atom. In a similar approach, the disulfide **125** was transformed into the corresponding sulfinamide **129**, following a literature procedure.^[105] A LC-MS analysis of the reaction mixture showed the formation of the desired product **129** in traces, however no product could be isolated. Another literature procedure^[106] describes the conversion of thiols and disulfides to sulfonylchlorides using TMSCl/H₂O₂. However, in this reaction (aiming at **128**) the same oxidation products as with SO₂Cl₂ (aiming at **127**) were found. Finally, the direct activation of the disulfide group was abandoned and it was first reduced to the thiol. Since mild reduction conditions like dithiothreitol already failed to reduce the disulfide bond, lithium aluminum hydride was tested, which could successfully cleave the disulfide bond, but also reduced the ester to the hydroxy group and gave compound **130**.

Compound **130** was used in turn as a starting point for further synthetic approaches towards HCysSIA (Scheme 19).

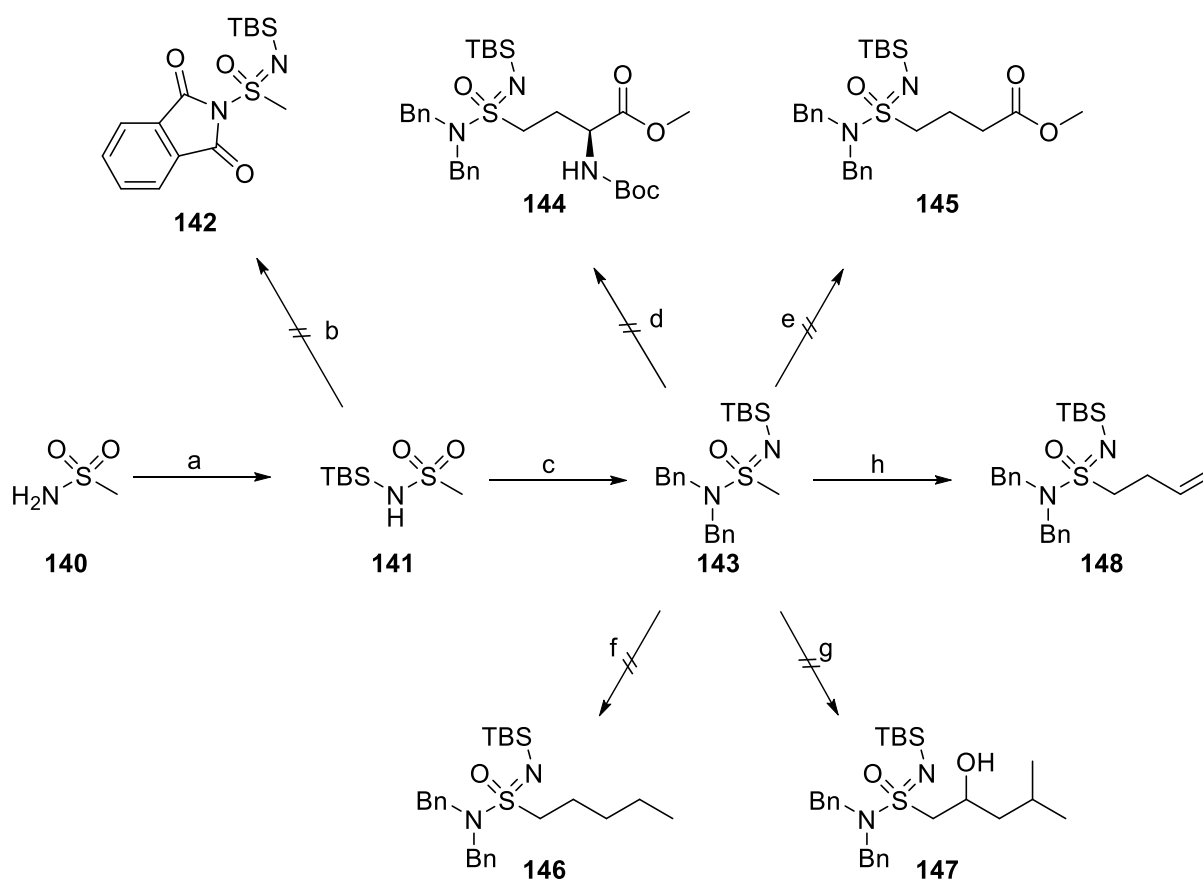


Scheme 19. Synthesis attempts towards HCysSIA **121**, part 2. Reagents and conditions: a) NCS, TEA, dry DCM, 0 °C – rt, 5 h; b) TBDPSCl, imidazole, dry DCM, rt, 20 h; c) SO₂Cl₂, DCM, 0 °C – rt, 4 h, then add benzylamine, rt, 16 h; d) NCS, TEA, DCM, rt, 3 h; e) SO₂Cl₂, TEA, DCM, 0 °C – rt, 15 min, then add phthalimide, TEA, 0 °C – rt, 4 h; f) TMSCl, H₂O₂, MeCN, rt, 1 h, then add aq. NH₃, rt, 80 min; g) TEA, dry THF, rt, 5 min, then add TBDPSCl, reflux, 18 h; h) AcCl, TEA, 0 °C – rt, 17 h; i) Ac₂O, SO₂Cl₂, dry DCE, -10 °C, 30 min, then add benzylamine, *N*-methylmorpholine, -10 °C – rt, 1 h.

A reaction of thiol **130** with NCS to form sulfenamide **131** again showed no product formation on LC-MS analysis. In a different approach, the hydroxy group was protected by TBDPS,^[107] yielding **132**. However, further conversions to sulfenamides **133**, **134** or **135** were not successful. Only the oxidation to the sulfonamide **136** showed product formation and could be isolated, under the same conditions which previously did not work for disulfide **125** (aiming at **128**). TBDPS protection of the sulfonamide **136** (towards **137**) was attempted in order to form a sulfonimidamide in analogy to **72** (Chapter 3.5). Unfortunately, no consumption of the starting material **136** could be observed and this route was abandoned. In a different approach, thiol **130** was converted to the respective thioacetate **138**, where the alcohol was simultaneously acetylated. Thioacetate **138** was then subjected to a literature

protocol,^[108] which aimed to form a sulfinyl chloride, which was then reacted with an amine to form the respective sulfenamide **139a**. While the starting material was consumed, no product formation could be observed. The only signals of the LC-MS analysis that could be assigned to a product would correlate to an intramolecular sulfenamide **139b** or sulfenamide **139c**, respectively. Even the addition of excessive amine did not break up the intramolecular cyclization. After this observation, it was considered that any activation of the sulfur atom would be futile as long as the γ -amino group was present in the same molecule.

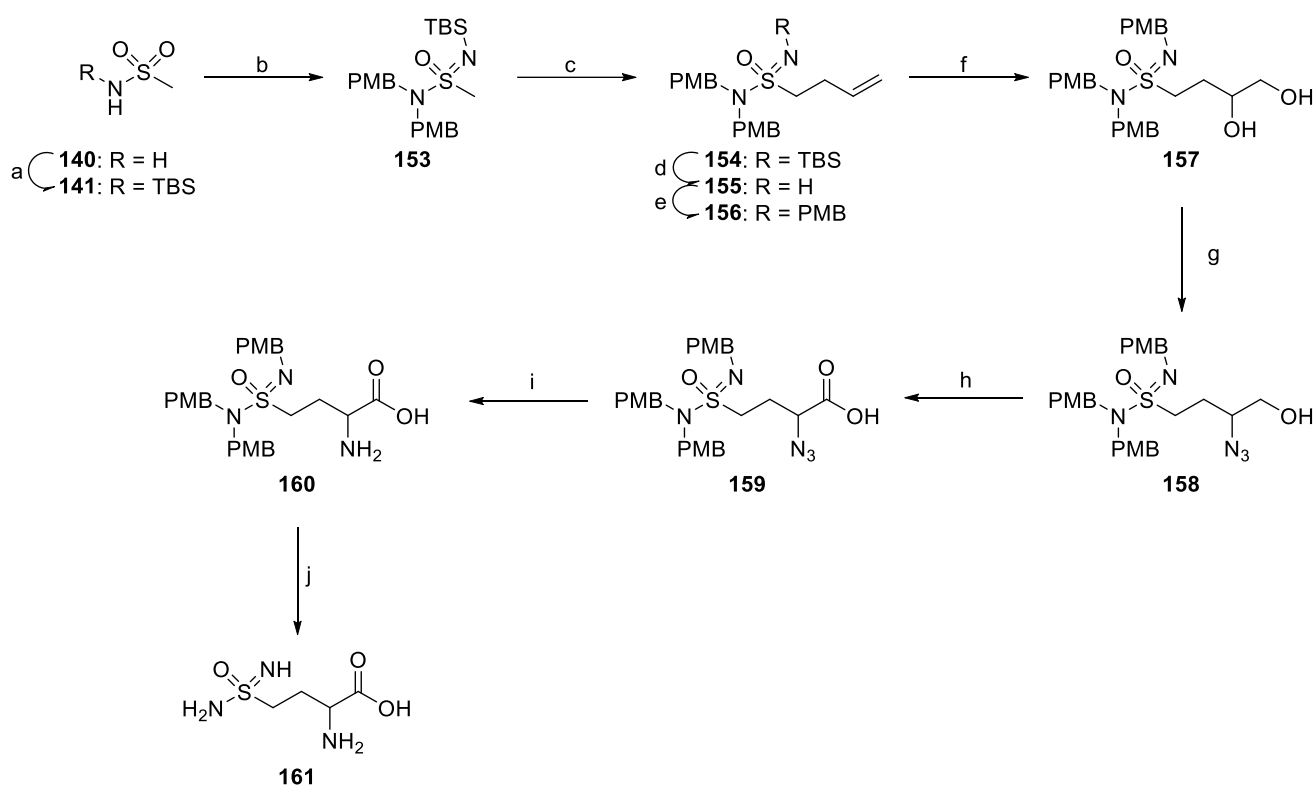
In the next strategy, the sulfonimidamide moiety was attempted to be synthesized separately from the amino acid (Scheme 20).



Scheme 20. Synthesis attempts towards HCysIA **121**, part 3. Reagents and conditions: a) TBDPSCI, THF, dry THF, 45 °C, 16 h; b) Ph_3PCl_2 , TEA, dry CHCl_3 , rt, 10 min, then add **141**, 0 °C, 20 min, then add phthalimide, 0 °C – rt, 16 h; c) Ph_3PCl_2 , TEA, dry CHCl_3 , rt, 10 min, then add **141**, 0 °C, 50 min, then add dibenzylamine, 0 °C – rt, 4 d; d) TMEDA, $^n\text{BuLi}$, dry THF, -84 °C, 10 min, then add Boc-iodo-L-alanine methyl ester **149**, -84 °C – rt, 30 min; e) TMEDA, $^n\text{BuLi}$, dry THF, -84 °C, 10 min, then add methyl acrylate **150**, -84 °C – rt, 16 h; f) TMEDA, $^n\text{BuLi}$, dry THF, -84 °C, 15 min, then add 1-iodobutane **151**, -84 °C – rt, 1 h; g) TMEDA, $^n\text{BuLi}$, dry THF, -84 °C, 15 min, then add isovaleraldehyde **152**, -84 °C – rt, 1 h; h) TMEDA, $^n\text{BuLi}$, dry THF, -84 °C, 10 min, then add allyl bromide, -84 °C – rt, 19 h.

Conversion of methanesulfonamide **140** to the TBS-protected methanesulfonamide **141** proceeded as described in literature.^[109] Deoxygenative chlorination of **141** to the TBS-protected methanesulfonimidoyl chloride was performed as described in literature^[109] and further coupling with

dibenzylamine yielded sulfonimidamide **143**. The same conditions did not yield the desired product **142** when the intermediary sulfonimidoyl chloride was mixed with phthalimide. The reaction of sulfonimidamides with electrophiles was already described in 1988,^[110] and this reaction was attempted to couple sulfonimidamide **143** to an amino acid building block. Reactions with iodo-alanine **149** (towards **144**) or methyl acrylate **150** (towards **145**) showed no product formation, and even test reactions with simpler electrophiles like 1-iodobutane **151** (towards **146**) or isovaleraldehyde **152** (towards **147**) showed no product formation. The only electrophile which reacted with sulfonimidamide **143** was allyl bromide, which formed **148** in a satisfying yield. Therefore, it was decided to go further with this intermediate and build the amino acid from the terminal double bond. After little optimization, the final synthetic route (Scheme 21) was set up.



Scheme 21. Reagents and conditions: a) TBSCl, TEA, dry THF, 45 °C, 23 h, 98 %; b) Ph₃PCl₂, TEA, dry CHCl₃ 0 °C, 10 min, then **141**, 0 °C, 30 min, then PMB₂NH, 0 °C – rt, 16 h, 62 %; c) BuLi, TMEDA, allyl bromide, dry THF, -84 °C – rt, 3 h, 86 %; d) TBAF, THF, rt, 3 h, 86 %; e) NaH, PMBCl, dry THF, 0 °C – rt, 24 h, 62 %; f) 2,6-Lutidine, NMO, OsO₄, acetone/water (10:1), 0 °C – rt, 2 h, 87 %; g) PPh₃, DIAD, 0 °C, 2 h, then TMSN₃, 0 °C – rt, 16 h, 60 %; h) Jones reagent, acetone, 0 °C – rt, 19 h, 47 %; i) PPh₃, THF, rt, 55 h, then 1 M NaOH, rt, 19 h, 87 %; j) TFA, reflux, 23 h, 3 %.

Methanesulfonamide **140** was TBS protected and converted to sulfonimidamide **153** under conditions described by CHEN and GIBSON.^[109] As amine, bis(4-methoxybenzyl)amine was used, since the benzyl groups in previous trials proved difficult to remove. After the allylation reaction (**154**), the TBS

protective group was exchanged for a more stable PMB (**156**) to avoid an intramolecular reaction in later steps. The terminal double bond was dihydroxylated with OsO₄, which gave **157** as a mixture of diastereomers. A regioselective Mitsunobu reaction, as described by HE *et al.*^[111] yielded azide **158**. Regioselectivity was confirmed by ¹³C-NMR shifts and reactivity in a Jones oxidation. The terminal hydroxy group was oxidized to the carboxylic acid **159** using Jones reagent. A Staudinger reduction converted the azide into the respective amine **160**. However, a water-stable intermediate was observed on LC-MS analysis which would be assigned to the respective 1,3,2-oxazaphospholidin-5-one. One example of such an intermediate is described in literature,^[112] and in this case the cyclic intermediate could be cleaved to the desired amino acid **160** with 1 M NaOH. Finally, deprotection of all PMB groups released the target molecule, racemic homocysteine sulfonimidamide **161**. The PMB deprotection did not work under oxidative conditions like CAN or DDQ, and acidic conditions at room temperature showed only traces of product. Pure TFA under reflux was able to cleave all three PMB groups. The purification of **161** turned out to be the final big hurdle in this synthesis. Reverse-phase HPLC, which was used more like a filtration since the product showed no retention, removed all unpolar side products. Cation exchange solid phase extraction, which was used to purify all MSO analogs in Chapter 3.8, increased the purity of **161** but not to a satisfying degree. After many other attempts (HPLC over HILIC column, cation exchange chromatography, siliga gel column chromatography) the final purification was performed by thick layer chromatography or preparative TLC. Due to the tedious purification optimization, the final yield was very low.

The biological activity of **161** was analyzed by Christian Meyners in a glutamine synthetase activity assay (Figure 43), using commercially available L-MSO as a control.

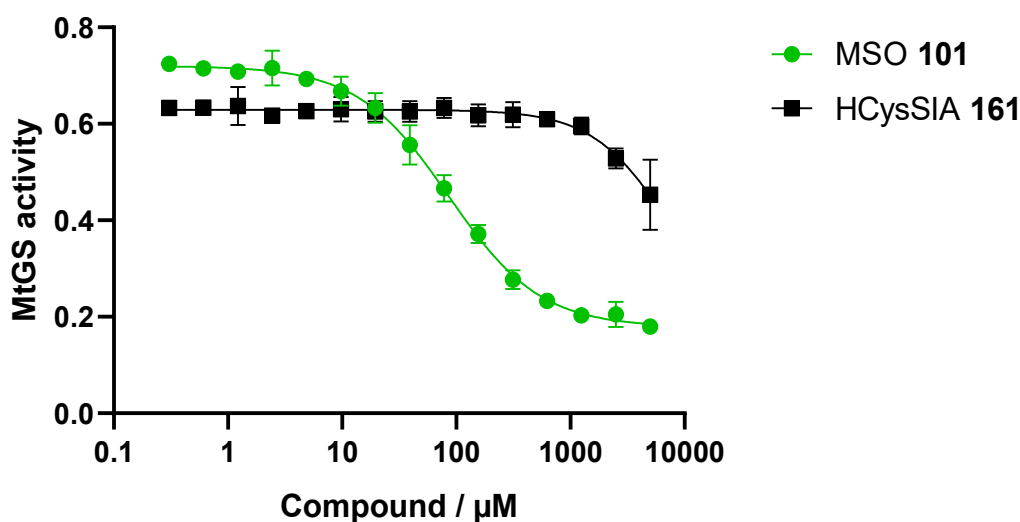


Figure 43. GS inhibition of L-MSO and compound **161**.

The novel compound **161** showed a much lower inhibitory effect than MSO ($IC_{50} = 6,900 \pm 870 \mu\text{M}$ vs. $86 \pm 4 \mu\text{M}$). This observation suggests that the enzyme's catalytic mechanism is more complex. The postulated attractive interactions of the novel amino group with the surrounding carboxylic acid side chains did not improve the inhibitory effect compared to the methyl group in MSO. Part of the lower activity could be explained by the configuration of the amino acid in both compounds. While MSO was used as a single (*S*)-epimer concerning the C_{α} , HCysSIA **161** was synthesized as a mixture of enantiomers.^[82] Another explanation might be that the amino function of HCysSIA is not a better transition state mimetic than the methyl group of MSO. The HCysSIA amino protons are likely able to form a generally stronger bond to the surrounding carboxylic acids. On the other hand, the amino group can only mimic two of the three interactions present in the natural transition state, where the corresponding amine is in its protonated ammonium form ($-\text{NH}_3^+$). The protons of the MSO methyl group are likely less polarized than those of an amine, but adjacent to a sulfoximine their acidity increases.^[113] The three protons of the MSO methyl group could potentially form bonds with all three surrounding carboxylic acids of GS (Glu219, Glu336, Asp54', see Figure 42). In combination, the attractive interactions of the MSO methyl group might be stronger than those of the HCysSIA amino group. Further insight would be necessary to understand this weak inhibition of **161**, for example a cocrystal structure could reveal the position and interactions of **161** in the active site of GS.

4. Conclusion and Outlook

In this research, multiple series of novel FKBP ligands and one series of ligands for GS-like enzymes were synthesized and biochemically assessed. The FKBP ligands expanded the knowledge of FKBP-ligand interactions and can be used as valuable tool compounds in further research. The ligands for GS-like enzymes helped to understand the mechanism of GlnA4 and the nitrogen metabolism of the model actinobacterium *Streptomyces coelicolor*.

The synthesis of a FKBP ligand with a contracted ring system in the core provided a structurally closely related molecule which barely binds FKBP anymore. This negative control is highly useful in future biochemical and biological experiments to identify an observed effect as FKBP-specific.

The derivatization of known FKBP ligands with a carboxylic acid in the R1 position resulted in a small series of compounds, of which one turned out to be metabolically stable. The metabolic stability was thus far a problem yet to be solved in the long process of developing drug-like FKBP ligands. However, this is but a starting point for the deeper understanding of what makes a FKBP ligand of this class metabolically stable or unstable. Furthermore, the highly polar groups of this compound make it more water-soluble and therefore more suitable as a tool compound in biochemical experiments, which sometimes require high ligand concentrations in aqueous media. At the same time, the high polarity of the ligand impedes the passage of a cell membrane, making it an excellent control compound in cellular experiments.

The derivatization of the R2 position in the known FKBP ligand scaffold identified a structural motif which leads to ultra-binding FKBP12 ligands with an unprecedented selectivity against FKBP51 and FKBP52. Further optimization pushed the binding affinity of these ligands to the low pM range and the cause of this high affinity and selectivity could be elucidated. These ultra-affinity FKBP12 ligands provide a scaffold on which novel tool compounds can be developed.

The systematic replacement of the conserved sulfonamide gave a series of FKBP ligands consisting of a sulfenamide, sulfinamides and sulfonimidamides. All diastereomers could be separated and assigned. The binding affinities of these compounds allowed the calculation of energetic contributions of each sulfonamide oxygen atom to the binding of the ligand. The interactions of the sulfonimidamide motif with the FKBP12 binding pocket could be identified from multiple cocrystal structures. Furthermore, the sulfonimidamide motif could be alkylated to expand the bicyclic scaffold into a new direction. This series of substituted sulfonimidamides revealed an interesting structure-affinity relationship which might

suggest a transient binding pocket in FKBP12. This binding mode should be further investigated to clarify this puzzling structure-affinity relationship.

In a screening for bacterial Mips, some of the presented bicyclic FKBP ligands also showed Mip binding, with the strongest ones in the low nM range. Further experiments with *L. pneumophila* confirmed that LpMip ligands which can pass the cell membrane can have a growth inhibiting effect on the bacterium. This antibacterial property of FKBP and Mip ligands should be further optimized to develop antibacterial drug candidates and to better understand the importance of Mip proteins for the respective pathogens.

The rational modification of the known GS inhibitor MSO led to the first inhibitors for the GS-like enzyme GlnA4. The inhibitory activity could be shown in a biochemical assay as well as in a cellular growth experiment. This novel inhibitor supported the hypothesized enzymatic mechanism of GlnA4 and gave further insights into the nitrogen metabolism of the model organism *S. coelicolor*. More importantly, this design concept provides a basis on which other inhibitors for ATP-dependent acid-amide synthases (EC 6.3) can be developed.

5. Experimental Part

5.1. General Methods

If not indicated otherwise, reactions were performed in quartz glass round bottom flasks. Air- or water-sensitive reagents were handled in dry solvents under argon atmosphere. For this purpose, the reaction vessel was sealed with a septum, evacuated in a high vacuum and heated with a heat gun. Afterwards, it was filled with argon (ALPHAGAZ™ 1 Argon, 99.999 %).

Reagents and solvents were purchased from commercial suppliers and used without further treatment.

Nuclear Magnetic Resonance Spectroscopy

NMR spectroscopy was performed by the NMR department at TU Darmstadt. NMR spectra were recorded either on a 300 MHz Avance II NMR spectrometer from Bruker BioSpin GmbH (for ¹H-NMR only), a 300 MHz Avance III NMR spectrometer from Bruker BioSpin GmbH (for ¹H-, ¹³C-NMR), or a 500 MHz NMR spectrometer DRX 500 from Bruker BioSpin GmbH (for ¹H- and ¹³C-NMR). NMR spectra were recorded at room temperature. Chemical shifts are given in parts per million, referenced to the respective solvent (¹H: CDCl₃ = 7.26 ppm, DMSO-d₆ = 2.50 ppm, D₂O = 4.79 ppm, CD₃OD = 3.31 ppm, ¹³C: CDCl₃ = 77.16 ppm, DMSO-d₆ = 39.52 ppm, CD₃OD = 49.00 ppm). Coupling constants (*J*) are given in hertz (Hz), peak multiplicities are given as singlet (s), doublet (d), triplet (t), quartet (q) or multiplet (m).

Liquid Chromatography – Mass Spectrometry

LC was performed either with a Beckman Coulter System Gold 126 solvent module, Beckman Coulter System Gold 508 autosampler and Beckman Coulter System Gold 166 detector, with a YMC-Pack Pro C8 3 μm 120 Å, 100x4.6 mm column from YMC, or with an Agilent 1260 Infinity II system with a Poroshell 120 EC-C18 1.9 μm, 2.1 x 50 mm column from Agilent. Eluents were 0.1 % formic acid in water (Eluent A) and 0.1 % formic acid in acetonitrile (Eluent B), the used method was 5 % B to 100 % B in either 19 min or in 2 min, respectively. MS was recorded either with a Thermo Finnigan LCQ Deca XP Plus or an Agilent InfinityLab G6125B LC/MSD, respectively.

High Resolution Mass Spectrometry

HR-MS was performed by the mass spectrometry department at TU Darmstadt. Mass spectra were recorded on an Impact II, quadrupol-time-of-flight spectrometer from Bruker Daltonics.

Semi-Preparative High Performance Liquid Chromatography

Semi-Preparative HPLC was performed either with a Beckman Coulter System Gold programmable solvent module 126NMP, Beckman Coulter System Gold programmable detector module 166 and

Beckman Coulter SC 100 fraction collector with a Jupiter 10 μm Proteo 90 Å, 250x10.00 mm column from Phenomenex, or with an Interchim PuriFlash 5250 system with a Luna[®] 5 μm C18(2) 100 Å, 250x21.2 mm column from Phenomenex. Eluents were 0.1 % TFA in water (Eluent A) and 0.1 % TFA in acetonitrile (Eluent B), methods are given in percentage B.

Column chromatography

Column chromatography was performed manually with silica gel 60 (0.04-0.063 mm, 230-400 mesh) from Carl Roth GmbH.

Flash column chromatography

Flash silica gel column chromatography was performed with a Biotage[®] Isolera One system with Biotage[®] Sfär Silica HC D columns.

Thin layer chromatography

TLC was performed on TLC Silica gel 60 F₂₅₄ Aluminum sheets from Merck Millipore.

Cation exchange solid phase extraction

Cation exchange solid phase extraction was performed with Dowex 50WX2 100-200 in a syringe equipped with a filter. The sample was loaded in 0.1 M aqueous HCl solution and the resin was washed with water three times. The product was eluted with 30 % aq. NH₃ solution.

Fluorescence Polarization assay

FP-Assays were performed either by myself, Stephanie Merz or Wisely Oki Sugiarto. For most pipetting steps, a Beckman Coulter FX^P Laboratory Automation Workstation was used. FKBP12, 12.6, 51 and 52 were expressed and purified in house, LpMip, TcMip and BpMip were provided by Ute Hellmich from the Friedrich Schiller University Jena. For FKBP51 and 52, only their respective Fk1 domains were used. As tracer, the fluorescent ligand **Pomplun2018-16g** developed by POMPLUN *et al.*^[57] was used. The compound was diluted in a 1:2 serial dilution in DMSO and then mixed in pseudo-duplicates with Protein and tracer in buffer (20 mM Hepes, pH 8, 0.002 % v/v Triton X-100, 150 mM NaCl) in a black, non-binding 384-well plate, and then incubated in the dark for 30 min. Polarization is measured on a Tecan Spark at room temperature with an excitation wavelength of 535 nm and an emission wavelength of 595 nm. The competition curves were visualized using GraphPad Prism 6.0, K_D values were calculated from the fitting according to KOZANY *et al.*^[45] The final parameters for each protein are shown in Table 13.

Table 13. Fit parameters for analyzing the fluorescence polarization assays.

Protein	FKBP12	FKBP12.6	FKBP51FK1	FKBP52FK1	LpMip	TcMip	BpMip
Protein concentration in nM	1	10	15	10	100	100	10
Tracer concentration in nM	0.5	1.0	1.0	1.0	1.0	1.0	1.0
Tracer K_D in nM	0.3	1.7	5.7	4.1	70	15	1.1

Homogenous Time-Resolved Fluorescence assay

HTRF assays were performed by Thomas Geiger or Wisely Oki Sugiarto. For most pipetting steps, a Beckman Coulter FX^P Laboratory Automation Workstation was used. FKBP12 and 12.6 were generated as GST-fusion proteins. As tracer, an Alexa FluorTM 647 labelled FKBP ligand of the 3,10-diazabicyclo[4.3.1]decan-2-one class was used. The compound was diluted in a 1:2 serial dilution in DMSO and then mixed with GST-tagged Protein, tracer and terbium-labelled anti-GST antibody in buffer (20 mM Hepes, pH 8, 0.002 % v/v Triton X-100, 150 mM NaCl) in a black, non-binding 384-well plate, and then incubated in the dark for 30 min. The sample is excited at 340 nm and emission is measured at 620 and 665 nm on a Tekan Spark at room temperature. The competition curves were visualized using GraphPad Prism 6, K_D values were calculated from the HTRF ratio according to KOZANY *et al.*^[45] The final parameters are shown in Table 14.

Table 14. Fit parameters for analyzing the HTRF assays.

Protein	FKBP12	FKBP12.6
Protein concentration in nM	5	5
Tracer concentration in nM	75	75
Antibody concentration in nM	0.4	0.4

Tracer K_D in nM	0.23	0.30
-----------------------------------	------	------

Nano-Bioluminescence Resonance Energy Transfer assay

NanoBRET assays were performed by Thomas Geiger in accordance to procedures previously published by GNATZY AND GEIGER *et al.*^[114] The fluorescent ligands were dissolved in Opti-MEM I Reduced Serum Media at the eightfold concentration required for the final sample. HEK293T cells expressing the FKBP-NanoLuc fusion protein were detached from the culture dish and resuspended in Opti-MEM I Reduced Serum Media. The cell number was adjusted to 4.6×10^5 cells/mL using transiently transfected cells or to 1.81×10^6 cells/mL using the stable FKBP-NanoLuc cell line. A cell-tracer mixture was prepared mixing one part of the tracer stock solution with three parts of the cell suspension (e.g. 500 μ L tracer stock solution + 1500 μ L cell suspension). Test ligands were dissolved in DMSO at thousandfold the concentration required for the final sample. This ligand stock was used to prepare a 1:2 serial dilution in DMSO. Each dilution was then diluted with Opti-MEM I Reduced Serum Media to generate a ligand dilution series with double the concentration required for the final sample. To a white non-binding 384-well assay plate (No.: 3574; Corning Life Sciences B.V., Schiphol-Rijk, Netherlands) 20 μ L of cell-tracer mixture and 20 μ L of test compound solution were added and the plate was incubated at 37 °C for two hours. Afterwards, the plate was equilibrated at room temperature for 15 minutes. For BRET detection, the Intracellular NanoGlo[®] Substrate/Inhibitor kit (No.: N2160; Promega) was used diluting the NanoBRET NanoGlo[®] Substrate 1:664 and the extracellular NanoLuc[®] inhibitor 1:2000 in Opti-MEM I Reduced Serum Media. 20 μ L of the detection solution was added per well and the plate was incubated for three minutes at room temperature. The donor emission was measured at 450 nm and the acceptor emission at 660 nm using a Clario Starplate reader (BMG Labtech, Ortenberg, Germany) or a Tecan Spark (Cailsheim, Germany). The BRET ratio and $K_{i,app}$ and $K_{D,app}$ values were calculated as shown in GNATZY AND GEIGER *et al.*^[114]

Cytotoxicity assay

Cytotoxicity assays were performed by Safa Karagöz at the Technical University Braunschweig. A549 cells were grown on RPMI + 10 % FCS at 37 °C and 5 % CO₂. The confluent cells were transferred via trypsinization process to the 96 well-plates with a number of 10^4 cells in 100 μ l volume of RPMI + 10 % FCS for each plate. The cells were grown at 37 °C and 5 % CO₂ for 24 hours. Thereafter, the culture medium was removed and substances solved in culture medium are given to the cells with a concentration ranging from 100 μ M to 3,125 μ M in a volume of 100 μ l for each well.

THP1 cells were grown under the same circumstances as A549, but in the transferring process, 100 nM PMA (phorbol-12-myristate-13-acetate) was given to the medium for the differentiation of monocytes to macrophages. After 48 hours, the medium is removed and substances were treated to the cells with the same procedure to A549.

20 μ l Resazurin solution (0.15 mg/ml Resazurin sodium salt were solved in PBS pH 7,4 and filtered through a 0.2 μ m filter) is given to each plate and incubated for 3 hours at 37 °C and 5 % CO₂. The produced resorufin is measured with 560 nm excitation / 590 nm emission filter set in a microplate fluorometer.

***L. pneumophila* Minimal Inhibitory Concentration assay**

MIC assays were performed by Safa Karagöz at the Technical University Braunschweig. *Legionella pneumophila* strain Corby was grown on YEB medium (10 g/L yeast extract, 10 g/L ACES buffer pH 6.9 supplemented with 0.4 g/L L-cysteine and 0.25 g/L iron (III) pyrophosphate) overnight at 37 °C. The bacteria were transferred at the stationary phase to 96-Well plates with the same bacterial load, starting at OD₆₀₀ = 0.05. The substances were solved in 100 μ L YEB medium with concentrations from 100 μ M to 3,125 μ M and given to the bacteria. *L. pneumophila* were grown at 37 °C in a plate shaker with 250 rpm supplemented with substances for 24h. The bacterial growth with and without substances, and with positive and negative controls were measured with OD₆₀₀ using a microplate reader. The growth of bacteria was analysed statistically.

Human Lung Tissue Explant assay

HLTE assays were performed by Safa Karagöz at the Technical University Braunschweig. Tumor-free pulmonary tissue samples of approximately 100 mg were obtained from surgery patients. The lung tissues were transferred to 12-well plates with 1 mL volume of HLTE medium (RPMI + 10 % FCS + 1 mM sodium pyruvate + 200 mM HEPES) for each plate as described by SCHEITHAUER *et al.*^[115] Samples were infected with the respective *L. pneumophila* strain and incubated at 37 °C and 5 % CO₂ for 2 h. Thereafter, the culture medium was removed and substances solved in culture medium are given to the cells with a concentration ranging from 100 μ M to 25 μ M in a volume of 1 mL for each well. For CFU determination, triplicate samples from each donor were infected. At the indicated time points, samples were weighed and homogenized in phosphate-buffered saline (PBS). Dilutions were plated on buffered charcoal-yeast extract (BCYE) and incubated at 37 °C with 5 % CO₂ for 4 days. The CFU/g of tissue were determined; means and standard deviations of results for samples were compared by using statistical analysis ANOVA.

Glutamine Synthetase activity assay

Christian Meyners modified a GS activity assay previously described by GAWRONSKI and BENSON.^[116] A serial dilution of the respective inhibitor in assay buffer (20 mM HEPES (pH 8.0), 50 mM MgCl₂) was placed in a 384-well microplate and incubated for 10 minutes with 40 nM purified His-GlnA1_{Mt}, 2.8 μM GlnA3_{Mt} or 2 μM purified His-GlnA4_{Sc}. To start the enzymatic reaction, a substrate mixture containing 25 mM sodium glutamate monohydrate, 2.5 mM ATP and 50 mM ammonium chloride or 50 mM cadaverine or 50 mM ethanolamine hydrochloride was added and the plate was incubated for 1 hour at 30 °C. The reaction was stopped by addition of an equal volume (30 μL) of a solution consisting of 2 parts 12 % w/v L-ascorbic acid in 1 M HCl and 1 part 2 % ammonium molybdate in H₂O. After 5 minutes, color development was stopped by addition of 30 μL of a solution containing 2 % sodium citrate tribasic and 2 % acetic acid in H₂O. Raw absorbance readings at 635 nm were normalized to enzymatic activity in the absence of inhibitors, and the 50 % inhibitory concentration (IC₅₀) value was determined using 4PL-fit implemented in GraphPad Prism 6.

Bacterial Growth assay

S. coelicolor growth assays were performed by Sergii Krysenko at the Eberhard Karl University Tübingen. The *S. coelicolor* M145 strain was grown in defined Evans medium (modified after EVANS *et al.*^[117]). Evans medium was supplemented with 25 mM ammonium chloride, L-glutamine or ethanolamine hydrochloride as a sole nitrogen source (as described by KRYSENKO *et al.*^[76]). Additionally, the media were supplemented with inhibitors in following final concentrations: 100 μM, 50 μM, 25 μM, 12.5 μM, 6.25 μM, 3.125 μM, 1.562 μM, 0.781 μM, 0 μM. Bacteria were incubated for 7 days at 30 °C on a rotary shaker (180 rpm). Phase-contrast microscopic pictures were taken under x400 magnification.

Crystallography

FKBP12 cocrystallization was performed by Christian Meyners at the following conditions.

Table 15. Conditions for the cocrystallization of FKBP12 with novel ligands.

Compound	1	31	77b	78a
Conditions	2.2 M (NH ₄) ₂ SO ₄ 0.2 M CdSO ₄	2.3 M (NH ₄) ₂ SO ₄ 0.1 M Na ₃ -citrate	1.32 M Na/K- tartrate 0.1 M MES pH 6.5	1.4 M Na/K- tartrate 0.1 M MES pH 6.5

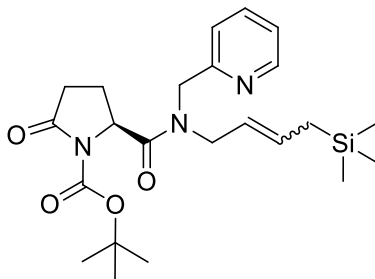
Protein and Ligand concentration	2.6 mM	2.4 mM	2.1 mM	2.1 mM
---	--------	--------	--------	--------

Crystals were fished and frozen by Christian Meyners. Analysis of the obtained crystals were performed at the Helmholtz-Zentrum BESSY II synchrotron in Berlin. Structure solution and refinement was again performed by Christian Meyners. Graphic figures were generated with the PyMol software.

5.2. Synthetic Procedures

5.2.1. Compound 4

(*S*)-tert-butyl 2-oxo-5-((pyridin-2-ylmethyl)(4-(trimethylsilyl)but-2-en-1-yl)carbamoyl)pyrrolidine-1-carboxylate



3 (2065 mg, 8809 μmol , 1.0 eq.), L-Pyroglutamic acid **6** (1145 mg, 8868, 1.0 eq.), EDC-HCl (1970 mg, 10276 μmol , 1.2 eq.) and HOBT-H₂O (1585 mg, 10350 μmol , 1.2 eq.) were dissolved in DMF (100 mL) at 0 °C under argon atmosphere. The reaction was allowed to warm to room temperature and stirred for 17 h. Brine was added to the reaction mixture and it was extracted with Et₂O. The organic phase was dried over MgSO₄, filtered and concentrated *in vacuo*.

The crude intermediate was dissolved in DCM (60 mL) and Boc₂O (11 mL, 47881 μmol , 5.4 eq.) and DIPEA (10 mL, 57408 μmol , 6.5 eq.) were added. Then DMAP was added in portions until gas formation was visible. The reaction was stirred at room temperature for 15 h, then brine was added and it was extracted with DCM. The organic phase was dried over MgSO₄, filtered and concentrated *in vacuo*. The crude product was purified twice by silica gel column chromatography (EA, then Cy/EA 1:1) to afford **4** as a mixture of *E/Z*-isomers.

Yield: 2248 mg, 57 % over two steps

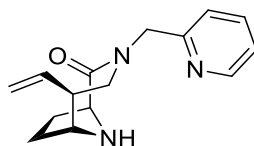
TLC: R_f = 0.36 (Cy/EA 1:1)

MS (ESI): *m/z* calculated: [M+H]⁺ = 446.25, found: [M+H]⁺ = 446.21

¹H-NMR (300 MHz, CDCl₃): δ = -0.06-0.04 (m, 9H), 1.41-1.54 (m, 11H), 1.79-2.00 (m, 1H), 2.07-2.57 (m, 2H), 2.57-2.87 (m, 1H), 3.81-4.04 (m, 1H), 4.05-4.24 (m, 1H), 4.46-4.63 (m, 1H), 4.67-4.90 (m, 1H), 4.90-4.54 (m, 1H), 5.20-5.39 (m, 1H), 5.55-5.77 (m, 1H), 7.12-7.28 (m, 1H), 7.27-7.39 (m, 1H), 7.58-7.78 (m, 1H), 8.46-8.63 (m, 1H) ppm.

5.2.2. Compound 5

(1*S*,5*S*,6*R*)-3-(pyridin-2-ylmethyl)-5-vinyl-3,9-diazabicyclo[4.2.1]nonan-2-one



4 (2187 mg, 4908 μmol , 1.0 eq.) was dissolved in dry THF (60 mL) under argon atmosphere and cooled to $-98\text{ }^\circ\text{C}$. DIBAH (1 M in THF, 8.4 mL, 8400 μmol , 1.7 eq.) was added dropwise. After stirring for 5 min at $-98\text{ }^\circ\text{C}$, Glauber's salt was added and it was allowed to warm to room temperature. The mixture was diluted with Et_2O , filtered over celite and concentrated *in vacuo*. The residue was taken up in DCM (200 mL) and cooled to $-84\text{ }^\circ\text{C}$. HF-pyridine (70 wt.-%, 14 mL, 530 mmol, 110 eq.) was added slowly and the reaction was allowed to warm to $0\text{ }^\circ\text{C}$. After 3 h the reaction was carefully quenched by addition of aqueous CaCO_3 slurry (200 mL) and NaOH (10 M, 200 mL). The mixture was filtered and extracted with DCM. The organic phase was dried over MgSO_4 , filtered and concentrated *in vacuo*. The crude product was purified twice by silica gel column chromatography (EA + 5 % MeOH + 3 % TEA, then Cy/EA 3:1 + 3 % TEA \rightarrow EA + 5 % MeOH + 3 % TEA) to afford 5.

Yield: 506 mg, 40 % over two steps

Appearance: orange oil

TLC: $R_f = 0.27$ (EA + 5 % MeOH + 3 % TEA)

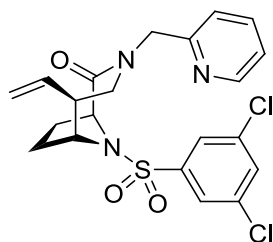
MS (ESI): m/z calculated: $[\text{M}+\text{H}]^+ = 258.16$, found: $[\text{M}+\text{H}]^+ = 258.28$

$^1\text{H-NMR}$ (500 MHz, CDCl_3): $\delta = 1.67\text{-}1.75$ (m, 1H), 1.92-2.04 (m, 2H), 2.12-2.19 (m, 1H), 2.22-2.31 (m, 1H), 3.00-3.25 (s, 1H), 3.32 (dd, 1H, $J = 14.9/4.5$ Hz), 3.51-3.56 (m, 1H), 3.59 (d, 1H, $J = 14.9$ Hz), 4.16 (d, 1H, $J = 9.8$ Hz), 4.38 (d, 1H, $J = 14.8$ Hz), 4.88 (d, 1H, $J = 14.8$ Hz), 5.00-5.09 (m, 2H), 5.69-5.79 (m, 1H), 7.10-7.16 (m, 1H), 7.23 (d, 1H, $J = 7.9$ Hz), 7.56-7.63 (m, 1H), 8.42-8.48 (m, 1H) ppm.

$^{13}\text{C-NMR}$ (125 MHz, CDCl_3): $\delta = 27.1, 30.2, 46.5, 49.8, 55.5, 60.8, 63.6, 116.8, 122.4, 122.8, 136.8, 137.6, 149.0, 157.6, 177.9$ ppm.

5.2.3. Compound 2

(1*S*,5*S*,6*R*)-9-((3,5-dichlorophenyl)sulfonyl)-3-(pyridin-2-ylmethyl)-5-vinyl-3,9-diazabicyclo[4.2.1]nonan-2-one



5 (31 mg, 121 μmol , 1.0 eq.) and 3,5-dichlorobenzenesulfonyl chloride **7** (55 mg, 222 μmol , 1.8 eq.) were dissolved in dry MeCN (15 mL) under argon atmosphere. DIPEA (50 μL , 287 μmol , 2.4 eq.) was added and the reaction was stirred at room temperature for 18 h. The solvent was evaporated *in vacuo* and the crude product was purified by silica gel column chromatography (Cy/EA 1:1) to afford **2**.

Yield: 45 mg, 80 %

Purity: 99 % (HPLC, UV-absorption 220 nm)

Appearance: colourless solid

TLC: $R_f = 0.15$ (Cy/EA 1:1)

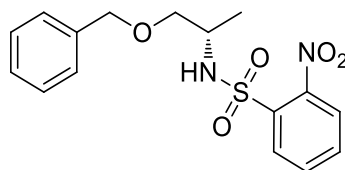
HR-MS (ESI): m/z calculated: $[\text{M}+\text{H}]^+ = 466.07534$, found: $[\text{M}+\text{H}]^+ = 466.07580$

$^1\text{H-NMR}$ (500 MHz, CDCl_3): $\delta = 1.65\text{-}1.79$ (m, 2H), 2.06-2.22 (m, 2H), 2.29-2.37 (m, 1H), 3.50-2.61 (m, 2H), 4.62 (d, 1H, $J = 15.0$ Hz), 4.75 (d, 1H, $J = 15.0$ Hz), 4.82 (dd, 1H, $J = 10.0/2.7$ Hz), 4.98 (d, 1H, $J = 10.4$ Hz), 5.07 (d, 1H, $J = 17.2$ Hz), 5.60-5.71 (m, 1H), 7.23 (dd, 1H, $J = 7.1/5.3$ Hz), 7.30 (d, 1H, $J = 7.9$ Hz), 7.55-7.58 (m, 1H), 7.68-7.72 (m, 1H), 7.73 (d, 2H, $J = 1.9$ Hz), 8.49 (d, 1H, $J = 4.8$ Hz) ppm.

$^{13}\text{C-NMR}$ (125 MHz, CDCl_3): $\delta = 28.3, 29.8, 30.3, 48.8, 50.7, 55.2, 63.7, 117.4, 122.9, 123.3, 125.6, 133.1, 136.2, 136.4, 137.8, 142.8, 148.4, 156.7, 172.3$ ppm.

5.2.4. Compound 10

(S)-N-(1-(benzyloxy)propan-2-yl)-2-nitrobenzenesulfonamide



S-2-Amino-1-propanol **9** (14.5 mL, 186.4 mmol, 1.0 eq.) was dissolved in THF (200 mL) under argon atmosphere. NaH (60 % in mineral oil, 7.49 g, 187.3 mmol, 1.0 eq.) was added and the mixture was refluxed for 30 min. Benzyl chloride (22.1 mL, 192.0 mmol, 1.0 eq.) was added and refluxed for 1 h. After cooling to room temperature, water (20 mL) was added and the solvent was evaporated. The residue was taken up in aqueous 1 M NaOH (200 mL) and extracted with DCM. The combined organic phases were dried over MgSO₄, filtered and the solvent was evaporated to afford a colourless liquid, which solidified after a short time (162 g). The crude intermediate was dissolved in MeCN (400 mL) under argon atmosphere. DIPEA (64 mL, 376.3 mmol, 2.0 eq.) and 2-nitrobenzenesulfonyl chloride (41.40 g, 186.8 mmol, 1.0 eq.) were added and the mixture was stirred at room temperature for 1 h. Aqueous 1 M NaOH (200 mL) was added and extracted with DCM. The combined organic phases were dried over MgSO₄, filtered and concentrated *in vacuo*. The crude product was purified by silica gel column chromatography (Cy/EA 5:1), crystallised from ethyl acetate and cyclohexane and the supernatant was purified again by column chromatography (Cy/EA 5:1) to afford **10**.

Yield: 38.12 g, 58 %

TLC: R_f = 0.21 (Cy/EA 3:1)

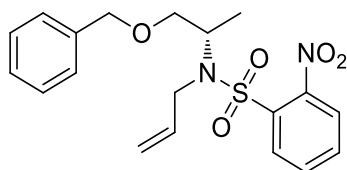
MS (ESI): m/z calculated: [M+H]⁺ = 351.10, found: [M+H]⁺ = 351.10

¹H-NMR (300 MHz, CDCl₃): δ = 1.13 (d, 1H, *J* = 6.7 Hz), 3.20–3.33 (m, 2H), 3.55–3.70 (m, 1H), 4.24 (s, 1H), 5.60 (d, 1H, *J* = 7.2 Hz), 7.03–7.11 (m, 2H), 7.14–7.25 (m, 3H), 7.49–7.61 (m, 2H), 7.66 (dd, 1H, *J* = 7.2/2.1 Hz), 8.03 (dd, 1H, *J* = 7.2/2.0 Hz) ppm.

¹³C-NMR (75 MHz, CDCl₃): δ = 18.8, 50.8, 73.2, 73.2, 125.4, 127.7, 127.8, 128.5, 130.7, 132.8, 133.3, 134.9, 137.6, 147.7 ppm.

5.2.5. Compound 11

(S)-N-allyl-N-(1-(benzyloxy)propan-2-yl)-2-nitrobenzenesulfonamide



10 (48.76 g, 139.2 mmol, 1.0 eq.) was dissolved in DMF (400 mL). K_2CO_3 (38.74 g, 280.3 mmol, 2.0 eq.) and allyl bromide (16 mL, 184.9 mmol, 1.3 eq.) were added and the mixture was stirred at 60 °C under argon atmosphere for 5 h. After cooling to room temperature, Et_2O was added and it was washed with brine. The organic phase was dried over $MgSO_4$, filtered and the solvent was evaporated. The crude product was purified by silica gel column chromatography (Cy/EA 5:1) to afford **11**.

Yield: 50.14 g, 92 %

Appearance: yellow oil

TLC: $R_f = 0.43$ (Cy/EA 3:1)

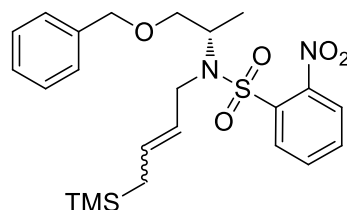
MS (ESI): m/z calculated: $[M+H]^+ = 391.13$, found: $[M+H]^+ = 391.30$

1H -NMR (300 MHz, $CDCl_3$): $\delta = 1.19$ (d, 1H, $J = 6.9$ Hz), 3.39 (dd, 1H, $J = 10.2/5.4$ Hz), 3.52 (dd, 1H, $J = 10.2/7.9$ Hz), 3.93 (qdt, 2H, $J = 16.6/6.0/1.4$ Hz), 4.16–4.29 (m, 1H), 4.30–4.42 (m, 2H), 5.02 (dq, 1H, $J = 10.2/1.3$ Hz), 5.13 (dq, 1H, $J = 17.2/1.4$ Hz), 5.71–5.88 (m, 1H), 7.15–7.22 (m, 2H), 7.22–7.32 (m, 3H), 7.39 (ddd, 1H, $J = 8.0/6.8/2.1$ Hz), 7.45–7.55 (m, 2H), 8.02 (dd, 1H, $J = 8.0/1.2$ Hz) ppm.

^{13}C -NMR (75 MHz, $CDCl_3$): $\delta = 16.8, 46.8, 53.8, 71.7, 73.0, 117.4, 123.9, 127.7, 127.8, 128.4, 131.0, 131.5, 133.2, 134.1, 136.0, 137.8, 148.1$ ppm.

5.2.6. Compound 12

(*S*)-*N*-(1-(benzyloxy)propan-2-yl)-2-nitro-*N*-(4-(trimethylsilyl)but-2-en-1-yl)benzenesulfonamide



11 (1.00 g, 2.56 mmol, 1.0 eq.), *p*-benzoquinone (33.4 mg, 309 μ mol, 0.12 eq.), Grubbs Catalyst 2nd gen. (173.4 mg, 204 μ mol, 8 mol-%) and allyltrimethylsilane (4.0 mL, 25.17 mmol, 9.8 eq.) were dissolved in DCM (25 mL) under argon atmosphere and refluxed for 6 h. Tris(hydroxymethyl)phosphine (1 M aqueous solution, 2.5 mL, 0.98 eq.) was added and refluxed over night. The reaction mixture was washed with brine, dried over MgSO₄, filtered and the solvent was evaporated. The crude product was purified by silica gel column chromatography (Cy - Cy/EA 7:1) to afford **12**.

Yield: 890 mg, 73 %

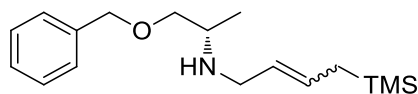
TLC: R_f = 0.41 (Cy/EA 3:1)

MS (ESI): m/z calculated: $[M+Na]^+$ = 499.17, found: $[M+Na]^+$ = 499.27

¹H-NMR (300 MHz, CDCl₃): δ = -0.02–0.04 (m, 9H), 1.26 (d, 3H, J = 7.0 Hz), 1.40 (d, 1H, J = 8.1 Hz), 1.48 (d, 1H, J = 8.8 Hz), 3.40–3.50 (m, 1H), 3.53–3.65 (m, 1H), 3.80–4.09 (m, 2H), 4.19–4.36 (m, 1H), 4.37–4.51 (m, 2H), 5.23–5.37 (m, 1H), 5.39–5.63 (m, 1H), 7.22–7.29 (m, 2H), 7.30–7.39 (m, 3H), 7.41–7.52 (m, 1H), 7.52–7.62 (m, 2H), 8.05–8.14 (m, 1H) ppm.

5.2.7. Compound 13

(*S*)-*N*-(1-(benzyloxy)propan-2-yl)-4-(trimethylsilyl)but-2-en-1-amine



12 (890 mg, 1.87 mmol, 1.0 eq.) and K_2CO_3 (647 mg, 5.99 mmol, 3.2 eq.) were dissolved in DMF (20 mL) under argon atmosphere. Thiophenol (250 μ L, 2.45 mmol, 1.3 eq.) was added and the reaction mixture was stirred at room temperature for 16 h. Et_2O was added and washed with 1 M NaOH, the organic phase was dried over $MgSO_4$, filtered and the solvent was evaporated. The crude product was purified by silica gel column chromatography (Cy - EA + 3 % TEA) to afford **13**.

Yield: 507 mg, 93 %

TLC: R_f = 0.37 (EA + 2 % MeOH + 2 % TEA)

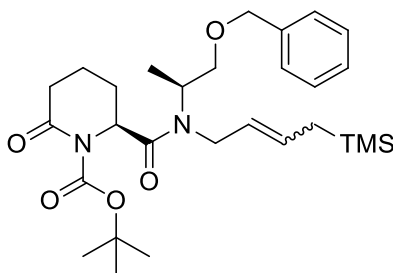
MS (ESI): m/z calculated: $[M+H]^+$ = 292.21, found: $[M+H]^+$ = 292.14

1H -NMR (300 MHz, $CDCl_3$): δ = -0.03–0.03 (m, 9H), 1.00–1.07 (m, 3H), 1.41–1.53 (m, 2H), 1.93 (s, 1H), 2.90–3.03 (m, 1H), 3.06–3.19 (m, 1H), 3.20–3.32 (m, 1H), 3.33–3.38 (m, 1H), 3.39–3.46 (m, 1H), 4.52 (s, 1H), 5.30–5.64 (m, 2H), 7.24–7.36 (m, 5H) ppm.

^{13}C -NMR (75 MHz, $CDCl_3$): δ = -1.9, 17.1, 22.8, 49.4, 51.8, 73.3, 74.9, 127.0, 127.7, 127.7, 128.4, 129.1, 138.5 ppm.

5.2.8. Compound 14

(*S*)-tert-butyl 2-(((*S*)-1-(benzyloxy)propan-2-yl)(4-(trimethylsilyl)but-2-en-1-yl)carbamoyl)-6-oxopiperidine-1-carboxylate



13 (9.11 g, 31.25 mmol, 1.0 eq.) was dissolved in DMF (200 mL) under argon atmosphere and cooled to 0 °C. *S*-6-Oxo-2-piperidinecarboxylic acid (5.81 g, 40.59 mmol, 1.3 eq.), HATU (15.87 g, 41.74 mmol, 1.3 eq.) and DIPEA (14 mL, 82.32 mmol, 2.6 eq.) were added. The reaction mixture was allowed to warm to room temperature and stirred for 19 h. Et₂O was added and washed with brine, the aqueous phase was extracted three times with Et₂O. The combined organic phases were dried over MgSO₄, filtered and the solvent was evaporated. The crude intermediate was dissolved in DCM (200 mL) under argon atmosphere, DIPEA (40 ml, 235.20 mmol, 7.5 eq.) and Boc₂O (54 mL, 235.05 mmol, 7.5 eq.) were added. DMAP was added in small portions until a continuous gas formation was visible. The reaction mixture was stirred at room temperature for 15 h. It was washed with brine and the aqueous phase was extracted three times with DCM. The combined organic phases were dried over MgSO₄, filtered and the solvent was evaporated. The crude product was purified by silica gel column chromatography (Cy/EA 5:1 + 3 % TEA) to afford **14**.

Yield: 14.65 g, 91 %

TLC: R_f = 0.51 (Cy/EA 1:1)

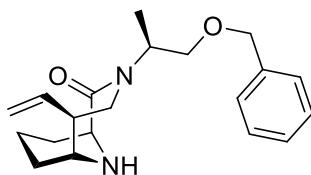
MS (ESI): *m/z* calculated: [M+Na]⁺ = 539.29, [M-Boc+H]⁺ = 417.26, found: [M+Na]⁺ = 539.34, [M-Boc+H]⁺ = 417.46

¹H-NMR (300 MHz, CDCl₃): δ = -0.06–0.06 (m, 9H), 1.19 (d, 3H, *J* = 7.0 Hz), 1.23–1.28 (m, 2H), 1.47–1.51 (m, 9H), 1.58–1.98 (m, 4H), 2.33–2.49 (m, 1H), 2.50–2.64 (m, 1H), 3.36–3.77 (m, 3H), 3.78–4.19 (m, 2H), 4.45–4.57 (m, 2H), 4.77–5.07 (m, 1H), 5.22–5.46 (m, 1H), 5.46–5.71 (m, 1H), 7.21–7.39 (m, 5H) ppm.

¹³C-NMR (75 MHz, CDCl₃): δ = -1.7, 15.2, 18.3, 22.9, 26.1, 28.1, 34.6, 47.4, 51.2, 56.4, 72.0, 73.0, 83.0, 125.0, 127.6, 127.7, 127.8, 128.4, 128.5, 130.4, 138.4, 153.6, 171.7, 171.8 ppm.

5.2.9. Compound 15

(1*S*,5*S*,6*R*)-3-((*S*)-1-(benzyloxy)propan-2-yl)-5-vinyl-3,10-diazabicyclo[4.3.1]decan-2-one



14 (15.32 g, 29.65 mmol, 1.0 eq.) was dissolved in THF (300 mL) under argon atmosphere. The solution was cooled to -98 °C and DIBAH (1 M in THF, 55 mL, 55.0 mmol, 1.9 eq.) was added dropwise. Glauber's salt was added excessively and the solution was allowed to warm to room temperature, then additional Glauber's salt was added. The mixture was diluted with Et₂O, filtered over celite and the solvent was evaporated. The crude intermediate was dissolved in DCM (600 mL) and cooled to -84 °C. Then HF-pyridine (70 wt.-%, 65 mL, 2503 mol, 84 eq.) was added and the reaction mixture was warmed to 0 °C. It was stirred at 0 °C for 3 h, then sat. aq. CaCO₃ (600 mL) and NaOH (10 M, 950 mL) was added carefully. The slurry was filtered over celite and extracted with DCM, dried over MgSO₄, filtered and concentrated *in vacuo*. The crude product was purified by silica gel column chromatography (Cy/EA 1:1 + 3 % TEA - EA + 5 % MeOH + 3 % TEA) to afford **15**.

Yield: 4.59 g, 48 %

Appearance: colourless oil

TLC: R_f = 0.35 (EA + 5 % MeOH + 3 % TEA)

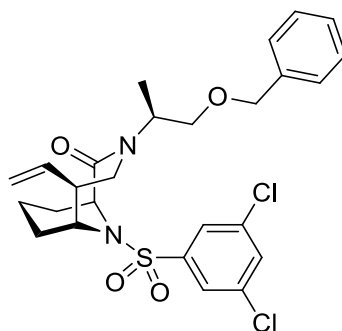
MS (ESI): m/z calculated: [M+H]⁺ = 329.22, found: [M+H]⁺ = 329.52

¹H-NMR (500 MHz, CDCl₃): δ = 1.12 (d, 3H, *J* = 6.9 Hz), 2.25–2.32 (m, 1H), 2.50 (q, 1H, *J* = 8.9 Hz), 2.78–2.83 (m, 1H), 3.00 (d, 1H, *J* = 14.1 Hz), 3.42 (dd, 1H, *J* = 10.5/5.1 Hz), 3.50 (dd, 1H, *J* = 10.5/8.1 Hz), 3.68 (dd, 1H, *J* = 14.2/10.7 Hz), 3.76–3.80 (m, 1H), 4.45 (d, 1H, *J* = 12.0 Hz), 4.55 (d, 1H, *J* = 12.1 Hz), 4.98 (s, 1H), 5.01 (d, 1H, *J* = 7.4 Hz), 5.07–5.15 (m, 1H), 5.62–5.71 (m, 1H), 7.27–7.37 (m, 5H) ppm.

¹³C-NMR (125 MHz, CDCl₃): δ = 14.5, 17.0, 28.1, 29.7, 44.4, 49.6, 50.5, 53.1, 58.2, 71.7, 72.8, 115.0, 127.8, 127.8, 128.5, 138.4, 139.4, 174.9 ppm.

5.2.10. Compound 16

(1*S*,5*S*,6*R*)-3-((*S*)-1-(benzyloxy)propan-2-yl)-10-((3,5-dichlorophenyl)sulfonyl)-5-vinyl-3,10-diazabicyclo[4.3.1]decan-2-one



15 (4.58 g, 13.9 mmol, 1.0 eq.) and 3,5-dichlorobenzenesulfonyl chloride **7** (6.58 g, 26.8 mmol, 1.9 eq.) were dissolved in MeCN (350 mL) under argon atmosphere and DIPEA (5.0 mL, 29.4 mmol, 2.1 eq.) was added. The reaction mixture was stirred for 15 h at room temperature. The solvent was evaporated and the crude product was purified by silica gel column chromatography (Cy/EA 5:1) to afford **16**.

Yield: 4.74 g, 63 %

TLC: $R_f = 0.32$ (Cy/EA 3:1)

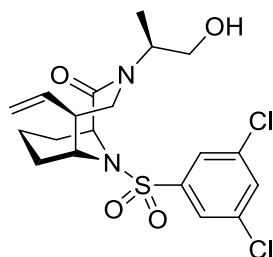
MS (ESI): m/z calculated: $[M+H]^+ = 537.14$, found: $[M+H]^+ = 537.62$

¹H-NMR (500 MHz, CDCl₃): $\delta = 1.07$ (d, 3H, $J = 6.9$ Hz), 1.10–1.29 (m, 3H), 1.38–1.51 (m, 2H), 2.22 (d, 1H, $J = 13.7$ Hz), 2.39 (q, 1H, $J = 9.2$ Hz), 2.97 (dd, 1H, $J = 14.7/1.8$ Hz), 3.34 (dd, 1H, $J = 10.2/5.1$ Hz), 3.43 (dd, 1H, $J = 10.2/7.3$ Hz), 3.66 (dd, 1H, $J = 14.6/10.6$ Hz), 3.88–3.94 (m, 1H), 4.39 (d, 1H, $J = 12.0$ Hz), 4.48 (d, 1H, $J = 12.1$ Hz), 4.63–4.69 (m, 1H), 4.86–4.95 (m, 1H), 4.96–5.05 (m, 2H), 5.65–5.75 (m, 1H), 7.18–7.22 (m, 1H), 7.24–7.30 (m, 4H), 7.46 (t, 1H, $J = 1.9$ Hz), 7.63 (d, 2H, $J = 1.8$ Hz) ppm.

¹³C-NMR (125 MHz, CDCl₃): $\delta = 14.5, 15.6, 26.4, 27.9, 45.7, 50.2, 51.2, 55.2, 57.2, 71.6, 73.0, 116.7, 125.1, 127.7, 127.7, 128.5, 132.7, 136.4, 137.6, 138.2, 144.4, 170.0$ ppm.

5.2.11. Compound 17

(1*S*,5*S*,6*R*)-10-((3,5-dichlorophenyl)sulfonyl)-3-((*S*)-1-hydroxypropan-2-yl)-5-vinyl-3,10-diazabicyclo[4.3.1]decan-2-one



16 (4295 mg, 7.99 mmol, 1.0 eq.) was dissolved in DCM (100 mL) under argon atmosphere and $\text{BCl}_3\text{-SMe}_2$ (2 M in DCM, 20 mL, 40 mmol, 5.0 eq.) was added. The reaction was stirred at room temperature for 5 h, then it was quenched with sat. aq. NaHCO_3 solution and stirred over night. It was extracted with DCM, the organic phase was dried over MgSO_4 , filtered and concentrated *in vacuo*. The crude product was purified by silica gel column chromatography (Cy/EA 1:2) to afford **17**.

Yield: 3058 mg, 86 %

Purity: >99 % (HPLC, UV-absorption 220 nm)

Appearance: yellowish solid

TLC: $R_f = 0.59$ (EA)

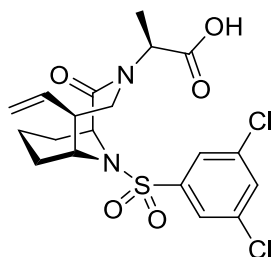
HR-MS (ESI): m/z calculated: $[\text{M}+\text{H}]^+ = 447.09066$, found: $[\text{M}+\text{H}]^+ = 447.09047$

$^1\text{H-NMR}$ (500 MHz, CDCl_3): $\delta = 1.13$ (d, 3H, $J = 6.9$ Hz), 1.19-1.29 (m, 1H), 1.33-1.43 (m, 1H), 1.50-1.60 (m, 3H), 2.28 (d, 1H, $J = 13.9$ Hz), 2.48-2.57 (m, 1H), 2.98 (dd, 1H, $J = 14.5/1.4$ Hz), 3.53-3.62 (m, 2H), 3.74 (dd, 1H, $J = 14.5/10.7$ Hz), 3.99-4.06 (m, 1H), 4.62-4.67 (m, 1H), 4.76-4.85 (m, 1H), 5.11 (d, 1H, $J = 4.7$ Hz), 5.14 (s, 1H), 5.75-5.86 (m, 1H), 7.55 (t, 1H, $J = 1.8$ Hz), 7.69 (d, 2H, $J = 1.8$ Hz) ppm.

$^{13}\text{C-NMR}$ (125 MHz, CDCl_3): $\delta = 13.9, 15.6, 26.5, 27.7, 45.5, 49.9, 54.2, 55.3, 57.2, 64.5, 117.1, 125.1, 132.9, 136.5, 137.4, 144.0, 171.3$ ppm.

5.2.12. Compound 8

(S)-2-((1S,5S,6R)-10-((3,5-dichlorophenyl)sulfonyl)-2-oxo-5-vinyl-3,10-diazabicyclo[4.3.1]decan-3-yl)propanoic acid



17 (200 mg, 447 μmol , 1.0 eq.) was dissolved in acetone (20 mL) and cooled to 0 °C. Jones reagent (450 μL , 900 μmol , 2.0 eq.) was added and the reaction was allowed to warm to room temperature. After 4 h $^i\text{PrOH}$ was added and it was stirred for 30 min to quench the reaction. The pH value of the mixture was adjusted to pH \sim 3 by adding sat. aq. NaHCO_3 solution, then it was extracted with DCM. The organic phase was dried over MgSO_4 , filtered and concentrated *in vacuo*. The crude product was purified by silica gel column chromatography (Cy/EA 2:1 + 1 % HCOOH) to afford **8**.

Yield: 197 mg, 96 %

Purity: >99 % (HPLC, UV-absorption 220 nm)

Appearance: colourless solid

TLC: $R_f = 0.51$ (Cy/EA 1:1 + 1 % HCOOH)

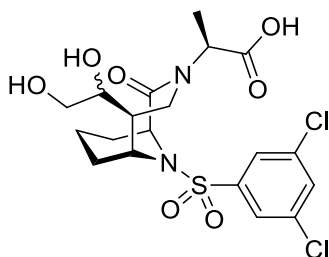
HR-MS (ESI): m/z calculated: $[\text{M}+\text{H}]^+ = 461.06992$, found: $[\text{M}+\text{H}]^+ = 461.06969$

$^1\text{H-NMR}$ (500 MHz, CDCl_3): $\delta = 1.19\text{-}1.42$ (m, 2H), 1.44 (d, 3H, $J = 7.1$ Hz), 1.49-1.63 (m, 3H), 2.25 (d, 1H, $J = 13.4$ Hz), 2.55-2.71 (m, 1H), 2.88 (dd, 1H, $J = 14.5/1.4$ Hz), 3.88-4.04 (m, 2H), 4.79 (d, 1H, $J = 5.8$ Hz), 4.96 (q, 1H, $J = 7.1$ Hz), 5.10 (s, 1H), 5.15 (d, 1H, $J = 5.4$ Hz), 5.67-5.86 (m, 1H), 7.56 (t, 1H, $J = 1.8$ Hz), 7.70 (d, 2H, $J = 1.8$ Hz), 9.17 (s, 1H) ppm.

$^{13}\text{C-NMR}$ (125 MHz, CDCl_3): $\delta = 14.5, 15.5, 26.6, 27.9, 49.7, 50.1, 55.1, 56.8, 57.5, 117.2, 125.1, 132.9, 136.5, 137.1, 144.0, 170.6, 175.8$ ppm.

5.2.13. Compound 19

(S)-2-((1S,5S,6R)-10-((3,5-dichlorophenyl)sulfonyl)-5-(1,2-dihydroxyethyl)-2-oxo-3,10-diazabicyclo[4.3.1]decan-3-yl)propanoic acid



8 (52 mg, 113 μmol , 1.0 eq.) was dissolved in acetone/water (9:1, 2 mL), then 2,6-Lutidine (38 μL , 327 μmol , 2.9 eq.), NMO (23 mg, 196 μmol , 1.7 eq.) and OsO_4 (2.5 wt.-% in $t\text{BuOH}$, 70 μL , 5.6 μmol , 5 mol-%) were added and the reaction was stirred at room temperature. After 6h additional NMO (18 mg, 154 μmol , 1.4 eq.) and OsO_4 (2.5 wt.-% in $t\text{BuOH}$, 70 μL , 5.6 μmol , 5 mol-%) were added and it was stirred for another 19 h. The reaction was quenched with sat. aq. $\text{Na}_2\text{S}_2\text{O}_3$ solution and stirred for 30 min, then the solution was acidified with 1 M HCl and extracted with EA. The organic phase extracted with 1 M NaOH, then the acidic phase was again acidified with 1 M HCl and extracted with EA. The organic phase was dried over MgSO_4 , filtered and concentrated *in vacuo*. The crude product was purified by semi-prep. HPLC (30-40 % MeCN in H_2O) to afford **19**.

Yield: 33 mg, 59 %

Purity: 98 % (HPLC, UV-absorption 220 nm)

Appearance: colourless solid

TLC: $R_f = 0.23$ (EA + 1 % HCOOH)

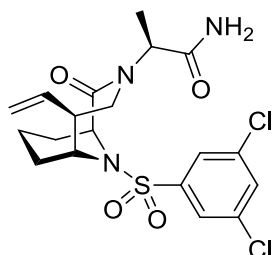
HR-MS (ESI): m/z calculated: $[\text{M}+\text{H}]^+ = 495.07540$, found: $[\text{M}+\text{H}]^+ = 495.07534$

$^1\text{H-NMR}$ (500 MHz, DMSO-d_6): $\delta = 1.11-1.25$ (m, 2H), 1.25-1.33 (m, 3H), 1.34-1.44 (m, 2H), 1.44-1.54 (m, 1H), 1.95-2.13 (m, 2H), 3.02-3.24 (m, 1H), 3.30-3.57 (m, 4H), 4.08-4.32 (m, 1H), 4.70-4.79 (m, 1H), 4.91-5.07 (m, 1H), 7.86-8.04 (m, 3H) ppm.

$^{13}\text{C-NMR}$ (125 MHz, DMSO-d_6): $\delta = 14.3, 14.8, 14.9, 26.9, 27.8, 28.0, 44.4, 45.5, 46.2, 47.3, 51.0, 51.9, 55.2, 55.3, 56.3, 56.4, 63.1, 71.7, 72.4, 125.1, 132.6, 135.4, 143.8, 168.9, 169.0, 172.4, 172.4$ ppm.

5.2.14. Compound 18

(S)-2-((1S,5S,6R)-10-((3,5-dichlorophenyl)sulfonyl)-2-oxo-5-vinyl-3,10-diazabicyclo[4.3.1]decan-3-yl)propanamide



8 (61 mg, 132 μmol , 1.0 eq.) and CDI (187 mg, 1153 μmol , 8.7 eq.) were dissolved in dry THF (15 mL) under argon atmosphere. After stirring for 3 h at room temperature NH_3 (30 wt.-% in H_2O , 850 μL , 13326 μmol , 101 eq.) was added and it was stirred for another 2 h at room temperature. Water was added and it was extracted with DCM, the organic phase was dried over MgSO_4 , filtered and concentrated *in vacuo*. The crude product was purified by silica gel column chromatography (Cy/EA 1:2) to afford **18**.

Yield: 50 mg, 82 %

Purity: >99 % (HPLC, UV-absorption 220 nm)

Appearance: colourless solid

TLC: $R_f = 0.30$ (Cy/EA 1:1 + 1 % HCOOH)

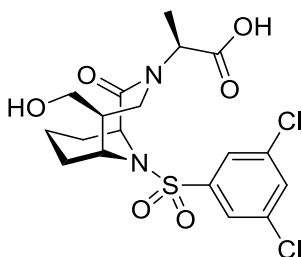
HR-MS (ESI): m/z calculated: $[\text{M}+\text{H}]^+ = 460.08591$, found: $[\text{M}+\text{H}]^+ = 460.08598$

$^1\text{H-NMR}$ (500 MHz, CDCl_3): $\delta = 1.22\text{-}1.32$ (m, 1H), 1.33 (d, 3H, $J = 7.0$ Hz), 1.36-1.46 (m, 1H), 1.49-1.63 (m, 3H), 2.26 (d, 1H, $J = 13.8$ Hz), 2.48-2.58 (m, 1H), 2.96 (dd, 1H, $J = 14.7/1.4$ Hz), 3.80 (dd, 1H, $J = 14.8/11.0$ Hz), 4.02-4.08 (m, 1H), 4.61 (d, 1H, $J = 6.1$ Hz), 5.09-5.13 (d, 1H, $J = 4.6$ Hz), 5.13-5.15 (m, 1H), 5.37 (q, 1H, $J = 7.0$ Hz), 5.67-5.81 (m, 2H), 6.22 (s, 1H), 7.56 (t, 1H, $J = 1.8$ Hz), 7.69 (d, 2H, $J = 1.8$ Hz) ppm.

$^{13}\text{C-NMR}$ (125 MHz, CDCl_3): $\delta = 13.4, 15.5, 26.6, 27.6, 46.9, 49.7, 54.5, 55.3, 57.0, 117.5, 125.1, 133.1, 136.5, 136.6, 143.7, 171.0, 172.7$ ppm.

5.2.15. Compound 20

(S)-2-((1S,5S,6R)-10-((3,5-dichlorophenyl)sulfonyl)-5-(hydroxymethyl)-2-oxo-3,10-diazabicyclo[4.3.1]decan-3-yl)propanoic acid



8 (54 mg, 117 μmol , 1.0 eq.) and NaIO_4 (106 mg, 496 μmol , 4.2 eq.) were dissolved in Dioxan/ H_2O (3:1, 15 mL). 2,6-Lutidine (25 μL , 215 μmol , 1.8 eq.) and OsO_4 (2.5 wt.-% in $t\text{BuOH}$, 70 μL , 5.6 μmol , 5 mol.-%) were added and the reaction was stirred at room temperature for 18 h. Sat. aq. $\text{Na}_2\text{S}_2\text{O}_3$ was added to quench the reaction, after stirring for 30 min it was extracted with EA. The organic phase was dried over MgSO_4 , filtered and concentrated *in vacuo*. The crude mixture was purified by silica gel column chromatography (Cy/EA 1:1 + 1 % HCOOH) to afford the intermediate aldehyde (56 mg). The intermediate was dissolved in THF (5 mL) and cooled to 0 $^\circ\text{C}$. NaBH_4 (8.8 mg, 233 μmol , 2.0 eq.) was added and the reaction was allowed to warm to room temperature. After 1 h additional NaBH_4 (8.2 mg, 217 μmol , 1.9 eq.) was added and the reaction was stirred for 20 h. It was quenched with sat. aq. NaHCO_3 , acidified with 1 M HCl and extracted with DCM. The organic phase was dried over MgSO_4 , filtered and concentrated *in vacuo*. The crude product was purified by silica gel column chromatography (Cy/EA 1:1 + 1 % HOOH \rightarrow Cy/EA 1:2 + 1 % HCOOH) followed by semi-prep. HPLC (40-100 % MeCN in H_2O) to afford **20**.

Yield: 14 mg, 26 % over two steps

Purity: 97 % (HPLC, UV-absorption 220 nm)

Appearance: colourless solid

TLC: $R_f = 0.56$ (EA + 1 % HCOOH)

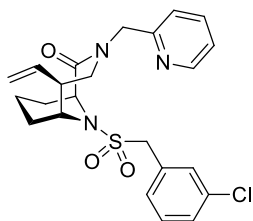
HR-MS (ESI): m/z calculated: $[\text{M}+\text{H}]^+ = 465.06484$, found: $[\text{M}+\text{H}]^+ = 465.06509$

$^1\text{H-NMR}$ (500 MHz, CDCl_3): $\delta = 1.09\text{-}1.20$ (m, 1H), 1.20-1.27 (m, 1H), 1.29 (d, 3H, $J = 7.2$ Hz), 1.34-1.51 (m, 3H), 1.97-2.07 (m, 1H), 2.13 (d, 1H, $J = 13.2$ Hz), 3.05 (dd, 1H, $J = 14.7/1.3$ Hz), 3.30-3.43 (m, 2H), 3.55 (dd, 1H, $J = 14.7/10.9$ Hz), 3.73-3.81 (m, 1H), 4.65 (m, 1H, $J = 5.8$ Hz), 5.04 (q, 1H, $J = 7.2$ Hz), 6.06 (br s, 1H), 7.44 (t, 1H, $J = 1.8$ Hz), 7.59 (d, 2H, $J = 1.8$ Hz) ppm.

$^{13}\text{C-NMR}$ (125 MHz, CDCl_3): $\delta = 14.4, 15.4, 27.7, 28.1, 45.9, 47.4, 52.3, 55.7, 56.9, 62.7, 124.8, 132.5, 136.1, 143.9, 169.6, 172.8$ ppm.

5.2.16. Compound 22

(1*S*,5*S*,6*R*)-10-((3-chlorobenzyl)sulfonyl)-3-(pyridin-2-ylmethyl)-5-vinyl-3,10-diazabicyclo[4.3.1]decan-2-one



21 (18.4 mg, 67.8 μmol , 1.0 eq.) and DMAP (31.6 mg, 259 μmol , 3.8 eq.) were dissolved in MeCN (5 mL) under argon atmosphere and cooled to 0 °C. (3-chlorophenyl)methanesulfonyl chloride **25** (75.0 mg, 333 μmol , 4.9 eq.) was dissolved in MeCN (5 mL) and added to the mixture. The reaction was allowed to warm to room temperature and was stirred for 30 h. Water was added and it was extracted with DCM, the organic phase was dried over MgSO_4 , filtered and concentrated *in vacuo*. The crude product was purified by silica gel column chromatography (DCM/MeOH 50:1 \rightarrow DCM/MeOH 20:1) to afford **22**.

Yield: 26 mg, 84 %

Purity: 99 % (HPLC, UV-absorption 220 nm)

Appearance: colourless solid

TLC: $R_f = 0.41$ (DCM/MeOH 20:1)

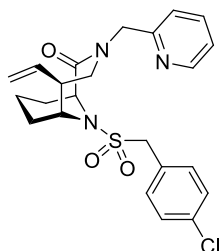
HR-MS (ESI): m/z calculated: $[\text{M}+\text{H}]^+ = 460.14562$, found: $[\text{M}+\text{H}]^+ = 460.14578$

$^1\text{H-NMR}$ (500 MHz, CDCl_3): $\delta = 1.46\text{-}1.53$ (m, 2H), 1.53-1.62 (m, 3H), 2.30 (d, 1H, $J = 13.8$ Hz), 2.58-2.68 (m, 1H), 3.03 (dd, 1H, $J = 14.1/1.7$ Hz), 3.63-3.69 (m, 1h), 4.03 (dd, 1H, $J = 14.3/11.0$ Hz), 4.22 (s, 2H), 4.44 (d, 1H, $J = 6.0$ Hz), 4.73 (d, 1H, $J = 15.5$ Hz), 4.92 (d, 1H, $J = 15.5$ Hz), 4.94 (d, 1H, $J = 17.0$ Hz), 4.97 (d, 1H, $J = 10.1$ Hz), 5.58-5.71 (m, 1H), 7.20 (t, 1H, $J = 6.1$ Hz), 7.31-7.36 (m, 3H), 7.36-7.39 (m, 1H), 7.41 (s, 1H), 7.70 (t, 1H, $J = 7.6$ Hz), 8.51 (d, 1H, $J = 4.8$ Hz) ppm.

$^{13}\text{C-NMR}$ (125 MHz, CDCl_3): $\delta = 15.6, 27.2, 28.4, 49.6, 52.2, 55.3, 56.2, 57.5, 59.1, 116.7, 122.3, 122.7, 129.0, 129.4, 130.3, 130.7, 131.0, 134.8, 137.5, 137.7, 148.7, 156.9, 171.1$ ppm.

5.2.17. Compound 23

(1*S*,5*S*,6*R*)-10-((4-chlorobenzyl)sulfonyl)-3-(pyridin-2-ylmethyl)-5-vinyl-3,10-diazabicyclo[4.3.1]decan-2-one



21 (16.3 mg, 60.1 μ mol, 1.0 eq.) and DMAP (27.4 mg, 224 μ mol, 3.8 eq.) were dissolved in MeCN (5 mL) under argon atmosphere and cooled to 0 °C. (4-chlorophenyl)methanesulfonyl chloride **26** (77.1 mg, 343 μ mol, 5.7 eq.) was dissolved in MeCN (5 mL) and added to the mixture. The reaction was allowed to warm to room temperature and was stirred for 45 h. Water was added and it was extracted with DCM, the organic phase was dried over MgSO₄, filtered and concentrated *in vacuo*. The crude product was purified by silica gel column chromatography (DCM/MeOH 50:1 → DCM/MeOH 20:1) to afford **23**.

Yield: 20 mg, 71 %

Purity: 95 % (HPLC, UV-absorption 220 nm)

Appearance: colourless solid

TLC: R_f = 0.49 (DCM/MeOH 20:1)

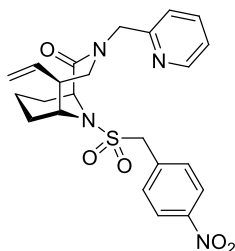
HR-MS (ESI): m/z calculated: [M+H]⁺ = 460.14562, found: [M+H]⁺ = 460.14569

¹H-NMR (500 MHz, CDCl₃): δ = 1.35-1.61 (m, 5H), 2.30 (d, 1H, *J* = 13.4 Hz), 2.57-2.67 (m, 1H), 3.03 (dd, 1H, *J* = 14.4/2.0 Hz), 3.60-3.67 (m, 1H), 4.03 (dd, 1H, *J* = 14.4/10.9 Hz), 4.22 (s, 2H), 4.42-4.47 (m, 1H), 4.72 (d, 1H, *J* = 15.4 Hz), 4.92 (d, 1H, *J* = 15.4 Hz), 4.93 (d, 1H, *J* = 17.0 Hz), 4.97 (dd, 1H, *J* = 10.1/1.2 Hz), 5.59-5.69 (m, 1H), 7.20 (dd, 1H, *J* = 7.5/4.9 Hz), 7.28-7.39 (m, 5H), 7.69 (td, 1H, *J* = 7.7/1.7 Hz), 8.51 (d, 1H, *J* = 5.0 Hz) ppm.

¹³C-NMR (125 MHz, CDCl₃): δ = 15.6, 27.2, 28.4, 49.6, 52.2, 55.2, 56.2, 57.4, 58.9, 116.7, 122.2, 122.7, 127.3, 129.2, 132.1, 135.4, 137.5, 137.6, 148.7, 156.9, 171.1 ppm.

5.2.18. Compound 24

(1*S*,5*S*,6*R*)-10-((4-nitrobenzyl)sulfonyl)-3-(pyridin-2-ylmethyl)-5-vinyl-3,10-diazabicyclo[4.3.1]decan-2-one



21 (16.3 mg, 60.1 μmol , 1.0 eq.) and DMAP (35.7 mg, 292 μmol , 4.9 eq.) were dissolved in MeCN (5 mL) under argon atmosphere and cooled to 0 °C. (4-chlorophenyl)methanesulfonyl chloride **27** (65.8 mg, 279 μmol , 4.6 eq.) was dissolved in MeCN (5 mL) and added to the mixture. The reaction was allowed to warm to room temperature and was stirred for 45 h. Water was added and it was extracted with DCM, the organic phase was dried over MgSO_4 , filtered and concentrated *in vacuo*. The crude product was purified twice by silica gel column chromatography (twice DCM/MeOH 50:1 \rightarrow DCM/MeOH 20:1) to afford **24**.

Yield: 23 mg, 82 %

Purity: >99 % (HPLC, UV-absorption 220 nm)

Appearance: colourless solid

TLC: $R_f = 0.35$ (DCM/MeOH 20:1)

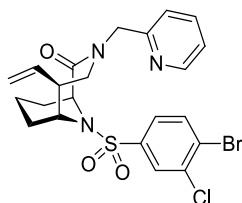
HR-MS (ESI): m/z calculated: $[\text{M}+\text{H}]^+ = 471.16967$, found: $[\text{M}+\text{H}]^+ = 471.17004$

$^1\text{H-NMR}$ (500 MHz, CDCl_3): $\delta = 1.23\text{-}1.35$ (m, 1H), 1.35-1.44 (m, 1H), 1.48-1.56 (m, 1H), 1.56-1.67 (m, 2H), 2.36 (d, 1H, $J = 13.2$ Hz), 2.60-2.71 (m, 1H), 3.05 (dd, 1H, $J = 14.4/2.0$ Hz), 3.65-3.74 (m, 1H), 4.02 (dd, 1H, $J = 14.4/10.9$ Hz), 4.33 (s, 2H), 4.52 (d, 1H, $J = 5.9$ Hz), 4.76 (d, 1H, $J = 15.3$ Hz), 4.82 (d, 1H, $J = 15.3$ Hz), 4.94 (d, 1H, $J = 17.0$ Hz), 4.98 (dd, 1H, $J = 10.1/1.2$ Hz), 5.56-5.74 (m, 1H), 7.18 (ddd, 1H, $J = 7.4/4.9/0.9$ Hz), 7.30 (d, 1H, $J = 7.9$ Hz), 7.62 (d, 2H, $J = 8.7$ Hz), 7.66 (td, 1H, $J = 7.7/1.8$ Hz), 8.25 (d, 2H, $J = 8.7$ Hz), 8.50 (d, 1H, $J = 5.0$ Hz) ppm.

$^{13}\text{C-NMR}$ (125 MHz, CDCl_3): $\delta = 15.6, 27.4, 28.7, 49.5, 52.1, 55.3, 56.3, 57.4, 59.0, 116.9, 122.1, 122.6, 124.1, 131.9, 135.9, 137.3, 137.3, 148.4, 149.1, 157.0, 170.7$ ppm.

5.2.19. Compound 29

(1*S*,5*S*,6*R*)-10-((4-bromo-3-chlorophenyl)sulfonyl)-3-(pyridin-2-ylmethyl)-5-vinyl-3,10-diazabicyclo[4.3.1]decan-2-one



(1*S*,5*S*,6*R*)-3-(pyridin-2-ylmethyl)-5-vinyl-3,10-diazabicyclo[4.3.1]decan-2-one **21** (217 mg, 800 μ mol, 1.0 eq.), 4-bromo-3-chlorobenzenesulfonyl chloride **28** (273 mg, 942 μ mol, 1.2 eq.) and ZnO (122 mg, 1499 μ mol, 1.9 eq.) were dissolved in dry MeCN (20 mL) under argon atmosphere and stirred at room temperature. After 22 h the reaction mixture was diluted with DCM, filtered over celite and concentrated *in vacuo*. The crude product was purified by silica gel column chromatography (Cy/EA 1:1) to afford **29**.

Yield: 396 mg, 94 %

Purity: >99 % (HPLC, UV-absorption 220 nm)

Appearance: colourless solid

TLC: R_f = 0.18 (Cy/EA 1:1)

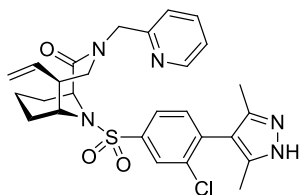
MS (ESI): m/z calculated: $[M+H]^+$ = 524.04, found: $[M+H]^+$ = 524.71

$^1\text{H-NMR}$ (300 MHz, CDCl_3): δ = 1.10–1.39 (m, 2H), 1.43–1.65 (m, 3H), 2.31 (d, 1H, J = 13.5 Hz), 2.56–2.75 (m, 1H), 3.13 (dd, 1H, J = 14.2/1.7 Hz), 3.96–4.03 (m, 1H), 4.08 (dd, 1H, J = 14.3/11.1 Hz), 4.79 (d, 1H, J = 6.2 Hz), 4.84–5.11 (m, 4H), 5.60–5.82 (m, 1H), 7.32 (dd, 1H, J = 7.5/5.3 Hz), 7.40 (d, 1H, J = 7.8 Hz), 7.56 (ddd, 1H, J = 8.4/2.2/0.4 Hz), 7.78 (d, 1H, J = 8.4 Hz), 7.81 (ddd, 1H, J = 7.7/7.7/1.7 Hz), 7.90 (d, 1H, J = 2.2 Hz), 8.66 (d, 1H, J = 4.9 Hz) ppm.

$^{13}\text{C-NMR}$ (75 MHz, CDCl_3): δ = 15.6, 26.4, 27.5, 49.1, 52.7, 54.9, 56.3, 57.0, 117.3, 123.0, 123.4, 125.6, 128.1, 128.3, 135.0, 136.2, 136.9, 138.8, 141.7, 149.3, 156.5, 172.0 ppm.

5.2.20. Compound 31

(1*S*,5*S*,6*R*)-10-((3-chloro-4-(3,5-dimethyl-1*H*-pyrazol-4-yl)phenyl)sulfonyl)-3-(pyridin-2-ylmethyl)-5-vinyl-3,10-diazabicyclo[4.3.1]decan-2-one



Aryl bromide **29** (22.0 mg, 41.9 μmol , 1.0 eq.), *tert*-butyl 3,5-dimethyl-4-(4,4,5,5-tetramethyl-1,3,2-dioxaborolan-2-yl)-1*H*-pyrazole-1-carboxylate **44** (25 mg, 77.6 μmol , 1.9 eq.), K_3PO_4 (29 mg, 137 μmol , 3.3 eq.), $\text{Pd}(\text{OAc})_2$ (2.6 mg, 11.6 μmol , 0.3 eq.) and XPhos (11 mg, 23.1 μmol , 0.6 eq.) were dissolved in THF (5 mL) under argon atmosphere and stirred at 60 °C. After 17 h, **44** (14 mg, 43.4 μmol , 1.0 eq.), $\text{Pd}(\text{OAc})_2$ (1.6 mg, 7.1 μmol , 0.2 eq.) and XPhos (7.6 mg, 15.9 μmol , 0.4 eq.) were added and the temperature was increased to 75 °C (reflux). After another 24 h, **44** (13 mg, 40.3 μmol , 1.0 eq.), $\text{Pd}(\text{OAc})_2$ (4.0 mg, 17.8 μmol , 0.4 eq.) and XPhos (16 mg, 33.6 μmol , 0.8 eq.) was added again. 24 h later water was added and it was extracted with DCM. The organic phase was dried over MgSO_4 , filtered and concentrated *in vacuo*. The crude intermediate was roughly purified by column chromatography (DCM/MeOH 50:1) to afford **162** (9.0 mg). Intermediate **162** was dissolved in DCM (5 mL). TFA (150 μL) was added and the reaction mixture was stirred at room temperature. After 65 h water was added and it was extracted with DCM. The organic phase was dried over MgSO_4 , filtered and concentrated *in vacuo*. The crude product was purified by silica gel column chromatography (twice: DCM/MeOH 20:1, then Cy/EA 1:2 + 3 % TEA \rightarrow EA + 5 % MeOH + 3 % MeOH) to afford **31**.

Yield: 3.9 mg, 17 % over 2 steps

Purity: >99 % (HPLC, UV-absorption 220 nm)

Appearance: colourless solid

TLC: $R_f = 0.24$ (DCM/MeOH 20:1)

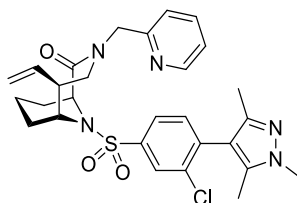
HR-MS (ESI): m/z calculated: $[\text{M}+\text{H}]^+ = 540.18306$, found: $[\text{M}+\text{H}]^+ = 540.18333$

$^1\text{H-NMR}$ (500 MHz, CDCl_3): $\delta = 1.27\text{--}1.35$ (m, 1H), 1.36–1.45 (m, 1H), 1.51–1.60 (m, 2H), 1.60–1.68 (m, 1H), 2.22 (s, 6H), 2.33 (d, 1H, $J = 13.2$ Hz), 2.68–2.78 (m, 1H), 3.13 (dd, 1H, $J = 14.0/1.5$ Hz), 4.04–4.12 (m, 2H), 4.79 (d, 1H, $J = 5.8$ Hz), 4.81–4.89 (m, 2H), 5.01 (d, 1H, $J = 17.1$ Hz), 5.05 (d, 1H, $J = 10.2$ Hz), 5.68–5.79 (m, 1H), 7.23 (dd, 1H, $J = 7.5/5.1$ Hz), 7.35–7.39 (m, 2H), 7.72 (ddd, 1H, $J = 7.6/7.5/1.8$ Hz), 7.75 (dd, 1H, $J = 8.0/1.9$ Hz), 7.97 (d, 1H, $J = 1.9$ Hz), 5.84 (d, 1H, $J = 5.0$ Hz) ppm.

¹³C-NMR (125 MHz, CDCl₃): δ = 11.4, 15.8, 26.7, 27.8, 49.3, 52.3, 54.9, 56.2, 57.0, 116.9, 122.4, 122.7, 124.9, 128.1, 133.4, 136.1, 136.7, 137.4, 137.6, 141.9, 143.0, 148.9, 157.0, 170.9 ppm.

5.2.21. Compound 32

(1*S*,5*S*,6*R*)-10-((3-chloro-4-(1,3,5-trimethyl-1*H*-pyrazol-4-yl)phenyl)sulfonyl)-3-(pyridin-2-ylmethyl)-5-vinyl-3,10-diazabicyclo[4.3.1]decan-2-one



Aryl bromide **29** (20.0 mg, 38.1 μmol , 1.0 eq.), 1,3,5-trimethyl-4-(4,4,5,5-tetramethyl-1,3,2-dioxaborolan-2-yl)-1*H*-pyrazole **163** (26 mg, 110 μmol , 2.9 eq.), K_3PO_4 (31 mg, 146 μmol , 3.8 eq.), $\text{Pd}(\text{OAc})_2$ (2.0 mg, 8.9 μmol , 0.2 eq.) and XPhos (10 mg, 21.0 μmol , 0.6 eq.) were dissolved in THF (10 mL) under argon atmosphere and refluxed at 70 °C. After 16 h additional $\text{Pd}(\text{OAc})_2$ (2.6 mg, 11.6 μmol , 0.3 eq.) and XPhos (10 mg, 21.0 μmol , 0.6 eq.) were added. After another 24 h water was added and it was extracted with DCM. The organic phase was dried over MgSO_4 , filtered and concentrated *in vacuo*. The crude product was purified by silica gel column chromatography (twice: DCM/MeOH 50:1, then EA \rightarrow EA + 5 %MeOH) to afford **32**.

Yield: 2.2 mg, 10 %

Purity: 97 % (HPLC, UV-absorption 220 nm)

Appearance: colourless solid

TLC: R_f = 0.31 (DCM/MeOH 20:1)

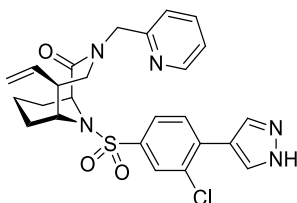
HR-MS (ESI): m/z calculated: $[\text{M}+\text{H}]^+ = 554.19872$, found: $[\text{M}+\text{H}]^+ = 554.19905$

$^1\text{H-NMR}$ (500 MHz, CDCl_3): δ = 1.20–1.38 (m, 2H), 1.37–1.49 (m, 1H), 1.59–1.71 (m, 2H), 2.12 (s, 6H), 2.30 (d, 1H, $J = 13.7$ Hz), 2.71–2.81 (m, 1H), 3.16 (d, 1H, $J = 14.2$ Hz), 3.81 (s, 3H), 4.06–4.17 (m, 2H), 4.76 (d, 1H, $J = 5.6$ Hz), 4.87 (d, 1H, $J = 15.8$ Hz), 5.02–5.11 (m, 2H), 5.69–5.80 (m, 1H), 7.35 (dd, 1H, $J = 8.1/1.4$ Hz), 7.36–7.44 (m, 1H), 7.50–7.59 (m, 1H), 7.72 (dd, 1H, $J = 8.1/2.0$ Hz), 7.85–7.96 (m, 1H), 7.94 (d, 1H, $J = 1.9$ Hz), 8.58 (d, 1H, $J = 4.9$ Hz) ppm.

$^{13}\text{C-NMR}$ (125 MHz, CDCl_3): δ = 10.7, 12.5, 15.7, 26.7, 27.7, 36.3, 49.3, 52.7, 54.9, 56.9, 117.2, 123.4, 123.4, 124.7, 128.0, 133.5, 136.0, 137.1, 141.1, 171.3 ppm.

5.2.22. Compound 33

(1*S*,5*S*,6*R*)-10-((3-chloro-4-(1*H*-pyrazol-4-yl)phenyl)sulfonyl)-3-(pyridin-2-ylmethyl)-5-vinyl-3,10-diazabicyclo[4.3.1]decan-2-one



Aryl bromide **29** (23.0 mg, 43.8 μmol , 1.0 eq.), (1-(*tert*-butoxycarbonyl)-3,5-dimethyl-1*H*-pyrazol-4-yl)boronic acid **164** (20 mg, 94.3 μmol , 2.2 eq.), K_3PO_4 (29 mg, 137 μmol , 3.1 eq.), $\text{Pd}(\text{OAc})_2$ (2.2 mg, 9.8 μmol , 0.2 eq.) and XPhos (11 mg, 23.1 μmol , 0.5 eq.) were dissolved in THF (5 mL) under argon atmosphere and stirred at 60 °C. After 65 h additional **164** (14 mg, 66.0 μmol , 1.5 eq.), $\text{Pd}(\text{OAc})_2$ (1.6 mg, 7.1 μmol , 0.2 eq.) and XPhos (10 mg, 21.0 μmol , 0.5 eq.) were added and the temperature was increased to 75 °C (reflux). Another 24 h later again **164** (12 mg, 56.6 μmol , 1.3 eq.), $\text{Pd}(\text{OAc})_2$ (3.0 mg, 13.3 μmol , 0.3 eq.) and XPhos (14 mg, 29.4 μmol , 0.7 eq.) were added and it was stirred for 24 h afterwards. Then water was added and it was extracted with DCM. The organic phase was dried over MgSO_4 , filtered and concentrated *in vacuo*. The crude intermediate was purified by column chromatography (DMC/MeOH 50:1) to afford **165** (10 mg).

Intermediate **165** was dissolved in DCM (5 mL) and TFA (150 μL) was added. The reaction mixture was stirred for 65 h, then water was added and it was extracted with DCM. The organic phase was dried over MgSO_4 , filtered and concentrated *in vacuo*. The crude product was purified by semi-preparative HPLC to afford **33**.

Yield: 1.0 mg, 4 % over two steps

Purity: 96 % (HPLC, UV-absorption 220 nm)

Appearance: colourless solid

TLC: $R_f = 0.49$ (DCM/MeOH 20:1)

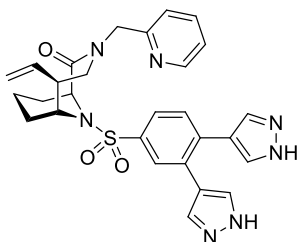
HR-MS (ESI): m/z calculated: $[\text{M}+\text{H}]^+ = 512.15176$, found: $[\text{M}+\text{H}]^+ = 512.15223$

$^1\text{H-NMR}$ (500 MHz, CDCl_3): $\delta = 1.28\text{--}1.38$ (m, 2H), 1.38–1.49 (m, 1H), 1.55–1.68 (m, 2H), 2.25 (d, 1H, $J = 13.1$ Hz), 2.77–2.87 (m, 1H), 3.17 (d, 1H, $J = 14.1$ Hz), 4.08–4.20 (m, 2H), 4.64–4.76 (m, 2H), 5.11–5.21 (m, 2H), 5.63–5.73 (m, 1H) 5.72–5.83 (m, 1H), 7.65 (d, 1H, $J = 8.2$ Hz), 7.67–7.75 (m, 2H), 7.82 (d, 1H, $J = 8.1$ Hz), 7.94 (d, 1H, $J = 1.8$ Hz), 8.14 (s, 1H), 8.26 (ddd, 1H, $J = 8.0/7.8/1.2$ Hz), 8.31 (s, 1H), 8.80 (d, 1H, $J = 5.4$ Hz), 9.20 (s, 1H) ppm.

¹³C-NMR (125 MHz, CDCl₃): δ = 15.6, 26.6, 27.4, 49.2, 53.2, 53.6, 54.9, 56.8, 117.8, 124.8, 124.9, 125.1, 128.8, 130.8, 136.4, 136.5, 140.5, 143.2, 144.1, 144.2, 154.3, 172.1 ppm.

5.2.23. Compound 38

(1*S*,5*R*,6*R*)-10-((3,4-di(1*H*-pyrazol-4-yl)phenyl)sulfonyl)-3-(pyridin-2-ylmethyl)-5-vinyl-3,10-diazabicyclo[4.3.1]decan-2-one



A side product from the Suzuki reaction in **33** was isolated where the bromine and the chlorine from **29** were both coupled (9 mg).

This intermediate was dissolved in DCM (5 mL) and TFA (150 μ L) was added. The reaction mixture was stirred for 3 d at room temperature, then water was added and it was extracted with DCM. The organic phase was dried over MgSO_4 , filtered and concentrated *in vacuo*. The crude product was purified by silica gel column chromatography twice (DCM/MeOH 20:1, then EA + 5 % MeOH + 3 % TEA \rightarrow EA + 10 % MeOH + 3 % TEA) to afford **38**.

Yield: 1.7 mg, 7 % over two steps

Purity: >99 % (HPLC, Uv-absorption 220 nm)

Appearance: colourless solid

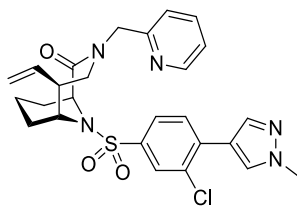
TLC: $R_f = 0.18$ (DCM/MeOH 10:1)

HR-MS (ESI): m/z calculated: $[\text{M}+\text{H}]^+ = 544.21254$, found: $[\text{M}+\text{H}]^+ = 544.21266$

$^1\text{H-NMR}$ (500 MHz, CDCl_3): $\delta = 1.40\text{-}1.60$ (m, 5H), 2.13-2.20 (m, 1H), 2.49-2.53 (m, 2H), 2.68-2.77 (m, 1H), 4.02-4.12 (m, 2H), 4.65-4.72 (m, 1H), 4.77-4.86 (m, 1H), 5.01-5.09 (m, 2H), 5.64-5.75 (m, 1H), 7.42 (d, 1H, $J = 4.2$ Hz), 7.48 (d, 1H, $J = 8.2$ Hz), 7.54-7.59 (m, 1H), 7.64 (dd, 1H, $J = 8.2/2.1$ Hz), 7.67-7.70 (m, 1H), 7.72 (d, 1H, $J = 2.0$ Hz), 8.06-8.16 (m, 1H), 8.55-8.59 (m, 1H) ppm.

5.2.24. Compound 34

(1*S*,5*S*,6*R*)-10-((3-chloro-4-(1-methyl-1*H*-pyrazol-4-yl)phenyl)sulfonyl)-3-(pyridin-2-ylmethyl)-5-vinyl-3,10-diazabicyclo[4.3.1]decan-2-one



Aryl bromide **29** (22.0 mg, 41.9 μ mol, 1.0 eq.), 1-methyl-4-(4,4,5,5-tetramethyl-1,3,2-dioxaborolan-2-yl)-1*H*-pyrazole **166** (46 mg, 221 μ mol, 5.3 eq.), K_3PO_4 (35 mg, 165 μ mol, 3.9 eq.), $Pd(OAc)_2$ (4.0 mg, 17.8 μ mol, 0.4 eq.) and XPhos (11 mg, 23.1 μ mol, 0.6 eq.) were dissolved in THF (5 mL) under argon atmosphere and stirred at 60 °C. After 19 h additional $Pd(OAc)_2$ (1.6 mg, 7.1 μ mol, 0.2 eq.) and XPhos (7.0 mg, 14.7 μ mol, 0.4 eq.) were added and the temperature was increased to 75 °C (reflux). After another 22 h water was added and it was extracted with DCM. The organic phase was dried over $MgSO_4$, filtered and concentrated *in vacuo*. The crude product was purified twice by silica gel column chromatography (DCM/MeOH 50:1 \rightarrow DCM/MeOH 20:1, then DCM/MeOH 50:1) to afford **34**.

Yield: 1.9 mg, 9 %

Purity: >99 % (HPLC, UV-absorption 220 nm)

Appearance: colourless solid

TLC: R_f = 0.43 (DCM/MeOH 20:1)

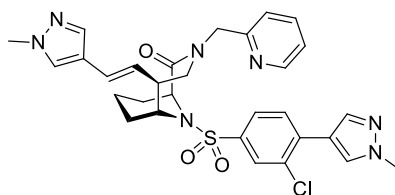
HR-MS (ESI): m/z calculated: $[M+H]^+$ = 526.16741, found: $[M+H]^+$ = 526.16760

1H -NMR (500 MHz, $CDCl_3$): δ = 1.27–1.34 (m, 1H), 1.34–1.44 (m, 1H), 1.49–1.58 (m, 2H), 1.58–1.67 (m, 1H), 2.27 (d, 1H, J = 13.5 Hz), 2.69–2.78 (m, 1H), 3.14 (d, 1H, J = 14.2 Hz), 3.91 (s, 1H), 3.99 (s, 3H), 4.04–4.12 (m, 2H), 4.77 (d, 1H, J = 6.0 Hz), 4.86 (d, 1H, J = 15.7 Hz), 5.04 (d, 1H, J = 13.6 Hz), 5.07 (d, 1H, J = 9.7 Hz), 5.68–5.80 (m, 1H), 7.32–7.40 (m, 1H), 7.46–7.52 (m, 1H), 7.61 (d, 1H, J = 8.2 Hz), 7.68 (dd, 1H, J = 8.2/1.9 Hz), 7.81–7.96 (m, 1H), 7.87 (s, 1H), 7.90 (d, 1H, J = 1.9 Hz), 7.93 (s, 1H), 8.56 (d, 1H, 5.0 Hz) ppm.

^{13}C -NMR (125 MHz, $CDCl_3$): δ = 15.7, 26.5, 27.5, 39.4, 49.3, 52.6, 53.6, 54.8, 56.9, 117.2, 118.4, 123.2, 123.3, 125.1, 126.6, 128.8, 130.2, 130.5, 132.0, 132.4, 136.2, 137.1, 137.2, 139.2, 139.8, 171.3 ppm.

5.2.25. Compound 39

(1*S*,5*S*,6*R*)-10-((3-chloro-4-(1-methyl-1*H*-pyrazol-4-yl)phenyl)sulfonyl)-5-((*E*)-2-(1-methyl-1*H*-pyrazol-4-yl)vinyl)-3-(pyridin-2-ylmethyl)-3,10-diazabicyclo[4.3.1]decan-2-one



In the synthesis of **34**, a side product was observed in which boronic ester **166** was not only coupled in a Suzuki reaction to the aryl bromide of **29** but also to the terminal alkene in a Heck reaction. This side product was purified by silica gel column chromatography (DCM/MeOH 50:1 → DCM/MeOH 20:1) to afford **39**.

Yield: 5.8 mg, 23 %

Purity: 92 % (HPLC, UV-absorption 220 nm)

Appearance: colourless solid

TLC: $R_f = 0.33$ (DCM/MeOH 20:1)

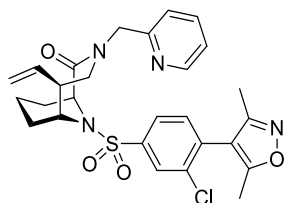
HR-MS (ESI): m/z calculated: $[M+H]^+ = 606.20486$, found: $[M+H]^+ = 606.20523$

¹H-NMR (500 MHz, CDCl₃): $\delta = 1.51$ - 1.70 (m, 5H), 2.30 (d, 1H, $J = 13.6$ Hz), 2.78-2.87 (m, 1H), 3.17 (dd, 1H, $J = 14.2/1.6$ Hz), 3.87 (s, 3H), 4.01 (s, 3H), 4.08-4.12 (m, 1H), 4.16 (dd, 1H, $J = 14.2/10.8$ Hz), 4.80 (d, 1H, $J = 6.0$ Hz), 4.85 (d, 1H, $J = 15.6$ Hz), 4.98-5.09 (m, 1H), 5.81 (dd, 1H, $J = 15.8/9.1$ Hz), 6.19 (d, 1H, $J = 15.8$ Hz), 7.29-7.35 (m, 2H), 7.42-7.48 (m, 1H), 7.50 (s, 1H), 7.63 (d, 1H, $J = 8.3$ Hz), 7.70 (dd, 1H, $J = 8.2/1.9$ Hz), 7.81-7.85 (m, 1H), 7.88 (s, 1H), 7.93 (d, 1H, $J = 1.9$ Hz), 7.94 (s, 1H), 8.56 (d, 1H, $J = 4.9$ Hz), ppm.

¹³C-NMR (125 MHz, CDCl₃): $\delta = 15.6, 26.4, 27.4, 38.9, 39.3, 48.7, 52.9, 55.2, 55.5, 56.8, 118.3, 119.7, 122.1, 122.7, 122.9, 124.9, 126.5, 127.7, 128.7, 130.1, 130.2, 132.3, 136.0, 137.2, 139.1, 139.7, 156.4, 171.0$ ppm.

5.2.26. Compound 35

(1*S*,5*S*,6*R*)-10-((3-chloro-4-(3,5-dimethylisoxazol-4-yl)phenyl)sulfonyl)-3-(pyridin-2-ylmethyl)-5-vinyl-3,10-diazabicyclo[4.3.1]decan-2-one



Aryl bromide **29** (28.0 mg, 53.3 μmol , 1.0 eq.), (3,5-dimethylisoxazol-4-yl)boronic acid **63** (9.0 mg, 63.9 μmol , 1.2 eq.), Pd(dppf)Cl₂ (5.4 mg, 6.6 μmol , 0.1 eq.) and K₂CO₃ (16.0 mg, 116 μmol , 2.2 eq.) were dissolved in dioxane/water (5:1, 1 mL, degassed) under argon atmosphere and stirred at 80 °C. After 17 h water was added and it was extracted with DCM. The organic phase was dried over MgSO₄, filtered and concentrated *in vacuo*. The crude product was purified by semi-preparative HPLC (20-75 % MeCN in water) to afford **35**.

Yield: 11.9 mg, 41 %

Purity: >99 % (HPLC, UV-absorption 220 nm)

Appearance: colourless solid

TLC: R_f = 0.41 (EA)

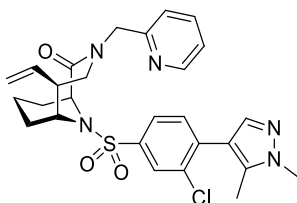
HR-MS (ESI): m/z calculated: [M+H]⁺ = 541.16708, found: [M+H]⁺ = 541.16717

¹H-NMR (500 MHz, CDCl₃): δ = 1.26–1.33 (m, 1H), 1.33–1.44 (m, 1H), 1.50–1.59 (m, 2H), 1.59–1.70 (m, 1H), 2.16 (s, 3H), 2.26–2.37 (m, 4H), 2.69–2.77 (m, 1H), 3.13 (d, 1H, *J* = 14.2 Hz), 4.01–4.12 (m, 2H), 4.74–4.91 (m, 3H), 5.00 (d, 1H, *J* = 17.1 Hz), 5.05 (d, 1H, *J* = 10.1 Hz), 5.67–5.78 (m, 1H), 7.18–7.24 (m, 1H), 7.34–7.39 (m, 1H), 7.37 (d, 1H, *J* = 8.0 Hz), 7.68–7.75 (m, 1H), 7.77 (dd, 1H, *J* = 8.0/1.9 Hz), 7.98 (d, 1H, *J* = 1.9 Hz), 8.53 (d, 1H, *J* = 4.8 Hz) ppm.

¹³C-NMR (125 MHz, CDCl₃): δ = 10.8, 12.0, 15.7, 26.7, 27.8, 49.3, 52.3, 55.0, 56.2, 57.0, 113.6, 117.0, 122.3, 122.7, 125.1, 128.3, 133.1, 134.2, 136.1, 137.4, 137.5, 142.7, 148.9, 156.9, 158.8, 166.9, 170.7 ppm.

5.2.27. Compound 36

(1*S*,5*S*,6*R*)-10-((3-chloro-4-(1,5-dimethyl-1*H*-pyrazol-4-yl)phenyl)sulfonyl)-3-(pyridin-2-ylmethyl)-5-vinyl-3,10-diazabicyclo[4.3.1]decan-2-one



Aryl bromide **29** (25.7 mg, 49.0 μmol , 1.0 eq.), 1,5-dimethyl-4-(4,4,5,5-tetramethyl-1,3,2-dioxaborolan-2-yl)-1*H*-pyrazole **61** (12.7 mg, 57.2 μmol , 1.2 eq.), Pd(dppf)Cl₂ (4.6 mg, 5.6 μmol , 0.1 eq.) and K₂CO₃ (21.2 mg, 153 μmol , 3.1 eq.) were dissolved in dioxane/water (5:1, 1 mL, degassed) under argon atmosphere and stirred at 80 °C. After 2 h water was added and it was extracted with DCM. The organic phase was dried over MgSO₄, filtered and concentrated *in vacuo*. The crude product was purified by semi-preparative HPLC (20-65 % MeCN in water) to afford **36**.

Yield: 11.2 mg, 42 %

Purity: >99 % (HPLC, UV-absorption 220 nm)

Appearance: colourless solid

TLC: R_f = 0.26 (DCM/MeOH 20:1)

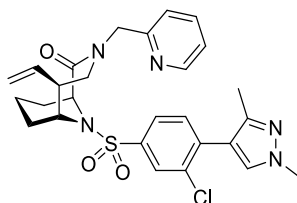
HR-MS (ESI): *m/z* calculated: [M+H]⁺ = 540.18306, found: [M+H]⁺ = 540.18290

¹H-NMR (500 MHz, CDCl₃): δ = 1.27–1.44 (d, 2H), 1.49–1.57 (m, 2H), 1.57–1.68 (m, 1H), 2.24 (s, 3H), 2.30 (d, 1H, *J* = 13.8 Hz), 2.66–2.76 (m, 1H), 3.11 (dd, 1H, *J* = 14.2/1.8 Hz), 3.87 (s, 3H), 4.02–4.12 (m, 2H), 4.79 (d, 1H, *J* = 6.0 Hz), 4.85 (s, 2H), 5.0 (d, 1H, *J* = 17.1 Hz), 5.04 (dd, 1H, *J* = 10.1/0.9 Hz), 5.67–5.78 (m, 1H), 7.22 (dd, 1H, *J* = 7.2/5.3 Hz), 7.34–7.40 (m, 2H), 7.57 (s, 1H), 7.68–7.75 (m, 2H), 7.92 (d, 1H, *J* = 1.9 Hz), 8.53 (d, 1H, *J* = 4.9 Hz) ppm.

¹³C-NMR (125 MHz, CDCl₃): δ = 10.8, 15.8, 26.5, 27.7, 36.8, 49.3, 52.3, 54.8, 56.1, 57.0, 116.8, 116.9, 122.4, 122.7, 124.8, 128.2, 132.5, 134.8, 137.0, 137.5, 137.6, 138.4, 140.8, 148.8, 157.0, 170.9 ppm.

5.2.28. Compound 37

(1*S*,5*S*,6*R*)-10-((3-chloro-4-(1,3-dimethyl-1*H*-pyrazol-4-yl)phenyl)sulfonyl)-3-(pyridin-2-ylmethyl)-5-vinyl-3,10-diazabicyclo[4.3.1]decan-2-one



Aryl bromide **29** (25.0 mg, 47.6 μ mol, 1.0 eq.), 1,3-dimethyl-4-(4,4,5,5-tetramethyl-1,3,2-dioxaborolan-2-yl)-1*H*-pyrazole **62** (15.7 mg, 70.7 μ mol, 1.5 eq.), Pd(dppf)Cl₂ (4.1 mg, 5.0 μ mol, 0.1 eq.) and K₂CO₃ (15.4 mg, 111 μ mol, 2.3 eq.) were dissolved in dioxane/water (5:1, 1 mL, degassed) under argon atmosphere and stirred at 80 °C. After 2 h water was added and it was extracted with DCM. The organic phase was dried over MgSO₄, filtered and concentrated *in vacuo*. The crude product was purified by semi-preparative HPLC (20-60 % MeCN in water) to afford **37**.

Yield: 13.1 mg, 51 %

Purity: 98 % (HPLC, UV-absorption 220 nm)

Appearance: colourless solid

TLC: R_f = 0.24 (DCM/MeOH 20:1)

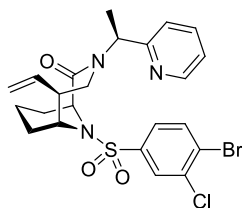
HR-MS (ESI): m/z calculated: [M+H]⁺ = 540.18306, found: [M+H]⁺ = 540.18320

¹H-NMR (500 MHz, CDCl₃): δ = 1.26–1.44 (m, 2H), 1.47–1.56 (m, 2H), 1.56–1.69 (m, 1H), 2.55 (s, 3H), 2.30 (d, 1H, *J* = 13.6 Hz), 2.67–2.75 (m, 1H), 3.11 (dd, 1H, *J* = 14.2/1.6 Hz), 3.91 (s, 3H), 4.01–4.11 (m, 2H), 4.78 (d, 1H, *J* = 5.9 Hz), 4.84 (s, 2H), 4.99 (d, 1H, *J* = 17.0 Hz), 5.04 (d, 1H, *J* = 10.2 Hz), 5.67–5.78 (m, 1H), 7.21 (dd, 1H, *J* = 6.7/5.6 Hz), 7.36 (d, 1H, *J* = 7.9 Hz), 7.43 (d, 1H, *J* = 8.1 Hz), 7.54 (s, 1H), 7.67–7.74 (m, 2H), 7.92 (d, 1H, *J* = 1.9 Hz), 8.53 (d, 1H, *J* = 4.9 Hz) ppm.

¹³C-NMR (125 MHz, CDCl₃): δ = 12.9, 15.8, 26.5, 27.7, 39.0, 49.3, 52.3, 54.8, 56.2, 57.0, 116.6, 116.9, 122.3, 122.7, 124.7, 128.2, 131.1, 132.2, 134.4, 137.3, 137.5, 140.6, 147.0, 148.9, 157.0, 170.9 ppm.

5.2.29. Compound 43

(1*S*,5*S*,6*R*)-10-((4-bromo-3-chlorophenyl)sulfonyl)-3-((*S*)-1-(pyridin-2-yl)ethyl)-5-vinyl-3,10-diazabicyclo[4.3.1]decan-2-one



(1*S*,5*S*,6*R*)-3-((*S*)-1-(pyridin-2-yl)ethyl)-5-vinyl-3,10-diazabicyclo[4.3.1]decan-2-one **42** (63 mg, 221 μ mol, 1.0 eq.) was dissolved in MeCN (12 mL) under argon atmosphere, then DIPEA (100 μ L, 588 μ mol, 2.7 eq.) and 4-bromo-3-chlorobenzene-1-sulfonyl chloride **28** (108 mg, 372 μ mol, 1.7 eq.) were added and the reaction mixture was stirred at room temperature for 3 days. The solvent was evaporated and the crude product was purified by silica gel column chromatography (Cy/EA 3:1 \rightarrow EA + 10 % MeOH + 3 % TEA) to afford **43**.

Yield: 22 mg, 18 %

Appearance: colourless solid

TLC: R_f = 0.14 (Cy/EA 3:1)

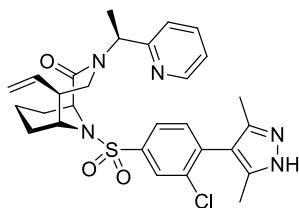
MS (ESI): m/z calculated: $[M+H]^+$ = 538.06, found: $[M+H]^+$ = 538.02

$^1\text{H-NMR}$ (500 MHz, CDCl_3): δ = 1.26-1.30 (m, 1H), 1.30-1.40 (m, 1H), 1.50-1.57 (m, 3H), 1.58 (d, 3H, J = 7.0 Hz), 2.32 (d, 1H, J = 13.6 Hz), 2.49-2.59 (m, 1H), 2.87 (dd, 1H, J = 14.7/1.5 Hz), 3.39 (dd, 1H, J = 14.7/10.8 Hz), 3.95-4.02 (m, 1H), 4.72-4.78 (m, 1H), 5.06 (dd, 1H, J = 10.2/1.0 Hz), 5.10 (dd, 1H, J = 17.0/1.0 Hz), 5.62-5.75 (m, 1H), 6.13 (q, 1H, J = 7.0 Hz), 7.21 (dd, 1H, J = 7.0/5.3 Hz), 7.28 (d, 1H, J = 7.9 Hz), 7.53 (dd, 1H, J = 8.4/2.2 Hz), 7.70 (td, 2H, J = 7.7/1.7 Hz), 7.75 (d, 1H, J = 8.4 Hz), 7.88 (d, 1H, J = 2.2 Hz), 8.56 (d, 1H, J = 4.6 Hz) ppm.

$^{13}\text{C-NMR}$ (125 MHz, CDCl_3): δ = 15.2, 15.7, 26.6, 28.0, 46.3, 50.2, 55.1, 57.1, 117.0, 122.7, 123.1, 125.6, 128.0, 128.3, 134.9, 136.2, 137.2, 137.3, 141.9, 149.7, 159.0, 170.3 ppm.

5.2.30. Compound 40

(1*S*,5*S*,6*R*)-10-((3-chloro-4-(3,5-dimethyl-1*H*-pyrazol-4-yl)phenyl)sulfonyl)-3-((*S*)-1-(pyridin-2-yl)ethyl)-5-vinyl-3,10-diazabicyclo[4.3.1]decan-2-one



Aryl bromide **43** (23.0 mg, 42.7 μ mol, 1.0 eq.), *tert*-butyl 3,5-dimethyl-4-(4,4,5,5-tetramethyl-1,3,2-dioxaborolan-2-yl)-1*H*-pyrazole-1-carboxylate **44** (30.0 mg, 93.1 μ mol, 2.2 eq.), Pd(OAc)₂ (2.0 mg, 8.9 μ mol, 0.2 eq.), XPhos (9.5 mg, 19.9 μ mol, 0.5 eq.) and K₂CO₃ (18.0 mg, 130 μ mol, 3.0 eq.) were dissolved in THF/water (9:1, 2.5 mL, degassed) under argon atmosphere and refluxed. After 6 h water was added and it was extracted with DCM. The organic phase was dried over MgSO₄, filtered and concentrated *in vacuo*. The crude intermediate was purified by silica gel column chromatography (Cy/EA 1:1 \rightarrow 1:2) to afford boc-protected **40**. The intermediate was dissolved in DCM (2 mL) and TFA (270 μ L) was added. The mixture was stirred at room temperature for 19 h, then water was added and it was extracted with DCM. The organic phase was dried over MgSO₄, filtered and concentrated *in vacuo*. The crude product was purified by semi-preparative HPLC (50-100 % MeCN in water) to afford **40**.

Yield: 16 mg, 40 % over 2 steps

Purity: 97 % (HPLC, UV-absorption 220 nm)

Appearance: colourless solid

TLC: R_f = 0.33 (EA + 5 % MeOH)

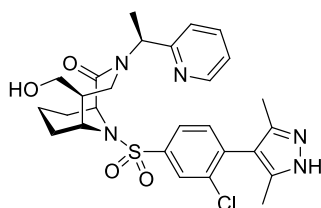
HR-MS (ESI): *m/z* calculated: [M+H]⁺ = 554.19872, found: [M+H]⁺ = 554.19908

¹H-NMR (500 MHz, CDCl₃): δ = 1.22-1.34 (m, 1H), 1.38-1.49 (m, 1H), 1.55-1.69 (m, 3H), 1.78 (d, 1H, *J* = 7.0 Hz), 2.21 (d, 1H, *J* = 13.8 Hz), 2.32 (s, 6H), 2.79-2.90 (m, 1H), 3.08 (dd, 1H, *J* = 14.2/1.4 Hz), 3.85 (dd, 1H, *J* = 14.4/10.9 Hz), 4.08-4.14 (m, 1H), 4.67 (d, 1H, *J* = 6.1 Hz), 5.15 (dd, 1H, *J* = 10.2/0.8 Hz), 5.21 (d, 1H, *J* = 17.0 Hz), 5.74-5.84 (m, 1H), 5.95 (q, 1H, *J* = 7.0 Hz), 7.40 (d, 1H, *J* = 8.1 Hz), 7.63-7.68 (m, 1H), 7.74 (d, 1H, *J* = 8.1 Hz), 7.80 (dd, 1H, *J* = 8.0/1.9 Hz), 7.99 (d, 1H, *J* = 1.9 Hz), 8.20 (td, 1H, *J* = 7.9/1.6 Hz), 8.89 (d, 1H, *J* = 5.6 Hz) ppm.

¹³C-NMR (125 MHz, CDCl₃): δ = 10.6, 15.3, 15.6, 26.9, 27.9, 48.6, 49.7, 55.2, 56.1, 57.0, 117.6, 124.5, 124.6, 125.3, 128.4, 133.4, 133.6, 136.3, 136.6, 143.1, 143.1, 143.2, 144.3, 157.3, 171.4 ppm.

5.2.31. Compound 41

(1*S*,5*S*,6*R*)-10-((3-chloro-4-(3,5-dimethyl-1*H*-pyrazol-4-yl)phenyl)sulfonyl)-5-(hydroxymethyl)-3-((*S*)-1-(pyridin-2-yl)ethyl)-3,10-diazabicyclo[4.3.1]decan-2-one



40 (9.0 mg, 16.2 μmol , 1.0 eq.) and NaIO_4 (18 mg, 84.2 μmol , 5.2 eq.) were dissolved in dioxane/water (3:1, 4 mL), then 2,6-lutidine (4.0 μL , 43.3 μmol , 2.1 eq.) and OsO_4 (2.5 wt.-% in $^t\text{BuOH}$, 11 μL , 0.8 μmol , 0.05 eq.) were added and the mixture was stirred for 23 h at room temperature. The reaction was quenched with sat. aq. $\text{Na}_2\text{S}_2\text{O}_3$ solution and extracted with EA. The organic phase was dried over MgSO_4 , filtered and concentrated *in vacuo*. The crude intermediate was purified by silica gel column chromatography (EA + 5 % MeOH) to afford the respective aldehyde (3 mg). The intermediate was dissolved in EtOH (2 mL) and cooled to 0 °C. Then NaBH_4 (1.8 mg, 47.6 μmol , 8.8 eq.) was added and the mixture was stirred for 1 h at room temperature. The reaction was quenched with sat. aq. NaHCO_3 solution and extracted with DCM. The organic phase was dried over MgSO_4 , filtered and concentrated *in vacuo*. The crude product was purified by silica gel column chromatography (DCM/MeOH 20:1 \rightarrow 15:1) to afford **41**.

Yield: 2.3 mg, 25 % over 2 steps

Purity: >99 % (HPLC, UV-absorption 220 nm)

Appearance: colourless solid

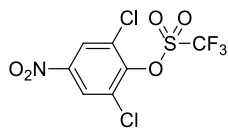
TLC: $R_f = 0.44$ (DCM/MeOH 10:1)

HR-MS (ESI): m/z calculated: $[\text{M}+\text{H}]^+ = 558.19363$, found: $[\text{M}+\text{H}]^+ = 558.19355$

$^1\text{H-NMR}$ (500 MHz, CDCl_3): $\delta = 1.29\text{-}1.38$ (m, 1H), 1.38-1.51 (m, 1H), 1.51-1.68 (m, 3H), 1.81 (d, 3H, $J = 7.0$ Hz), 2.18-2.24 (m, 2H), 2.29 (s, 3H), 2.39 (d, 1H, $J = 0.8$ Hz), 1.56-2.68 (m, 1H), 3.51-3.72 (m, 4H), 3.83-3.92 (m, 1H), 4.67-4.76 (m, 1H), 5.58 (q, 1H, $J = 6.8$ Hz), 7.35-7.44 (m, 1H), 7.52-7.58 (m, 1H), 7.67-7.73 (m, 1H), 7.73-7.79 (m, 1H), 7.92-7.99 (m, 1H), 8.04-8.11 (m, 1H), 8.66-8.73 (m, 1H) ppm.

5.2.32. Compound 46

2,6-dichloro-4-nitrophenyl trifluoromethanesulfonate



2,6-Dichloro-4-nitrophenol **45** (1027 mg, 4938 μmol , 1.0 eq.) was dissolved in dry DCM under argon atmosphere and pyridine (800 μL , 9912 μmol , 2.0 eq.) was added. The mixture was cooled to 0 °C and triflic anhydride (1 M in DCM, 5 mL, 5000 μmol , 1.0 eq.) was added dropwise. The reaction mixture was allowed to warm to room temperature and stirred for 18 h. Then, 1 M HCl was added and it was extracted with DCM. The organic phase was dried over MgSO_4 , filtered and concentrated *in vacuo*. The crude product was purified by flash silica gel column chromatography (0-20 % EA in Cy) to afford **46**.

Yield: 1528 mg (93 %)

Appearance: yellow solid

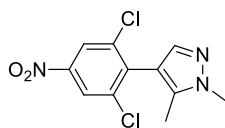
TLC: $R_f = 0.54$ (Cy/EA 9:1)

$^1\text{H-NMR}$ (500 MHz, CDCl_3): $\delta = 8.34$ (s, 2H) ppm.

$^{13}\text{C-NMR}$ (125 MHz, CDCl_3): $\delta = 118.4$ (q, $J = 321$ Hz), 125.0, 131.0, 146.5, 147.0 ppm.

5.2.33. Compound 47

4-(2,6-dichloro-4-nitrophenyl)-1,5-dimethyl-1H-pyrazole



Aryl triflate **46** (261 mg, 768 μmol , 1.0 eq.), 1,5-dimethyl-4-(4,4,5,5-tetramethyl-1,3,2-dioxaborolan-2-yl)-1H-pyrazole **61** (175 mg, 788 μmol , 1.0 eq.), Pd(dppf)Cl₂ (35 mg, 43 μmol , 5 mol-%) and K₂CO₃ (216 mg, 1563 μmol , 2.0 eq.) were dissolved in dioxane/H₂O (20:1, 10 mL, degassed with argon) under argon atmosphere and stirred at 80 °C. After 19 h water was added and it was extracted with DCM. The organic phase was dried over MgSO₄, filtered and concentrated *in vacuo*. The crude oproduct was purified by flash silica gel column chromatography (12-100 % EA in Cy) to afford **47**.

Yield: 86 mg (39 %)

Appearance: orange solid

TLC: R_f = 0.51 (Cy/EA 1:1)

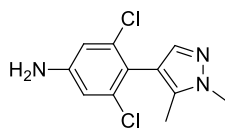
MS (ESI): m/z calculated: [M+H]⁺ = 286.0, found: [M+H]⁺ = 286.0

¹H-NMR (500 MHz, CDCl₃): δ = 2.13 (s, 3H), 3.86 (s, 3H), 7.42 (s, 1H), 8.24 (s, 2H) ppm.

¹³C-NMR (125 MHz, CDCl₃): δ = 10.7, 36.7, 113.8, 123.1, 137.3, 137.5, 138.1, 138.8, 147.0 ppm.

5.2.34. Compound 50

3,5-dichloro-4-(1,5-dimethyl-1*H*-pyrazol-4-yl)aniline



47 (86 mg, 321 μmol , 1.0 eq.) was dissolved in EtOH (10 mL), then Zn powder (238 mg, 3639 μmol , 11.3 eq.) and NH_4Cl (188 mg, 3515 μmol , 11.0 eq.) were added and the reaction mixture was stirred at room temperature for 3 h. To complete conversion, it was then refluxed for 1 h. After cooling to room temperature, the mixture was filtered and concentrated *in vacuo*. The crude product was purified by flash silica gel column chromatography (12-100 % EA in Cy) to afford **50**.

Yield: 106 mg, impure

TLC: $R_f = 0.46$ (Cy/EA 1:1)

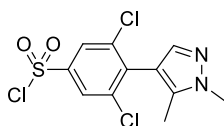
MS (ESI): m/z calculated: $[\text{M}+\text{H}]^+ = 256.0$, found: $[\text{M}+\text{H}]^+ = 256.0$

$^1\text{H-NMR}$ (500 MHz, CD_3OD): $\delta = 2.14$ (s, 3H), 3.96 (s, 3H), 6.75 (s, 2H), 7.52 (s, 1H) ppm.

$^{13}\text{C-NMR}$ (125 MHz, CD_3OD): $\delta = 10.2, 36.9, 114.7, 117.7, 117.9, 137.4, 140.9, 142.6, 151.2$ ppm.

5.2.35. Compound 53

3,5-dichloro-4-(1,5-dimethyl-1H-pyrazol-4-yl)benzene-1-sulfonyl chloride



SOCl_2 (2 mL, 27.57 mmol, 86 eq.) was dropwise added to water (6 mL) at 0 °C.

50 (82 mg, 321 μmol , 1.0 eq.) was dissolved in MeCN (10 mL) and conc. HCl (500 μL) was added. NaNO_2 (28 mg, 406 μmol , 1.3 eq.) was dissolved in water (500 μL) and added to the reaction. After 10 min the reaction was cooled to 0 °C, then the $\text{SOCl}_2/\text{H}_2\text{O}$ solution and CuCl (26 mg, 263 μmol , 0.8 eq.) were added. The reaction was allowed to warm to room temperature and stirred for 1 h. Then brine was added and it was extracted with EA. The organic phase was dried over MgSO_4 , filtered and concentrated *in vacuo*. The crude sulfonyl chloride was attempted to be purified on semi-prep. HPLC (20-100 % MeCN in H_2O) where it was hydrolysed to the sulfonic acid **167** (41 mg, 39 %).

The sulfonic acid **167** (13.7 mg, 42.7 μmol , 1.0 eq.) was dissolved in dry MeCN (2 mL) under argon atmosphere, then POCl_3 (15 μL , 164 μmol , 3.8 eq.) was added and the reaction was stirred at 55 °C. After 4 h additional POCl_3 (50 μL , 548 μmol , 12.8 eq.) was added and the reaction was stirred for another 19 h at 55 °C. Then the mixture was filtered and concentrated *in vacuo*. The crude product was purified by flash silica gel column chromatography (12-100 % EA in Cy) to afford **53**.

Yield: 8.0 mg (21 % over three steps)

TLC: $R_f = 0.41$ (Cy/EA 1:1)

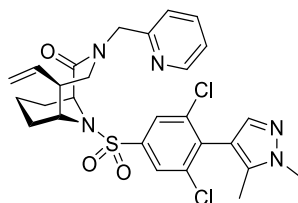
MS (ESI): m/z calculated: $[\text{M}+\text{H}]^+ = 339.0$, found: $[\text{M}+\text{H}]^+ = 339.0$

$^1\text{H-NMR}$ (500 MHz, CDCl_3): $\delta = 2.17$ (s, 3H), 3.91 (s, 3H), 7.48 (s, 1H), 8.05 (s, 2H) ppm.

$^{13}\text{C-NMR}$ (125 MHz, CDCl_3): $\delta = 10.8, 36.8, 113.8, 126.3, 137.9, 138.0, 138.0, 139.4, 144.0$ ppm.

5.2.36. Compound 56

(1*S*,5*S*,6*R*)-10-((3,5-dichloro-4-(1,5-dimethyl-1*H*-pyrazol-4-yl)phenyl)sulfonyl)-3-(pyridin-2-ylmethyl)-5-vinyl-3,10-diazabicyclo[4.3.1]decan-2-one



21 (11.5 mg, 42.4 μmol , 1.8 eq.), sulfonyl chloride **53** (8.0 mg, 23.6 μmol , 1.0 eq.) and DIPEA (15 μL , 88.2 μmol , 3.7 eq.) were dissolved in dry MeCN (1 mL) under argon atmosphere and stirred at room temperature. After 21 h the solvent was removed *in vacuo* and the crude product was purified by semi-prep. HPLC (20-60 % MeCN in H₂O) to afford **56**.

Yield: 1.9 mg (14 %)

Purity: >99 % (HPLC, UV-absorption 220 nm)

Appearance: colourless solid

TLC: $R_f = 0.20$ (DCM/MeOH 20:1)

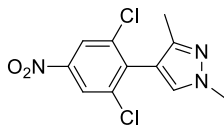
HR-MS (ESI): m/z calculated: $[\text{M}+\text{H}]^+ = 574.14409$, found: $[\text{M}+\text{H}]^+ = 574.14438$

¹H-NMR (500 MHz, CDCl₃): $\delta = 1.33\text{-}1.44$ (m, 1H), 1.44-1.55 (m, 1H), 1.56-1.74 (m, 3H), 2.15 (s, 3H), 2.30 (d, 1H, $J = 13.8$ Hz), 2.79-2.90 (m, 1H), 3.21 (d, 1H, $J = 14.1$ Hz), 3.92 (s, 3H), 4.08-4.18 (m, 2H), 4.71 (d, 1H, $J = 6.0$ Hz), 4.75 (d, 1H, $J = 16.8$ Hz), 5.13-5.23 (m, 2H), 5.71-5.83 (m, 2H), 7.52 (s, 1H), 7.72 (t, 1H, $J = 6.6$ Hz), 7.79-7.87 (m, 3H), 8.29 (t, 1H, $J = 7.9$ Hz), 8.77 (d, 1H, $J = 5.4$ Hz) ppm.

¹³C-NMR (125 MHz, CDCl₃): $\delta = 10.7, 15.5, 26.8, 27.6, 36.6, 49.3, 52.9, 53.5, 55.1, 56.9, 114.1, 118.0, 124.9, 125.0, 125.9, 126.0, 136.2, 136.4, 137.8, 137.9, 137.9, 138.2, 141.9, 142.7, 144.6, 154.1, 171.8$ ppm.

5.2.37. Compound 48

4-(2,6-dichloro-4-nitrophenyl)-1,3-dimethyl-1H-pyrazole



Aryl triflate **46** (502 mg, 1476 μmol , 1.0 eq.), 1,3-dimethyl-4-(4,4,5,5-tetramethyl-1,3,2-dioxaborolan-2-yl)-1H-pyrazole **62** (364 mg, 1639 μmol , 1.1 eq.), Pd(dppf)Cl₂ (81 mg, 99 μmol , 7 mol-%), K₂CO₃ (411 mg, 2974 μmol , 2.0 eq.) were dissolved in dioxane/H₂O (20:1, 10 mL, degassed with argon) under argon atmosphere and stirred at 80 °C. After 19 h water was added and it was extracted with DCM. The organic phase was dried over MgSO₄, filtered and concentrated *in vacuo*. The crude product was purified by flash silica gel column chromatography (12-100 % EA in Cy) to afford **48**.

Yield: 238 mg (56 %)

Appearance: orange oil

TLC: R_f = 0.40 (Cy/EA 1:1)

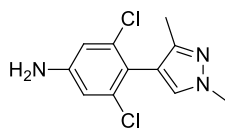
MS (ESI): m/z calculated: [M+H]⁺ = 286.0, found: [M+H]⁺ = 286.0

¹H-NMR (500 MHz, CDCl₃): δ = 2.13 (s, 3H), 3.94 (s, 3H), 7.36 (s, 1H), 8.25 (s, 2H) ppm.

¹³C-NMR (125 MHz, CDCl₃): δ = 12.5, 39.1, 114.1, 123.1, 130.8, 137.5, 138.7, 147.2, 147.2 ppm.

5.2.38. Compound 51

3,5-dichloro-4-(1,3-dimethyl-1*H*-pyrazol-4-yl)aniline



48 (238 mg, 832 μmol , 1.0 eq.) was dissolved in EtOH (10 mL), then Zn powder (547 mg, 8366 μmol , 10.1 eq.) and NH_4Cl (447 mg, 8357 μmol , 10.0 eq.) were added and the reaction mixture was refluxed for 5 h. After cooling to room temperature, the mixture was filtered and concentrated *in vacuo*. The crude product was purified by flash silica gel column chromatography (12-100 % EA in Cy) to afford **51**.

Yield: 276 mg, impure

TLC: $R_f = 0.36$ (Cy/EA 1:1)

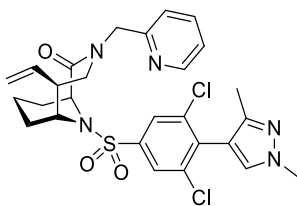
MS (ESI): m/z calculated: $[\text{M}+\text{H}]^+ = 256.0$, found: $[\text{M}+\text{H}]^+ = 256.0$

$^1\text{H-NMR}$ (500 MHz, CDCl_3): $\delta = 2.15$ (s, 3H), 3.99 (s, 3H), 6.72 (s, 2H), 7.29 (s, 1H) ppm.

$^{13}\text{C-NMR}$ (125 MHz, CDCl_3): $\delta = 12.1, 39.1, 113.9, 155.9, 118.9, 132.1, 136.4, 147.7, 148.9$ ppm.

5.2.39. Compound 57

(1*S*,5*S*,6*R*)-10-((3,5-dichloro-4-(1,3-dimethyl-1*H*-pyrazol-4-yl)phenyl)sulfonyl)-3-(pyridin-2-ylmethyl)-5-vinyl-3,10-diazabicyclo[4.3.1]decan-2-one



SOCl_2 (7.5 mL, 103387 μmol , 96 eq.) was dropwise added to water (22.5 mL) at 0 °C. Then CuCl (64 mg, 646 μmol , 0.6 eq.) was added.

51 (276 mg, 1078 μmol , 1.0 eq.) was dissolved in MeCN (20 mL) and conc. HCl (2 mL) was added. NaNO_2 (97 mg, 1406 μmol , 1.3 eq.) was dissolved in water (500 μL) and added to the reaction. After 30 min the reaction mixture was cooled to 0 °C and the aqueous $\text{SOCl}_2/\text{CuCl}$ solution was added. The reaction was allowed to warm to room temperature and stirred for 3 h. Then water was added and it was extracted with DCM. The organic phase was dried over MgSO_4 , filtered and concentrated *in vacuo*. The crude sulfonyl chloride **54** was purified by flash silica gel column chromatography and yielded 146 mg (40 %). Upon preparation of the NMR sample, the sulfonyl chloride slowly hydrolysed to the sulfonic acid **168**. The sulfonic acid was then dissolved in MeCN (10 mL) and POCl_3 (400 μL , 4383 μmol , 10.2 eq.) was added. The reaction mixture was stirred at 55 °C for 2 h, then again POCl_3 (400 μL , 4383 μmol , 10.2 eq.) was added and it was stirred at 55 °C for another 15 h. The solvent was evaporated *in vacuo* and the sulfonyl chloride **54** was purified by flash silica gel column chromatography (274 mg).

21 (14.9 mg, 54.9 μmol , 1.0 eq.) and freshly prepared **54** (42.1 mg, 124 μmol , 2.3 eq.) were dissolved in dry MeCN (1 mL) under argon atmosphere and DIPEA (24 μL , 141 μmol , 2.6 eq.) was added. The reaction mixture was stirred at room temperature for 19 h. A colourless solid precipitated from the solution, addition of DIPEA (24 μL , 141 μmol , 2.6 eq.) dissolved it again. The reaction was stirred for another 26 h at room temperature before the solvent was evaporated *in vacuo* and the crude product was purified by semi-prep. HPLC to afford **57**.

Yield: 1.7 mg (2 % over four steps)

Purity: >99 % (HPLC, UV-absorption 220 nm)

Appearance: off-white solid

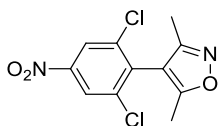
TLC: $R_f = 0.18$ (DCM/MeOH 20:1)

HR-MS (ESI): m/z calculated: $[\text{M}+\text{H}]^+ = 574.14409$, found: $[\text{M}+\text{H}]^+ = 574.14460$

¹H-NMR (500 MHz, CDCl₃): δ = 1.26-1.39 (m, 1H), 1.39-1.50 (m, 1H), 1.50-1.69 (m, 3H), 2.08 (s, 3H), 2.24 (d, 1H, *J* = 13.5 Hz), 2.78-2.87 (m, 1H), 3.22 (d, 1H, *J* = 13.9 Hz), 3.91 (s, 3H), 4.00-4.13 (m, 2H), 4.64 (d, 1H, *J* = 5.3 Hz), 4.87 (d, 1H, *J* = 16.9 Hz), 5.12 (d, 1H, *J* = 10.4 Hz), 5.16 (d, 1H, *J* = 17.1 Hz), 5.67-5.80 (m, 1H), 5.85 (d, 1H, *J* = 16.6 Hz), 7.36 (s, 1H), 7.72-7.81 (m, 3H), 7.85 (d, 1H, *J* = 7.7 Hz), 8.30-8.39 (m, 1H), 8.58-8.67 (m, 1H) ppm.

5.2.40. Compound 49

4-(2,6-dichloro-4-nitrophenyl)-3,5-dimethylisoxazole



Aryl triflate **46** (589 mg, 1732 μmol , 1.0 eq.), (3,5-dimethylisoxazol-4-yl)boronic acid **63** (274 mg, 1944 μmol , 1.1 eq.), Pd(dppf)Cl₂ (72 mg, 88 μmol , 5 mol-%) and K₂CO₃ (510 mg, 3690 μmol , 2.1 eq.) were dissolved in dioxane/H₂O (20:1, 10 mL, degassed with argon) under argon atmosphere and stirred at 80 °C. After 5 h additional Pd(dppf)Cl₂ (90 mg, 110 μmol , 6 mol-%) was added and stirring was continued at 80 °C. After 17 h water was added and it was extracted with DCM. The organic phase was dried over MgSO₄, filtered and concentrated *in vacuo*. The crude product was purified by flash silica gel column chromatography (0-20 % EA in Cy) to afford **49**.

Yield: 148 mg (30 %)

Appearance: colourless solid

TLC: R_f = 0.29 (Cy/EA 9:1)

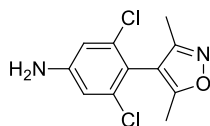
MS (ESI): m/z calculated: [M+H]⁺ = 287.0, found: [M+H]⁺ = 287.0

¹H-NMR (500 MHz, CDCl₃): δ = 2.13 (s, 3H), 2.27 (s, 3H), 8.30 (s, 2H) ppm.

¹³C-NMR (125 MHz, CDCl₃): δ = 10.7, 11.9, 111.3, 123.3, 135.3, 138.0, 148.2, 158.8, 167.5 ppm.

5.2.41. Compound 52

3,5-dichloro-4-(3,5-dimethylisoxazol-4-yl)aniline



49 (148 mg, 516 μmol , 1.0 eq.) was dissolved in EtOH (10 mL), then Zn powder (336 mg, 5139 μmol , 10.0 eq.) and NH_4Cl (273 mg, 5104 μmol , 9.9 eq.) were added and the reaction mixture was refluxed for 4 h. After cooling to room temperature, the mixture was filtered and concentrated *in vacuo*. The crude product was purified by flash silica gel column chromatography (0-35 % EA in Cy) to afford **52**.

Yield: 125 mg (94 %)

Appearance: yellowish oil

TLC: $R_f = 0.34$ (Cy/EA 3:1)

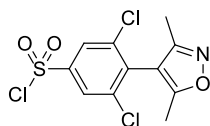
MS (ESI): m/z calculated: $[\text{M}+\text{H}]^+ = 257.0$, found: $[\text{M}+\text{H}]^+ = 257.0$

$^1\text{H-NMR}$ (500 MHz, CDCl_3): $\delta = 2.10$ (s, 3H), 2.22 (s, 3H), 6.71 (s, 2H) ppm.

$^{13}\text{C-NMR}$ (125 MHz, CDCl_3): $\delta = 10.6, 11.7, 112.5, 114.2, 116.9, 137.0, 148.2, 160.1, 167.1$ ppm.

5.2.42. Compound 55

3,5-dichloro-4-(3,5-dimethylisoxazol-4-yl)benzene-1-sulfonyl chloride



SOCl_2 (3.2 mL, 44112 μmol , 91 eq.) was slowly added to water (9 mL) at 0 °C. After stirring for 30 min, CuCl (29 mg, 293 μmol , 0.6 eq.) was added.

52 (125 mg, 486 μmol , 1.0 eq.) was dissolved in MeCN (10 mL) and conc. HCl (1 mL) and then NaNO_2 (42 mg, 609 μmol , 1.3 eq.) were added. After 10 min, the reaction mixture was cooled to 0 °C and the $\text{SOCl}_2/\text{CuCl}$ solution was added. The reaction was allowed to warm to room temperature and stirred for 3 h. Then water was added and it was extracted with DCM. The organic phase was dried over MgSO_4 , filtered and concentrated *in vacuo*. The crude product was purified on flash silica gel column chromatography to afford **55**.

Yield: 78 mg (47 %)

Appearance: yellowish oil

TLC: R_f = 0.51 (Cy/EA 5:1)

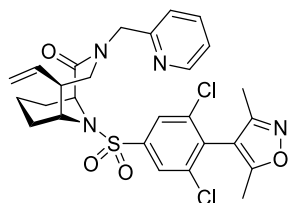
HR-MS (ESI): m/z calculated: $[\text{M}+\text{H}]^+ = 339.9$, found: $[\text{M}+\text{H}]^+ = 340.0$

$^1\text{H-NMR}$ (500 MHz, CDCl_3): δ = 2.16 (s, 3H), 2.31 (s, 3H), 8.10 (s, 2H) ppm.

$^{13}\text{C-NMR}$ (125 MHz, CDCl_3): δ = 10.7, 12.0, 111.1, 126.3, 136.1, 138.4, 145.2, 158.7, 167.6 ppm.

5.2.43. Compound 58

(1*S*,5*S*,6*R*)-10-((3,5-dichloro-4-(3,5-dimethylisoxazol-4-yl)phenyl)sulfonyl)-3-(pyridin-2-ylmethyl)-5-vinyl-3,10-diazabicyclo[4.3.1]decan-2-one



21 (13.1 mg, 48.1 μmol , 1.0 eq.) and **55** (20.4 mg, 59.9 μmol , 1.2 eq.) were dissolved in MeCN (1.5 mL), then DIPEA (20 μL , 118 μmol , 2.5 eq.) was added and the reaction mixture was stirred at room temperature for 17 h. The solvent was evaporated *in vacuo* and the crude product was purified by semi-prep. HPLC (25-65 % MeCN in H₂O) to afford **58**.

Yield: 11.8 mg (42 %)

Purity: >99 % (HPLC, UV-absorption 220 nm)

Appearance: colourless solid

TLC: R_f = 0.23 (DCM/MeOH 20:1)

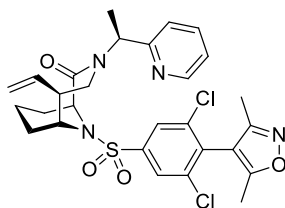
HR-MS (ESI): m/z calculated: $[\text{M}+\text{H}]^+ = 575.12811$, found: $[\text{M}+\text{H}]^+ = 575.12895$

¹H-NMR (500 MHz, CDCl₃): δ = 1.30-1.41 (m, 1H), 1.42-1.53 (m, 1H), 1.57-1.74 (m, 3H), 2.13 (s, 3H), 2.28 (s, 3H), 2.32 (d, 1H, J = 13.8 Hz), 2.78-2.89 (m, 1H), 3.18 (d, 1H, J = 14.4 Hz), 4.07-4.19 (m, 2H), 4.63-4.74 (m, 2H), 5.11-5.20 (m, 2H), 5.60 (d, 1H, J = 16.5 Hz), 5.70-5.83 (m, 1H), 7.66 (t, 1H, J = 6.5 Hz), 7.77 (d, 1H, J = 8.1 Hz), 7.86 (s, 2H), 8.21 (t, 1H, J = 8.0 Hz), 8.80 (d, 1H, J = 5.2 Hz) ppm.

¹³C-NMR (125 MHz, CDCl₃): δ = 10.7, 12.0, 15.5, 26.9, 27.7, 49.3, 53.1, 53.4, 55.2, 56.9, 111.4, 117.9, 124.6, 124.7, 126.1, 133.4, 136.3, 138.2, 143.1, 143.5, 143.9, 154.4, 158.9, 167.5, 171.5 ppm.

5.2.44. Compound 59

(1*S*,5*S*,6*R*)-10-((3,5-dichloro-4-(3,5-dimethylisoxazol-4-yl)phenyl)sulfonyl)-3-((*S*)-1-(pyridin-2-yl)ethyl)-5-vinyl-3,10-diazabicyclo[4.3.1]decan-2-one



42 (29.6 mg, 104 μ mol, 1.0 eq.) and **55** (44.3 mg, 130 μ mol, 1.3 eq.) were dissolved in dry MeCN (2 mL) and DIPEA (36 μ L, 212 μ mol, 2.0 eq.) was added. The reaction mixture was stirred for 66 h, then the solvent was evaporated *in vacuo* and the crude product was purified twice by semi-prep. HPLC (5-70 % MeCN in H₂O, then 30-70 % MeCN in H₂O) to afford **59** and recover residual **42** (13.7 mg, 46 %).

Yield: 9.8 mg (16 %, 30 % brsm.)

Purity: 99 % (HPLC, UV-absorption 220 nm)

Appearance: colourless solid

TLC: R_f = 0.69 (EA)

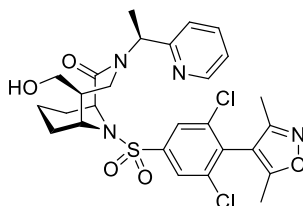
HR-MS (ESI): m/z calculated: [M+H]⁺ = 589.14376, found: [M+H]⁺ = 589.14398

¹H-NMR (500 MHz, CDCl₃): δ = 1.26-1.38 (m, 1H), 1.40-1.51 (m, 1H), 1.57-1.72 (m, 3H), 1.75 (d, 3H, *J* = 6.9 Hz), 2.12 (s, 3H), 2.21-2.31 (m, 4H), 2.78-2.89 (m, 1H), 3.08 (d, 1H, *J* = 14.3 Hz), 3.79 (dd, 1H, *J* = 14.2/11.1 Hz), 4.05-4.14 (m, 1H), 4.66 (d, 1H, *J* = 5.6 Hz), 5.15 (d, 1H, *J* = 10.1 Hz), 5.20 (d, 1H, *J* = 17.1 Hz), 5.72-5.84 (m, 1H), 5.93 (q, 1H, *J* = 6.8 Hz), 7.60 (t, 1H, *J* = 6.4 Hz), 7.69 (d, 1H, *J* = 8.1 Hz), 7.85 (s, 2H), 8.15 (t, 1H, *J* = 7.8 Hz), 8.87 (d, 1H, *J* = 5.1 Hz) ppm.

¹³C-NMR (125 MHz, CDCl₃): δ = 10.7, 12.0, 15.3, 15.5, 27.0, 28.0, 48.5, 49.7, 55.3, 56.2, 57.1, 111.4, 117.7, 124.3, 124.5, 126.1, 133.3, 136.5, 138.2, 142.6, 143.2, 144.6, 157.5, 158.9, 167.5, 171.1 ppm.

5.2.45. Compound 60

(1*S*,5*S*,6*R*)-10-((3,5-dichloro-4-(3,5-dimethylisoxazol-4-yl)phenyl)sulfonyl)-5-(hydroxymethyl)-3-((*S*)-1-(pyridin-2-yl)ethyl)-3,10-diazabicyclo[4.3.1]decan-2-one



59 (6.2 mg, 11.0 μ mol, 1.0 eq.) was dissolved in dioxane/H₂O (3:1, 400 μ L) and 2,6-lutidine (3 μ L, 25.8 μ mol, 2.3 eq.) was added. The mixture was cooled to 0 °C, then OsO₄ (2.5 wt-% in ^tBuOH, 6 μ L, 4 mol-%), and NaIO₄ (13 mg, 60.8 μ mol, 5.5 eq.) were added and the reaction was allowed to warm to room temperature. After 20 h the reaction was quenched by addition of sat. aq. Na₂S₂O₃ solution and stirring for 30 min. The mixture was extracted with EA, the organic phase was dried over MgSO₄, filtered and concentrated *in vacuo* to yield the corresponding aldehyde as a colourless oil (7.5 mg).

The crude intermediate was dissolved in EtOH (1 mL) under argon atmosphere, cooled to 0 °C and NaBH₄ (4.4 mg, 116 μ mol, 10.5 eq.) was added. The reaction was allowed to warm to room temperature and stirred for 50 min. The solvent was evaporated *in vacuo* and the crude product was purified by semi-prep. HPLC (30-70 % MeCN in H₂O) to afford **60**.

Yield: 2.9 mg (47 % over two steps)

Purity: >99 % (HPLC, UV-absorption 220 nm)

Appearance: colourless solid

TLC: R_f = 0.51 (DCM/MeOH 10:1)

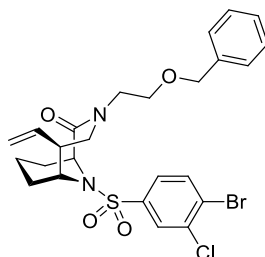
HR-MS (ESI): m/z calculated: [M+H]⁺ = 593.13867, found: [M+H]⁺ = 583.13900

¹H-NMR (500 MHz, CDCl₃): δ = 1.27-1.39 (m, 1H), 1.42-1.54 (m, 1H), 1.54-1.70 (m, 3H), 1.82 (d, 3H, *J* = 7.0 Hz), 2.12 (s, 3H), 2.19 (d, 1H, *J* = 2.15-2.23 (m, 1H), 2.27 (s, 3H), 2.50-2.62 (m, 1H), 3.54-3.68 (m, 4H), 3.84-3.92 (m, 1H), 4.65 (d, 1H, *J* = 5.5 Hz), 5.78 (q, 1H, *J* = 6.8 Hz), 7.70 (t, 1H, *J* = 6.5 Hz), 7.80-7.86 (m, 3H), 8.25 (t, 1H, *J* = 8.8 Hz), 8.88 (d, 1H, *J* = 5.4 Hz) ppm.

¹³C-NMR (125 MHz, CDCl₃): δ = 10.7, 12.0, 14.5, 15.6, 28.2, 28.2, 46.8, 47.8, 52.5, 56.9, 57.2, 63.2, 111.4, 124.8, 125.8, 126.1, 133.3, 138.2, 143.2, 143.5, 143.8, 156.8, 158.9, 167.5, 171.0 ppm.

5.2.46. Compound 65

(1*S*,5*S*,6*R*)-3-(2-(benzyloxy)ethyl)-10-((4-bromo-3-chlorophenyl)sulfonyl)-5-vinyl-3,10-diazabicyclo[4.3.1]decan-2-one



64 (185 mg, 588 μmol , 1.0 eq.) was dissolved in MeCN (20 mL) under argon atmosphere, then DIPEA (200 μL , 1176 μmol , 2.0 eq.) and 4-bromo-3-chlorobenzenesulfonyl chloride **28** (330 mg, 1138 μmol , 1.9 eq.) were added and the reaction was stirred at room temperature for 18 h. The solvent was evaporated and the crude product was purified by silica gel column chromatography (Cy/EA 4:1 \rightarrow Cy/EA 2:1) to afford **65**.

Yield: 196 mg, 59 %

TLC: R_f = 0.20 (Cy/EA 3:1)

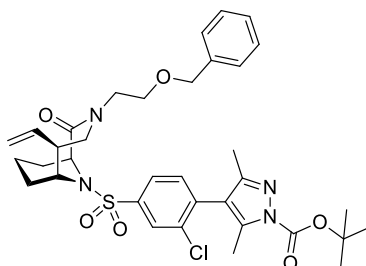
MS (ESI): m/z calculated: $[\text{M}+\text{H}]^+ = 567.07$, found: $[\text{M}+\text{H}]^+ = 567.94$

$^1\text{H-NMR}$ (500 MHz, CDCl_3): δ = 1.11-1.41 (m, 2H), 1.41-1.59 (m, 3H), 2.27 (d, 1H, $J = 12.7$ Hz), 2.63-2.79 (m, 1H), 3.14 (d, 1H, $J = 14.2$ Hz), 3.37-3.51 (m, 1H), 3.59-3.69 (m, 1H), 3.69-3.80 (m, 1H), 3.92-4.04 (m, 2H), 4.04-4.21 (m, 1H), 4.55 (s, 2H), 4.71 (d, 1H, $J = 4.7$ Hz), 4.95 (d, 1H, $J = 17.1$ Hz), 5.05 (d, 1H, $J = 10.2$ Hz), 5.66-5.85 (m, 1H), 7.27-7.42 (m, 5H), 7.58 (d, 1H, $J = 8.4$ Hz), 7.81 (d, 1H, $J = 8.4$ Hz), 7.93 (s, 1H) ppm.

$^{13}\text{C-NMR}$ (125 MHz, CDCl_3): δ = 15.6, 26.6, 27.8, 49.2, 52.0, 53.3, 54.9, 57.0, 69.0, 73.6, 116.6, 125.7, 127.9, 128.1, 128.4, 128.5, 134.9, 136.1, 137.6, 138.1, 142.0, 170.1 ppm.

5.2.47. Compound 66

tert-butyl 4-(4-(((1*S*,5*S*,6*R*)-3-(2-(benzyloxy)ethyl)-2-oxo-5-vinyl-3,10-diazabicyclo[4.3.1]decan-10-yl)sulfonyl)-2-chlorophenyl)-3,5-dimethyl-1*H*-pyrazole-1-carboxylate



65 (196 mg, 345 μ mol, 1.0 eq.), *tert*-butyl 3,5-dimethyl-4-(4,4,5,5-tetramethyl-1,3,2-dioxaborolan-2-yl)-1*H*-pyrazole-1-carboxylate **44** (249 mg, 773 μ mol, 2.2 eq.), Pd(OAc)₂ (4.6 mg, 20 μ mol, 6 mol-%), XPhos (23.9 mg, 50 μ mol, 14 mol-%) and K₂CO₃ (108 mg, 1019 μ mol, 3.0 eq.) were dissolved in THF/H₂O (9:1, 20 mL, degassed with argon) under argon atmosphere. The reaction was refluxed for 18 h, then water was added and it was extracted with DCM. The organic phase was dried over MgSO₄, filtered and concentrated *in vacuo*. The crude product was purified by silica gel column chromatography (Cy/EA 2:1 → EA) to afford **66**.

Yield: 178 mg, 75 %

TLC: R_f = 0.21 (Cy/EA 2:1)

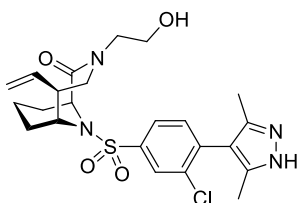
HR-MS (ESI): *m/z* calculated: [M+H]⁺ = 683.26646, found: [M+H]⁺ = 683.26650

¹H-NMR (500 MHz, CDCl₃): δ = 1.17-1.22 (m, 1H), 1.30-1.37 (m, 1H), 1.44-1.52 (m, 3H), 1.66 (s, 9H), 2.13 (s, 3H), 2.22-2.26 (m, 1H), 2.32 (s, 3H), 2.64-2.72 (m, 1H), 3.11 (d, 1H, *J* = 14.1 Hz), 3.34-3.43 (m, 1H), 3.58-3.65 (m, 1H), 3.66-3.73 (m, 1H), 3.91-4.02 (m, 2H), 4.06-4.14 (m, 1H), 4.46-4.54 (m, 2H), 4.69 (d, 1H, *J* = 5.8 Hz), 4.90 (d, 1H, *J* = 17.1 Hz), 5.00 (d, 1H, *J* = 10.2 Hz), 5.68-5.77 (m, 1H), 7.26-7.35 (m, 6H), 7.73 (dd, 1H, *J* = 8.0/1.9 Hz), 7.94 (d, 1H, *J* = 1.8 Hz) ppm.

¹³C-NMR (125 MHz, CDCl₃): δ = 13.0, 13.7, 15.6, 25.0, 25.0, 26.8, 27.9, 28.1, 49.2, 52.0, 53.3, 54.9, 56.9, 69.0, 73.6, 85.4, 116.5, 120.3, 124.9, 127.9, 128.1, 128.5, 133.3, 136.2, 137.6, 138.1, 141.9, 142.3, 148.7, 150.5, 170.2 ppm.

5.2.48. Compound 67

(1*S*,5*S*,6*R*)-10-((3-chloro-4-(3,5-dimethyl-1*H*-pyrazol-4-yl)phenyl)sulfonyl)-3-(2-hydroxyethyl)-5-vinyl-3,10-diazabicyclo[4.3.1]decan-2-one



66 (111 mg, 163 μmol , 1.0 eq.) was dissolved in DCM (10 mL) under argon atmosphere. $\text{BCl}_3\text{-SMe}_2$ (2 M in DCM, 750 μL , 1500 μmol , 9.2 eq.) was added and the reaction was stirred at room temperature for 3 d. It was quenched with sat. aq. NaHCO_3 and extracted with DCM. The organic phase was dried over MgSO_4 , filtered and concentrated *in vacuo*. The crude product was purified by silica gel column chromatography (EA \rightarrow EA + 5 % MeOH) to afford **67**.

Yield: 42 mg, 52 %

Appearance: colourless solid

TLC: $R_f = 0.19$ (EA + 5 % MeOH)

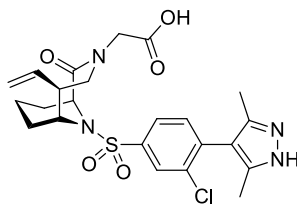
HR-MS (ESI): m/z calculated: $[\text{M}+\text{H}]^+ = 493.16708$, found: $[\text{M}+\text{H}]^+ = 493.16741$

$^1\text{H-NMR}$ (500 MHz, CDCl_3): $\delta = 1.21\text{-}1.32$ (m, 1H), $1.33\text{-}1.43$ (m, 1H), $1.51\text{-}1.70$ (m, 3H), $2.18\text{-}2.25$ (m, 6H), 2.28 (d, 1H, $J = 12.6$ Hz), $2.71\text{-}2.81$ (m, 1H), 3.02 (dd, 1H, $J = 14.2/1.4$ Hz), 3.39 (dt, 1H, $J = 14.1/4.2$ Hz), $3.74\text{-}3.86$ (m, 2H), $3.90\text{-}3.98$ (m, 1H), $4.02\text{-}4.08$ (m, 1H), 4.17 (dd, 1H, $J = 14.3/11.0$ Hz), 4.72 (d, 1H, $J = 5.8$ Hz), $5.10\text{-}5.19$ (m, 2H), $5.75\text{-}5.87$ (m, 1H), 7.38 (d, 1H, $J = 8.1$ Hz), 7.75 (dd, 1H, $J = 8.0/1.6$ Hz), 7.96 (d, 1H, $J = 1.6$ Hz) ppm.

$^{13}\text{C-NMR}$ (125 MHz, CDCl_3): $\delta = 11.4, 15.7, 26.5, 27.7, 49.4, 53.0, 54.5, 55.0, 57.0, 61.2, 117.2, 124.9, 125.0, 128.2, 133.4, 136.1, 137.4, 141.7, 141.8, 142.9, 172.3$ ppm.

5.2.49. Compound 68

2-((1*S*,5*S*,6*R*)-10-((3-chloro-4-(3,5-dimethyl-1*H*-pyrazol-4-yl)phenyl)sulfonyl)-2-oxo-5-vinyl-3,10-diazabicyclo[4.3.1]decan-3-yl)acetic acid



67 (42 mg, 85 μ mol, 1.0 eq.) was dissolved in acetone (4 mL) and cooled to 0 °C. Jones reagent (85 μ L, 170 μ mol, 2.0 eq.) was added and the reaction was allowed to warm to room temperature. After 17 h it was quenched with ⁱPrOH, stirred for another 30 min, then water was added and it was extracted with DCM. The organic phase was dried over MgSO₄, filtered and concentrated *in vacuo*. The crude product was purified by silica gel column chromatography (EA + 1 % HCOOH) and semi-prep. HPLC (5-100 % MeCN in H₂O) to afford **68**.

Yield: 9 mg, 21 %

Purity: 94 % (HPLC, UV-absorption 220 nm)

Appearance: colourless solid

TLC: R_f = 0.37 (EA + 1 % HCOOH)

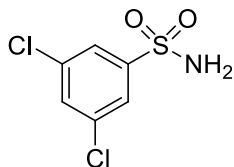
HR-MS (ESI): m/z calculated: [M+H]⁺ = 507.14635, found: [M+H]⁺ = 507.14675

¹H-NMR (500 MHz, CDCl₃): δ = 1.22-1.41 (m, 2H), 1.50-1.64 (m, 2H), 1.64-1.77 (m, 1H), 2.25 (d, 1H, *J* = 12.8 Hz), 2.34 (s, 6H), 2.95 (d, 1H, *J* = 13.8 Hz), 2.98-3.07 (m, 1H), 4.00-4.08 (m, 2H), 4.22 (dd, 1H, *J* = 14.2/10.9 Hz), 4.48 (d, 1H, *J* = 17.5 Hz), 4.81 (d, 1H, *J* = 5.8 Hz), 5.10-5.21 (m, 2H), 5.73-5.86 (m, 1H), 7.42 (d, 1H, *J* = 8.0 Hz), 7.81 (dd, 1H, *J* = 8.0/1.6 Hz), 8.00 (d, 1H, *J* = 1.7 Hz), 8.14 (br s, 1H) ppm.

¹³C-NMR (125 MHz, CDCl₃): δ = 10.6, 15.6, 26.7, 27.9, 48.8, 53.6, 54.0, 55.0, 56.8, 117.3, 117.5, 125.4, 128.4, 133.2, 133.5, 136.3, 137.1, 143.4, 143.4, 172.1, 172.4 ppm.

5.2.50. Compound 70

3,5-dichlorobenzenesulfonamide



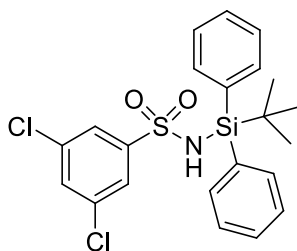
3,5-Dichlorobenzenesulfonyl chloride **7** (530 mg, 2.16 mmol, 1.0 eq.) was suspended in 30 % aq. NH_3 solution (10 mL) and stirred for 18 h at room temperature. It was extracted with EA, the organic phase was dried over MgSO_4 , filtered and concentrated *in vacuo*. The crude product was purified by silica gel column chromatography (Cy/EA 3:1 \rightarrow Cy/EA 1:1) to afford **70**.

Yield: 309 mg, 63 %

TLC: $R_f = 0.41$ (Cy/EA 3:1)

5.2.51. Compound 71

N-(*tert*-butyldiphenylsilyl)-3,5-dichlorobenzenesulfonamide



70 (102 mg, 451 μmol , 1.0 eq.) was dissolved in dry THF (10 mL) under argon atmosphere, then TEA (250 μL , 1804 μmol , 4.0 eq.) and TBDPSCl (1.1 mL, 4242 μmol , 9.4 eq.) were added. The reaction was refluxed for 3 d, then cooled to room temperature and filtered over celite. The filtrate was concentrated *in vacuo* and the crude product was purified by silica gel column chromatography twice (Cy/EA 9:1, then Cy/EA 20:1) to afford **71**.

Yield: 163 mg, 78 %

Appearance: colourless solid

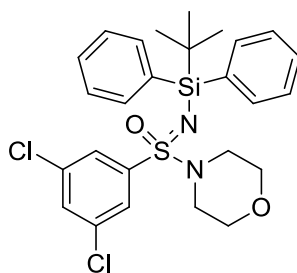
TLC: R_f = 0.44 (Cy/EA 9:1)

$^1\text{H-NMR}$ (300 MHz, CDCl_3): δ = 1.08 (s, 9), 5.63 (br. s, 1H), 7.18 (d, 1H, J = 1.8 Hz), 7.32-7.42 (m, 5H), 7.43-7.52 (m, 2H), 7.61-7.69 (m, 4H) ppm.

$^{13}\text{C-NMR}$ (75 MHz, CDCl_3): δ = 18.6, 27.2, 124.9, 127.9, 130.3, 130.7, 131.9, 135.4, 136.3, 145.6 ppm.

5.2.52. Compound 72

4-(3,5-dichloro-*N*-(*tert*-butyldiphenylsilyl)phenylsulfonimidoyl)morpholine



Triphenylphosphine dichloride (17 mg, 51 μmol , 1.5 eq.) was suspended in dry CHCl_3 under argon atmosphere, then TEA (8 μL , 58 μmol , 1.7 eq.) was added and the mixture was stirred at room temperature for 20 min. It was cooled to 0 $^\circ\text{C}$ and a solution of **71** (16 mg, 34 μmol , 1.0 eq.) in dry CHCl_3 (500 μL) was added. The reaction was stirred at 0 $^\circ\text{C}$ for 20 min, then morpholine (10 μL , 115 μmol , 3.4 eq.), dissolved in dry CHCl_3 (500 μL), was added. The reaction was allowed to warm to room temperature and stirred for 16 h. The solvent was evaporated *in vacuo* and the crude product was purified by silica gel column chromatography (Cy/EA 9:1) to afford **72**.

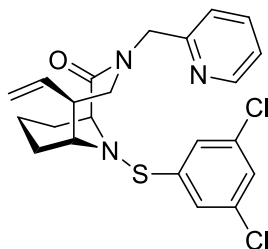
Yield: 14 mg, 74 %

TLC: $R_f = 0.43$ (Cy/EA 9:1)

MS (ESI): m/z calculated: $[\text{M}+\text{H}]^+ = 533.12$, found: $[\text{M}+\text{H}]^+ = 533.61$

5.2.53. Compound 75

(1*S*,5*S*,6*R*)-10-((3,5-dichlorophenyl)thio)-3-(pyridin-2-ylmethyl)-5-vinyl-3,10-diazabicyclo[4.3.1]decan-2-one



3,5-Dichlorobenzene-thiol **74** (105 mg, 586 μmol , 1.0 eq.) was wetted with acetic acid (32 μL , 560 μmol , 1.0 eq.) and cooled to $-40\text{ }^{\circ}\text{C}$. Sulfuryl chloride (100 μL , 1237 μmol , 2.1 eq.) was added and the reaction mixture was allowed to warm to room temperature without stirring. At room temperature, the reaction mixture was completely liquid. Coproducts were removed *in vacuo* to give the crude sulfenyl chloride. (1*S*,5*R*,6*R*)-3-(pyridin-2-ylmethyl)-5-vinyl-3,10-diazabicyclo[4.3.1]decan-2-one **21** (95 mg, 350 μmol , 0.6 eq.) was dissolved in MeCN (20 mL) under argon atmosphere. DIPEA (300 μL , 1764 μmol , 3.0 eq.) was added and the reaction mixture was cooled to $0\text{ }^{\circ}\text{C}$. The crude sulfenyl chloride was dissolved in a small amount of MeCN and added to the reaction mixture. The solution was allowed to warm to room temperature and stirred for 19 h under argon atmosphere. The reaction was quenched with water and extracted with DCM. The organic phase was dried over MgSO_4 , filtered and concentrated *in vacuo*. The crude product was purified by column chromatography (Cy/EA 2:1) to afford **75**.

Yield: 87 mg, 55 %

Purity: 88 % (HPLC, UV-absorption 220 nm)

TLC: $R_f = 0.42$ (Cy/EA 1:1)

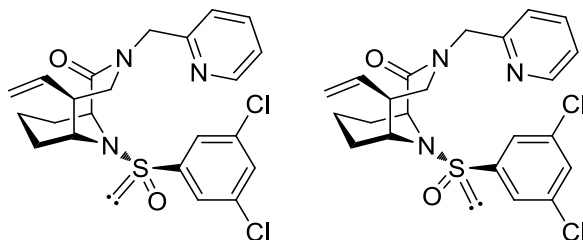
HR-MS (ESI): m/z calculated: $[\text{M}+\text{H}]^+ = 448.10117$, found: $[\text{M}+\text{H}]^+ = 448.10139$

$^1\text{H-NMR}$ (300 MHz, CDCl_3): $\delta = 1.52\text{--}1.74$ (m, 3H), 1.85–2.07 (m, 2H), 2.38 (d, 1H, $J = 13.5$ Hz), 2.66–2.81 (m, 1H), 3.09–3.17 (m, 1H), 3.21 (dd, 1H, $J = 14.4/1.8$ Hz), 3.92–4.07 (m, 2H), 4.76–5.00 (m, 4H), 5.54–5.70 (m, 1H), 7.10 (s, 3H), 7.21 (dd, 1H, $J = 7.4/5.3$ Hz), 7.35 (d, 1H, $J = 7.9$ Hz), 7.69 (ddd, 1H, $J = 7.7/7.7/1.7$ Hz), 8.55 (d, 1H, $J = 4.7$ Hz) ppm.

$^{13}\text{C-NMR}$ (75 MHz, CDCl_3): $\delta = 15.4, 28.6, 29.7, 50.1, 51.8, 56.3, 65.7, 69.0, 116.2, 120.4, 122.3, 122.6, 125.6, 135.8, 137.1, 138.5, 146.3, 149.3, 157.5, 173.4$ ppm.

5.2.54. Compound 76a and 76b

(1*S*,5*S*,6*R*)-10-((*R*)-(3,5-dichlorophenyl)sulfinyl)-3-(pyridin-2-ylmethyl)-5-vinyl-3,10-diazabicyclo[4.3.1]decan-2-one and (1*S*,5*S*,6*R*)-10-((*S*)-(3,5-dichlorophenyl)sulfinyl)-3-(pyridin-2-ylmethyl)-5-vinyl-3,10-diazabicyclo[4.3.1]decan-2-one



KF (12.1 mg, 210 μ mol, 1.9 eq.) and mCPBA (70 %, wet with water, 44.6 mg, 181 μ mol, 1.7 eq.) were dissolved in MeCN/H₂O 5:1 (5 mL) and cooled to 0 °C. After stirring for 30 min at 0 °C, sulfenamide 75 (49 mg, 109 μ mol, 1.0 eq.) was added to the reaction. The mixture was stirred at 0 °C for 4.5 h, then sat. aq. NaHCO₃ was added and it was extracted with EA. The organic phase was dried over MgSO₄, filtered and concentrated *in vacuo*. The crude product was purified by column chromatography (Cy/EA 1:2) to afford both diastereomers 76a and 76b.

76b:

Yield: 2.4 mg, 5 %

Purity: 93 % (HPLC, UV-absorption 220 nm)

Appearance: colourless solid

TLC: R_f = 0.44 (Cy/EA 1:1)

HR-MS (ESI): m/z calculated: [M+H]⁺ = 464.09608, found: [M+H]⁺ = 494.09640

¹H-NMR (500 MHz, CDCl₃): δ = 1.48–1.61 (m, 2H), 1.61–1.78 (m, 2H), 1.82–1.92 (m, 1H), 2.39 (d, 1H, *J* = 13.5 Hz), 2.69–2.77 (m, 1H), 3.21 (d, 1H, *J* = 13.8 Hz), 3.37–3.43 (m, 1H), 4.22 (dd, 1H, *J* = 13.9/10.8 Hz), 4.38 (d, 1H, *J* = 6.0 Hz), 4.88 (d, 1H, *J* = 15.5 Hz), 4.97–5.11 (m, 3H), 5.61–5.71 (m, 1H), 7.38–7.46 (m, 2H), 7.48 (t, 1H, *J* = 1.8 Hz), 7.54 (d, 2H, *J* = 1.9 Hz), 7.87–7.96 (m, 1H), 8.58 (d, 1H, *J* = 5.0 Hz) ppm.

¹³C-NMR (125 MHz, CDCl₃): δ = 15.9, 27.5, 29.8, 48.9, 52.9, 57.7, 59.6, 117.1, 123.7, 123.8, 124.5, 131.7, 136.4, 137.0, 147.3, 171.8 ppm.

76a:

Yield: 3.6 mg, 7 %

Purity: 92 % (HPLC, UV-absorption 220 nm)

Appearance: colourless solid

TLC: $R_f = 0.41$ (Cy/EA 1:2)

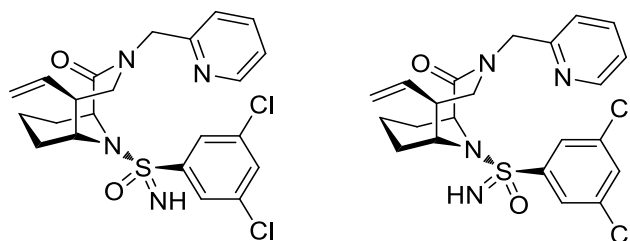
HR-MS (ESI): calculated: $[M+H]^+ = 464.09608$, found: $[M+H]^+ = 494.09663$

$^1\text{H-NMR}$ (500 MHz, CDCl_3): $\delta = 1.46\text{--}1.59$ (m, 1H), $1.65\text{--}1.74$ (m, 3H), $1.77\text{--}1.90$ (m, 1H), 2.27 (d, 1H, $J = 13.4$ Hz), $2.67\text{--}2.78$ (m, 1H), 3.09 (dd, 1H, $J = 14.1/1.7$ Hz), $3.58\text{--}3.65$ (m, 1H), 4.04 (dd, 1H, $J = 13.9/11.2$ Hz), 4.17 (d, 1H, $J = 5.9$ Hz), 4.85 (d, 1H, $J = 15.7$ Hz), 4.91 (d, 1H, $J = 17.0$ Hz), 4.98 (d, 1H, $J = 10.2$ Hz), $5.01\text{--}5.10$ (m, 1H), $5.35\text{--}5.46$ (m, 1H), $7.30\text{--}7.38$ (m, 1H), 7.49 (t, 1H, $J = 1.9$ Hz), $7.50\text{--}7.55$ (m, 1H), 7.56 (d, 2H, $J = 1.9$ Hz), $7.83\text{--}7.92$ (m, 1H), 8.57 (d, 1H, $J = 4.8$ Hz) ppm.

$^{13}\text{C-NMR}$ (125 MHz, CDCl_3): $\delta = 16.0, 28.7, 29.2, 48.7, 52.8, 55.2, 57.9, 58.6, 116.8, 123.2, 124.6, 131.6, 136.3, 137.3, 147.4, 156.3, 171.8$ ppm.

5.2.55. Compound 77a and 77b

(1*S*,5*S*,6*R*)-10-((*S*)-(3,5-dichlorophenyl)sulfonimidoyl)-3-(pyridin-2-ylmethyl)-5-vinyl-3,10-diazabicyclo[4.3.1]decan-2-one and (1*S*,5*S*,6*R*)-10-((*R*)-(3,5-dichlorophenyl)sulfonimidoyl)-3-(pyridin-2-ylmethyl)-5-vinyl-3,10-diazabicyclo[4.3.1]decan-2-one



Sulfenamide **75** (130 mg, 290 μmol , 1.0 eq.), (Diacetoxyiodo)benzene (305 mg, 947 μmol , 3.3 eq.) and ammonium acetate (104 mg, 1350 μmol , 4.7 eq.) were dissolved in MeOH (8 mL) and stirred at room temperature. After 19 h, water was added and the mixture was extracted with DCM. The organic phase was dried over MgSO_4 , filtered and concentrated *in vacuo*. The crude product was purified by column chromatography (Cy/EA 1:2) to afford pure diastereomers **77a** and **77b**.

77a:

Yield: 36 mg, 26 %

Purity: 96 % (HPLC, UV-absorption 220 nm)

Appearance: colourless solid

TLC: $R_f = 0.26$ (Cy/EA 1:2)

HR-MS (ESI): m/z calculated: $[\text{M}+\text{H}]^+ = 479.10698$, found: $[\text{M}+\text{H}]^+ = 479.10704$

$^1\text{H-NMR}$ (500 MHz, CDCl_3): $\delta = 1.13\text{--}1.23$ (m, 1H), 1.27–1.36 (m, 1H), 1.50–1.53 (m, 1H), 1.53–1.61 (m, 1H), 2.22–2.29 (m, 1H), 2.63–2.73 (m, 1H), 3.13 (dd, 1H, $J = 14.0/1.5$ Hz), 3.38 (dd, 1H, $J = 14.0/10.8$ Hz), 4.26–5.33 (m, 1H), 4.81–4.84 (m, 2H), 4.84–4.87 (m, 1H), 5.00 (d, 1H, $J = 17.1$ Hz), 5.05 (d, 1H, $J = 10.2$ Hz), 5.64–5.75 (m, 1H), 7.22–7.26 (m, 1H), 7.37 (d, 1H, $J = 7.9$ Hz), 7.52 (t, 1H, $J = 1.8$ Hz), 7.74 (dd, 1H, $J = 7.7/7.7$ Hz), 7.80 (d, 1H, $J = 1.8$ Hz), 8.53 (d, 1H, $J = 4.7$ Hz) ppm.

$^{13}\text{C-NMR}$ (125 MHz, CDCl_3): $\delta = 15.8, 26.7, 27.7, 48.9, 52.4, 55.1, 55.9, 57.0, 116.8, 122.6, 122.9, 125.3, 132.3, 136.2, 137.4, 137.9, 146.2, 148.5, 156.9, 171.2$ ppm.

77b:

Yield: 53 mg, 35 %

Purity: 98 % (HPLC, UV-absorption 220 nm)

Appearance: colourless solid

TLC: $R_f = 0.17$ (Cy/EA 1:2)

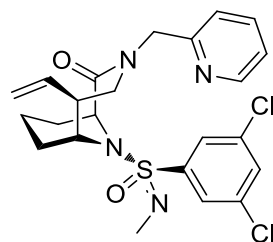
HR-MS (ESI): m/z calculated: $[M+H]^+ = 479.10698$, found: $[M+H]^+ = 479.10739$

$^1\text{H-NMR}$ (500 MHz, CDCl_3): $\delta = 1.15\text{--}1.23$ (m, 1H), 1.27–1.35 (m, 1H), 1.45–1.52 (m, 1H), 1.52–1.56 (m, 1H), 1.56–1.63 (m, 1H), 2.23–2.31 (m, 1H), 2.72–2.80 (m, 1H), 3.01 (dd, 1H, $J = 14.1/1.6$ Hz), 4.06–4.11 (m, 1H), 4.11–4.15 (m, 1H), 4.41 (d, 1H, $J = 15.7$ Hz), 4.87–4.92 (m, 1H), 5.01–5.07 (m, 2H), 5.30 (d, 1H, $J = 15.7$ Hz), 5.70–5.80 (m, 1H), 7.72 (dd, 1H, $J = 7.5/5.3$ Hz), 7.27 (d, 1H, $J = 8.0$ Hz), 7.50 (t, 1H, $J = 1.9$ Hz), 7.69 (ddd, 1H, $J = 7.8/7.7/1.7$ Hz), 7.85 (d, 1H, $J = 1.9$ Hz), 8.55 (d, 1H, $J = 5.0$ Hz) ppm.

$^{13}\text{C-NMR}$ (125 MHz, CDCl_3): $\delta = 15.7, 26.4, 27.3, 49.0, 53.4, 54.9, 56.0, 57.7, 116.8, 122.4, 122.7, 125.0, 132.0, 136.1, 137.4, 137.6, 146.1, 149.0, 156.4, 172.5$ ppm.

5.2.56. Compound 78a

(1*S*,5*S*,6*R*)-10-((*S*)-3,5-dichloro-*N*-methylphenylsulfonimidoyl)-3-(pyridin-2-ylmethyl)-5-vinyl-3,10-diazabicyclo[4.3.1]decan-2-one



Sulfonimidamide **77a** (5.0 mg, 10.4 μ mol, 1.0 eq.) was dissolved in THF (1.0 mL) under argon atmosphere and cooled to 0 °C. NaH (60 % in mineral oil, 3.8 mg, 95.0 μ mol, 9.1 eq.) was added and it was stirred for 30 min at 0 °C. MeI (7.0 μ L, 112 μ mol, 10.8 eq.) was added and the reaction mixture was stirred for 24 h at room temperature. The reaction was quenched with MeOH and water and extracted with DCM. The organic phase was dried over MgSO₄, filtered and concentrated *in vacuo*. The crude product was purified by column chromatography (Cy/EA 1:2) to afford **78a**.

Yield: 4.2 mg, 82 %

Purity: 98 % (HPLC, UV-absorption 220 nm)

Appearance: colourless solid

TLC: R_f = 0.43 (Cy/EA 1:2)

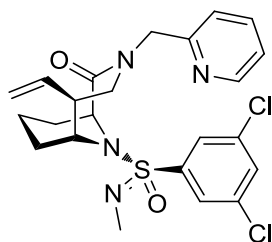
HR-MS (ESI): m/z calculated: [M+H]⁺ = 493.12263, found: [M+H]⁺ = 493.12305

¹H-NMR (500 MHz, CDCl₃): δ = 1.26–1.33 (m, 1H), 1.35–1.46 (m, 1H), 1.46–1.51 (m, 1H), 1.51–1.57 (m, 1H), 1.57–1.65 (m, 1H), 2.23 (d, 1H, *J* = 13.5 Hz), 2.64–2.73 (m, 1H), 2.80 (s, 3H), 3.09 (d, 1H, *J* = 14.1 Hz), 3.85 (dd, 1H, *J* = 13.8/11.0 Hz), 4.18–4.28 (m, 1H), 4.80 (d, 1H, *J* = 6.0 Hz), 4.83–4.90 (m, 2H), 5.01 (d, 1H, *J* = 17.0 Hz), 5.06 (d, 1H, *J* = 10.1 Hz), 5.64–5.75 (m, 1H), 7.29–7.37 (m, 1H), 7.37–7.47 (m, 1H), 7.50 (t, 1H, *J* = 1.9 Hz), 7.74 (d, 2H, *J* = 1.9 Hz), 7.78–7.88 (m, 1H), 8.54 (d, 1H, *J* = 4.8 Hz) ppm.

¹³C-NMR (125 MHz, CDCl₃): δ = 15.8, 26.6, 27.5, 29.1, 49.0, 52.0, 54.7, 55.2, 57.2, 116.8, 123.2, 125.7, 132.1, 136.2, 137.9, 144.3, 156.5, 171.6 ppm.

5.2.57. Compound 78b

(1*S*,5*S*,6*R*)-10-((*R*)-3,5-dichloro-*N*-methylphenylsulfonimidoyl)-3-(pyridin-2-ylmethyl)-5-vinyl-3,10-diazabicyclo[4.3.1]decan-2-one



Sulfonimidamide **77b** (8.3 mg, 17.3 μ mol, 1.0 eq.) was dissolved in THF (1.0 mL) under argon atmosphere and cooled to 0 °C. NaH (60 % in mineral oil, 4.2 mg, 105 μ mol, 8.7 eq.) was added and it was stirred for 30 min at 0 °C. MeI (11 μ L, 177 μ mol, 10.2 eq.) was added and the reaction mixture was stirred for 24 h at room temperature. The reaction was quenched with MeOH and water and extracted with DCM. The organic phase was dried over MgSO₄, filtered and concentrated *in vacuo*. The crude product was purified by column chromatography (Cy/EA 1:2) to afford **78b**.

Yield: 5.4 mg, 64 %

Purity: 96 % (HPLC, UV-absorption 220 nm)

Appearance: colourless solid

TLC: R_f = 0.40 (Cy/EA 1:2)

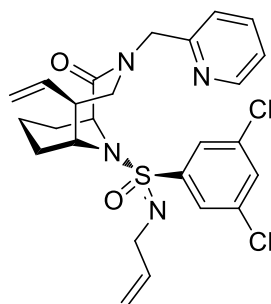
HR-MS (ESI): m/z calculated: [M+H]⁺ = 493.12263, found: [M+H]⁺ = 493.12303

¹H-NMR (500 MHz, CDCl₃): δ = 1.06–1.13 (m, 1H), 1.13–1.21 (m, 1H), 1.37–1.48 (m, 2H), 1.48–1.62 (m, 1H), 2.21 (d, 1H, *J* = 13.7 Hz), 2.64–2.72 (m, 1H), 2.77 (s, 3H), 3.19 (dd, 1H, *J* = 14.0/1.6 Hz), 3.98–4.05 (m, 1H), 4.14 (dd, 1H, *J* = 14.0/10.8 Hz), 4.84–4.90 (m, 3H), 4.99 (d, 1H, *J* = 17.0 Hz), 5.04 (d, 1H, *J* = 10.2 Hz), 5.69–5.79 (m, 1H), 7.26–7.30 (m, 1H), 7.41 (d, 1H, *J* = 7.7 Hz), 7.50 (t, 1H, *J* = 1.9 Hz), 7.71–7.77 (m, 1H), 7.79 (d, 2H, *J* = 1.9 Hz), 5.84 (d, 1H, *J* = 4.8 Hz) ppm.

¹³C-NMR (125 MHz, CDCl₃): δ = 15.7, 25.9, 27.0, 28.0, 49.4, 52.3, 54.3, 55.8, 57.6, 116.8, 123.0, 123.2, 125.2, 132.1, 136.1, 137.7, 138.0, 144.9, 148.2, 156.7, 171.6 ppm.

5.2.58. Compound 79a

(1*S*,5*S*,6*R*)-10-((*S*)-*N*-allyl-3,5-dichlorophenylsulfonimidoyl)-3-(pyridin-2-ylmethyl)-5-vinyl-3,10-diazabicyclo[4.3.1]decan-2-one



Sulfonimidamide **77a** (5.8 mg, 12.1 μmol , 1.0 eq.) was dissolved in THF (1.0 mL) under argon atmosphere and cooled to 0 °C. NaH (60 % in mineral oil, 3.7 mg, 55.3 μmol , 4.6 eq.) was added and it was stirred for 30 min at 0 °C. Allylbromide (20 μL , 231 μmol , 19.1 eq.) was added and the reaction mixture was allowed to reach room temperature. After 17 h the solution was again cooled to 0 °C, NaH (60 % in mineral oil, 7.2 mg, 108 μmol , 8,9 eq.) and allylbromide (20 μL , 231 μmol , 19.1 eq.) were added and the reaction mixture was allowed to reach room temperature. After another 25 h water was added and the mixture was extracted with DCM. The organic phase was dried over MgSO_4 , filtered and concentrated *in vacuo*. The crude product was purified by column chromatography (Cy/EA 2:1–1:1) to afford **79a**.

Yield: 6.3 mg, 100 %

Purity: 95 % (HPLC, UV-absorption 220 nm)

Appearance: colourless solid

TLC: $R_f = 0.38$ (Cy/EA 1:1)

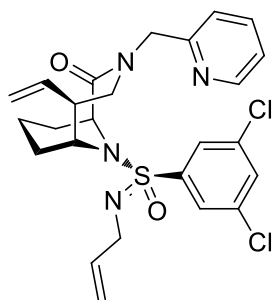
HR-MS (ESI): m/z calculated: $[\text{M}+\text{H}]^+ = 519.13828$, found: $[\text{M}+\text{H}]^+ = 519.13826$

$^1\text{H-NMR}$ (500 MHz, CDCl_3): $\delta = 1.19\text{--}1.30$ (m, 1H), 1.43–1.52 (m, 1H), 1.52–1.66 (m, 3H), 2.18 (d, 1H, $J = 13.0$ Hz), 2.71–2.81 (m, 1H), 3.13 (d, 1H, $J = 13.9$ Hz), 3.59–3.71 (m, 2H), 4.08–4.16 (m, 1H), 4.40–4.47 (m, 1H), 4.62–4.73 (m, 2H), 5.06–5.10 (m, 1H), 5.11 (s, 1H), 5.14 (d, 1H, $J = 7.7$ Hz), 5.21–5.28 (m, 1H), 5.57 (d, 1H, $J = 16.5$ Hz), 5.69–6.79 (m, 1H), 5.85–5.94 (m, 1H), 7.53 (t, 1H, $J = 1.8$ Hz), 7.70 (d, 2H, $J = 1.8$ Hz), 7.71–7.75 (m, 1H), 7.84 (d, 1H, $J = 8.0$ Hz), 8.26–8.33 (m, 1H), 8.80 (d, 1H, $J = 5.2$ Hz) ppm.

$^{13}\text{C-NMR}$ (125 MHz, CDCl_3): $\delta = 14.3, 15.7, 26.7, 27.5, 45.6, 49.2, 53.0, 53.3, 55.0, 56.5, 115.0, 117.4, 125.0, 125.4, 125.9, 132.5, 136.4, 136.6, 136.9, 142.8, 144.0, 144.7, 154.1, 172.8$ ppm.

5.2.59. Compound 79b

(1*S*,5*S*,6*R*)-10-((*R*)-*N*-allyl-3,5-dichlorophenylsulfonimidoyl)-3-(pyridin-2-ylmethyl)-5-vinyl-3,10-diazabicyclo[4.3.1]decan-2-one



Sulfonimidamide **77b** (5.3 mg, 11.1 μmol , 1.0 eq.) was dissolved in THF (1.0 mL) under argon atmosphere and cooled to 0 °C. NaH (60 % in mineral oil, 3.9 mg, 58.3 μmol , 5.3 eq.) was added and it was stirred for 30 min at 0 °C. Allylbromide (20 μL , 231 μmol , 20.8 eq.) was added and the reaction mixture was allowed to reach room temperature. After 17 h the solution was again cooled to 0 °C, NaH (60 % in mineral oil, 7.5 mg, 112 μmol , 10.1 eq.) and allylbromide (20 μL , 231 μmol , 20.8 eq.) were added and the reaction mixture was allowed to reach room temperature. After another 25 h water was added and the mixture was extracted with DCM. The organic phase was dried over MgSO_4 , filtered and concentrated *in vacuo*. The crude product was purified by column chromatography (Cy/EA 1:1–1:2) to afford **79b**.

Yield: 4.6 mg, 81 %

Purity: 96 % (HPLC, UV-absorption 220 nm)

Appearance: colourless solid

TLC: $R_f = 0.45$ (Cy/EA 1:1)

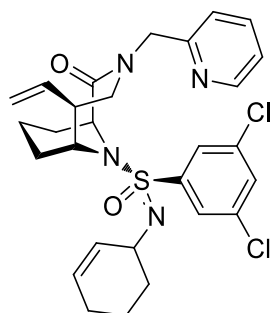
HR-MS (ESI): m/z calculated: $[\text{M}+\text{H}]^+ = 519.13828$, found: $[\text{M}+\text{H}]^+ = 519.13865$

$^1\text{H-NMR}$ (500 MHz, CDCl_3): $\delta = 1.08\text{--}1.21$ (m, 2H), 1.38–1.50 (m, 2H), 1.50–1.62 (m, 1H), 2.22 (d, 1H, $J = 13.1$ Hz), 2.65–2.74 (m, 1H), 3.18 (dd, 1H, $J = 13.9/1.5$ Hz), 3.58–3.66 (m, 1H), 3.76–3.83 (m, 1H), 4.00–4.07 (m, 1H), 4.14 (dd, 1H, $J = 13.9/10.7$ Hz), 4.79 (d, 1H, $J = 15.3$ Hz), 4.92 (d, 1H, $J = 6.1$ Hz), 5.02 (d, 1H, $J = 17.0$ Hz), 5.06 (d, 1H, $J = 10.2$ Hz), 5.07–5.11 (m, 1H), 5.23–5.29 (m, 1H), 4.70–4.80 (m, 1H), 4.86–4.95 (m, 1H), 7.29–7.37 (m, 1H), 7.44–7.50 (m, 1H), 7.51 (t, 1H, $J = 1.9$ Hz), 7.75–7.85 (m, 3H), 8.55 (d, 1H, $J = 5.1$ Hz) ppm.

$^{13}\text{C-NMR}$ (125 MHz, CDCl_3): $\delta = 15.7, 25.9, 27.1, 44.7, 49.4, 52.5, 54.2, 55.4, 57.8, 115.2, 116.9, 123.3, 123.5, 125.3, 132.2, 136.2, 136.8, 137.5, 144.9, 156.4, 171.7$ ppm.

5.2.60. Compound 80a

(1*S*,5*S*,6*R*)-10-((*S*)-3,5-dichloro-*N*-(cyclohex-2-en-1-yl)phenylsulfonimidoyl)-3-(pyridin-2-ylmethyl)-5-vinyl-3,10-diazabicyclo[4.3.1]decan-2-one



Sulfonimidamide **77a** (15.5 mg, 32.3 μmol , 1.0 eq.) was dissolved in THF (1.0 mL) under argon atmosphere and cooled to 0 °C. NaH (60 % in mineral oil, 11 mg, 165 μmol , 5.1 eq.) was added and it was stirred for 30 min at 0 °C. 3-Bromocyclohexene (73 μL , 626 μmol , 19.4 eq.) was added and the reaction mixture was allowed to reach room temperature. After 45 h the solution was again cooled to 0 °C, NaH (60 % in mineral oil, 10 mg, 150 μmol , 4.6 eq.) and 3-bromocyclohexene (73 μL , 626 μmol , 19.4 eq.) were added and the reaction mixture was allowed to reach room temperature. After another 3 d water was added and the mixture was extracted with DCM. The organic phase was dried over MgSO_4 , filtered and concentrated *in vacuo*. The crude product was purified by column chromatography (Cy/EA 2:1–1:1) to afford **80a** as a mixture of (*R*)- and (*S*)-cyclohex-2-en-1-yl epimers.

Yield: 11.9 mg, 66 %

Purity: 97 % (HPLC, UV-absorption 220 nm)

Appearance: colourless solid

TLC: $R_f = 0.38$ (Cy/EA1:1)

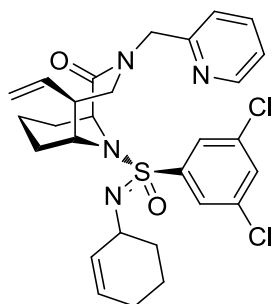
HR-MS (ESI): m/z calculated: $[\text{M}+\text{H}]^+ = 559.16958$, found: $[\text{M}+\text{H}]^+ = 559.16916$

$^1\text{H-NMR}$ (500 MHz, CDCl_3): $\delta = 1.26\text{--}1.35$ (m, 1H), 1.40–1.58 (m, 4H), 1.58–1.73 (m, 2H), 1.73–1.83 (m, 1H), 1.83–1.89 (m, 1H), 1.89–1.97 (m, 1H), 1.97–2.06 (m, 1H), 2.25 (d, 1H, $J = 13.5$ Hz), 2.59–2.73 (m, 1H), 3.02 (dd, 1H, $J = 14.0/1.3$ Hz), 3.75–3.91 (m, 2H), 4.29–4.39 (m, 1H), 4.67–4.80 (m, 2H), 4.79–4.88 (m, 1H), 4.98 (d, 1H, $J = 16.9$ Hz), 5.02 (d, 1H, $J = 10.1$ Hz), 5.53–5.65 (m, 1H), 5.65–5.71 (m, 1H), 5.70–5.78 (m, 1H), 7.22–7.29 (m, 1H), 7.35 (d, 1H, $J = 7.9$ Hz), 7.45–7.49 (m, 1H), 7.69–7.73 (m, 2H), 7.73–7.79 (m, 1H), 8.52 (m, 1H, $J = 4.9$ Hz) ppm.

$^{13}\text{C-NMR}$ (125 MHz, CDCl_3): $\delta = 15.9, 20.2, 20.4, 24.9, 24.9, 26.8, 26.9, 27.8, 27.9, 29.8, 33.0, 33.0, 49.1, 49.1, 49.4, 49.9, 52.0, 54.9, 55.7, 56.6, 56.7, 116.6, 122.7, 122.8, 125.8, 125.8, 128.7, 128.9, 131.0, 131.4, 132.0, 136.0, 136.0, 137.8, 138.1, 145.3, 145.4, 148.2, 156.9, 171.7$ ppm.

5.2.61. Compound 80b

(1*S*,5*S*,6*R*)-10-((*R*)-3,5-dichloro-*N*-(cyclohex-2-en-1-yl)phenylsulfonimidoyl)-3-(pyridin-2-ylmethyl)-5-vinyl-3,10-diazabicyclo[4.3.1]decan-2-one



Sulfonimidamide **77b** (15.9 mg, 33.2 μ mol, 1.0 eq.) was dissolved in THF (1.0 mL) under argon atmosphere and cooled to 0 °C. NaH (60 % in mineral oil, 9.0 mg, 135 μ mol, 4.1 eq.) was added and it was stirred for 30 min at 0 °C. 3-Bromocyclohexene (73 μ L, 626 μ mol, 18.9 eq.) was added and the reaction mixture was allowed to reach room temperature. After 42 h water was added and the mixture was extracted with DCM. The organic phase was dried over MgSO₄, filtered and concentrated *in vacuo*. The crude product was purified by column chromatography (Cy/EA 2:1–1:1) to afford **80b** as a mixture of (*R*)- and (*S*)-cyclohex-2-en-1-yl epimers.

Yield: 15.8 mg, 85 %

Purity: >99 % (HPLC, UV-absorption 220 nm)

Appearance: colourless oil

TLC: R_f = 0.41 (Cy/EA 1:1)

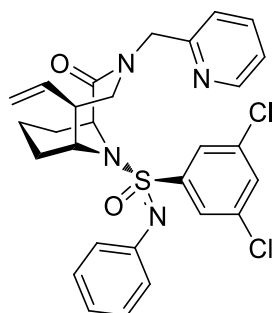
HR-MS (ESI): m/z calculated: [M+H]⁺ = 559.16958, found: [M+H]⁺ = 559.16995

¹H-NMR (500 MHz, CDCl₃): δ = 1.05–1.20 (m, 2H), 1.35–1.47 (m, 3H), 1.53–1.59 (m, 1H), 1.62–1.72 (m, 1H), 1.73–1.83 (m, 1H), 1.86–1.92 (m, 1H), 1.92–1.98 (m, 1H), 1.98–2.08 (m, 1H), 2.20 (d, 1H, *J* = 13.5 Hz), 2.65–2.74 (m, 1H), 3.14 (ddd, 1H, *J* = 13.9/7.2/1.6 Hz), 3.87–4.02 (m, 1H), 4.02–4.06 (m, 1H), 4.06–4.19 (m, 1H), 4.62 and 5.07 (d, 1H, *J* = 15.1 Hz, each 50 %), 4.79 and 4.87 (d, 1H, *J* = 15.1 Hz, each 50 %), 4.90–5.05 (m, 3H), 5.58–5.80 (m, 3H), 7.19–7.25 (m, 1H), 7.37 (dd, 1H, *J* = 12.2/7.9 Hz), 7.47–7.50 (m, 1H), 7.63–7.70 (m, 1H), 7.79 (t, 1H, *J* = 1.6 Hz), 8.49–8.56 (m, 1H) ppm.

¹³C-NMR (125 MHz, CDCl₃): δ = 15.7, 20.3, 24.9, 24.9, 25.8, 26.9, 32.4, 33.4, 49.0, 49.2, 49.5, 49.6, 52.1, 52.3, 54.3, 55.9, 56.0, 57.9, 116.7, 116.7, 122.7, 122.7, 122.8, 123.1, 125.3, 125.3, 128.5, 129.2, 130.9, 131.5, 131.9, 131.9, 136.0, 136.0, 137.4, 137.6, 137.7, 137.8, 145.4, 145.5, 148.6, 148.9, 157.0, 171.5, 171.6 ppm.

5.2.62. Compound 81a

(1*S*,5*S*,6*R*)-10-((*S*)-3,5-dichloro-*N*-phenylphenylsulfonimidoyl)-3-(pyridin-2-ylmethyl)-5-vinyl-3,10-diazabicyclo[4.3.1]decan-2-one



Sulfonimidamide **77a** (8.6 mg, 17.9 μmol , 1.0 eq.), phenylboronic acid (18.3 mg, 150 μmol , 8.4 eq.) and $\text{Cu}(\text{OAc})_2$ (7.3 mg, 40.2 μmol , 2.2 eq.) were dissolved in MeCN (1 mL) under argon atmosphere, then TEA (5 μL , 36.1 μmol , 2.0 eq.) was added. The reaction mixture was stirred at room temperature for 42 h, then water was added and it was extracted with EA. The organic phase was dried over MgSO_4 , filtered and concentrated *in vacuo*. The crude product was purified by column chromatography (Cy/EA 2:1–1:1) to afford **81a**.

Yield: 10.0 mg, 100 %

Purity: 96 % (HPLC, UV-absorption 220 nm)

Appearance: colourless solid

TLC: $R_f = 0.34$ (Cy/EA 1:1)

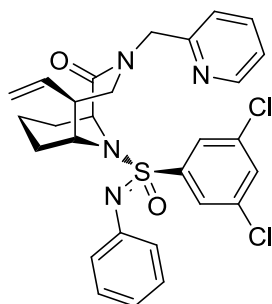
HR-MS (ESI): m/z calculated: $[\text{M}+\text{H}]^+ = 555.13828$, found: $[\text{M}+\text{H}]^+ = 555.13832$

$^1\text{H-NMR}$ (500 MHz, CDCl_3): $\delta = 1.08\text{--}1.18$ (m, 1H), 1.18–1.31 (m, 1H), 1.39–1.48 (m, 2H), 1.41–1.61 (m, 1H), 2.17 (d, 1H, $J = 13.6$ Hz), 2.52–2.61 (m, 1H), 2.75 (d, 1H, $J = 14.1$ Hz), 3.44 (dd, 1H, $J = 14.0/10.9$ Hz), 4.18–4.24 (m, 1H), 4.76 (d, 1H, $J = 15.4$ Hz), 4.79–4.99 (m, 4H), 5.30–5.42 (m, 1H), 6.94–7.00 (m, 1H), 7.15–7.23 (m, 4H), 7.28–7.32 (m, 1H), 7.32–7.36 (m, 1H), 7.53 (t, 1H, $J = 1.9$ Hz), 7.78–7.84 (m, 1H), 7.89 (d, 1H, $J = 1.9$ Hz), 8.52 (d, 1H, $J = 4.8$ Hz) ppm.

$^{13}\text{C-NMR}$ (125 MHz, CDCl_3): $\delta = 15.7, 25.8, 27.0, 48.9, 51.3, 55.3, 55.4, 57.5, 116.8, 122.9, 123.1, 123.3, 124.2, 125.9, 129.4, 132.6, 136.3, 137.6, 138.7, 142.4, 144.4, 147.6, 156.5, 171.5$ ppm.

5.2.63. Compound 81b

(1*S*,5*S*,6*R*)-10-((*R*)-3,5-dichloro-*N*-phenylphenylsulfonimidoyl)-3-(pyridin-2-ylmethyl)-5-vinyl-3,10-diazabicyclo[4.3.1]decan-2-one



Sulfonimidamide **77b** (7.4 mg, 15.4 μ mol, 1.0 eq.), phenylboronic acid (14.9 mg, 122 μ mol, 7.9 eq.) and Cu(OAc)₂ (9.9 mg, 54.5 μ mol, 3.5 eq.) were dissolved in MeCN (1 mL) under argon atmosphere, then TEA (5 μ L, 36.1 μ mol, 2.3 eq.) was added. The reaction mixture was stirred at room temperature for 18 h, then water was added and it was extracted with EA. The organic phase was dried over MgSO₄, filtered and concentrated *in vacuo*. The crude product was purified by column chromatography (Cy/EA 2:1–1:2) to afford **81b**.

Yield: 7.5 mg, 87 %

Purity: 98 % (HPLC, UV-absorption 220 nm)

Appearance: colourless solid

TLC: R_f = 0.33 (Cy/EA 1:1)

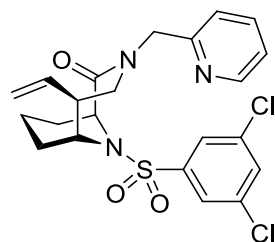
HR-MS (ESI): *m/z* calculated: [M+H]⁺ = 555.13828, found: [M+H]⁺ = 555.13811

¹H-NMR (500 MHz, CDCl₃): δ = 1.03–1.16 (m, 1H), 1.16–1.29 (m, 1H), 1.37–1.58 (m, 3H), 2.21 (d, 1H, *J* = 13.3 Hz), 2.52–2.64 (m, 1H), 2.27 (d, 1H, *J* = 13.8 Hz), 3.64 (dd, 1H, *J* = 13.3/11.2 Hz), 4.05–4.25 (m, 2H), 4.84 (d, 1H, *J* = 15.7 Hz), 4.93 (d, 1H, *J* = 17.0 Hz), 5.01 (d, 1H, *J* = 10.2 Hz), 5.04 (d, 1H, *J* = 6.0 Hz), 5.62–5.74 (m, 1H), 7.02–7.09 (m, 1H), 7.16 (d, 1H, *J* = 7.8 Hz), 7.24–7.30 (m, 4H), 7.55 (t, 1H, *J* = 1.9 Hz), 7.65–7.75 (m, 1H), 7.93 (d, 2H, *J* = 1.9 Hz), 8.49 (d, 1H, *J* = 4.9 Hz) ppm.

¹³C-NMR (125 MHz, CDCl₃): δ = 15.7, 26.1, 27.1, 49.5, 51.2, 54.4, 54.8, 58.1, 116.8, 122.9, 123.0, 123.7, 124.9, 125.5, 129.4, 132.5, 136.3, 137.5, 139.3, 142.0, 144.7, 147.3, 156.4, 171.0 ppm.

5.2.64. Compound 1

(1*S*,5*S*,6*R*)-10-(3,5-dichlorophenylsulfonyl)-3-(pyridin-2-ylmethyl)-5-vinyl-3,10-diazabicyclo[4.3.1]decan-2-one



(1*S*,5*S*,6*R*)-3-(pyridin-2-ylmethyl)-5-vinyl-3,10-diazabicyclo[4.3.1]decan-2-one **21** (83 mg, 306 μ mol, 1.0 eq.) was dissolved in dry MeCN (5 mL) under argon atmosphere. DIPEA (100 μ L, 588 μ mol, 1.9 eq.) and 3,5-dichlorobenzenesulfonyl chloride **7** (130 mg, 530 μ mol, 1.7 eq.) were added and the reaction mixture was stirred at room temperature. After 19 h water was added and it was extracted with DCM. The organic phase was dried over MgSO₄, filtered and concentrated *in vacuo*. The crude product was purified by semi-preparative HPLC (40-80 % MeCN in water) to afford **1**.

Yield: 70.4 mg, 48 %

Purity: >99 % (HPLC, UV-absorption 220 nm)

Appearance: colourless solid

TLC: R_f = 0.30 (Cy/EA 1:2)

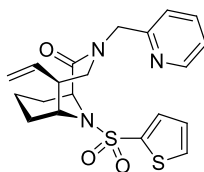
MS (ESI): m/z calculated: [M+H]⁺ 480.1 = , found: [M+H]⁺ = 480.0

¹H-NMR (500 MHz, CDCl₃): δ = 1.16–1.36 (m, 2H), 1.46–1.55 (m, 2H), 1.55–1.67 (m, 1H), 2.30 (d, 1H, *J* = 13.5 Hz), 2.64–2.75 (m, 1H), 3.10 (dd, 1H, *J* = 14.2/1.7 Hz), 3.95–4.05 (m, 2H), 4.70–4.77 (m, 2H), 4.86 (d, 1H, *J* = 15.2 Hz), 4.97 (d, 1H, *J* = 17.0 Hz), 5.03 (d, 1H, *J* = 10.1 Hz), 5.63–5.76 (m, 1H), 7.18 (dd, 1H, *J* = 7.4/4.8 Hz), 7.30 (d, 1H, *J* = 7.8 Hz), 7.55 (t, 1H, *J* = 1.8 Hz), 7.64–7.68 (m, 1H), 7.69 (d, 2H, *J* = 1.8 Hz), 8.51 (d, 1H, *J* = 4.8 Hz) ppm.

¹³C-NMR (125 MHz, CDCl₃): δ = 15.6, 26.5, 27.7, 49.2, 52.1, 55.0, 56.3, 57.0, 117.0, 122.2, 122.6, 125.0, 132.8, 136.4, 137.1, 137.3, 144.2, 149.2, 157.0, 170.5 ppm.

5.2.65. Compound 82

(1*S*,5*S*,6*R*)-3-(pyridin-2-ylmethyl)-10-(thiophen-2-ylsulfonyl)-5-vinyl-3,10-diazabicyclo[4.3.1]decan-2-one



Bicycle **21** (15.3 mg, 56 μ mol, 1.0 eq.) and thiophene-2-sulfonyl chloride **95** (19.9 mg, 109 μ mol, 1.9 eq.) were dissolved in dry MeCN (500 μ L) under argon atmosphere and DIPEA (19 μ L, 112 μ mol, 2.0 eq.) was added. The reaction mixture was stirred at room temperature for 17 h, then the solvent was removed *in vacuo* and the crude mixture was purified by silica gel column chromatography (Cy/EA 2:1 \rightarrow Cy/EA 1:2) to afford **82**.

Yield: 10.9 mg, 46 %

Purity: >99 % (HPLC, UV-absorption 220 nm)

Appearance: colourless solid

TLC: R_f = 0.39 (EA)

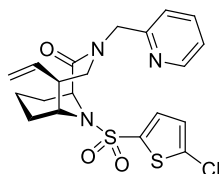
HR-MS (ESI): m/z calculated: $[M+H]^+ = 418.12536$, found: $[M+H]^+ = 418.12556$

$^1\text{H-NMR}$ (500 MHz, CDCl_3): δ = 1.30-1.45 (m, 2H), 1.46-1.54 (m, 2H), 1.55-1.67 (m, 1H), 2.28 (d, 1H, $J = 13.5$ Hz), 2.68 (q, 1H, $J = 8.7$ Hz), 3.08 (dd, 1H, $J = 14.1/1.7$ Hz), 3.98-4.08 (m, 2H), 4.79-4.88 (m, 3H), 4.98 (d, 1H, $J = 16.9$ Hz), 5.02 (d, 1H, $J = 14.1$ Hz), 5.64-5.76 (m, 1H), 7.08 (dd, 1H, $J = 5.0/3.8$ Hz), 7.18-7.23 (m, 1H), 7.33 (d, 1H, $J = 7.9$ Hz), 7.56-7.61 (m, 2H), 7.66-7.73 (m, 1H), 8.52 (d, 1H, $J = 4.9$ Hz) ppm.

$^{13}\text{C-NMR}$ (125 MHz, CDCl_3): δ = 15.7, 26.7, 27.4, 49.1, 52.3, 54.8, 56.2, 57.0, 116.8, 122.3, 122.6, 127.6, 131.9, 131.9, 137.4, 137.6, 142.2, 149.0, 157.1, 171.0 ppm.

5.2.66. Compound 83

(1*S*,5*S*,6*R*)-10-((5-chlorothiophen-2-yl)sulfonyl)-3-(pyridin-2-ylmethyl)-5-vinyl-3,10-diazabicyclo[4.3.1]decan-2-one



Bicycle **21** (15.8 mg, 58 μ mol, 1.0 eq.) was dissolved in dry MeCN (500 μ L) under argon atmosphere, then 5-chlorothiophene-2-sulfonyl chloride **96** (12 μ L, 90 μ mol, 1.6 eq.) and DIPEA (19 μ L, 112 μ mol, 1.9 eq.) was added. The reaction mixture was stirred at room temperature for 17 h, then the solvent was removed *in vacuo* and the crude mixture was purified by silica gel column chromatography (Cy/EA 2:1 \rightarrow Cy/EA 1:2) to afford **83**.

Yield: 10.8 mg, 41 %

Purity: >99 % (HPLC, UV-absorption 220 nm)

Appearance: colourless solid

TLC: R_f = 0.24 (Cy/EA 1:2)

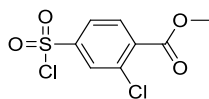
HR-MS (ESI): m/z calculated: $[M+H]^+ = 452.08639$, found: $[M+H]^+ = 452.08682$

$^1\text{H-NMR}$ (500 MHz, CDCl_3): δ = 1.36-1.69 (m, 5H), 2.31 (d, 1H, J = 13.6 Hz), 2.70 (q, 1H, J = 8.8 Hz), 3.11 (dd, 1H, J = 14.2/1.6 Hz), 3.96-4.05 (m, 2H), 4.78 (d, 1H, J = 6.0 Hz), 4.83 (s, 2H), 4.99 (d, 1H, J = 17.1 Hz), 5.03 (d, 1H, J = 10.1 Hz), 5.64-5.75 (m, 1H), 6.92 (d, 1H, J = 4.0 Hz), 7.19-7.25 (m, 1H), 7.31-7.36 (m, 1H), 7.38 (d, 1H, J = 4.0 Hz), 7.67-7.76 (m, 1H), 8.53 (d, 1H, J = 4.9 Hz) ppm.

$^{13}\text{C-NMR}$ (125 MHz, CDCl_3): δ = 15.7, 26.4, 27.5, 49.1, 52.3, 54.9, 56.1, 57.1, 116.9, 122.4, 122.7, 127.0, 131.3, 137.4, 137.6, 140.1, 148.9, 157.0, 170.8 ppm.

5.2.67. Compound 85

Methyl 2-chloro-4-(chlorosulfonyl)benzoate



Thionyl chloride (30 mL) was slowly added to water (100 mL) at 0 °C to create a SO₂/HCl solution. Methyl 4-amino-2-chlorobenzoate **84** (407 mg, 2.19 mmol, 1.0 eq.) were dissolved in MeCN (60 mL) and conc. HCl (2 mL) was added, which precipitated a colourless solid. NaNO₂ (225 mg, 3.26 mmol, 1.5 eq.) in water (1 mL) was added, which dissolved the precipitate again. After stirring for 10 min at room temperature, the reaction mixture was cooled to 0 °C. The SO₂/HCl solution (50 mL, 159 mmol, 73 eq.) and CuCl₂ (174 mg, 1.29 mmol, 0.6 eq.) were added and the reaction mixture was stirred at room temperature for 3 h. Brine was added and it was extracted with EA. The organic phase was dried over MgSO₄, filtered and concentrated *in vacuo*. The crude product was purified by silica gel column chromatography twice (Cy/EA 9:1, then Cy → Cy/EA 9:1) to afford **85**.

Yield: 295 mg, 48 %

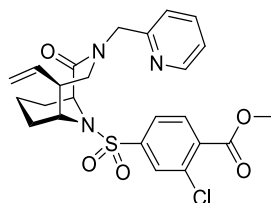
TLC: R_f = 0.46 (Cy/EA 3:1)

¹H-NMR (300 MHz, CDCl₃): δ = 3.99 (s, 3H, rotamer A+B), 7.95 (d, 0.2H, *J* = 1.8 Hz, rotamer A), 7.98 (d, 0.8H, *J* = 1.8 Hz, rotamer B), 8.00 (d, 0.8H, *J* = 0.5 Hz, rotamer B), 8.03 (d, 0.2H, *J* = 0.5 Hz, rotamer A), 8.11 (dd, 1H, *J* = 1.8/0.5 Hz, rotamer A+B) ppm.

¹³C-NMR (75 MHz, CDCl₃): δ = 55.3, 124.9, 129.3, 132.5, 135.2, 136.6, 146.8, 164.5 ppm.

5.2.68. Compound 86

Methyl 2-chloro-4-(((1*S*,5*S*,6*R*)-2-oxo-3-(pyridin-2-ylmethyl)-5-vinyl-3,10-diazabicyclo[4.3.1]decan-10-yl)sulfonyl)benzoate



Bicycle **21** (80.3 mg, 296 μmol , 1.0 eq.) and **85** (115.5 mg, 429 μmol , 1.4 eq.) were dissolved in dry MeCN (1 mL) under argon atmosphere and DIPEA (100 μL , 588 μmol , 2.0 eq.) was added. The reaction mixture was stirred at room temperature for 17 h, then the solvent was removed *in vacuo* and the crude mixture was purified by silica gel column chromatography (Cy/EA 2:1 \rightarrow Cy/EA 1:3) to afford **86**.

Yield: 116.4 mg, 63 %

Purity: 99 % (HPLC, UV-absorption 220 nm)

Appearance: off-white solid

TLC: $R_f = 0.31$ (DCM/MeOH 20:1)

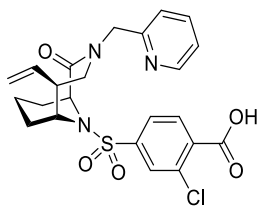
HR-MS (ESI): m/z calculated: $[M+H]^+ = 504.13545$, found: $[M+H]^+ = 504.13570$

$^1\text{H-NMR}$ (500 MHz, CDCl_3): $\delta = 1.14\text{-}1.34$ (m, 2H), 1.44-1.53 (m, 2H), 1.53-1.66 (m, 1H), 2.28 (d, 1H, $J = 13.5$ Hz), 2.70 (q, 1H, $J = 8.7$ Hz), 3.11 (dd, 1H, $J = 14.2/1.5$ Hz), 3.96 (s, 3H), 3.97-4.06 (m, 2H), 4.72-4.79 (m, 2H), 4.85 (d, 1H, $J = 15.3$ Hz), 4.98 (d, 1H, $J = 17.1$ Hz), 5.03 (d, 1H, $J = 10.2$ Hz), 5.64-5.75 (m, 1H), 7.17-7.22 (m, 1H), 7.31 (d, 1H, $J = 7.9$ Hz), 7.65-7.71 (m, 1H), 7.74 (dd, 1H, $J = 8.2/1.8$ Hz), 7.90 (d, 1H, $J = 1.8$ Hz), 7.93 (d, 1H, $J = 8.2$ Hz), 8.52 (d, 1H, $J = 5.0$ Hz) ppm.

$^{13}\text{C-NMR}$ (125 MHz, CDCl_3): $\delta = 15.6, 26.5, 27.6, 49.2, 52.2, 53.1, 55.0, 56.2, 57.0, 117.0, 122.3, 122.6, 124.5, 129.0, 132.4, 134.1, 135.1, 137.2, 137.3, 145.1, 149.1, 157.0, 165.0, 170.6$ ppm.

5.2.69. Compound 87

2-Chloro-4-(((1*S*,5*S*,6*R*)-2-oxo-3-(pyridin-2-ylmethyl)-5-vinyl-3,10-diazabicyclo[4.3.1]decan-10-yl)sulfonyl)benzoic acid



86 (106 mg, 210 μmol , 1.0 eq.) was dissolved in THF/H₂O 1:1 (10 mL) and LiOH (15.1 mg, 630 μmol , 3.0 eq.) was added. The reaction was stirred at room temperature for 2 h, then it was acidified with 1 M HCl and extracted with EA. The organic phase was dried over MgSO₄, filtered and concentrated *in vacuo*. The crude product was purified by silica gel column chromatography (EA + 1 % HCOOH) to afford **87**.

Yield: 104.5 mg, quant.

Purity: 97 % (HPLC, UV-absorption 220 nm)

Appearance: colourless solid

TLC: R_f = 0.40 (EA + 5 % MeOH + 1 % HCOOH)

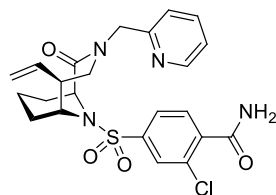
HR-MS (ESI): m/z calculated: [M+H]⁺ = 490.11980, found: [M+H]⁺ = 490.12009

¹H-NMR (500 MHz, CDCl₃): δ = 1.22-1.40 (m, 2H), 1.47-1.65 (m, 3H), 2.27 (d, 1H, *J* = 13.5 Hz), 2.69 (q, 1H, *J* = 8.6 Hz), 3.13 (d, 1H, *J* = 14.0 Hz), 3.99-4.10 (m, 2H), 4.77 (d, 1H, *J* = 15.6 Hz), 4.87 (d, 1H, *J* = 5.9 Hz), 5.00-5.10 (m, 2H), 5.19 (d, 1H, *J* = 15.6 Hz), 5.72 (ddd, 1H, *J* = 16.9, 10.1, 8.6 Hz), 7.40 (dd, 1H, *J* = 7.0/5.4 Hz), 7.50 (d, 1H, *J* = 7.9 Hz), 7.77 (dd, 1H, *J* = 8.1/1.6 Hz), 7.90 (t, 1H, *J* = 7.8 Hz), 7.93 (d, 1H, *J* = 1.6 Hz), 8.04 (d, 1H, *J* = 8.2 Hz), 8.67 (d, 1H, *J* = 4.6 Hz) ppm.

¹³C-NMR (125 MHz, CDCl₃): δ = 15.6, 26.4, 27.5, 49.1, 52.6, 55.0, 55.0, 56.9, 117.3, 123.2, 123.6, 124.5, 129.0, 132.7, 135.0, 135.2, 136.9, 139.7, 144.7, 147.2, 155.8, 167.8, 171.7 ppm.

5.2.70. Compound 88

2-Chloro-4-(((1*S*,5*S*,6*R*)-2-oxo-3-(pyridin-2-ylmethyl)-5-vinyl-3,10-diazabicyclo[4.3.1]decan-10-yl)sulfonyl)benzamide



87 (12.0 mg, 25 μ mol, 1.0 eq.) was dissolved in dry THF (1 mL) under argon atmosphere and CDI (21.0 mg, 130 μ mol, 5.2 eq.) was added. After 2 h aq. NH_3 (30 %, 160 μ L, 2.51 mmol, 100 eq.) was added and it was stirred for 15 h at room temperature. Water was added and it was extracted with DCM. The organic phase was dried over MgSO_4 , filtered and concentrated *in vacuo*. The crude product was purified by silica gel column chromatography (EA \rightarrow EA + 5 % MeOH), washed with 0.1 M HCl and purified again by silica gel column chromatography (EA \rightarrow EA + 5 % MeOH) to afford **88**.

Yield: 6.7 mg, 56 %

Purity: 97 % (HPLC, UV-absorption 220 nm)

Appearance: colourless solid

TLC: $R_f = 0.41$ (DCM/MeOH 10:1)

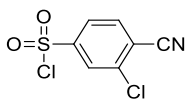
HR-MS (ESI): m/z calculated: $[\text{M}+\text{H}]^+ = 489.13578$, found: $[\text{M}+\text{H}]^+ = 489.13591$

$^1\text{H-NMR}$ (500 MHz, CDCl_3): $\delta = 1.18\text{-}1.36$ (m, 2H), 1.45-1.67 (m, 3H), 2.28 (d, 1H, $J = 13.4$ Hz), 2.71 (q, 1H, $J = 8.9$ Hz), 3.13 (dd, 1H, $J = 14.2/1.8$ Hz), 3.97-4.07 (m, 2H), 4.76 (d, 1H, $J = 6.0$ Hz), 4.85 (s, 2H), 5.00 (d, 1H, $J = 17.0$ Hz), 5.05 (dd, 1H, $J = 10.2/0.9$ Hz), 5.71 (ddd, 1H, $J = 17.0/10.1/8.7$ Hz), 6.19 (s, 1H), 6.39 (s, 1H), 7.23-7.27 (m, 1H), 7.37 (d, 1H, $J = 7.9$ Hz), 7.74 (td, 1H, $J = 7.7/1.4$ Hz), 7.76 (dd, 1H, $J = 8.1/1.8$ Hz), 7.87-7.90 (m, 2H), 8.54 (d, 1H, $J = 5.0$ Hz) ppm.

$^{13}\text{C-NMR}$ (125 MHz, CDCl_3): $\delta = 15.6, 26.5, 27.7, 49.2, 52.4, 55.0, 56.0, 57.0, 117.1, 122.6, 122.9, 125.1, 128.5, 131.7, 132.2, 137.2, 137.9, 138.0, 144.5, 148.6, 156.7, 166.7, 170.7$ ppm.

5.2.71. Compound 90

3-Chloro-4-cyanobenzene-1-sulfonyl chloride



Thionyl chloride (30 mL) was slowly added to water (100 mL) at 0 °C to create a SO₂/HCl solution. 4-Amino-2-chlorobenzonitrile **89** (417 mg, 2.73 mmol, 1.0 eq.) were dissolved in MeCN (60 mL) and conc. HCl (2 mL) was added, which precipitated a colourless solid. NaNO₂ (271 mg, 3.93 mmol, 1.4 eq.) in water (1 mL) was added, which dissolved the precipitate again. After stirring for 10 min at room temperature, the reaction mixture was cooled to 0 °C. The SO₂/HCl solution (60 mL, 191 mmol, 70 eq.) and CuCl₂ (191 mg, 1.42 mmol, 0.5 eq.) were added and the reaction mixture was stirred at room temperature for 3 h. Brine was added and it was extracted with EA. The organic phase was dried over MgSO₄, filtered and concentrated *in vacuo*. The crude product was purified by silica gel column chromatography twice (Cy/EA 9:1, then Cy → Cy/EA 9:1) to afford **90**.

Yield: 133 mg, 21 %

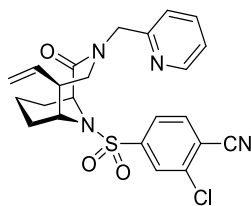
TLC: R_f = 0.44 (Cy/EA 3:1)

¹H-NMR (300 MHz, CDCl₃): δ = 7.96 (dd, 1H, *J* = 8.3/0.4 Hz), 8.05 (dd, 1H, *J* = 8.3/1.8 Hz), 8.19 (dd, 1H, *J* = 1.8/0.4 Hz) ppm.

¹³C-NMR (75 MHz, CDCl₃): δ = 114.2, 119.8, 125.4, 128.3, 135.4, 138.9, 148.0 ppm.

5.2.72. Compound 91

2-chloro-4-(((1*S*,5*S*,6*R*)-2-oxo-3-(pyridin-2-ylmethyl)-5-vinyl-3,10-diazabicyclo[4.3.1]decan-10-yl)sulfonyl)benzonitrile



Bicycle **21** (15.7 mg, 57.9 μmol , 1.0 eq.) and **90** (19.3 mg, 81.8 μmol , 1.4 eq.) were dissolved in dry MeCN (500 μL) under argon atmosphere and DIPEA (19 μL , 112 μmol , 1.9 eq.) was added. The reaction mixture was stirred at room temperature for 17 h, then the solvent was removed *in vacuo* and the crude mixture was purified by silica gel column chromatography (Cy/EA 2:1 \rightarrow Cy/EA 1:2) to afford **86**.

Yield: 14.5 mg, 53 %

Purity: 99 % (HPLC, UV-absorption 220 nm)

Appearance: colourless solid

TLC: $R_f = 0.29$ (Cy/EA 1:2)

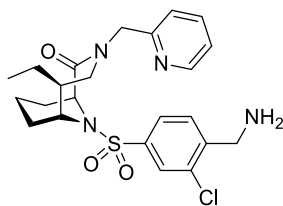
HR-MS (ESI): m/z calculated: $[\text{M}+\text{H}]^+ = 471.12522$, found: $[\text{M}+\text{H}]^+ = 471.12534$

$^1\text{H-NMR}$ (500 MHz, CDCl_3): $\delta = 1.13\text{-}1.34$ (m, 2H), 1.46-1.69 (m, 3H), 2.32 (d, 1H, $J = 13.6$ Hz), 2.74 (q, 1H, $J = 8.8$ Hz), 3.15 (dd, 1H, $J = 14.3/1.8$ Hz), 3.95-4.05 (m, 2H), 4.71-4.81 (m, 2H), 4.87 (d, 1H, $J = 15.2$ Hz), 5.00 (d, 1H, $J = 17.0$ Hz), 5.06 (dd, 1H, $J = 10.2/0.8$ Hz), 5.71 (ddd, 1H, $J = 17.0, 10.2, 8.8$ Hz), 7.23 (dd, 1H, $J = 7.5/5.0$ Hz), 7.33 (d, 1H, $J = 7.9$ Hz), 7.71 (td, 1H, $J = 7.7/1.7$ Hz), 7.78-7.86 (m, 2H), 7.97 (d, 1H, $J = 1.5$ Hz), 8.53 (d, 1H, $J = 4.9$ Hz) ppm.

$^{13}\text{C-NMR}$ (125 MHz, CDCl_3): $\delta = 15.6, 26.7, 27.8, 49.2, 52.2, 55.3, 56.2, 57.1, 114.7, 117.2, 117.4, 122.4, 122.8, 125.0, 128.0, 135.1, 137.1, 137.4, 138.5, 146.7, 149.0, 156.8, 170.3$ ppm.

5.2.73. Compound 92

(1*S*,5*S*,6*R*)-10-((4-(aminomethyl)-3-chlorophenyl)sulfonyl)-5-ethyl-3-(pyridin-2-ylmethyl)-3,10-diazabicyclo[4.3.1]decan-2-one



91 (4.8 mg, 10 μ mol, 1.0 eq.) was dissolved in dry MeOH under argon atmosphere. CoCl_2 (4.1 mg, 32 μ mol, 3.2 eq.) and NaBH_4 (3.0 mg, 79 μ mol, 7.9 eq.) were added at 0 $^\circ\text{C}$, then the reaction mixture was allowed to warm to room temperature. It was stirred for 4 h, then water and NH_4OH were added and it was extracted with DCM. The organic phase was dried over MgSO_4 , filtered and concentrated *in vacuo*. The crude product was purified by semi-preparative HPLC (10-50% MeCN in H_2O) to afford **92**.

Yield: 1.6 mg, 31 %

Purity: >99 % (HPLC, UV-absorption 220 nm)

Appearance: colourless solid

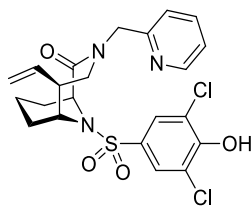
TLC: $R_f = 0.12$ (EA + 5 % MeOH + 3 % TEA)

HR-MS (ESI): m/z calculated: $[\text{M}+\text{H}]^+ = 477.17217$, found: $[\text{M}+\text{H}]^+ = 477.17212$

$^1\text{H-NMR}$ (500 MHz, CD_3OD): $\delta = 0.86$ (t, 3H, $J = 7.4$ Hz), 1.19-1.70 (m, 8H), 1.95-2.08 (m, 1H), 2.15 (d, 1H, $J = 13.0$ Hz), 3.22 (d, 1H, $J = 14.4$ Hz), 3.84-3.97 (m, 2H), 4.37 (s, 2H), 4.72-4.77 (m, 1H), 4.78-4.80 (m, 1H), 4.86-4.91 (m, 2H), 7.46-7.53 (m, 1H), 7.53-7.57 (d, 1H, $J = 7.7$ Hz), 7.77 (d, 1H, $J = 8.1$ Hz), 7.94 (dd, 1H, $J = 8.1/1.8$ Hz), 7.98-8.05 (m, 1H), 8.08 (d, 1H, $J = 1.8$ Hz), 8.59 (d, 1H, $J = 4.3$ Hz) ppm.

5.2.74. Compound 93

(1*S*,5*S*,6*R*)-10-((3,5-dichloro-4-hydroxyphenyl)sulfonyl)-3-(pyridin-2-ylmethyl)-5-vinyl-3,10-diazabicyclo[4.3.1]decan-2-one



Bicycle **21** (17.5 mg, 64 μ mol, 1.0 eq.) and 3,5-dichloro-4-hydroxybenzene-1-sulfonyl chloride **97** (20.7 mg, 79 μ mol, 1.2 eq.) were dissolved in dry MeCN (1 mL) under argon atmosphere. DIPEA (20 μ L, 118 μ mol, 1.8 eq.) was added and it was stirred for 18 h at room temperature. The solvent was evaporated *in vacuo* and the crude product was purified by semi-preparative HPLC (15-100 % MeCN in H₂O) to afford **93**.

Yield: 3.9 mg, 12 %

Purity: 96 % (HPLC, UV-absorption 220 nm)

Appearance: colourless solid

TLC: R_f = 0.39 (DCM/MeOH 10:1)

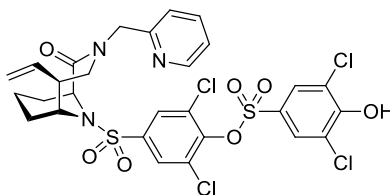
HR-MS (ESI): m/z calculated: $[M+H]^+ = 496.08591$, found: $[M+H]^+ = 496.08612$

¹H-NMR (500 MHz, CD₃OD): δ = 1.31-1.44 (m, 2H), 1.49-1.71 (m, 3H), 2.19 (d, 1H, J = 13.5 Hz), 2.87 (q, 1H, J = 8.5 Hz), 3.20 (d, 1H, J = 14.0 Hz), 4.04 (s, 1H), 4.09 (dd, 1H, J = 14.0/11.1 Hz), 4.72 (d, 1H, J = 5.8 Hz), 4.76 (d, 1H, J = 15.9 Hz), 5.03 (d, 1H, J = 15.9 Hz), 5.07-5.17 (m, 2H), 5.79 (ddd, 1H, J = 17.2/10.2/8.5 Hz), 7.58-7.67 (m, 2H), 7.82 (s, 2H), 8.19 (td, 1H, J = 7.8/1.7 Hz), 8.64 (d, 1H, J = 5.5 Hz) ppm.

¹³C-NMR (125 MHz, CD₃OD): δ = 16.4, 27.2, 28.4, 50.0, 54.3, 55.8, 55.9, 58.0, 117.4, 124.2, 124.8, 125.4, 128.2, 134.0, 138.5, 143.2, 146.8, 155.1, 156.5, 173.7 ppm.

5.2.75. Compound 94

2,6-Dichloro-4-(((1*S*,5*S*,6*R*)-2-oxo-3-(pyridin-2-ylmethyl)-5-vinyl-3,10-diazabicyclo[4.3.1]decan-10-yl)sulfonyl)phenyl 3,5-dichloro-4-hydroxybenzenesulfonate



Compound **94** was formed and isolated as a side product from the synthesis of **93**.

Yield: 14.5 mg, 31 %

Purity: 89 % (HPLC, UV-absorption 220 nm)

Appearance: colourless solid

TLC: $R_f = 0.49$ (DCM/MeOH 10:1)

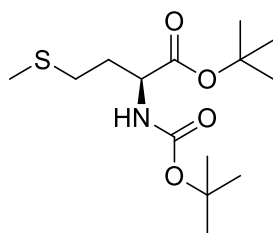
HR-MS (ESI): m/z calculated: $[M+H]^+ = 719.99608$, found: $[M+H]^+ = 719.99602$

$^1\text{H-NMR}$ (500 MHz, CD_3OD): $\delta = 1.30$ - 1.43 (m, 2H), 1.50 - 1.72 (m, 3H), 2.19 (d, 1H, $J = 13.7$ Hz), 2.89 (q, 1H, $J = 8.5$ Hz), 3.23 (d, 1H, $J = 14.2$ Hz), 4.02 - 4.14 (m, 3H), 4.75 - 4.83 (m, 2H), 5.02 (d, 1H, $J = 15.9$ Hz), 5.07 - 5.17 (m, 2H), 5.79 (ddd, 1H, $J = 17.0/10.2/8.5$ Hz), 7.59 - 7.69 (m, 2H), 7.93 (s, 2H), 8.07 (s, 2H), 8.15 - 8.23 (m, 1H), 8.64 (d, 1H, $J = 4.7$ Hz) ppm.

$^{13}\text{C-NMR}$ (125 MHz, CD_3OD): $\delta = 16.3$, 27.3 , 28.5 , 50.0 , 54.3 , 55.8 , 56.2 , 58.2 , 117.5 , 124.2 , 124.8 , 125.4 , 128.8 , 130.2 , 132.8 , 138.4 , 142.7 , 143.2 , 146.7 , 147.6 , 156.4 , 156.4 , 157.2 , 173.4 ppm.

5.2.76. Compound 112

(*S*)-*tert*-butyl 2-((*tert*-butoxycarbonyl)amino)-4-(methylthio)butanoate



Boc-L-Methionine **111** (3.64 g, 14.60 mmol, 1.0 eq.) and DMAP (200 mg, 1.64 mmol, 0.1 eq.) were dissolved in DCM (150 mL) under argon atmosphere. *tert*-Butanol (2.64 mL, 28.19 mmol, 1.9 eq.) was added and the mixture was cooled to 0 °C. DCC (3.79 g, 18.37 mmol, 1.3 eq.) was added and the reaction mixture was allowed to warm to room temperature. After 18 h, the colourless precipitate was filtered off and the filtrate was washed with 1M HCl, dried over MgSO₄, filtered and concentrated *in vacuo*. The crude product was purified by silica gel column chromatography (Cy/EA 9:1) to afford **112**.

Yield: 3.78 g, 85 %

Appearance: yellowish oil

TLC: R_f = 0.44 (Cy/EA 3:1, PMA stain)

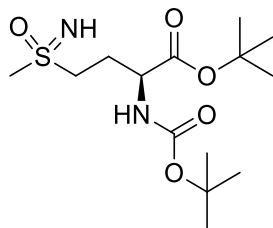
MS (ESI): m/z calculated [M+H]⁺ = 306.17, [M+Na]⁺ = 328.16, found [M+H]⁺ = 305.92, [M+Na]⁺ = 328.06

¹H-NMR (300 MHz, CDCl₃): δ = 1.14 (s, 9H), 1.46 (s, 9H), 1.79–1.99 (m, 1H), 1.99–2.18 (m, 4H), 2.41–2.62 (m, 2H), 4.26 (d, 1H, *J* = 4.6 Hz), 5.10 (d, 1H, *J* = 5.2 Hz) ppm.

¹³C-NMR (75 MHz, CDCl₃): δ = 15.6, 28.1, 28.5, 30.1, 32.8, 53.6, 79.9, 82.2, 155.4, 171.5 ppm.

5.2.77. Compound 113

(2*S*)-*tert*-butyl 2-((*tert*-butoxycarbonyl)amino)-4-(methylsulfonimidoyl)butanoate



112 (3.73 g, 12.21 mmol, 1.0 eq.), ammonium acetate (1.88 g, 24.42 mmol, 2.0 eq.) and PIDA (9.87 g, 30.64 mmol, 2.5 eq.) were dissolved in MeOH (150 mL) and stirred at room temperature. After 22 h the solvent was removed *in vacuo* and the residue was purified by silica gel column chromatography (EA) to afford **113**.

Yield: 3.58 g, 87 %

Appearance: yellowish solid

TLC: $R_f = 0.13$ (EA, Ninhydrin stain)

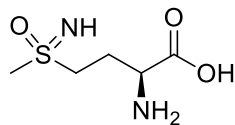
MS (ESI): m/z calculated $[M+H]^+ = 337.18$, $[M+Na]^+ = 359.16$, found $[M+H]^+ = 337.23$, $[M+Na]^+ = 359.20$

$^1\text{H-NMR}$ (300 MHz, CDCl_3): $\delta = 1.41$ (s, 9H), 1.44 (s, 9H), 2.04–2.18 (m, 1H), 2.26–2.44 (m, 1H), 2.97 (s, 3H), 3.02–3.27 (m, 2H), 4.14–4.36 (m, 1H), 5.21–5.44 (m, 1H) ppm.

$^{13}\text{C-NMR}$ (75 MHz, CDCl_3): $\delta = 26.6, 28.0, 28.4, 43.0, 52.7, 53.5, 80.3, 83.0, 155.5, 170.5$ ppm.

5.2.78. Compound 101

(2*S*)-2-amino-4-(*S*-methylsulfonimidoyl)butanoic acid



113 (102 mg, 303 μmol , 1.0 eq.) was dissolved in 1M HCl (5 mL) and stirred at 90 °C for 16 h. The solvent was removed at 120 °C and the crude product was purified by cation exchange solid phase extraction to afford **101**.

Yield: 38 mg, 69 %

Appearance: colourless solid

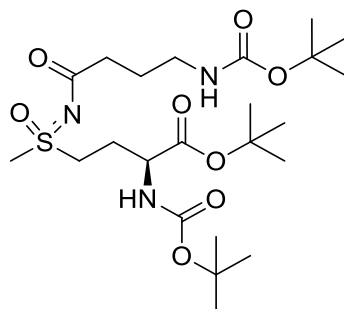
MS (ESI): m/z calculated: $[\text{M}+\text{H}]^+ = 181.06$, $[\text{M}+\text{Na}]^+ = 203.05$, found: $[\text{M}+\text{H}]^+ = 181.06$, $[\text{M}+\text{Na}]^+ = 203.09$

$^1\text{H-NMR}$ (300 MHz, D_2O): $\delta = 2.20\text{--}2.38$ (m, 2H), 3.19 (s, 3H), 3.34–3.55 (m, 2H), 3.74 (t, 1H, $J = 6.2$ Hz) ppm.

$^{13}\text{C-NMR}$ (75 MHz, D_2O): $\delta = 25.7, 41.1, 52.4, 53.6, 176.2$ ppm.

5.2.79. Compound 116

(2*S*)-*tert*-butyl 2-((*tert*-butoxycarbonyl)amino)-4-(*S*-methyl-*N*-(4-((*tert*-butoxycarbonyl)-amino)butanoyl)sulfonimidoyl)butanoate



113 (207 mg, 615 μmol , 1.0 eq.), Boc-GABA **119** (155 mg, 763 μmol , 1.2 eq.) and HATU (322 mg, 847 μmol , 1.4 eq.) were dissolved in DMF (30 mL) under argon atmosphere. DIPEA (415 μL , 2380 μmol , 3.9 eq.) was added and the reaction mixture was stirred at room temperature for 3 days. Water was added and it was extracted with DCM. The organic phase was dried over MgSO_4 , filtered and concentrated *in vacuo*. The crude product was purified by column chromatography (Cy/EA 1:1) to afford **116**.

Yield: 310 mg, quant.

Appearance: yellowish oil

TLC: $R_f = 0.58$ (EA)

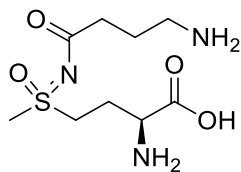
MS (ESI): m/z calculated: $[\text{M}+\text{H}]^+ = 522.28$, $[\text{M}+\text{Na}]^+ = 544.27$, found: $[\text{M}+\text{H}]^+ = 522.22$, $[\text{M}+\text{Na}]^+ = 544.21$

$^1\text{H-NMR}$ (500 MHz, CDCl_3): $\delta = 1.39$ (s, 9H), 1.40 (s, 9H), 1.44 (s, 9H), 1.75 (t, 2H, $J = 7.0$ Hz), 2.33 (t, 2H, $J = 7.1$ Hz), 2.75–2.77 (m, 4H), 3.07–3.14 (m, 2H), 3.18–3.24 (m, 3H), 4.21 (s, 1H), 4.78 (s, 1H), 5.39 (s, 1H) ppm.

$^{13}\text{C-NMR}$ (125 MHz, CDCl_3): $\delta = 25.4, 25.9, 28.0, 28.3, 28.5, 36.7, 38.7, 39.5, 40.1, 50.4, 52.6, 79.1, 80.3, 83.1, 156.0, 162.6, 170.1, 182.2$ ppm.

5.2.80. Compound 117

(2*S*)-2-amino-4-(*N*-(4-aminobutanoyl)-*S*-methylsulfonimidoyl)butanoic acid



116 (30 mg, 58 μ mol, 1.0 eq.) was dissolved in DCM (5 mL) and TFA (2.0 mL, 26.0 mmol, 450 eq.) was added. After 17 h at room temperature, the solvent was removed *in vacuo*. The crude product was purified by cation exchange solid phase extraction to afford **117**.

Yield: 18 mg, quant.

Appearance: yellowish solid

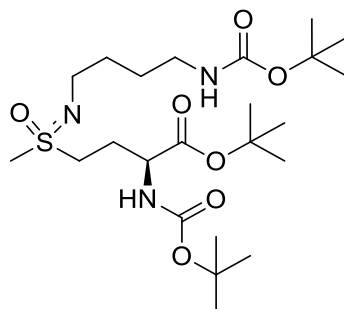
HR-MS (ESI): m/z calculated: $[M+H]^+ = 266.1169$, found: $[M+H]^+ = 266.1170$

$^1\text{H-NMR}$ (500 MHz, D_2O): $\delta = 1.90\text{--}2.03$ (m, 2H), 2.10–2.30 (m, 2H), 2.53 (t, 2H, $J = 7.3$ Hz), 3.06 (t, 2H, $J = 7.5$ Hz), 3.15–3.19 (m, 2H), 3.45 (s, 3H), 3.53 (t, 1H, $J = 6.3$ Hz) ppm.

$^{13}\text{C-NMR}$ (125 MHz, D_2O): $\delta = 23.0, 26.5, 36.5, 38.5, 38.9, 52.6, 54.1, 179.4, 183.9$ ppm.

5.2.81. Compound 115a

(2*S*)-*tert*-butyl 2-((*tert*-butoxycarbonyl)amino)-4-(*S*-ethyl-*N*-(4-((*tert*-butoxycarbonyl)amino)butyl)sulfonimidoyl)butanoate



116 (258 mg, 495 μmol , 1.0 eq.) was dissolved in DCM (25 mL) under argon atmosphere and cooled to 0 °C. A solution of $\text{BH}_3\text{-SMe}_2$ (5 M in Et_2O , 120 μL , 600 μmol , 1.2 eq.) was slowly added and the reaction mixture was allowed to get to room temperature. After 19 h, more BH_3SMe_2 (140 μL , 700 μmol , 1.4 eq.) was added at, and after another 5 h $\text{BH}_3\text{-SMe}_2$ (200 μL , 1000 μmol , 2.0 eq.) was added a third time, each at 0 °C. The mixture was stirred for 17 h at room temperature and MeOH was added to quench excessive borane. Water was added and it was extracted with DCM. The organic phase was dried over MgSO_4 , filtered and concentrated *in vacuo*. The crude product was purified by column chromatography (EA) to afford **115a**.

Yield: 42 mg, 17 %

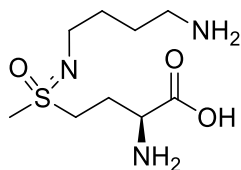
TLC: $R_f = 0.24$ (EA)

MS (ESI): m/z calculated: $[\text{M}+\text{H}]^+ = 508.31$, found: $[\text{M}+\text{H}]^+ = 508.43$

$^1\text{H-NMR}$ (300 MHz, CDCl_3): $\delta = 1.43$ (s, 9H), 1.44 (s, 9H), 1.47 (s, 9H), 2.05-2.20 (m, 1H), 2.26-2.43 (m, 1H), 2.91-2.96 (m, 3H), 3.01-3.19 (m, 5H), 3.20-3.34 (m, 1H), 3.44-3.76 (m, 2H), 4.12-4.38 (m, 1H), 4.71-4.79 (br. s, 1H), 5.45 (d, 1H, $J = 7.1$ Hz) ppm.

5.2.82. Compound 118a

(2S)-2-amino-4-(N-(4-aminobutyl)-S-methylsulfonimidoyl)butanoic acid



115a (42 mg, 83 μmol , 1.0 eq.) was dissolved in DCM (10 mL) and TFA (700 μL , 9090 μmol , 110 eq.) was added. After 20 h at room temperature, the solvent was removed *in vacuo*. The crude product was purified by cation exchange solid phase extraction to afford **118a**.

Yield: 15 mg, 71 %

Appearance: yellowish solid

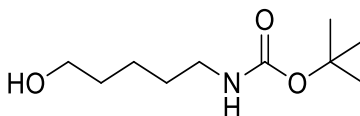
HR-MS (ESI): m/z calculated: $[\text{M}+\text{H}]^+ = 252.1376$, found: $[\text{M}+\text{H}]^+ = 252.1376$

$^1\text{H-NMR}$ (500 MHz, D_2O): $\delta = 1.48\text{--}1.77$ (m, 4H), 1.98–2.20 (m, 2H), 2.89–2.98 (m, 1H), 3.03–3.20 (m, 5H), 3.33–3.51 (m, 3H), 4.74–4.92 (m, 1H) ppm.

$^{13}\text{C-NMR}$ (125 MHz, D_2O): $\delta = 26.2, 28.6, 28.7, 38.1, 39.7, 42.4, 49.5, 54.7, 181.4$ ppm.

5.2.83. Compound 169

tert-butyl (5-hydroxypentyl)carbamate



5-Aminopentan-1-ol (1.00 g, 9.69 mmol, 1.0 eq.) was dissolved in DCM (25 mL) under argon atmosphere and TEA (2.00 mL, 14.43 mmol, 1.5 eq.) was added. The solution was cooled to 0 °C and Boc₂O (3.21 g, 14.71 mmol, 1.5 eq.) was added. The reaction mixture was stirred at room temperature for 17 h. The solvent was removed *in vacuo* and the residue was purified by silica gel column chromatography (Cy/EA 1:1) to afford **169b**.

Yield: 1.48 g, 75 %

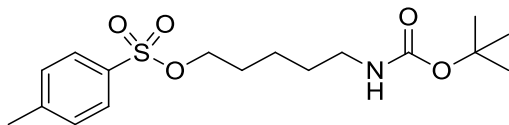
TLC: R_f = 0.32 (Cy/EA 1:1)

MS (ESI): m/z calculated: [M+H]⁺ = 204.16, [M+Na]⁺ = 226.14, found: [M+H]⁺ = 204.05, [M+Na]⁺ = 226.26

¹H-NMR (300 MHz, CDCl₃): δ = 1.31–1.41 (m, 2H), 1.43 (s, 9H), 1.46–1.53 (m, 2H), 1.53–1.65 (m, 2H), 3.11 (t, 2H, *J* = 6.8 Hz), 3.63 (t, 2H, *J* = 6.5 Hz) ppm.

5.2.84. Compound 114b

5-((*tert*-butoxycarbonyl)amino)pentyl 4-methylbenzenesulfonate



169b (1.45 g, 7.13 mmol, 1.0 eq.) was dissolved in DCM (20 mL) and put under argon atmosphere, then TEA (2.0 mL, 14.43 mmol, 2.0 eq.) was added. Tosyl chloride (2.39 g, 12.54 mmol, 1.8 eq.) was added and the reaction mixture was stirred at room temperature for 18 h. The solution was washed with water, dried over MgSO₄, filtered and the solvent was removed *in vacuo*. The crude product was purified by silica gel column chromatography (Cy/EA 3:1) to afford **114b**.

Yield: 2.35 g, 92 %

Appearance: yellowish solid

TLC: R_f = 0.34 (Cy/EA 3:1)

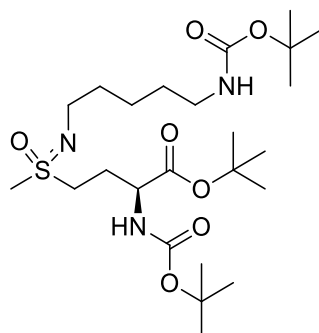
MS (ESI): m/z calculated: [M+H]⁺ = 358.17, [M+Na]⁺ = 380.15, found: [M+H]⁺ = 358.10, [M+Na]⁺ = 380.23

¹H-NMR (300 MHz, CDCl₃): δ = 1.27–1.35 (m, 2H), 2.36–1.45 (m, 11H), 1.58–1.68 (m, 2H), 2.42 (s, 3H), 3.03 (t, 2H, *J* = 6.2 Hz), 3.99 (t, 2H, *J* = 6.4 Hz), 4.53 (s, 1H), 7.32 (d, 2H, *J* = 8.2 Hz), 7.76 (d, 2H, *J* = 8.2 Hz) ppm.

¹³C-NMR (75 MHz, CDCl₃): δ = 21.7, 22.7, 28.5, 28.6, 29.5, 40.3, 70.4, 79.2, 127.9, 129.9, 133.3, 144.8, 156.0 ppm.

5.2.85. Compound 115b

(2*S*)-*tert*-butyl 2-((*tert*-butoxycarbonyl)amino)-4-(*S*-ethyl-*N*-(5-((*tert*-butoxycarbonyl)amino)pentyl)sulfonimidoyl)butanoate



113 (60 mg, 178 μmol , 1.0 eq.), **114b** (129 mg, 361 μmol , 2.0 eq.) and NaHCO_3 (33 mg, 393 μmol , 2.2 eq.) were dissolved in MeCN (5 mL) and refluxed for 2 days. DCM was added and the mixture was washed with water. The organic phase was dried over MgSO_4 , filtered and concentrated *in vacuo*. The crude product was purified by silica gel column chromatography (EA) to afford **115b**.

Yield: 52 mg, 56 %

TLC: $R_f = 0.31$ (EA)

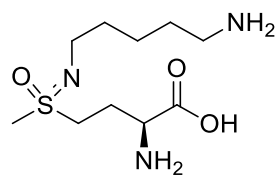
MS (ESI): m/z calculated: $[\text{M}+\text{H}]^+ = 522.32$, $[\text{M}+\text{Na}]^+ = 544.30$, found: $[\text{M}+\text{H}]^+ = 522.32$, $[\text{M}+\text{Na}]^+ = 544.11$

$^1\text{H-NMR}$ (300 MHz, CDCl_3): $\delta = 1.30\text{--}1.37$ (m, 2H), 1.38–1.42 (m, 18H), 1.43–1.47 (m, 11H), 1.49–1.57 (m, 2H), 2.02–2.14 (m, 1H), 2.23–2.38 (m, 1H), 2.88 (s, 3H), 2.96–3.02 (m, 2H), 3.04–3.09 (m, 2H), 3.10–3.15 (m, 1H), 3.15–3.26 (m, 1H), 3.35–3.56 (m, 1H), 4.20 (s, 1H), 4.64 (s, 1H) ppm.

$^{13}\text{C-NMR}$ (75 MHz, CDCl_3): $\delta = 18.8, 24.4, 26.9, 28.1, 28.4, 28.5, 29.7, 32.4, 39.7, 40.6, 43.0, 50.5, 66.5, 79.0, 80.2, 82.9, 155.5, 156.1, 170.6$ ppm.

5.2.86. Compound 118b

(2*S*)-2-amino-4-(*N*-(5-aminopentyl)-*S*-methylsulfonimidoyl)butanoic acid



115b (52 mg, 100 μmol , 1.0 eq.) was dissolved in 1M HCl (3 mL) and stirred at 90 °C for 17 h. The solvent was removed at 120 °C and the residue was purified by cation exchange solid phase extraction to afford **118b**.

Yield: 17 mg, 65 %

Appearance: colourless solid

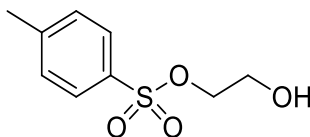
HR-MS (ESI): m/z calculated: $[\text{M}+\text{H}]^+ = 266.15329$, found: $[\text{M}+\text{H}]^+ = 266.15301$

$^1\text{H-NMR}$ (500 MHz, D_2O): $\delta = 1.44\text{--}1.54$ (m, 2H), 1.58–1.67 (m, 2H), 1.69–1.78 (m, 2H), 2.05–2.22 (m, 2H), 3.02–3.08 (m, 2H), 3.08–3.14 (m, 2H), 3.15 (s, 3H), 3.36–3.53 (m, 2H), 3.72–3.85 (m, 1H) ppm.

$^{13}\text{C-NMR}$ (125 MHz, D_2O): $\delta = 23.2, 26.5, 28.0, 30.9, 38.1, 39.5, 42.5, 49.3, 54.4, 58.9, 180.1$ ppm.

5.2.87. Compound 169c

2-hydroxyethyl 4-methylbenzenesulfonate



Ethylene glycol (4.40 mL, 78.68 mmol, 4.9 eq.) was dissolved in DCM (100 mL) under argon atmosphere. TEA (4.36 mL, 31.27 mmol, 1.9 eq.) and tosyl chloride (3.07 g, 16.10 mmol, 1.0 eq.) were added and the reaction mixture was stirred at room temperature for 16 h. It was washed with water, the organic phase was dried over MgSO_4 , filtered and concentrated *in vacuo*. The crude product was purified by silica gel column chromatography (Cy/EA 3:1–1:1) to afford **169c**.

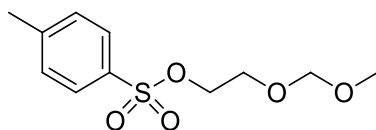
Yield: 1.44 g, 41 %

TLC: $R_f = 0.31$ (Cy/EA 1:1)

MS (ESI): m/z calculated $[\text{M}+\text{H}]^+ = 217.05$, found $[\text{M}+\text{H}]^+ = 217.25$

5.2.88. Compound 114c

2-(methoxymethoxy)ethyl 4-methylbenzenesulfonate



169c (506 mg, 2.34 mmol, 1.0 eq.) was dissolved in DCM (25 mL) under argon atmosphere. DIPEA (1.20 mL, 7.06 mmol, 3.0 eq.) and MOMCl (880 μ L, 11.59 mmol, 5.0 eq.) were added and the reaction mixture was stirred at room temperature. After 26 h it was washed with water, the organic phase was dried over MgSO_4 , filtered and concentrated *in vacuo*. The crude product was purified by column chromatography (Cy/EA 3:1) to afford **114c**.

Yield: 319 mg, 23 % over two steps

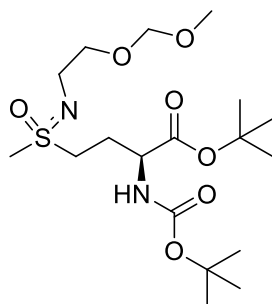
TLC: $R_f = 0.65$ (Cy/EA 1:1)

MS (ESI): m/z calculated $[\text{M}+\text{H}]^+ = 261.08$, found $[\text{M}+\text{H}]^+ = 261.26$

$^1\text{H-NMR}$ (300 MHz, CDCl_3): $\delta = 2.45$ (s, 3H), 3.31 (s, 3H), 3.71 (t, 2H, $J = 4.8$ Hz), 4.19 (t, 2H, $J = 4.8$ Hz), 4.56 (s, 2H), 7.34 (d, 2H, $J = 8.1$ Hz), 7.80 (d, 2H, $J = 8.2$ Hz) ppm.

5.2.89. Compound 115c

(2*S*)-*tert*-butyl 2-((*tert*-butoxycarbonyl)amino)-4-(*N*-(2-(methoxymethoxy)ethyl)-methylsulfonimidoyl)butanoate



113 (111 mg, 330 μmol , 1.0 eq.), **114c** (118 mg, 453 μmol , 1.4 eq.) and K_2CO_3 (99 mg, 716 μmol , 2.2 eq.) were dissolved in MeCN (30 mL) and refluxed for 6 days. After cooling to room temperature, the precipitate was filtered off and the filtrate was concentrated *in vacuo*. The crude product was purified by column chromatography three times (EA, DCM/MeOH 20:1, DCM/MeOH 30:1) to afford **115c**.

Yield: 19 mg, 14 %

TLC: R_f = 0.47 (DCM/MeOH 10:1)

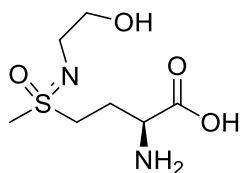
MS (ESI): m/z calculated $[\text{M}+\text{H}]^+ = 425.23$, $[\text{M}+\text{Na}]^+ = 447.21$, found $[\text{M}+\text{H}]^+ = 425.26$, $[\text{M}+\text{Na}]^+ = 447.13$

$^1\text{H-NMR}$ (500 MHz, CDCl_3): δ = 1.43 (s, 9H), 1.46 (s, 9H), 2.04–2.18 (m, 2H), 2.26–2.43 (m, 2H), 2.93–2.98 (m, 3H), 3.26 (t, 2H, $J = 5.7$ Hz), 3.34–3.37 (m, 3H), 3.60–3.65 (m, 2H), 4.23 (s, 1H), 4.65 (d, 2H, $J = 3.9$ Hz), 5.36 (dd, 1H, $J = 44.9/7.2$ Hz) ppm.

$^{13}\text{C-NMR}$ (125 MHz, CDCl_3): δ = 26.9, 28.1, 28.4, 40.1, 43.0, 51.0, 52.8, 55.4, 69.3, 80.3, 82.9, 96.7, 155.6, 170.6 ppm.

5.2.90. Compound 118c

(2S)-2-amino-4-(N-(2-hydroxyethyl)-methylsulfonimidoyl)butanoic acid



115c (19 mg, 45 μ mol, 1.0 eq.) was dissolved in DCM (5 mL) and TFA (2.0 mL, 26.0 mmol, 580 eq.) was added. The reaction mixture stirred at room temperature for 40 h, then the solvent was removed *in vacuo* and the residue was dissolved again in 15 % aq. NH_4OH . After 15 h at room temperature, the solvent was removed *in vacuo* and the crude product was purified by cation exchange chromatography to afford **118c**.

Yield: 8 mg, 80 %

Appearance: off-white solid

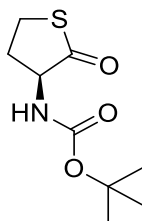
HR-MS (ESI): m/z calculated $[\text{M}+\text{H}]^+ = 225.09035$, found $[\text{M}+\text{H}]^+ = 225.09046$

$^1\text{H-NMR}$ (500 MHz, D_2O): $\delta = 2.16\text{--}2.38$ (m, 2H), 3.17 (s, 3H), 3.21 (td, 2H, $J = 5.8/2.2$ Hz), 3.39–3.58 (m, 2H), 3.68 (t, 2H, $J = 5.7$ Hz), 3.70–3.77 (m, 1H) ppm.

$^{13}\text{C-NMR}$ (125 MHz, D_2O): $\delta = 26.0, 38.2, 44.6, 49.4, 53.6, 62.4$ ppm.

5.2.91. Compound 107

(*S*)-*tert*-butyl (2-oxotetrahydrothiophen-3-yl)carbamate



L-Homocysteine thiolactone **106** (210 mg, 1.55 mmol, 1.0 eq.) was dissolved in THF/H₂O (1:1, 10 mL). NaHCO₃ (375 mg, 4.46 mmol, 2.9 eq.) and Boc₂O (350 μ L, 1.64 mmol, 1.1 eq.) were added and the mixture was stirred at room temperature. After 18 h and then after another 7 h, additional Boc₂O (each 200 μ L, 0.93 mmol, 0.6 eq.) was added. After 15 h, the reaction mixture was diluted with water and extracted with DCM. The organic phase was dried over MgSO₄, filtered and concentrated *in vacuo*. The crude product was purified by column chromatography (Cy/EA 3:1) to afford **107**.

Yield: 107 mg, 29 %

Appearance: colourless solid

TLC: R_f = 0.44 (Cy/EA 2:1)

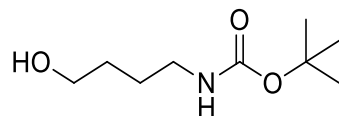
HR-MS (ESI): *m/z* calculated [M+H]⁺ = 218.08454, [M+Na]⁺ = 240.06649, found [M+H]⁺ = 218.08439, [M+Na]⁺ = 240.06638

¹H-NMR (500 MHz, CDCl₃): δ = 1.42 (s, 9H), 1.86–2.04 (m, 1H), 2.67–2.90 (m, 1H), 3.12–3.38 (m, 2H), 4.09–4.39 (m, 1H), 4.84–5.21 (s, 1H) ppm.

¹³C-NMR (125 MHz, CDCl₃): δ = 27.3, 28.4, 32.1, 60.6, 80.4, 155.6, 205.3 ppm.

5.2.92. Compound 170a

tert-butyl (4-hydroxybutyl)carbamate



4-Aminobutan-1-ol (1.03 mL, 11.2 mmol, 1.0 eq.) was dissolved in DCM (25 mL) under argon atmosphere. TEA (2.33 mL, 16.8 mmol, 1.5 eq.) was added and the solution was cooled to 0 °C. Boc₂O (3.88 g, 17.8 mmol, 1.6 eq.) was added and the reaction mixture was allowed to warm to room temperature. After 5 h the solvent was removed *in vacuo* and the crude product was purified by silica gel column chromatography (Cy/EA 1:1) to afford **170a**.

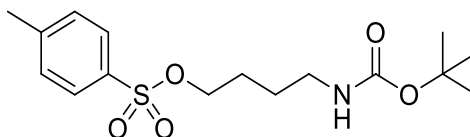
Yield: 1.75 g, 83 %

TLC: R_f = 0.22 (Cy/EA 1:1)

¹H-NMR (300 MHz, CDCl₃): δ = 1.43 (s, 9H), 1.49–1.66 (m, 4H), 3.10–3.19 (m, 2H), 3.61–3.72 (m, 2H) ppm.

5.2.93. Compound 108a

4-((*tert*-butoxycarbonyl)amino)butyl 4-methylbenzenesulfonate



170a (1.74 g, 9.20 mmol, 1.0 eq.) was dissolved in DCM (25 mL) under argon atmosphere. TEA (2.55 mL, 18.4 mmol, 2.0 eq.) and tosyl chloride (3.07 g, 16.1 mmol, 1.8 eq.) were added and the reaction mixture was stirred at room temperature for 18 h. It was washed with water, dried over MgSO₄, filtered and concentrated *in vacuo*. The crude product was purified by silica gel column chromatography (Cy/EA 4:1 → Cy/EA 2:1) to afford **108a**.

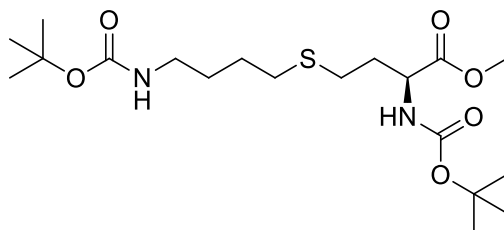
Yield: 2.17 g, 69 %

TLC: R_f = 0.25 (Cy/EA 3:1)

MS (ESI): m/z calculated: [M+Na]⁺ = 366.13, found: [M+Na]⁺ = 366.42

5.2.94. Compound 109a

(*S*)-Methyl 2-((*tert*-butoxycarbonyl)amino)-4-((4-((*tert*-butoxycarbonyl)amino)butyl)thio)butanoate



107 (299 mg, 1.38 mmol, 1.0 eq.) and NaOMe (157 mg, 2.91 mmol, 2.1 eq.) were dissolved in dry MeOH (25 mL) under argon atmosphere. After 30 min, **108a** (595 mg, 1.73 mmol, 1.3 eq.) was added. After 20 h, water was added and the reaction mixture was extracted with EA. The organic phase was dried over MgSO₄, filtered and concentrated *in vacuo*. The crude product was purified by column chromatography (DCM/MeOH 50:1) to afford **109a**.

Yield: 367 mg, 63 %

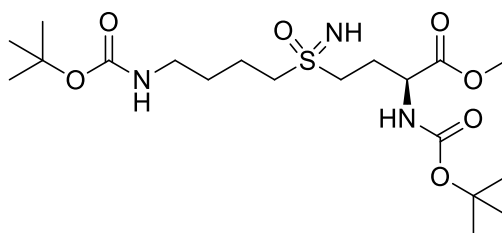
TLC: R_f = 0.21 (DCM/MeOH 20:1)

MS (ESI): m/z calculated: [M+H]⁺ = 421.24, [M+Na]⁺ = 443.22, found: [M+H]⁺ = 421.07, [M+Na]⁺ = 443.11

¹H-NMR (300 MHz, CDCl₃): δ = 1.42 (s, 9H), 1.46–1.56 (m, 2H), 1.61–1.73 (m, 2H), 2.44 (s, 1H), 3.07 (t, 2H, *J* = 6.9 Hz), 4.03 (t, 2H, *J* = 6.2 Hz), 7.34 (d, 2H, *J* = 8.0 Hz), 7.77 (d, 2H, *J* = 8.3 Hz) ppm.

5.2.95. Compound 110a

(2*S*)-methyl 2-((*tert*-butoxycarbonyl)amino)-4-(4-((*tert*-butoxycarbonyl)amino)butylsulfonimidoyl)butanoate



109a (367 mg, 0.87 mmol, 1.0 eq.), ammonium acetate (286 mg, 3.71 mmol, 4.3 eq.) and PIDA (862 mg, 2.21 mmol, 2.5 eq.) were dissolved in MeOH (15 mL) and stirred at room temperature for 17 h. The solvent was removed *in vacuo* and the crude product was purified by silica gel column chromatography (DCM/MeOH 20:1) to afford **110a**. Product **110a** still showed some impurities and was used in the next step without further purification.

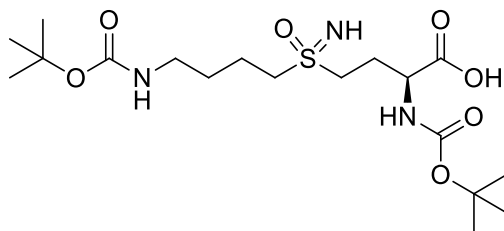
Yield: 109 mg, impure

TLC: $R_f = 0.28$ (DCM/MeOH 20:1)

MS (ESI): m/z calculated: $[M+H]^+ = 425.24$, found: $[M+H]^+ = 452.17$

5.2.96. Compound 171a

(2*S*)-2-((*tert*-butoxycarbonyl)amino)-4-(4-((*tert*-butoxycarbonyl)amino)butylsulfonimidoyl)butanoic acid



110a (109 mg, 41 μ mol, 1.0 eq.) was dissolved in THF/H₂O (1:1, 10 mL) and LiOH (14 mg, 603 μ mol, 2.5 eq.) was added. The reaction mixture was stirred at room temperature for 5 h. It was acidified with 1M HCl and extracted with EA. The organic phase was dried over MgSO₄, filtered and concentrated *in vacuo*. The crude product was purified by silica gel column chromatography (EA + 1 % HCOOH) to afford **171a**.

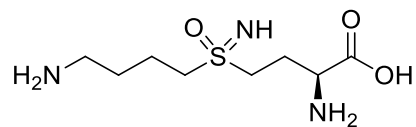
Yield: 63 mg, 16 % over two steps

TLC: R_f = 0.40 (DCM/MeOH 10:1 + 1 % HCOOH)

MS (ESI): m/z calculated: [M+H]⁺ = 438.23, [M+Na]⁺ = 460.21, found: [M+H]⁺ = 438.28, [M+Na]⁺ = 460.20

5.2.97. Compound 105a

(2*S*)-2-amino-4-(4-aminobutylsulfonimidoyl)butanoic acid



171a (63 mg, 144 μ mol, 1.0 eq.) was dissolved in DCM (5 mL) and TFA (170 μ L, 2.21 mmol, 15 eq.) was added. The reaction mixture was stirred at room temperature for 15 h and the solvent was removed *in vacuo*. The crude product was purified by cation exchange solid phase extraction to afford **105a**.

Yield: 29 mg, 85 %

Appearance: orange solid

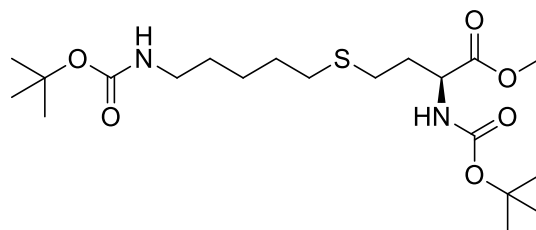
HR-MS (ESI): m/z calculated: $[M+H]^+ = 238.12199$, found: $[M+H]^+ = 238.12134$

$^1\text{H-NMR}$ (500 MHz, D_2O): $\delta = 1.78\text{--}2.04$ (m, 4H), 2.05–2.28 (m, 2H), 3.00–3.18 (m, 2H), 3.21–3.48 (m, 4H), 3.49–3.60 ppm.

$^{13}\text{C-NMR}$ (125 MHz, D_2O): $\delta = 19.1, 25.9, 27.0, 38.9, 50.8, 52.5, 54.4, 179.9$ ppm.

5.2.98. Compound 109b

(S)-methyl 2-((tert-butoxycarbonyl)amino)-4-((5-((tert-butoxycarbonyl)amino)pentyl)-thio)butanoate



107 (321 mg, 1.48 mmol, 1.0 eq.) and NaOMe (162 mg, 3.00 mmol, 2.0 eq.) were dissolved in dry MeOH (25 mL) under argon atmosphere. After 30 min, **114b** (625 mg, 1.75 mmol, 1.2 eq.) was added. After 20 h, water was added and the reaction mixture was extracted with EA. The organic phase was dried over MgSO₄, filtered and concentrated *in vacuo*. The crude product was purified by column chromatography (DCM/MeOH 50:1) to afford **109b**.

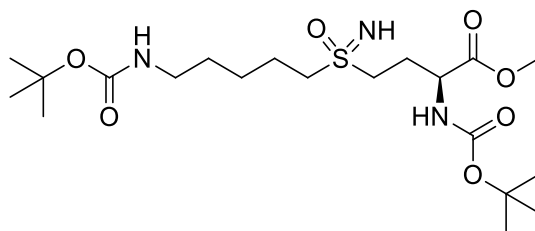
Yield: 430 mg, 67 %

TLC: R_f = 0.21 (DCM/MeOH 20:1)

MS (ESI): m/z calculated: [M+H]⁺ = 435.25, [M+Na]⁺ = 457.23, found: [M+H]⁺ = 435.14, [M+Na]⁺ = 457.18

5.2.99. Compound 110b

(*S*)-methyl 2-((*tert*-butoxycarbonyl)amino)-4-((5-((*tert*-butoxycarbonyl)amino)pentylsulfonimidoyl)butanoate



109b (430 mg, 0.99 mmol, 1.0 eq.), ammonium acetate (205 mg, 2.66 mmol, 2.7 eq.) and PIDA (862 mg, 2.60 mmol, 2.6 eq.) were dissolved in MeOH (15 mL) and stirred at room temperature for 17 h. The solvent was removed *in vacuo* and the crude product was purified by silica gel column chromatography (DCM/MeOH 50:1) to afford **110b**. Product **110b** still showed some impurities and was used in the next step without further purification.

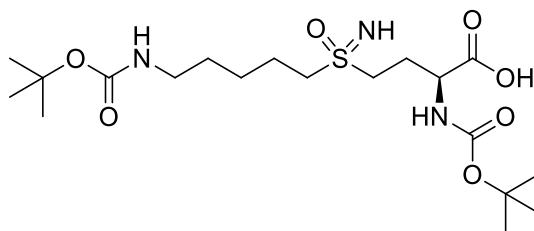
Yield: 261 mg, impure

TLC: $R_f = 0.49$ (DCM/MeOH 20:1)

MS (ESI): m/z calculated: $[M+H]^+ = 466.26$, $[M+Na]^+ = 488.24$, found: $[M+H]^+ = 466.25$, $[M+Na]^+ = 488.17$

5.2.100. Compound 171b

(*S*)-2-((*tert*-butoxycarbonyl)amino)-4-((5-((*tert*-butoxycarbonyl)amino)pentylsulfonimidoyl)butanoic acid



110b (261 mg, 561 μmol , 1.0 eq.) was dissolved in THF/H₂O (1:1, 20 mL) and LiOH (36 mg, 1503 μmol , 2.7 eq.) was added. The reaction mixture was stirred at room temperature for 3 h. It was acidified with 1M HCl and extracted with EA. The organic phase was dried over MgSO₄, filtered and concentrated *in vacuo*. The crude product was purified by column chromatography (EA + 1 % HCOOH) to afford **171b**.

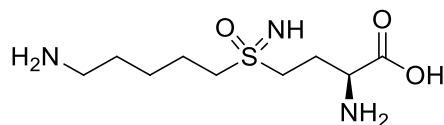
Yield: 67 mg, 26 % over two steps

TLC: R_f = 0.41 (DCM/MeOH 10:1 + 1 % HCOOH)

MS (ESI): m/z calculated: [M+H]⁺ = 452.24, [M+Na]⁺ = 474.22, found: [M+H]⁺ = 452.25, [M+Na]⁺ = 474.10

5.2.101. Compound 105b

(2S)-2-amino-4-(5-aminopentylsulfonimidoyl)butanoic acid



171b (67 mg, 148 μmol , 1.0 eq.) was dissolved in DCM (3 mL) and TFA (200 μL , 2.60 mmol, 18 eq.) was added. The reaction mixture was stirred at room temperature for 17 h and the solvent was removed *in vacuo*. The crude product was purified by cation exchange solid phase extraction to afford **105b**.

Yield: 34 mg, 92 %

Appearance: yellowish solid

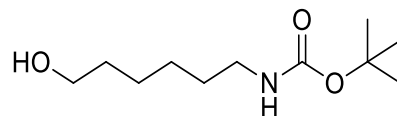
HR-MS (ESI): m/z calculated: $[\text{M}+\text{H}]^+ = 252.13764$, found: $[\text{M}+\text{H}]^+ = 252.13767$

$^1\text{H-NMR}$ (500 MHz, D_2O): $\delta = 1.51\text{--}1.70$ (m, 2H), 1.70–1.85 (m, 2H), 1.85–2.03 (m, 2H), 2.03–2.34 (m, 2H), 2.91–3.18 (m, 2H), 3.23–3.45 (m, 3H), 3.45–3.76 ppm.

$^{13}\text{C-NMR}$ (125 MHz, D_2O): $\delta = 21.3, 24.5, 26.5, 27.2, 39.2, 50.8, 52.8, 54.4, 180.3$ ppm.

5.2.102. Compound 170c

tert-butyl (6-hydroxyhexyl)carbamate



6-Aminohexan-1-ol (1.02 g, 8.70 mmol, 1.0 eq.) and Boc_2O (2.93 g, 13.42 mmol, 1.5 eq.) were dissolved in DCM (40 mL) under argon atmosphere. TEA (1.77 mL, 12.77 mmol, 1.5 eq.) was added and the reaction mixture was stirred at room temperature for 19 h. The solvent was removed *in vacuo* and the crude product was purified by silica gel column chromatography (Cy/EA 1:1) to afford **170c**.

Yield: 1.48 g, 78 %

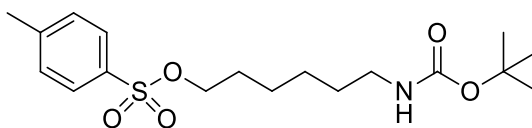
TLC: $R_f = 0.32$ (Cy/EA 1:1)

MS (ESI): m/z calculated: $[\text{M}+\text{H}]^+ = 218.18$, $[\text{M}+\text{Na}]^+ = 240.16$, found: $[\text{M}+\text{H}]^+ = 218.32$, $[\text{M}+\text{Na}]^+ = 240.41$

$^1\text{H-NMR}$ (500 MHz, CDCl_3): $\delta = 1.27\text{--}1.39$ (m, 4H), 1.41–1.44 (m, 9H), 1.44–1.51 (m, 2H), 1.51–1.61 (m, 2H), 3.09 (t, 2H, $J = 7.0$ Hz), 3.62 (t, 2H, $J = 6.5$ Hz) ppm.

5.2.103. Compound 108c

6-((*tert*-butoxycarbonyl)amino)hexyl 4-methylbenzenesulfonate



170c (1.46 g, 6.72 mmol, 1.0 eq.) was dissolved in DCM (25 mL) under argon atmosphere and TEA (1.86 mL, 13.44 mmol, 2.0 eq.) and tosyl chloride (1.55 g, 8.13 mmol, 1.2 eq.) were added. The reaction mixture was stirred at room temperature for 16 h and washed with water. The organic phase was dried over MgSO₄, filtered and concentrated *in vacuo*. The crude product was purified by silica gel column chromatography (Cy/EA 4:1) to afford **108c**.

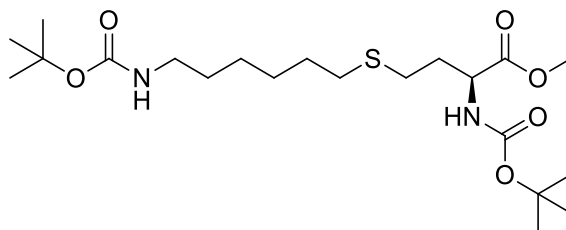
Yield: 2.00 g, 80 %

TLC: R_f = 0.32 (Cy/EA 3:1)

¹H-NMR (300 MHz, CDCl₃): δ = 1.18–1.40 (m, 6H), 1.43 (s, 9H), 1.56–1.69 (m, 2H), 2.44 (s, 3H), 3.05 (t, 2H, *J* = 7.0 Hz), 4.00 (t, 2H, *J* = 6.5 Hz), 4.48 (s, 1H), 7.34 (d, 2H, *J* = 8.3 Hz), 7.78 (d, 2H, *J* = 8.3 Hz) ppm.

5.2.104. Compound 109c

(S)-methyl 2-((*tert*-butoxycarbonyl)amino)-4-((6-((*tert*-butoxycarbonyl)amino)hexyl)-thio)butanoate



107 (353 mg, 1.62 mmol, 1.0 eq.) and NaOMe (204 mg, 3.78 mmol, 2.3 eq.) were dissolved in dry MeOH (25 mL) under argon atmosphere. After 30 min **108c** (767 mg, 2.06 mmol, 1.3 eq.) was added. After 20 h, water was added and the reaction mixture was extracted with EA. The organic phase was dried over MgSO₄, filtered and concentrated *in vacuo*. The crude product was purified by silica gel column chromatography (DCM/MeOH 50:1) to afford **109c**.

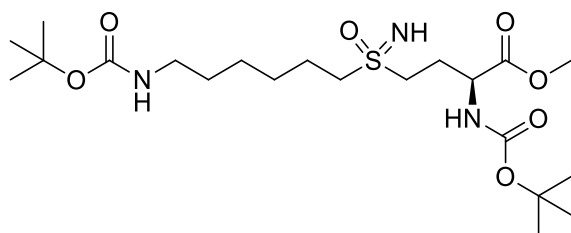
Yield: 575 mg, 79 %

TLC: R_f = 0.25 (DCM/MeOH 50:1)

MS (ESI): m/z calculated: [M+H]⁺ = 449.27, [M+Na]⁺ = 471.25, found: [M+H]⁺ = 449.19, [M+Na]⁺ = 471.29

5.2.105. Compound 110c

(2*S*)-methyl 2-((*tert*-butoxycarbonyl)amino)-4-(6-((*tert*-butoxycarbonyl)amino)hexylsulfonimidoyl)butanoate



109c (575 mg, 1.28 mmol, 1.0 eq.), ammonium acetate (252 mg, 3.27 mmol, 2.6 eq.) and PIDA (1038 mg, 3.22 mmol, 2.5 eq.) were dissolved in MeOH (40 mL) and stirred at room temperature for 17 h. The solvent was removed *in vacuo* and the crude product was purified by silica gel column chromatography (DCM/MeOH 30:1) to afford **110c**. Product **110c** still showed some impurities and was used in the next step without further purification.

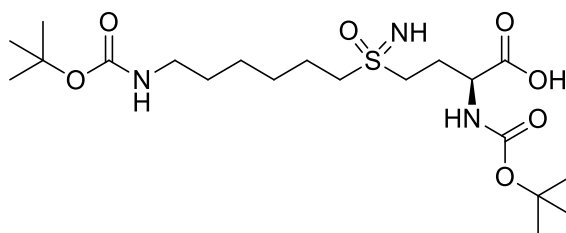
Yield: 252 mg, impure

TLC: $R_f = 0.26$ (DCM/MeOH 20:1)

MS (ESI): m/z calculated: $[M+H]^+ = 480.27$, $[M+Na]^+ = 502.26$, found: $[M+H]^+ = 480.41$, $[M+Na]^+ = 502.30$

5.2.106. Compound 171c

(2*S*)-2-((*tert*-butoxycarbonyl)amino)-4-(6-((*tert*-butoxycarbonyl)amino)hexylsulfon-imidoyl)butanoic acid



110c (252 mg, 525 μ mol, 1.0 eq.) was dissolved in THF/H₂O (1:1, 20 mL) and LiOH (34 mg, 1.42 mmol, 2.7 eq.) was added. The reaction mixture was stirred at room temperature for 4 h. It was acidified with 1M HCl and extracted with EA. The organic phase was dried over MgSO₄, filtered and concentrated *in vacuo*. The crude product was purified by silica gel column chromatography (DCM/MeOH 20:1 + 1 % HCOOH) to afford **171c**.

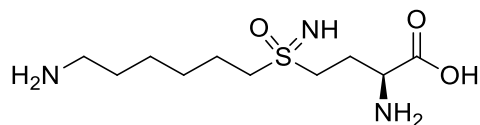
Yield: 152 mg, 62 % over two steps

TLC: R_f = 0.11 (DCM/MeOH 20:1 + 1 % HCOOH)

MS (ESI): m/z calculated: [M+H]⁺ = 466.26, [M+Na]⁺ = 488.24, found: [M+H]⁺ = 466.32, [M+Na]⁺ = 488.21

5.2.107. Compound 105c

(2*S*)-2-amino-4-(6-aminohexylsulfonimidoyl)butanoic acid



171c (137 mg, 294 μmol , 1.0 eq.) was dissolved in DCM (15 mL) and TFA (5.0 mL, 64.9 mmol, 220 eq.) was added. The reaction mixture was stirred at room temperature for 17 h and the solvent was removed *in vacuo*. The crude product was purified by cation exchange solid phase extraction to afford **105c**.

Yield: 64 mg, 82 %

Appearance: yellowish solid

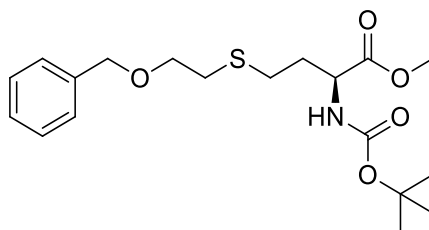
HR-MS (ESI): m/z calculated: $[\text{M}+\text{H}]^+ = 266.1533$, found: $[\text{M}+\text{H}]^+ = 266.1534$

$^1\text{H-NMR}$ (500 MHz, D_2O): $\delta = 1.42\text{--}1.49$ (m, 2H), 1.49–1.59 (m, 2H), 1.61–1.75 (m, 2H), 1.78–1.89 (m, 2H), 1.98–2.21 (m, 2H), 2.94 (t, 2H, $J = 7.0$ Hz), 3.21–3.38 (m, 4H), 3.41 (t, 1H, $J = 5.8$ Hz) ppm.

$^{13}\text{C-NMR}$ (125 MHz, D_2O): $\delta = 21.4, 25.1, 27.0, 27.5, 27.6, 39.6, 50.8, 53.0, 54.6, 181.2$ ppm.

5.2.108. Compound 109d

(S)-methyl 4-((2-(benzyloxy)ethyl)thio)-2-((tert-butoxycarbonyl)amino)butanoate



107 (255 mg, 1.17 mmol, 1.0 eq.) and NaOMe (382.1 mg, 7.07 mmol, 6 eq.) were dissolved in MeOH (20 ml) and stirred at room temperature. After 1 h, Benzyl-2-bromoethylether **108d** (273 mg, 1.27 mmol, 1.1 eq.) was added. After 16 h, the reaction mixture was extracted with ethyl acetate, the organic phase was dried over MgSO₄, the solvent evaporated *in vacuo* and the crude product was purified by silica gel column chromatography (Cy/EA 5:1) to afford **109d**.

Yield: 315 mg, 71 %

Appearance: colourless solid

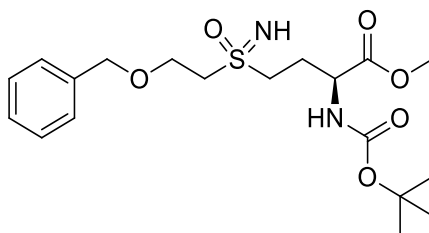
TLC: R_f = 0.20 (Cy/EA 5:1)

¹H-NMR (300 MHz, CDCl₃): δ = 1.37 (s, 9H), 1.73–1.95 (m, 1H), 1.96–2.11 (m, 1H), 2.53 (t, *J* = 7.6 Hz, 2H), 2.66 (t, 2H, *J* = 6.6 Hz), 3.56 (t, 2H, *J* = 6.6 Hz), 3.65 (s, 3H), 4.31 (s, 1H), 4.47 (s, 2H), 5.06 (s, 1H), 7.15–7.33 (m, 5H) ppm.

¹³C-NMR (75 MHz, CDCl₃): δ = 28.4, 28.5, 31.8, 32.9, 52.4, 52.9, 70.0, 73.1, 80.1, 127.8, 128.5, 138.2, 155.4, 172.8 ppm.

5.2.109. Compound 110d

(2*S*)-methyl 4-(2-(benzyloxy)ethylsulfonimidoyl)-2-((*tert*-butoxycarbonyl)amino) butanoate



109d (315 mg, 0.79 mmol, 1.0 eq.), MeCOONH₄ (126.24 mg, 1.64 mmol, 2.1 eq.) and PIDA (650 mg, 2.02 mmol, 2.6 eq.) were dissolved in methanol (25 ml) and stirred at room temperature for 18 h. The solvent was evaporated and the crude product was purified by silica gel column chromatography (Cy/EA 1:2 - EA). Product **110d** (239 mg) remained impure and was used in the next reaction as it was.

Yield: 239 mg, impure

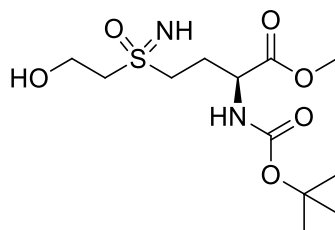
Appearance: yellow oil

TLC: R_f = 0.16 (Cy/EA 2:1)

MS (ESI): m/z calculated: [M+H]⁺ = 415.19, found: [M+H]⁺ = 415.44

5.2.110. Compound 172d

(2S)-methyl 4-(2-(benzyloxy)ethylsulfonimidoyl)-2-((*tert*-butoxycarbonyl)amino) butanoate



Crude **110d** (239 mg, 0.58 mmol, 1.0 eq.) was dissolved in ethanol (20 ml), degassed with argon for 10 minutes and put under an argon atmosphere. Palladium on carbon, 10 wt-% loading (613 mg, 0.58 mmol, 1.0 eq.) was added, hydrogen was introduced to the reaction mixture and it was stirred at room temperature. After 10 minutes, the mixture was put under a hydrogen atmosphere and continued to stir for additional 15 h. The palladium on carbon was then filtered over celite, the solvent evaporated and the crude product was purified by silica gel column chromatography (EA/MeOH 20:1) to afford **172d**.

Yield: 20 mg, 8 % over two steps

Appearance: colourless oil

TLC: $R_f = 0.15$ (Cy/MeOH 20:1)

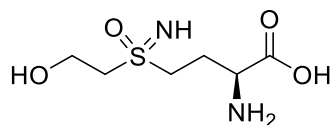
MS (ESI): m/z calculated: $[M+H]^+ = 325.15$, found: $[M+H]^+ = 325.09$

$^1\text{H-NMR}$ (300 MHz, CDCl_3): $\delta = 1.43$ (s, 9H), 2.10–2.26 (m, 1H), 2.25–2.54 (m, 1H), 3.11–3.47 (m, 6H), 3.76 (s, 3H), 3.96–4.24 (m, 2H), 4.40 (s, 1H), 5.45 (s, 1H) ppm.

$^{13}\text{C-NMR}$ (75 MHz, CDCl_3): $\delta = 19.2, 28.4, 51.2, 52.3, 52.8, 54.5, 61.4, 80.4, 155.7, 172.1$ ppm.

5.2.111. Compound 105d

(2*S*)-2-amino-4-(2-hydroxyethylsulfonimidoyl)butanoic acid



172d (20 mg, 0.06 mmol, 1.0 eq.) and LiOH (40 mg, 1.67 mmol, 28 eq.) were dissolved in a mixture of THF/H₂O (1:1, 5 ml) and stirred at room temperature for 18 h. The reaction mixture was acidified by addition of 1 M HCl and washed with EA. The aqueous phase was concentrated *in vacuo*. and the aqueous phase was collected. The crude product was purified by silica gel column chromatography (EA/MeOH 10:1 - MeOH/AcOH 50:1) and then by cation exchange solid phase extraction to afford **105d** (11 mg, 85 %).

Yield: 11 mg, 85 %

Appearance: colourless solid

TLC: R_f = 0.09 (MeOH/AcOH 50:1)

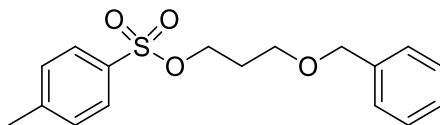
HR-MS (ESI): m/z calculated: [M+H]⁺ = 211.07470, found: [M+H]⁺ = 211.07482

¹H-NMR (500 MHz, D₂O): δ = 2.37–2.57 (m, 2H), 3.42–3.67 (m, 4H), 3.90–4.00 (m, 1H), 4.07–4.17 (m, 2H) ppm.

¹³C-NMR (125 MHz, D₂O): δ = 23.8, 51.7, 53.3, 55.7, 56.1, 173.1 ppm.

5.2.112. Compound 108e

3-(benzyloxy)propyl 4-methylbenzenesulfonate



3-(Benzyloxy)propan-1-ol **170e** (952 μ L, 6.02 mmol, 1.0 eq.) was dissolved in DCM (40 mL) under argon atmosphere. Pyridine (1.20 mL, 14.87 mmol, 2.5 eq.) and TsCl (2.36 g, 12.38 mmol, 2.1 eq.) were added and the reaction mixture was stirred at room temperature. After 16 h, TsCl (1.03 g, 5.40 mmol, 0.9 eq.) and NaH (60 % in mineral oil, 1.16 g, 29.30 mmol, 4.9 eq.) were added. The mixture was stirred for 3 days, then washed with water, the organic phase was dried over MgSO_4 , filtered and concentrated *in vacuo*. The crude product was purified by column chromatography (Cy/EA 5:1–3:1) to afford **108e**.

Yield: 488 mg, 25 %

Appearance: red liquid

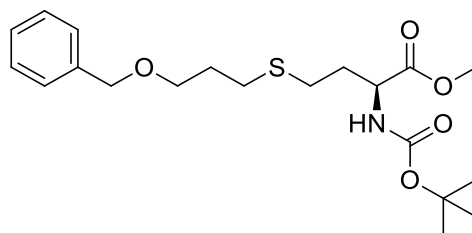
TLC: $R_f = 0.53$ (Cy/EA 3:1)

MS (ESI): m/z calculated $[\text{M}+\text{H}]^+ = 321.12$, found $[\text{M}+\text{H}]^+ = 321.43$

$^1\text{H-NMR}$ (300 MHz, CDCl_3): $\delta = 1.97$ (tt, 2H, $J = 6.1$ Hz), 2.45 (s, 3H), 3.53 (t, 2H, $J = 6.0$ Hz), 4.20 (t, 2H, $J = 6.2$ Hz), 4.44 (s, 2H), 7.24–7.40 (m, 7H), 7.82 (d, 2H, $J = 8.4$ Hz) ppm.

5.2.113. Compound 109e

(S)-methyl 4-((3-(benzyloxy)propyl)thio)-2-((tert-butoxycarbonyl)amino)butanoate



107 (215 mg, 1.00 mmol, 1.0 eq.) and NaOMe (134 mg, 2.48 mmol, 2.5 eq.) were dissolved in dry MeOH (20 mL) under argon atmosphere. After 30 min at room temperature, **108e** (477 mg, 1.49 mmol, 1.5 eq.) was added. After 18 h, more NaOMe (145 mg, 2.68 mmol, 2.7 eq.) was added and the mixture was stirred for another 2 h. Water was added and it was extracted with EA. The organic phase was dried over MgSO₄, filtered and concentrated *in vacuo*. The crude product was purified by column chromatography (Cy/EA 5:1) twice to afford **109e**.

Yield: 231 mg, 59 %

Appearance: yellowish oil

TLC: R_f = 0.46 (Cy/EA 3:1)

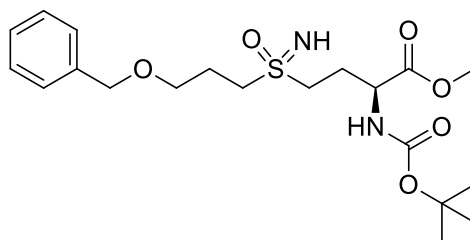
MS (ESI): m/z calculated [M+H]⁺ = 398.20, [M+Na]⁺ = 420.18, found [M+H]⁺ = 398.12, [M+Na]⁺ = 420.17

¹H-NMR (300 MHz, CDCl₃): δ = 1.45 (s, 9H), 1.82–2.00 (m, 3H), 2.03–2.20 (m, 1H), 2.55 (t, 2H, *J* = 7.5 Hz), 2.63 (t, 2H, *J* = 7.3 Hz), 3.56 (t, 2H, *J* = 6.2 Hz), 3.74 (s, 3H), 4.41 (s, 1H), 4.51 (s, 2H), 5.14 (s, 1H), 7.21–7.42 (m, 5H) ppm.

¹³C-NMR (125 MHz, CDCl₃): δ = 28.0, 28.4, 28.9, 29.8, 32.8, 52.5, 52.9, 68.8, 73.1, 80.1, 127.7, 127.7, 128.5, 138.5, 155.4, 172.9 ppm.

5.2.114. Compound 110e

(2S)-methyl 4-(3-(benzyloxy)propylsulfonimidoyl)-2-((tert-butoxycarbonyl)amino)butanoate



109e (231 mg, 581 μmol , 1.0 eq.), MeCOONH_4 (99 mg, 1.28 mmol, 2.2 eq.) and PIDA (527 mg, 1.64 mmol, 2.8 eq.) were dissolved in MeOH (20 mL) and stirred at room temperature for 16 h. The solvent was removed *in vacuo* and the crude product was purified by column chromatography (Cy/EA 1:1–EA) to afford **110e**. Product **110e** still showed some impurities and was used in the next step without further purification.

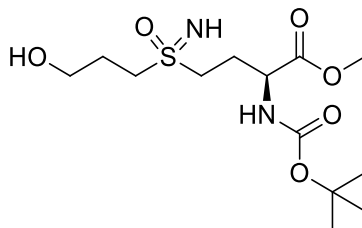
Yield: 302 mg, impure

TLC: $R_f = 0.10$ (Cy/EA 1:2)

MS (ESI): m/z calculated $[\text{M}+\text{H}]^+ = 429.21$, $[\text{M}+\text{Na}]^+ = 451.19$, found $[\text{M}+\text{H}]^+ = 429.30$, $[\text{M}+\text{Na}]^+ = 451.18$

5.2.115. Compound 172e

(2*S*)-methyl 2-((*tert*-butoxycarbonyl)amino)-4-(3-hydroxypropylsulfonimidoyl)butanoate



108c (302 mg, 705 μmol , 1.0 eq.) was dissolved in EtOH (10 mL) under argon atmosphere and degassed by introducing argon in the solution for 10 min. Pd/C (10 wt-%, 618 mg, 581 μmol , 0.8 eq.) was added and H_2 was introduced in the solution for 10 min. The reaction mixture stirred for 1 h under H_2 atmosphere, then it was filtered over celite. The solvent was evaporated *in vacuo* and the crude product was purified by column chromatography (EA + 5 % MeOH) to afford **172e**.

Yield: 86 mg, 44 % over two steps

TLC: $R_f = 0.09$ (EA + 5 % MeOH)

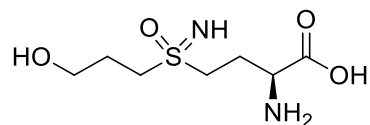
MS (ESI): m/z calculated $[\text{M}+\text{H}]^+ = 339.16$, $[\text{M}+\text{Na}]^+ = 361.14$, found $[\text{M}+\text{H}]^+ = 339.17$, $[\text{M}+\text{Na}]^+ = 361.08$

$^1\text{H-NMR}$ (300 MHz, CDCl_3): $\delta = 1.42$ (s, 9H), 2.03–2.46 (m, 4H), 3.16–3.26 (m, 3H), 3.26–3.40 (m, 2H), 3.75 (s, 3H), 4.38 (s, 1H), 5.54 (s, 1H) ppm.

$^{13}\text{C-NMR}$ (125 MHz, CDCl_3): $\delta = 25.6, 28.4, 29.8, 51.7, 52.2, 52.3, 52.9, 60.5, 80.6, 155.7, 172.0$ ppm.

5.2.116. Compound 105e

(2S)-2-amino-4-(3-hydroxypropylsulfonimidoyl)butanoic acid



172e (86 mg, 254 μ mol, 1.0 eq.) was dissolved in THF/H₂O (1:1, 10 mL) and LiOH (16 mg, 668 μ mol, 2.6 eq.) was added. After 14 h at room temperature, the solution was acidified by addition of 1M HCl and washed with EA. The aqueous phase was concentrated *in vacuo*. The crude product was purified first by column chromatography (EA + 5 % MeOH + 1 % HCOOH–MeOH + 2 % HCOOH) and then by cation exchange chromatography to afford **105e**.

Yield: 23 mg, 40 %

Appearance: colourless solid

TLC: R_f = 0.14 (MeOH + 2 % HCOOH)

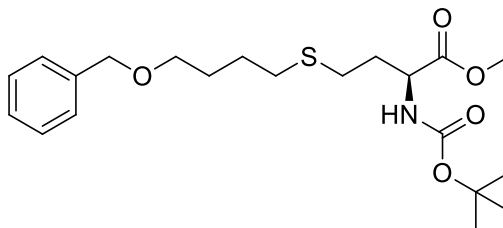
HR-MS (ESI): m/z calculated [M+H]⁺ = 225.0904, found [M+H]⁺ = 225.0905

¹H-NMR (500 MHz, D₂O): δ = 2.01–2.13 (m, 2H), 2.29–2.46 (m, 2H), 3.31–3.54 (m, 4H), 3.76 (t, 2H, *J* = 6.2 Hz), 3.82–3.90 (m, 1H) ppm.

¹³C-NMR (125 MHz, D₂O): δ = 24.2, 24.7, 50.2, 50.8, 53.3, 59.7, 174.1 ppm.

5.2.117. Compound 109f

(S)-methyl 4-((4-(benzyloxy)butyl)thio)-2-((tert-butoxycarbonyl)amino)butanoate



107 (250 mg, 1.15 mmol, 1.0 eq.) and NaOMe (193 mg, 3.57 mmol, 3.1 eq.) were dissolved in MeOH (20 ml) and stirred at room temperature. After 1 h, Benzyl-4-bromobutylether **108f** (330 μ L, 1.73 mmol, 1.5 eq.) was added. After 19 h, NaOMe (113 mg, 2.09 mmol, 1.8 eq.) was added and it was stirred for another 5 h. The reaction mixture was extracted with ethyl acetate, the organic phase was dried over MgSO₄, the solvent was evaporated *in vacuo* and the crude product was purified by silica gel column chromatography (Cy/EA 9:1) to afford **109f**.

Yield: 281 mg, 59 %

Appearance: colourless oil

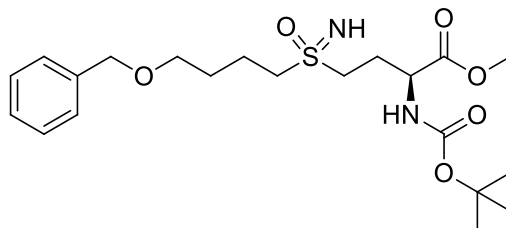
TLC: R_f = 0.51 (Cy/EA 9:1)

¹H-NMR (300 MHz, CDCl₃): δ = 1.46 (s, 9H), 1.60–1.79 (m, 4H), 1.83–1.99 (m, 1H), 2.03–2.18 (m, 1H), 2.48–2.61 (m, 3H), 3.49 (t, 2H, *J* = 5.9 Hz), 3.74 (s, 3H), 4.32–4.47 (m, 1H), 4.51 (s, 2H), 5.09–5.21 (m, 1H), 7.25–7.38 (m, 5H) ppm.

¹³C-NMR (125 MHz, CDCl₃): δ = 26.3, 27.8, 28.3, 28.9, 31.9, 32.7, 52.4, 52.8, 69.7, 72.9, 80.0, 127.5, 127.6, 128.4, 138.5, 155.3, 172.8 ppm.

5.2.118. Compound 110f

(2S)-methyl 4-(4-(benzyloxy)butylsulfonimidoyl)-2-((tert-butoxycarbonyl)amino) butanoate



109f (281 mg, 0.70 mmol, 1.0 eq.), MeCOONH₄ (109 mg, 1.41 mmol, 2 eq.) and PIDA (576 mg, 1.79 mmol, 2.6 eq.) were dissolved in methanol (20 ml) and stirred at room temperature for 18 h. The solvent was evaporated *in vacuo* and the crude product was purified by silica gel column chromatography (Cy/EA 2:1 - EA). Product **110** (173 mg) remained impure and was used in the next reaction as it was.

Yield: 173 mg, impure

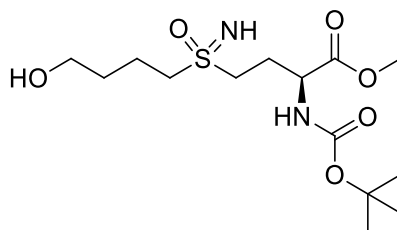
Appearance: colourless oil

TLC: R_f = 0.88 (Cy/EA 9:1)

MS (ESI): m/z calculated: [M+H]⁺ = 443.22, found: [M+H]⁺ = 443.32

5.2.119. Compound 172f

(2*S*)-methyl 2-((*tert*-butoxycarbonyl)amino)-4-(4-hydroxybutylsulfonimidoyl)butanoate



Crude **110f** (173 mg, 0.39 mmol, 1.0 eq.) was dissolved in ethanol (20 ml), stirred at room temperature and argon was introduced for 10 min. The reaction mixture was held under an argon atmosphere and palladium on carbon, 10 wt-% loading (462 mg, 434 mmol, 1.1 eq.) was added. Hydrogen was introduced to the reaction mixture for 10 min and afterwards held under a hydrogen atmosphere and stirred at room temperature for 6 h. The solvent was evaporated *in vacuo* and the crude product was purified by silica gel column chromatography (EA/MeOH 20:1 - EA/MeOH 10:1) to afford **172f**.

Yield: 53 mg, 22 % over two steps

Appearance: colourless oil

TLC: $R_f = 0.10$ (EA/MeOH 20:1)

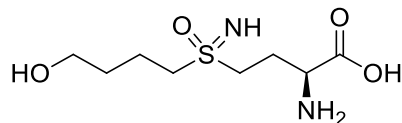
MS (ESI): m/z calculated: $[M+H]^+ = 353.18$, found: $[M+H]^+ = 353.19$

$^1\text{H-NMR}$ (300 MHz, CDCl_3): $\delta = 1.40$ (s, 9H), 1.57–1.74 (m, 2H), 1.83–1.98 (m, 2H), 2.06–2.21 (m, 1H), 2.25–2.44 (m, 1H), 2.95–3.22 (m, 5H), 3.56–5.69 (t, $J = 6$ Hz, 2H), 3.70–3.80 (s, 1H), 4.26 (s, 1H), 5.55–5.70 (m, 1H) ppm.

$^{13}\text{C-NMR}$ (125 MHz, CDCl_3): $\delta = 19.0, 25.6, 28.2, 30.8, 51.1, 52.1, 52.6, 54.3, 61.2, 80.3, 155.5, 171.9$ ppm.

5.2.120. Compound 105f

(2S)-2-amino-4-(4-hydroxybutylsulfonimidoyl)butanoic acid



172f (53 mg, 150 μmol , 1 eq.) was dissolved in THF/H₂O (1:1, 20 mL) and LiOH (10 mg, 417 μmol , 2.8 eq.) was added and stirred at room temperature for 3 h. The reaction mixture was acidified by addition of 1 M HCl and washed with EA. The aqueous phase was concentrated *in vacuo*. and the aqueous phase was collected. The crude product was purified by silica gel column chromatography (EA/MeOH 10:1 - MeOH/AcOH 50:1) and then by cation exchange solid phase extraction to afford **105f**.

Yield: 22 mg, 61 %

Appearance: colourless solid

TLC: R_f = 0.05 (DCM/MeOH 10:1)

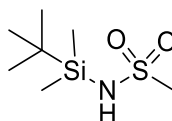
HR-MS (ESI): m/z calculated $[M+H]^+$ = 239.10600, found $[M+H]^+$ = 239.10606

¹H-NMR (500 MHz, D₂O): δ = 1.70–1.81 (m, 2H), 1.84–1.97 (m, 2H), 2.30–2.46 (m, 2H), 3.26–3.44 (m, 3H) 3.44–3.55 (m, 1H), 3.68 (t, 2H, J = 6.5 Hz), 3.88–3.97 (m, 1H) ppm.

¹³C-NMR (125 MHz, D₂O): δ = 18.6, 23.7, 30.1, 50.0, 53.2, 53.4, 60.1, 173.1 ppm.

5.2.121. Compound 141

N-(*tert*-butyldimethylsilyl)methanesulfonamide



Methanesulfonamide **140** (5125 mg, 53.9 mmol, 1.0 eq.) and TBSCl (9700 mg, 64.4 mmol, 1.2 eq.) were dissolved in dry THF (50 mL) under argon atmosphere and TEA (15 mL, 108 mmol, 2.0 eq.) was added. The reaction mixture was stirred at 45 °C for 23 h, over which time a colourless solid precipitated. Water was added and it was extracted with EA. The organic phase was dried over MgSO₄, filtered and concentrated *in vacuo*. The crude product was purified by silica gel column chromatography (Cy/EA 3:1 → EA) to afford **141**.

Yield: 11082 mg, 98 %

Appearance: off-white solid

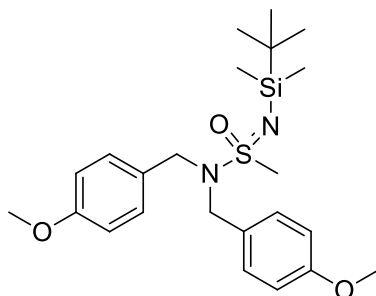
TLC: R_f = 0.37 (Cy/EA 2:1)

¹H-NMR (300 MHz, CDCl₃): δ = 0.26 (s, 6H), 0.92 (s, 9H), 2.99 (s, 3H), 4.88 (br. s, 1H) ppm.

¹³C-NMR (75 MHz, CDCl₃): δ = -4.3, 17.3, 25.8, 44.4 ppm.

5.2.122. Compound 153

N'-(*tert*-butyldimethylsilyl)-*N,N*-bis(4-methoxybenzyl)methanesulfonimidamide



Ph_3PCl_2 (4298 mg, 12.9 mmol, 1.3 eq.) was dissolved in dry CHCl_3 (40 mL) under argon atmosphere and cooled to 0 °C. TEA (3 mL, 21.6 mmol, 2.2 eq.) was added slowly and it was stirred at 0 °C for 10 min. **141** (2019 mg, 9.6 mmol, 1.0 eq.) was dissolved in dry CHCl_3 (5 mL) and added to the mixture. After stirring for 30 min at 0 °C, bis(4-methoxybenzyl)amine (2681 mg, 10.4 mmol, 1.1 eq.) dissolved in dry CHCl_3 (5 mL) was added. The reaction was allowed to warm to room temperature and stirred for 16 h, then the solvent was evaporated *in vacuo* and the crude product was purified by flash chromatography (2-20 % EA in Cy) to afford **153**.

Yield: 2677 mg, 62 %

Appearance: yellow oil

TLC: $R_f = 0.61$ (Cy/EA 3:1)

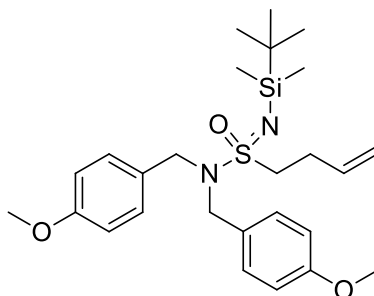
MS (ESI): m/z calculated $[\text{M}+\text{H}]^+ = 449.2$, found $[\text{M}+\text{H}]^+ = 449.2$

$^1\text{H-NMR}$ (300 MHz, CDCl_3): $\delta = -0.05$ (s, 3H), 0.00 (s, 3H), 0.76 (s, 9H), 2.52 (s, 3H), 3.63 (s, 6H), 3.94 (d, 2H, $J = 14.9$ Hz), 4.24 (d, 2H, $J = 14.9$ Hz), 6.69 (d, 4H, $J = 8.6$ Hz), 7.06 (d, 4H, $J = 8.6$ Hz) ppm.

$^{13}\text{C-NMR}$ (75 MHz, CDCl_3): $\delta = -2.4, -2.4, 18.2, 26.2, 44.6, 49.2, 55.4, 114.0, 128.8, 130.2, 159.2$ ppm.

5.2.123. Compound 154

N'-(*tert*-butyldimethylsilyl)-*N,N*-bis(4-methoxybenzyl)but-3-ene-1-sulfonimidamide



153 (2057 mg, 4.58 mmol, 1.0 eq.) was dissolved in dry THF (60 mL) under argon atmosphere. TMEDA (1.4 mL, 9.40 mmol, 2.1 eq.) was added and the solution was cooled to -84 °C. *n*-BuLi (2.3 M in hexanes, 2.4 mL, 5.52 mmol, 1.2 eq.) was added dropwise and after stirring for 30 min at -84 °C, allyl bromide (810 μ L, 9.22 mmol, 2.0 eq.) was dissolved in dry THF (4 mL) and added to the reaction. The reaction was allowed to warm to room temperature and stirred for 3 h. The reaction was quenched with sat. aq. NH₄Cl solution, then water was added and it was extracted with DCM. The organic phase was dried over MgSO₄, filtered and concentrated *in vacuo*. The crude product was purified by silica gel column chromatography (Cy/EA 30:1 \rightarrow 9:1) to afford **154**.

Yield: 1917 mg, 86 %

Appearance: pale-yellow oil

TLC: R_f = 0.31 (Cy/EA 9:1)

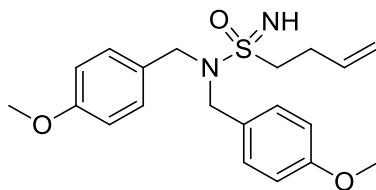
MS (ESI): m/z calculated [M+H-TBS]⁺ = 375.2, found [M+H-TBS]⁺ = 375.0

¹H-NMR (300 MHz, CDCl₃): δ = 0.12 (s, 3H), 0.18 (s, 3H), 0.93 (s, 9H), 2.40-2.56 (m, 2H), 2.75-2.92 (m, 2H), 3.81 (s, 6H), 4.12 (d, 2H, J = 15.0 Hz), 4.45 (d, 2H, J = 15.0 Hz), 4.93-5.08 (m, 2H), 5.74 (ddt, 1H, J = 17.6/9.7/6.6 Hz), 6.86 (d, 4H, J = 8.6 Hz), 7.20 (d, 4H, J = 8.6 Hz) ppm.

¹³C-NMR (75 MHz, CDCl₃): δ = -2.4, -2.3, 18.3, 26.2, 28.5, 49.4, 55.4, 56.2, 114.0, 116.3, 129.1, 130.1, 135.4, 159.2 ppm.

5.2.124. Compound 155

N,N-bis(4-methoxybenzyl)but-3-ene-1-sulfonimidamide



154 (2079 mg, 4.25 mmol, 1.0 eq.) was dissolved in THF (50 mL) and TBAF (1M in THF, 4.8 mL, 4.8 mmol, 1.1 eq.) was added. The reaction was stirred for 3 h at room temperature, then the solvent was evaporated *in vacuo*. The crude product was purified by flash chromatography (12-100 % EA in Cy) to afford **155**.

Yield: 1371 mg, 86 %

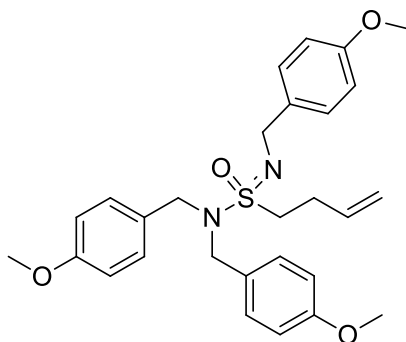
Appearance: colourless oil

TLC: $R_f = 0.37$ (Cy/EA 1:1)

MS (ESI): m/z calculated $[M+H]^+ = 375.2$, found $[M+H]^+ = 375.2$

5.2.125. Compound 156

N,N,N'-tris(4-methoxybenzyl)but-3-ene-1-sulfonimidamide



155 (745 mg, 1.99 mmol, 1.0 eq.) was dissolved in dry THF (20 mL) under argon atmosphere and cooled to 0 °C. NaH (60 % in mineral oil, 282 mg, 7.05 mmol, 3.5 eq.) was added and after stirring for 5 min at 0 °C, PMBCl (540 μ L, 4.00 mmol, 2.0 eq.) was added. The reaction was allowed to warm to room temperature and stirred for 24 h. Water was added and it was extracted with DCM. The organic phase was dried over MgSO₄, filtered and concentrated *in vacuo*. The crude product was purified by silica gel column chromatography (Cy/EA 9:1 \rightarrow 3:1) to afford **156**.

Yield: 608 mg, 62 %

Appearance: yellow oil

TLC: R_f = 0.34 (Cy/EA 3:1)

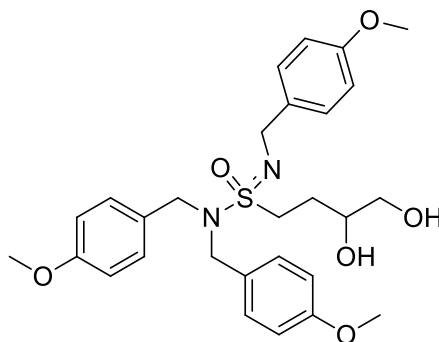
MS (ESI): m/z calculated $[M+H]^+$ = 495.2, found $[M+H]^+$ = 495.2

¹H-NMR (300 MHz, CDCl₃): δ = 2.42-2.70 (m, 2H), 2.83 (ddd, 1H, J = 13.4/10.6/5.4 Hz), 3.18 (ddd, 1H, J = 13.3/11.0/5.4 Hz), 3.78 (s, 3H), 3.82 (s, 6H), 3.95 (d, 1H, J = 14.1 Hz), 4.17 (d, 2H, J = 15.0 Hz), 4.30-4.47 (m, 3H), 4.95-5.09 (m, 2H), 5.63-5.83 (m, 1H), 6.84 (d, 2H, J = 8.6 Hz), 6.89 (d, 4H, J = 8.6 Hz), 7.24 (d, 4H, J = 8.6 Hz), 7.30 (d, 2H, J = 8.5 Hz) ppm.

¹³C-NMR (75 MHz, CDCl₃): δ = 28.0, 44.9, 49.6, 53.5, 55.4, 65.0, 113.8, 114.1, 116.7, 128.7, 128.8, 130.3, 133.7, 134.8, 158.4, 159.3 ppm.

5.2.126. Compound 157

3,4-Dihydroxy-*N,N,N'*-tris(4-methoxybenzyl)butane-1-sulfonimidamide



156 (608 mg, 1.23 mmol, 1.0 eq.) was dissolved in a mixture of acetone (20 mL) and water (2.4 mL) and cooled to 0 °C. 2,6-Lutidine (285 μ L, 2.45 mmol, 2.0 eq.), NMO (420 mg, 3.59 mmol, 2.9 eq.) and OsO₄ (2.5 wt-% in *t*BuOH, 950 μ L, 74 μ mol, 0.06 eq.) were added and the mixture was allowed to warm to room temperature. After 2 h the reaction was quenched with sat. aq. Na₂S₂O₃ solution and stirred for 10 min. It was extracted with EA, the organic phase was dried over MgSO₄, filtered and concentrated *in vacuo*. The crude product was purified by silica gel column chromatography (EA \rightarrow EA + 5 % MeOH) to afford **157** as a mixture of diastereomers.

Yield: 565 mg, 87 %

Appearance: yellowish oil

TLC: R_f = 0.46 (EA)

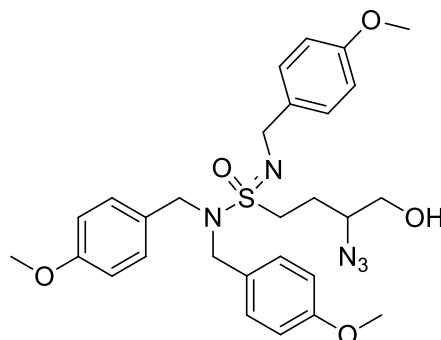
MS (ESI): *m/z* calculated [M+H]⁺ = 529.2, found [M+H]⁺ = 529.2

¹H-NMR (500 MHz, CDCl₃): δ = 1.76-1.94 (m, 1H), 1.98-2.14 (m, 1H), 2.76-2.87 (m, 1H), 3.18-3.31 (m, 1H), 3.34-3.40 (m, 1H), 3.46-3.55 (m, 1H), 3.63-3.69 (m, 0.5H), 3.76 (s, 3H), 3.80 (s, 6H), 3.83-3.89 (m, 0.5H), 3.96 (d, 1H, *J* = 13.9 Hz), 4.21 (dd, 2H, *J* = 15.0/2.2 Hz), 4.28-4.35 (m, 3H), 6.83 (d, 2H, *J* = 8.7 Hz), 6.88 (d, 4H, *J* = 8.7 Hz), 7.21 (d, 4H, *J* = 8.7 Hz), 7.24 (d, 2H, *J* = 8.7 Hz) ppm.

¹³C-NMR (125 MHz, CDCl₃): δ = 27.2, 27.3, 44.9, 45.0, 49.5, 50.5, 51.4, 55.3, 55.4, 66.1, 66.5, 69.2, 71.0, 113.9, 114.2, 118.2, 118.2, 128.9, 128.9, 130.3, 132.8, 133.0, 158.6, 159.4, 159.4 ppm.

5.2.127. Compound 158

3-Azido-4-hydroxy-*N,N,N'*-tris(4-methoxybenzyl)butane-1-sulfonimidamide



157 (565 mg, 1.07 mmol, 1.0 eq.) and PPh_3 (481 mg, 1.83 mmol, 1.7 eq.) were dissolved in toluene (15 mL) under argon atmosphere and cooled to 0 °C. DIAD (378 μL , 1.93 mmol, 1.8 eq.) was added and it was stirred at 0 °C for 2 h. Then TMSN_3 (212 μL , 1.60 mmol, 1.5 eq.) was added and the reaction was allowed to warm to room temperature. After 16 h water was added and it was extracted with DCM. The organic phase was dried over MgSO_4 , filtered and concentrated *in vacuo*. The crude product was purified by silica gel column chromatography (DCM/MeOH 50:1 \rightarrow 20:1), followed by semi-prep. HPLC (50-80 % MeCN in H_2O) to afford **158**, still as a mixture of diastereomers.

Yield: 358 mg, 60 % (94 % brsm)

Appearance: colourless oil

TLC: $R_f = 0.19$ (EA)

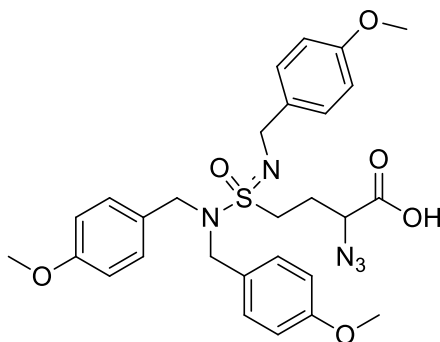
MS (ESI): m/z calculated $[\text{M}+\text{H}]^+ = 554.2$, found $[\text{M}+\text{H}]^+ = 554.2$

$^1\text{H-NMR}$ (300 MHz, CDCl_3): $\delta = 1.74\text{-}2.20$ (m, 2H), 2.91-3.14 (m, 1H), 3.34-3.71 (m, 3H), 3.78 (s, 3H), 3.82 (s, 6H), 3.96-4.19 (m, 2H), 4.21-4.46 (m, 5H), 6.85 (d, 2H, $J = 8.5$ Hz), 6.92 (d, 4H, $J = 8.5$ Hz), 7.10-7.25 (m, 6H) ppm.

$^{13}\text{C-NMR}$ (75 MHz, CDCl_3): $\delta = 24.0, 24.3, 43.5, 43.5, 48.4, 49.6, 50.0, 53.5, 55.4, 55.5, 60.5, 61.2, 63.0, 64.5, 114.4, 114.8, 125.1, 127.2, 127.3, 129.8, 129.9, 130.6, 159.8, 160.3$ ppm.

5.2.128. Compound 159

2-Azido-4-(*N,N,N'*-tris(4-methoxybenzyl)sulfamimidoyl)butanoic acid



158 (81 mg, 146 μmol , 1.0 eq.) was dissolved in acetone (3 mL) and cooled to 0 °C, then Jones reagent (146 μL , 292 μmol , 2.0 eq.) was added and the reaction was allowed to warm to room temperature. After 19 h the reaction was quenched with *i*PrOH and stirred for 30 min. The pH-value of the solution was adjusted to 3-4 by addition of sat. aq. NaHCO_3 , then water was added and it was extracted with DCM. The organic phase was dried over MgSO_4 , filtered and concentrated *in vacuo*. The crude product was purified by silica gel column chromatography (Cy/EA 3:1 + 1 % FA \rightarrow Cy/EA 3:2 + 1 % FA) to afford **159**.

Yield: 37 mg, 47 %

Appearance: colourless oil

TLC: $R_f = 0.41$ (Cy/EA + 1 % FA)

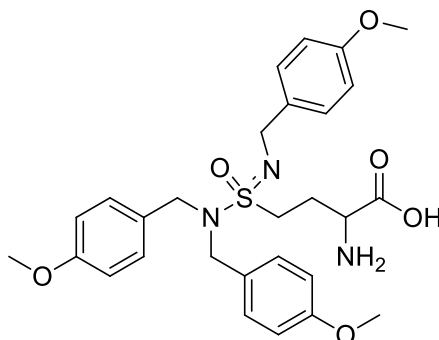
MS (ESI): m/z calculated $[\text{M}+\text{H}]^+ = 568.2$, found $[\text{M}+\text{H}]^+ = 568.2$

$^1\text{H-NMR}$ (500 MHz, CDCl_3): $\delta = 2.01\text{-}2.23$ (m, 1H), 2.23-2.42 (m, 1H), 3.11-3.30 (m, 1H), 3.78 (s, 3H), 3.82 (s, 6H), 3.94-4.05 (m, 1H), 4.05-4.21 (m, 2H), 4.24-4.43 (m, 5H), 6.84 (d, 2H, $J = 8.5$ Hz), 6.91 (d, 4H, $J = 8.5$ Hz), 7.12-7.17 (m, 4H), 7.19 (d, 2H, $J = 8.5$ Hz) ppm.

$^{13}\text{C-NMR}$ (125 MHz, CDCl_3): $\delta = 24.7, 24.9, 43.7, 43.8, 48.6, 49.1, 50.2, 55.4, 55.5, 59.4, 59.6, 114.5, 114.8, 125.1, 125.2, 127.0, 127.2, 129.9, 129.9, 130.6, 130.6, 159.8, 159.9, 160.3, 160.3, 170.7, 170.8$ ppm.

5.2.129. Compound 160

2-Amino-4-(*N,N,N'*-tris(4-methoxybenzyl)sulfamimidoyl)butanoic acid



159 (411 mg, 724 μmol , 1.0 eq.) was dissolved in THF (25 mL) and PPh_3 (234 mg, 892 μmol , 1.2 eq.) was added. The reaction stirred at room temperature for 48 h, when additional PPh_3 (119 mg, 454 μmol , 0.6 eq.) was added. Another 7 h later, 1 M NaOH (1.5 mL) was added and the reaction continued to stir for 19 h. The solvent was evaporated *in vacuo* and the crude product was purified by semi-prep. HPLC (35-50 % MeCN in H_2O) to afford **160**.

Yield: 358 mg, 87 %

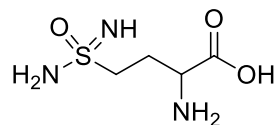
MS (ESI): m/z calculated $[\text{M}+\text{H}]^+ = 542.2$, found $[\text{M}+\text{H}]^+ = 542.2$

$^1\text{H-NMR}$ (500 MHz, D_2O): $\delta = 2.30\text{-}2.57$ (m, 2H), 3.00-3.10 (m, 0.5H), 3.12-3.22 (m, 0.5H), 3.33-3.38 (m, 0.5H), 3.38-3.47 (m, 0.5H), 3.76 (s, 3H), 3.79 (s, 6H), 3.93 (d, 1H, $J = 13.7$ Hz), 4.05-4.10 (m, 0.5H), 4.13-4.18 (m, 0.5H), 4.20 (dd, 2H, $J = 15.0/1.7$ Hz), 4.25 (dd, 1H, $J = 13.8/4.6$ Hz), 4.39 (d, 1H, $J = 12.8$ Hz), 4.42 (d, 1H, $J = 12.8$ Hz), 6.86 (d, 2H, $J = 8.6$ Hz), 6.90 (d, 4H, $J = 8.6$ Hz), 7.18-7.26 (m, 6H) ppm.

$^{13}\text{C-NMR}$ (125 MHz, D_2O): $\delta = 25.8, 26.0, 45.9, 50.2, 51.1, 51.2, 52.5, 53.0, 55.7, 55.8, 114.9, 115.2, 129.4, 130.1, 131.3, 133.7, 133.8, 160.2, 160.3, 161.0, 170.9, 171.0$ ppm.

5.2.130. Compound 161

2-Amino-4-sulfamimidoylbutanoic acid



160 (358 mg, 661 μmol , 1.0 eq.) was dissolved in TFA (10 mL) and refluxed for 23 h. The solvent was removed in an air stream and the crude product was purified by semi-prep. HPLC (5 % MeCN in H_2O , isocratic), cation exchange solid phase extraction and preparative TLC (MeOH + 2 % FA) to afford **161**.

Yield: 3 mg, 3 %

Appearance: colourless solid

TLC: $R_f = 0.19$ (MeOH + 2 % FA)

HRMS (ESI): m/z calculated $[\text{M}+\text{H}]^+ = 182.0594$, found $[\text{M}+\text{H}]^+ = 182.0592$

$^1\text{H-NMR}$ (500 MHz, D_2O): $\delta = 2.31\text{-}2.48$ (m, 2H), 3.32-3.42 (m, 1H), 3.42-3.52 (m, 1H), 3.90 (t, 1H, $J = 6.2$ Hz) ppm.

6. Appendix

6.1. List of abbreviations

Abbreviation	Meaning
ΔG	Difference in molar Gibbs free energy
6-OHDA	6-Hydroxydopamine
Å	Ångström
A549 cells	Adenocarcinomic human alveolar basal epithelial cells
aq.	Aqueous
AR	Androgen receptor
ATP	Adenosine triphosphate
Bcl-2	B-cell lymphoma 2
BCYE	Buffered charcoal-yeast extract
<i>Bp</i>	<i>Burkholderia pseudomallei</i>
CAN	Ceric ammonium nitrate
CDI	1,1'-Carbonyldiimidazol
CFU	Colony-forming unit
CL _{int}	Intrinsic clearance
Cy	Cyclohexane
d	Doublet
DCC	<i>N,N'</i> -Dicyclohexylcarbodiimide
DCM	Dichloromethane
DDQ	2,3-Dichlor-5,6-dicyano-1,4-benzochinon
DIAD	Diisopropyl azodicarboxylate
DIBAH	Diisobutylaluminiumhydrid
DIPEA	<i>N,N</i> -Diisopropylethylamine
DMAP	4-Dimethylaminopyridine
DMF	Dimethylformamide
DMSO	Dimethyl sulfoxide
DTT	Dithiothreitol
EA	Ethyl acetate
EDC	1-Ethyl-3-(3-dimethylaminopropyl)carbodiimide
FKBP	FK506 binding protein
FP	Fluorescence Polarization
GABA	γ -Aminobutyric acid
GlnA	Glutamine synthetase-like enzyme
GR	Glucocorticoid receptor
GS	Glutamine synthetase
GST	Glutathione <i>S</i> -transferase
HATU	1-[Bis(dimethylamino)methylene]-1 <i>H</i> -1,2,3-triazolo[4,5- <i>b</i>]pyridinium 3-oxide hexafluorophosphate
HCysSIA	Homocysteine sulfonimidamide
HEK293T	Human embryonic kidney 293 cells with mutated SV40 large T antigen
HEPES	4-(2-hydroxyethyl)-1-piperazineethanesulfonic acid
HILIC	hydrophilic interaction liquid chromatography
HLTE	Human lung tissue explant

<i>Hm</i>	<i>Haloferax mediterranei</i>
HOBt	Hydroxybenzotriazole
HPLC	High-performance liquid chromatography
HSP	Heat shock protein
HTRF	Homogeneous Time Resolved Fluorescence
HTS	High-throughput screening
IC ₅₀	Half maximal inhibitory concentration
K _D	Dissociation constant
K _i	Inhibition constant
LAH	Lithium aluminium hydride
LC	Liquid chromatography
<i>Lp</i>	<i>Legionella pneumophila</i>
m	multiplet
mCPBA	<i>meta</i> -Chloroperoxybenzoic acid
MES	2-(<i>N</i> -morpholino)ethanesulfonic acid
MIC	Minimal inhibitory concentration
Mip	Macrophage infectivity potentiator
MOM	Methoxymethyl
MS	Mass spectrometry
MSO	Methionine sulfoximine
<i>Mt</i>	<i>Mycobacterium tuberculosis</i>
mTOR	mechanistic target of rapamycin
NanoBRET	Nano-bioluminescence resonance energy transfer
NCS	<i>N</i> -Chlorosuccinimide
NLuc	Nanoluciferase
NMO	<i>N</i> -Methylmorpholine <i>N</i> -oxide
NMR	Nuclear magnetic resonance
OD ₆₀₀	Optical density at 600 nm
Opti-MEM I	Optimised minimal essential medium I
PauA	Pimeloyl-CoA synthetase
PBS	Phosphate-buffered saline
PDB	Protein data bank
PIDA	(Diacetoxyiodo)benzene
PMA	Phorbol-12-myristate-13-acetate
PMB	<i>p</i> -Methoxybenzyl
PPIase	Peptidylprolyl isomerase
PPT	Phosphinothricin
q	Quartet
R	Ideal gas constant
rpm	Revolutions per minute
RPMI	Roswell Park Memorial Institute
RyR	Ryanodine receptor
s	Singlet
sat.	Saturated
<i>Sc</i>	<i>Streptomyces coelicolor</i>
SIM	Selected ion monitoring
T	Temperature
t	Triplet

TBAF	Tetra- <i>n</i> -butylammonium fluoride
TBAI	Tetra- <i>n</i> -butylammonium iodide
TBDPS	<i>tert</i> -Butyldiphenylsilyl
<i>Tc</i>	<i>Trypanosoma cruzi</i>
TEA	Triethylamine
TFA	Trifluoroacetic acid
THF	Tetrahydrofuran
THP-1 cells	Human monocytic cell line derived from acute monocytic leukemia
TLC	Thin-layer chromatography
TMEDA	Tetramethylethylenediamine
TMS	Trimethylsilyl
TPR	Tetratricopeptide repeat
YEB	Yeast extract beef

6.2. List of Figures

Figure 1. 3,10-Diazabicyclo[4.3.1]decan-2-ones, a) scaffold (black) with substitutions at positions 3 (R1, red), 5 (R3, green) and 10 (R2, blue); b) reference ligand for this scaffold with standard substitutions R1 = pyridine-2-ylmethyl, R2 = (3,5-dichlorophenyl)sulfonyl, R3 = vinyl.	1
Figure 2. a) Methionine sulfoximine, b) MSO-derivatives as novel GlnA3 and GlnA4 inhibitors, c) Homocysteine sulfonimidamide.	2
Figure 3. Structures of natural FKBP ligands FK506 and rapamycin. Pipecolate motif highlighted in blue.	8
Figure 4. FKBP12 ligands developed by a) SmithKline Beecham Pharmaceuticals, ^[42] $K_D = 2$ nM and b) Vertex Pharmaceuticals, ^[41] $K_D = 1$ nM, c) Guilford Pharmaceuticals. ^[10]	9
Figure 5. „Bumped“ FKBP12 ligands with specific binding to the mutated FKBP12-F36V. a) $IC_{50} = 1.5$ nM, ^[43] b) $IC_{50} = 5$ nM. ^[44]	9
Figure 6. Fluorescent FKBP12 ligand for a high throughput fluorescence polarization assay with FKBP12, 12.6, 51 and 52. ^[45]	10
Figure 7. SAFit1 ($K_i = 4$ nM for FKBP51) and SAFit2 ($K_i = 6$ nM for FKBP51), the first ligands optimized for FKBP51 selectivity over FKBP52. ^[46]	10
Figure 8. Macrocyclic SAFit-analog with FKBP51 selectivity over FKBP12, 12.6 and 52. ^[48]	11
Figure 9. FKBP ligands bearing pipecolate sulfonamides, a) $IC_{50} = 0.23$ μ M for FKBP12, $IC_{50} = 16$ μ M for FKBP51, $IC_{50} = 18$ μ M for FKBP52 ; b) $IC_{50} = 72$ nM for BpMip, $IC_{50} = 5.7$ nM for LpMip. ...	11
Figure 10. Bicyclic FKBP ligands by a) Agouron Pharmaceuticals, $K_i = 54$ nM for FKBP12, ^[51] b) Guilford Pharmaceuticals, $IC_{50} = 650$ nM for FKBP12, ^[52] c) Pfizer, $K_i = 34$ nM for FKBP12. ^[53] ..	12
Figure 11. 3,10-Diazabicyclo[4.3.1]decan-2-ones as FKBP ligands. a) First developed scaffold; ^[54] b) Improvement by C5-attachment; ^[55] c) exemplary ligand with the new scaffold, $K_i = 0.2$ nM for FKBP12, $K_i = 21$ nM for FKBP51. ^[56]	12
Figure 12. Introduction of an α -methyl group in R1 improves binding affinity: a) $K_D = 0.52$ nM for FKBP12, $K_D = 33$ nM for FKBP51; b) $K_D = 0.29$ nM for FKBP12, $K_D = 2.9$ nM for FKBP51.....	13
Figure 13. Cocrystal structure of MtGS with phosphorylated MSO, ADP, Mg^{2+} and Cl^- (PDB: 2BVC). The subunits are alternately colored in light and dark blue. The cocrystal structure shows 6 subunits forming one ring.	14
Figure 14. a) Well-characterized [4.3.1]-bicyclic FKBP-ligand 1 , b) analogous [4.2.1]-bicyclic compound 2	19
Figure 15. Structures of carboxylic acid and amide without α -methyl group in the R1 position.....	23
Figure 16. a) FKBP-inhibitor developed by the HAUSCH lab, ^[57] with the arylsulfonamide highlighted in blue, Pomplun2018-15e R = 3-Cl, $K_D = 8.8$ nM against FKBP12. b) FKBP12-inhibitor developed	

by Guilford Pharmaceuticals, ^[52] with the benzylsulfonamide highlighted in blue, IC ₅₀ = 1300 nM against FKBP12. c) LpMip and BpMip-inhibitor developed by the HOLZGRABE lab, ^[50] with the benzylsulfonamide highlighted in blue, Seufert2016-5n R = 3-Cl, IC ₅₀ = 230 nM against BpMip.	25
Figure 17. Chemical structures of a) Phenylsulfonamide 1 , b) modeled bicyclic benzylsulfonamide and b) benzylsulfonamide SF354	27
Figure 18. A) Cocrystal structures of 1 (green) with FKBP12 (olive) and of SF354 (purple) with BpMip (blue) (PDB:5V8T); B) Cocrystal structure of benzyl sulfonamide modeled from 1 (green) with FKBP12 (olive) and of SF354 (purple) with BpMip (blue) (PDB:5V8T).	27
Figure 19. Cocrystal structure of 31 with FKBP12. Sticks and transparent surface shown, important ligand-protein-interactions indicated by yellow dotted lines. Distances are given in Å.....	34
Figure 20. A) Cocrystal structure of 31 (green sticks) with FKBP12 (white surface), cavity next to Ile90 highlighted in purple, B) Same cocrystal structure superimposed with FKBP51FK1 (pink, PDB: 5OBK), cocrystallized with a similar ligand (not shown).....	35
Figure 21. Structures of reference compounds Kolos2021-16 ^{(S)-Me} and Kolos2021-18 ^{(S)-Me}	36
Figure 22. Crystal structure of FKBP12, cocrystallized with 31 . Ile90 highlighted in magenta, ligand's chlorine atoms highlighted in orange. A) Original crystal structure of 31 , B) 57 modeled, C) 56 modeled, D) 58 modeled. Biaryl dihedral angle measured as 57° for 31 (A), modeled as 90° for 3,5-dichloro analogs (B-D).	42
Figure 23. a) Sulfonamide 1 and b) analogous sulfenamide, sulfinamide, sulfonimidamide.....	45
Figure 24. a) Structure of FKBP51-selective SAFit2 (69), b) Structure of a bicyclic FKBP-ligand-scaffold with a cyclohexyl attached via a sulfonimidamide.	46
Figure 25. ¹ H- ¹ H coupling of H ²⁰ visible in the NOESY-spectra of 78a and 78b	48
Figure 26. NOESY spectrum of compound 78a , assignment of ¹ H- ¹ H-coupling in reference to the compound structure in Figure 25.....	49
Figure 27. NOESY spectrum of compound 78b , assignment of ¹ H- ¹ H-coupling in reference to the compound structure in Figure 25.....	50
Figure 28. SIM LC-MS analysis of the iminiation reactions of sulfinamides 76a and 76b , co-injected with diastereomerically pure sulfonimidamides 77a and 77b	51
Figure 29. Stereoconfiguration of sulfinamides 76a and 76b	51
Figure 30. Calculated Gibbs free energie differences between sulfenamide 75 , sulfinamides 76a and 76b , and sulfonamide 1	54
Figure 31. Cocrystal structures of FKBP12 with compounds A) FK506 (PDB: 1FKJ), B) 1 , C) 77b and D) 78a . All protein complexes per asymmetric unit of each cocrystal structure are overlaid.	

Hydrogen bonds are shown in blue, CH...O interactions are shown in yellow. Distances of dashed lines are given in Å.	55
Figure 32. One (Chain A) of the two protein complexes per asymmetric unit of the 1 -FKBP12 cocrystal structure. A) 3D- and B) 2D-Interaction network of 1 with FKBP12. Hydrogen bonds are shown in blue, haloge- π -interactions are shown in red, CH...O interactions are shown in yellow, other polar contacts are shown in light blue. Distances of dashed lines are given in Å.	56
Figure 33. Two (Chain D and C) of the four protein complexes per asymmetric unit of the 77b -FKBP12 cocrystal structure. A+B) 3D- and C+D) 2D-Interaction network of 77b with FKBP12, A+B overlaid with 1 . Hydrogen bonds are shown in blue, haloge- π -interactions are shown in red, CH...O interactions are shown in yellow, other polar contacts are shown in light blue. Distances of dashed lines are given in Å.	57
Figure 34. Both (Chain B and A) of the two protein complexes per asymmetric unit of the 78a -FKBP12 cocrystal structure. A+B) 3D- and C+D) 2D-Interaction network of 78a with FKBP12, A+B overlaid with 1 . Hydrogen bonds are shown in blue, haloge- π -interactions are shown in red, CH...O interactions are shown in yellow, other polar contacts are shown in light blue. Distances of dashed lines are given in Å.	59
Figure 35. A) R2-para carboxylic acid modelled into the cocrystal structure of 1 and FKBP12; B) R2-para carboxylic acid modelled into the cocrystal structure of Pomplun2018-16h and FKBP51Fk1 (PDB: 5OBK). Distances of the carboxylic acid to the Ile90 (A) and Lys121 (B) backbone nitrogen are indicated as yellow dotted lines.	64
Figure 36. Structures of FKBP ligands with binding affinities measured for LpMip, TcMip and BpMip.	67
Figure 37. Synthesized GlnA3 _{sc} and GlnA4 _{sc} inhibitors. Amine-mimicking moiety shown in green.	73
Figure 38. Enzyme activity assays with GlnA1, GlnA3 and GlnA4, normalized to the activity without inhibitor. 5 mM inhibitor, 2.5 mM ATP, 25 mM glutamate, a) 50 mM NH ₄ Cl, 40 nM GlnA1 _{MT} ; b) 50 mM cadaverine, 2.8 μ M GlnA3 _{MT} ; c) 50 mM ethanolamine, 2 μ M GlnA4 _{sc}	73
Figure 39. GlnA4 _{sc} activity at different concentrations of inhibitors 118c and 105d-f	74
Figure 40. <i>S. Coelicolor</i> growth with different concentrations of inhibitor 105e using ethanolamine as a nitrogen source.	76
Figure 41. Structures of a) P-MSO, b) the natural transition state of the GS-catalysed Gln formation and c) P-HCysSIA.	77
Figure 42. Cocrystal structure of P-MSO 102 and MtGS (PDB: 2BVC). Distances of the terminal methyl group to surrounding carboxylic acids are shown as dashed yellow lines and given in Å.	78
Figure 43. GS inhibition of L-MSO and compound 161	84

6.3. List of Tables

Table 1. Members of the mammalian FKBP, with gene name and classification.	5
Table 2. Binding affinities of compound 1 and 2 against different FKBP. All K_D values were measured in the same assay.	21
Table 3. Binding affinities of (<i>S</i>)-2-(2-oxo-3,10-diazabicyclo[4.3.1]decan-3-yl)propanoic acids for FKBP12, 12.6, 51 and 52. ^a Values taken from POMPLUN <i>et al.</i> ^[57] ^{b-d} Values taken from the same assay, respectively.	23
Table 4. Binding affinities of (1 <i>S</i> ,5 <i>S</i> ,6 <i>R</i>)-10-benzylsulfonyl-3,10-diazabicyclo[4.3.1]decan-2-ones 22 , 23 and 24 , and reference 3-chlorobenzenesulfonamide Pomplun2018-15e for FKBP. ^a Values taken from POMPLUN <i>et al.</i> ^[57] Values for all other compounds are taken from the same assay.	26
Table 5. Binding affinities of compounds 30a-1 for FKBP12, 51 and 52. ^a Values taken from POMPLUN <i>et al.</i> ^[57] Values for all other compounds are taken from the same assay.....	29
Table 6. K_D -values of 30g analogs for FKBP12, 12.6, 51 and 52 by FP assay. * K_D -values determined in HTRF assay. ^a Values taken from POMPLUN <i>et al.</i> ^[57] ^{b-f} Values taken from the same assay, respectively.	32
Table 7. Binding affinities of optimized FKBP12 ligands 40 and 41 . * K_D -values determined in HTRF-assay. ^a Values taken from KOLOS <i>et al.</i> ^[90] ^{b-f} Values taken from the same assay, respectively.	36
Table 8. Binding affinities of the 30g -analogous 3,5-dichloro variants and respective reference compounds. * K_D -values determined by HTRF assay. ^{a-l} Values taken from the same assay, respectively.....	39
Table 9. Binding affinities of compound 68 and previous intermediates. * K_D -values determined by HTRF-assay. ^{a-c} Values taken from the same assay, respectively.	44
Table 10. Binding affinities of SIA-FKBP-ligands for FKBP 51, 52, 12 and 12.6. Core = (1 <i>S</i> ,5 <i>S</i> ,6 <i>R</i>)-2-oxo-3-(pyrin-2-ylmethyl)-5-vinyl-3,10-diazabicyclo[4.3.1]decan-10-yl, Ar = 3,5-dichlorophenyl. *Cocrystal structure with FKBP12 solved. ^{a-c} Values taken from the same assay, respectively. ^c Values measured in real triplicates instead of pseudoduplicates.....	52
Table 11. Binding affinities of miscellaneous bicycles 82-94 for FKBP12, 12.6, 51 and 52. Core* = ethyl group in R3 instead of vinyl group. ^a Values taken from POMPLUN <i>et al.</i> ^[57] ^{b-c} Values taken from the same assay, respectively.	62
Table 12. K_D values for newly synthesised bicyclic FKBP ligands for LpMip, TcMip, BpMip and FKBP12, sorted by affinity for each protein. 1 highlighted in blue as reference. *No binding was observed at 10 μ M, no dose-response curves were measured. ** K_D value determined in a HTRF assay. ^{a-p} Values taken from the same assay, respectively.....	65

Table 13. Fit parameters for analyzing the fluorescence polarization assays.	91
Table 14. Fit parameters for analyzing the HTRF assays.	91
Table 15. Conditions for the cocrystallization of FKBP12 with novel ligands.	94

6.4. List of Schemes

Scheme 1. Enzymatic mechanism of glutamine synthetase.....	14
Scheme 2. Inhibitory mechanism of MSO.	16
Scheme 3. Reagents and conditions: a) L-Pyroglutamic acid 6 , EDC, HOBT, DMF, 0 °C – rt, 17 h, then Boc ₂ O, DIPEA, DMAP, DCM, rt, 15 h, 57 % over two steps; b) DIBAH, THF, -98 °C, 5 min, then HF-pyridine, -84 °C – 0 °C, 3 h, 40 % over two steps; c) 3,5-Dichlorobenzesulfonyl chloride 7 , DIPEA, MeCN, rt, 18 h, 80 %.....	20
Scheme 4. Reagents and conditions: a) NaH, BnCl, THF, reflux, 1 h; b) DIPEA, NsCl, MeCN, rt, 1 h, 58 % (over 2 steps); c) K ₂ CO ₃ , allyl bromide, DMF, 60 °C, 5 h, 92 %; d) p-benzoquinone, Grubbs cat. 2 nd gen., allyltrimethylsilane, DCM, reflux, 6 h, 73 %; e) K ₂ CO ₃ , thiophenol, DMF, rt, 16 h, 93 %; f) S-6-Oxo-2-piperidinecarboxylic acid, HATU, DIPEA, DMF, rt, 19 h; g) Boc ₂ O, DIPEA, DMAP, rt, 15 h, 91 % (over 2 steps); h) DIBAH, THF, -98 °C, 5 min; i) HF-pyridine, DCM, -84 – 0 °C, 3 h, 48 % (over 2 steps); j) 3,5-Dichlorobenzesulfonyl chloride 7 , DIPEA, MeCN, rt, 15 h, 63 %; k) BCl ₃ -SMe ₂ , DCM, 5 h, 86 %; l) Jones reagent, acetone, 0 °C – rt, 4 h, 96 %; m) CDI, THF, rt, 3 h, then aq. NH ₃ , rt, 2 h, 82 % ; n) 2,6-Lutidine, NMO, OsO ₄ , acetone/water (9:1), rt, 25 h, 59 %; o) 2,6-Lutidine, OsO ₄ , NaIO ₄ , dioxan/water (3:1), rt, 18 h; p) NaBH ₄ , THF, 0 °C – rt, 21 h, 26 % (over 2 steps).	22
Scheme 5. Reagents and conditions: a) <i>meta</i> -chlorobenzylsulfonyl chloride 25 , DMAP, MeCN, 0 °C – rt, 30 h, 84 %; b) <i>para</i> -chlorobenzylsulfonyl chloride 26 , DMAP, MeCN, 0 °C – rt, 45 h, 71 %; c) <i>para</i> -nitrobenzylsulfonyl chloride 27 , DMAP, MeCN, 0 °C – rt, 45 h, 82 %.....	26
Scheme 6. Synthesis of a FKBP ligand library with different R ₂ -para substituents.....	29
Scheme 7. Reagents and conditions: Suzuki reactions for a,b,c,d) Pd(OAc) ₂ , XPhos, K ₃ PO ₄ , respective boronic acid or ester, THF, reflux, 2-5 d, 10 % 32 , 9 % 34 ; Boc-cleavage for a,c) TFA, DCM, rt, 65 h, yields over two steps: 17 % 31 , 4 % 33 , 7 % 38 ; Suzuki reactions for e,f,g) Pd(dppf)Cl ₂ , K ₂ CO ₃ , respective boronic acid or ester, dioxane/water, 80 °C, 2-17 h, 41 % 35 , 42 % 36 , 51 % 37	31
Scheme 8. Reagents and conditions: a) 4-bromo-3-chlorobenzene-1-sulfonyl chloride 28 , DIPEA, MeCN, rt, 3 d, 18 %; b) <i>tert</i> -butyl 3,5-dimethyl-4-(4,4,5,5-tetramethyl-1,3,2-dioxaborolan-2-yl)-1 <i>H</i> -pyrazole-1-carboxylate 44 , Pd(OAc) ₂ , XPhos, K ₂ CO ₃ , THF/water 9:1, reflux, 6 h, then TFA, DCM, rt, 19 h, 40 % over two steps; c) NaIO ₄ , 2,6-lutidine, OsO ₄ , dioxane/water 3:1, rt, 23 h, then NaBH ₄ , EtOH, 0 °C – rt, 1 h, 25 % over two steps.	35
Scheme 9. Reagents and conditions: a) Tf ₂ O, pyridine, DCM, 0 °C – rt, 18 h, 93 %; b) boronic acid or ester 61 , 62 or 63 , Pd(dppf)Cl ₂ , K ₂ CO ₃ , dioxane/water 20:1, 80 °C, 5-19 h, 39 % 47 , 56 % 48 , 30 % 49 ; c) Zn-powder, NH ₄ Cl, EtOH, reflux, 1-5 h, impure 50 , impure 51 , 94 % 52 ; d) NaNO ₂ , HCl, MeCN/H ₂ O, 10 min, rt, then SOCl ₂ /H ₂ O/CuCl, 0 °C – rt, 1 h, then POCl ₃ , dry MeCN, 55 °C, 23 h,	

21 % 53 over three steps, 54 used in the next reaction without complete purification; e) NaNO ₂ , HCl, MeCN/H ₂ O, 10 min, rt, then SOCl ₂ /H ₂ O/CuCl, 0 °C – rt, 3 h, 47 % 55 ; f) 21 , DIPEA, dry MeCN, rt, 17-21 h, 14 % 56 , 2 % 57 over four steps, 42 % 58 ; g) 55 , DIPEA, dry MeCN, rt, 66 h, 16 %; h) 2,6-lutidine, NaIO ₄ , OsO ₄ , dioxane/water 3:1, 0 °C – rt, 20 h, then NaBH ₄ , EtOH, 0 °C – rt, 50 min, 47 % over two steps.	38
Scheme 10. Reagents and conditions: a) 4-Bromo-3-chlorobenzenesulfonyl chloride 28 , DIPEA, MeCN, rt, 18 h, 59 %; b) <i>tert</i> -butyl 3,5-dimethyl-4-(4,4,5,5-tetramethyl-1,3,2-dioxaborolan-2-yl)-1 <i>H</i> -pyrazole-1-carboxylate 44 , Pd(OAc) ₂ , XPhos, THF/water 9:1, reflux, 18 h, 75 %; c) BCl ₃ -SMe ₂ , DCM, rt, 3 d, 52 %; d) Jones reagent, acetone, 0 °C – rt, 17 h, 21 %.....	43
Scheme 11. Synthetic attempt to form bicyclic sulfonimidamide FKBP-ligands.....	46
Scheme 12. Reagents and conditions: a) 3,5-dichlorobenzenethiol 74 , HOAc, SO ₂ Cl ₂ , -40 °C -> rt, then 21 , DIPEA, MeCN, rt, 55 %; b) KF, mCPBA, MeCN/H ₂ O 5:1, 30 min, 0 °C, then 75 , 5 h, 0 °C, 5 % 76b and 7 % 76a (separated diastereomers); c) PIDA, AcONH ₄ , MeOH, rt, 26 % 77a and 35 % 77b (separated diastereomers); d) NaH, MeI, THF, 0 °C -> rt, 82 % 78a , 64 % 78b ; e) NaH, allyl bromide, THF, 0 °C -> rt, 100 % 79a , 81 % 79b ; f) NaH, 3-bromocyclohexene, 0 °C -> rt, 66 % 80a , 85 % 80b ; g) PhB(OH) ₂ , Cu(OAc) ₂ , TEA, MeCN, rt, 100 % 81a , 87 % 81b	47
Scheme 13. Reagents and conditions: a) Thiophene-2-sulfonyl chloride 95 , DIPEA, dry MeCN, rt, 17 h, 46 %; b) 5-Chlorothiophene-2-sulfonyl chloride 96 , DIPEA, dry MeCN, rt, 17 h, 41 %; c) NaNO ₂ , HCl, MeCN, rt, 10 min, then SO ₂ /HCl/CuCl ₂ , 0 °C – rt, 3 h, 48 %; d) 85 , DIPEA, dry MeCN, rt, 17 h, 63 %; e) LiOH, THF/H ₂ O (1:1), rt, 2 h, quant.; f) CDI, aq. NH ₃ , THF, rt, 15 h, 56 %; g) NaNO ₂ , HCl, MeCN, rt, 10 min, then SO ₂ /HCl/CuCl ₂ , 0 °C – rt, 3 h, 21 %; h) 90 , DIPEA, dry MeCN, rt, 17 h, 53 %; i) CoCl ₂ , NaBH ₄ , dry MeOH, 0 °C – rt, 4 h, 31 %; j) 3,5-Dichloro-4-hydroxybenzene-1-sulfonyl chloride 97 , DIPEA, dry MeCN, rt, 18 h, 12% 93 , 31 % 94	61
Scheme 14. a) Mechanism of GS-catalyzed conversion of glutamate 98 to glutamine 100 . b) Mechanism of GS inhibition by MSO 101 . c) Putative mechanism of GlnA3 _{sc} -catalyzed conversion of polyamine to γ-glutamylpolyamine 103 . d) Putative mechanism of GlnA4 _{sc} -catalyzed conversion of ethanolamine to γ-glutamylethanolamine 104	69
Scheme 15. Possible MSO substitutions to achieve GS-like selectivity: a) elongating the terminal methyl group, b) elongating the sulfoximine nitrogen.....	70
Scheme 16. Synthesis of C-substituted MSO analogs. Reagents and conditions: (a) Boc ₂ O, NaHCO ₃ , THF/H ₂ O (1:1), rt, 40 h, 29 %; (b) NaOMe, MeOH, rt, then 108a, b, c, d, e or f , rt, 16-24 h, 59-79 %; (c) PIDA, MeCOONH ₄ , MeOH, rt. 16-18 h; (d) LiOH, THF/H ₂ O (1:1), rt, 3-5 h, 16-62 % over two steps, (e) TFA, DCM, rt, 15-17 h, 82-92 %; (f) Pd/C, H ₂ , EtOH, rt, 1-15 h, 8-44 % over two steps; (g) LiOH, THF/H ₂ O (1:1), rt, 3-18 h then HCl, 40-85 %.....	71

Scheme 17. Synthesis of N-substituted MSO. Reagents and conditions: (a) DCC, *tert*-Butanol, DMAP, 0 °C - rt, 18 h, 85 %; (b) PIDA, MeCOONH₄, MeOH, rt, 22 h, 87 %; (c) **114b**, NaHCO₃ or **114c**, K₂CO₃, MeCN, reflux, 2-6 d, 14-56 % ; (d) Boc-GABA, HATU, DIPEA, DMF, rt, 3 d, quant.; (e) BH₃-SMe₂, DCM, 0 °C - rt, 17 %; (f) TFA, DCM, rt, 17 h, quant.; (g) TFA, DCM, rt - 90 °C, 17-40 h, 65-80 %; (h) 1 M HCl, 90 °C, 16 h, 69 %.....72

Scheme 18. Synthesis attempts towards HCysSIA **121**, part 1. Reagents and conditions: a) BnBr, TBAI, K₂CO₃, dry MeCN, 0-50 °C, 4 d; b) NaOMe, NCS, dry MeOH, rt, 16 h; c) NaOMe, dry MeOH, rt - 75 °C, 2 d; d) DMAP, DCC, MeOH, DCM, rt, 5 d; e) DTT, H₂O, rt, 21 h; f) SO₂Cl₂, DCM, -15 °C - rt, 7 h, then add benzylamine, DIPEA, rt, 18 h; g) TMSCl, H₂O₂, MeCN, rt, 90 min; h) AcOH, SO₂Cl₂, -40 °C - rt, 1 h, then add benzylamine, DIPEA, MeCN, rt, 17 h; i) LAH, dry THF, -84 °C - rt, 30 min.....79

Scheme 19. Synthesis attempts towards HCysSIA **121**, part 2. Reagents and conditions: a) NCS, TEA, dry DCM, 0 °C - rt, 5 h; b) TBDPSCl, imidazole, dry DCM, rt, 20 h; c) SO₂Cl₂, DCM, 0 °C - rt, 4 h, then add benzylamine, rt, 16 h; d) NCS, TEA, DCM, rt, 3 h; e) SO₂Cl₂, TEA, DCM, 0 °C - rt, 15 min, then add phthalimide, TEA, 0 °C - rt, 4 h; f) TMSCl, H₂O₂, MeCN, rt, 1 h, then add aq. NH₃, rt, 80 min; g) TEA, dry THF, rt, 5 min, then add TBDPSCl, reflux, 18 h; h) AcCl, TEA, 0 °C - rt, 17 h; i) Ac₂O, SO₂Cl₂, dry DCE, -10 °C, 30 min, then add benzylamine, *N*-methylmorpholine, -10 °C - rt, 1 h.....81

Scheme 20. Synthesis attempts towards HCysSIA **121**, part 3. Reagents and conditions: a) TBDPSCl, THF, dry THF, 45 °C, 16 h; b) Ph₃PCL₂, TEA, dry CHCl₃, rt, 10 min, then add **141**, 0 °C, 20 min, then add phthalimide, 0 °C - rt, 16 h; c) Ph₃PCL₂, TEA, dry CHCl₃, rt, 10 min, then add **141**, 0 °C, 50 min, then add dibenzylamine, 0 °C - rt, 4 d; d) TMEDA, ⁿBuLi, dry THF, -84 °C, 10 min, then add Boc-iodo-L-alanine methyl ester **149**, -84 °C - rt, 30 min; e) TMEDA, ⁿBuLi, dry THF, -84 °C, 10 min, then add methyl acrylate **150**, -84 °C - rt, 16 h; f) TMEDA, ⁿBuLi, dry THF, -84 °C, 15 min, then add 1-iodobutane **151**, -84 °C - rt, 1 h; g) TMEDA, ⁿBuLi, dry THF, -84 °C, 15 min, then add isovaleraldehyde **152**, -84 °C - rt, 1 h; h) TMEDA, ⁿBuLi, dry THF, -84 °C, 10 min, then add allyl bromide, -84 °C - rt, 19 h.....82

Scheme 21. Reagents and conditions: a) TBSCl, TEA, dry THF, 45 °C, 23 h, 98 %; b) Ph₃PCL₂, TEA, dry CHCl₃ 0 °C, 10 min, then **141**, 0 °C, 30 min, then PMB₂NH, 0 °C - rt, 16 h, 62 %; c) BuLi, TMEDA, allyl bromide, dry THF, -84 °C - rt, 3 h, 86 %; d) TBAF, THF, rt, 3 h, 86 %; e) NaH, PMBCl, dry THF, 0 °C - rt, 24 h, 62 %; f) 2,6-Lutidine, NMO, OsO₄, acetone/water (10:1), 0 °C - rt, 2 h, 87 %; g) PPh₃, DIAD, 0 °C, 2 h, then TMSN₃, 0 °C - rt, 16 h, 60 %; h) Jones reagent, acetone, 0 °C - rt, 19 h, 47 %; i) PPh₃, THF, rt, 55 h, then 1 M NaOH, rt, 19 h, 87 %; j) TFA, reflux, 23 h, 3 %.....83

7. References

- [1] a) J. M. Armitage, R. L. Kormos, B. P. Griffith, R. L. Hardesty, F. J. Fricker, R. S. Stuart, G. C. Marrone, S. Todo, J. Fung, T. E. Starzl, *Transplantation proceedings* **1991**, *23*, 1149–1152; b) A. J. Demetris, J. J. Fung, S. Todo, B. Banner, T. Zerbe, G. Sysyn, T. E. Starzl, *Transplantation proceedings* **1990**, *22*, 25–34; c) J. J. Fung, S. Todo, A. Jain, J. McCauley, M. Alessiani, C. Scotti, T. E. Starzl, *Transplantation proceedings* **1990**, *22*, 6–12; d) R. Shapiro, M. Jordan, J. Fung, J. McCauley, J. Johnston, Y. Iwaki, A. Tzakis, T. Hakala, S. Todo, T. E. Starzl, *Transplantation proceedings* **1991**, *23*, 920–923; e) T. E. Starzl, J. Fung, M. Jordan, R. Shapiro, A. Tzakis, J. McCauley, J. Johnston, Y. Iwaki, A. Jain, M. Alessiani, *JAMA* **1990**, *264*, 63–67; f) T. E. Starzl, S. Todo, J. Fung, A. J. Demetris, R. Venkataramman, A. Jain, *The Lancet* **1989**, *2*, 1000–1004; g) S. Todo, J. J. Fung, A. J. Demetris, A. Jain, R. Venkataramanan, T. E. Starzl, *Transplantation proceedings* **1990**, *22*, 13–16; h) S. Todo, J. J. Fung, T. E. Starzl, A. Tzakis, A. J. Demetris, R. Kormos, A. Jain, M. Alessiani, S. Takaya, R. Shapiro, *Annals of surgery* **1990**, *212*, 295–305; discussion 306–7; i) Z.-H. Zhang, L. X. Li, P. Li, S.-C. Lv, B. Pan, Q. He, *Journal of investigative surgery : the official journal of the Academy of Surgical Research* **2019**, *32*, 632–641;
- [2] L. A. Banaszynski, C. W. Liu, T. J. Wandless, *Journal of the American Chemical Society* **2005**, *127*, 4715–4721.
- [3] a) C. J. Sabers, M. M. Martin, G. J. Brunn, J. M. Williams, F. J. Dumont, G. Wiederrecht, R. T. Abraham, *Journal of Biological Chemistry* **1995**, *270*, 815–822; b) J. P. Steiner, T. M. Dawson, M. Fotuhi, C. E. Glatt, A. M. Snowman, N. Cohen, S. H. Snyder, *Nature* **1992**, *358*, 584–587;
- [4] a) S. Fischer, S. Michnick, M. Karplus, *Biochemistry* **1993**, *32*, 13830–13837; b) M. W. Harding, A. Galat, D. E. Uehling, S. L. Schreiber, *Nature* **1989**, *341*, 758–760; c) J. J. Siekierka, S. H. Hung, M. Poe, C. S. Lin, N. H. Sigal, *Nature* **1989**, *341*, 755–757;
- [5] S. L. Rulten, R. A. Kinloch, H. Tateossian, C. Robinson, L. Gettins, J. E. Kay, *Mammalian genome : official journal of the International Mammalian Genome Society* **2006**, *17*, 322–331.
- [6] a) A. B. Brillantes, K. Ondrias, A. Scott, E. Kobrinsky, E. Ondriasová, M. C. Moschella, T. Jayaraman, M. Landers, B. E. Ehrlich, A. R. Marks, *Cell* **1994**, *77*, 513–523; b) T. Jayaraman, A. M. Brillantes, A. P. Timerman, S. Fleischer, H. Erdjument-Bromage, P. Tempst, A. R. Marks, *The Journal of biological chemistry* **1992**, *267*, 9474–9477; c) A. P. Timerman, E. Ogunbumni, E. Freund, G. Wiederrecht, A. R. Marks, S. Fleischer, *Journal of Biological Chemistry* **1993**, *268*, 22992–22999; d) A. P. Timerman, H. Onoue, H. B. Xin, S. Barg, J. Copello, G. Wiederrecht, S. Fleischer, *The Journal of biological chemistry* **1996**, *271*, 20385–20391;
- [7] E. Venturi, E. Galfré, F. O'Brien, S. J. Pitt, S. Bellamy, R. B. Sessions, R. Sitsapesan, *Biophysical Journal* **2014**, *106*, 824–833.

-
- [8] C. Long, L. G. Cook, G.-Y. Wu, B. M. Mitchell, *Arteriosclerosis, thrombosis, and vascular biology* **2007**, *27*, 1580–1586.
- [9] a) M. Avramut, C. L. Achim, *Physiology & behavior* **2002**, *77*, 463–468; b) W. E. Lyons, J. P. Steiner, S. H. Snyder, T. M. Dawson, *J. Neurosci.* **1995**, *15*, 2985–2994;
- [10] J. P. Steiner, G. S. Hamilton, D. T. Ross, H. L. Valentine, H. Guo, M. A. Connolly, S. Liang, C. Ramsey, J. H. Li, W. Huang et al., *Proceedings of the National Academy of Sciences of the United States of America* **1997**, *94*, 2019–2024.
- [11] C. Zhang, J. P. Steiner, G. S. Hamilton, T. P. Hicks, M. O. Poulter, *The Journal of neuroscience : the official journal of the Society for Neuroscience* **2001**, *21*, RC156.
- [12] E. Lam, M. Martin, G. Wiederrecht, *Gene* **1995**, *160*, 297–302.
- [13] a) X. Bai, D. Ma, A. Liu, X. Shen, Q. J. Wang, Y. Liu, Y. Jiang, *Science (New York, N.Y.)* **2007**, *318*, 977–980; b) M. Shirane, K. I. Nakayama, *Nature cell biology* **2003**, *5*, 28–37;
- [14] a) F. Edlich, M. Weiwad, F. Erdmann, J. Fanghänel, F. Jarczowski, J.-U. Rahfeld, G. Fischer, *The EMBO journal* **2005**, *24*, 2688–2699; b) H.-Q. Wang, Y. Nakaya, Z. Du, T. Yamane, M. Shirane, T. Kudo, M. Takeda, K. Takebayashi, Y. Noda, K. I. Nakayama et al., *Human molecular genetics* **2005**, *14*, 1889–1902;
- [15] F. Edlich, F. Erdmann, F. Jarczowski, M.-C. Moutty, M. Weiwad, G. Fischer, *The Journal of biological chemistry* **2007**, *282*, 15341–15348.
- [16] a) C. R. Sinars, J. Cheung-Flynn, R. A. Rimerman, J. G. Scammell, D. F. Smith, J. Clardy, *Proceedings of the National Academy of Sciences of the United States of America* **2003**, *100*, 868–873; b) B. Wu, P. Li, Y. Liu, Z. Lou, Y. Ding, C. Shu, S. Ye, M. Bartlam, B. Shen, Z. Rao, *Proceedings of the National Academy of Sciences of the United States of America* **2004**, *101*, 8348–8353;
- [17] D. L. Cioffi, T. R. Hubler, J. G. Scammell, *Current opinion in pharmacology* **2011**, *11*, 308–313.
- [18] a) D. L. Riggs, P. J. Roberts, S. C. Chirillo, J. Cheung-Flynn, V. Prapapanich, T. Ratajczak, R. Gaber, D. Picard, D. F. Smith, *The EMBO journal* **2003**, *22*, 1158–1167; b) J. C. Young, W. M. Obermann, F. U. Hartl, *The Journal of biological chemistry* **1998**, *273*, 18007–18010;
- [19] J. Cheung-Flynn, V. Prapapanich, M. B. Cox, D. L. Riggs, C. Suarez-Quian, D. F. Smith, *Molecular endocrinology (Baltimore, Md.)* **2005**, *19*, 1654–1666.
- [20] J. J. Sabbagh, J. C. O'Leary, L. J. Blair, T. Klengel, B. A. Nordhues, S. N. Fontaine, E. B. Binder, C. A. Dickey, *PloS one* **2014**, *9*, e107241.
- [21] a) J. Hartmann, K. V. Wagner, C. Liebl, S. H. Scharf, X.-D. Wang, M. Wolf, F. Hausch, T. Rein, U. Schmidt, C. Touma et al., *Neuropharmacology* **2012**, *62*, 332–339; b) M. V. Schmidt, M. Paez-Pereda, F. Holsboer, F. Hausch, *ChemMedChem* **2012**, *7*, 1351–1359;

- [22] S. Albu, C. P. N. Romanowski, M. Letizia Curzi, V. Jakubcakova, C. Flachskamm, N. C. Gassen, J. Hartmann, M. V. Schmidt, U. Schmidt, T. Rein et al., *Journal of sleep research* **2014**, *23*, 176–185.
- [23] L. A. Stechschulte, B. Qiu, M. Warriar, T. D. Hinds, M. Zhang, H. Gu, Y. Xu, S. S. Khuder, L. Russo, S. M. Najjar et al., *Endocrinology* **2016**, *157*, 3888–3900.
- [24] M. Maiarù, O. B. Morgan, T. Mao, M. Breitsamer, H. Bamber, M. Pöhlmann, M. V. Schmidt, G. Winter, F. Hausch, S. M. Géranton, *Pain* **2018**, *159*, 1224–1234.
- [25] H.-Q. Cai, M.-J. Zhang, Z.-J. Cheng, J. Yu, Q. Yuan, J. Zhang, Y. Cai, L.-Y. Yang, Y. Zhang, J.-J. Hao et al., *Journal of biomedical science* **2021**, *28*, 13.
- [26] a) H.-H. Chang, C.-H. Lee, C.-J. Chang, F.-J. Jan, *Molecular plant pathology* **2022**, *23*, 561–575; b) A. Galat, *European journal of biochemistry* **2000**, *267*, 4945–4959; c) S. M. Horne, T. J. Kottom, L. K. Nolan, K. D. Young, *Infection and immunity* **1997**, *65*, 806–810; d) A. G. Lundemose, D. A. Rouch, S. Birkelund, G. Christiansen, J. H. Pearce, *Molecular microbiology* **1992**, *6*, 2539–2548; e) T. Maruyama, R. Suzuki, M. Furutani, *Frontiers in bioscience : a journal and virtual library* **2004**, *9*, 1680–1720; f) P. Monaghan, A. Bell, *Molecular and biochemical parasitology* **2005**, *139*, 185–195; g) R. Suzuki, K. Nagata, F. Yumoto, M. Kawakami, N. Nemoto, M. Furutani, K. Adachi, T. Maruyama, M. Tanokura, *Journal of molecular biology* **2003**, *328*, 1149–1160;
- [27] N. P. Cianciotto, B. I. Eisenstein, C. H. Mody, G. B. Toews, N. C. Engleberg, *Infection and immunity* **1989**, *57*, 1255–1262.
- [28] A. Riboldi-Tunncliffe, B. König, S. Jessen, M. S. Weiss, J. Rahfeld, J. Hacker, G. Fischer, R. Hilgenfeld, *Nature structural biology* **2001**, *8*, 779–783.
- [29] C. Wagner, A. S. Khan, T. Kamphausen, B. Schmausser, C. Unal, U. Lorenz, G. Fischer, J. Hacker, M. Steinert, *Cellular microbiology* **2007**, *9*, 450–462.
- [30] J. Rasch, C. M. Ünal, A. Klages, Ü. Karsli, N. Heinsohn, R. M. H. J. Brouwer, M. Richter, A. Dellmann, M. Steinert, *Infection and immunity* **2019**, *87*.
- [31] A. Moro, F. Ruiz-Cabello, A. Fernández-Cano, R. P. Stock, A. González, *The EMBO journal* **1995**, *14*, 2483–2490.
- [32] P. J. B. Pereira, M. C. Vega, E. González-Rey, R. Fernández-Carazo, S. Macedo-Ribeiro, F. X. Gomis-Rüth, A. González, M. Coll, *EMBO reports* **2002**, *3*, 88–94.
- [33] I. H. Norville, K. O'Shea, M. Sarkar-Tyson, S. Zheng, R. W. Titball, G. Varani, N. J. Harmer, *The Biochemical journal* **2011**, *437*, 413–422.
- [34] I. H. Norville, N. J. Harmer, S. V. Harding, G. Fischer, K. E. Keith, K. A. Brown, M. Sarkar-Tyson, R. W. Titball, *Infection and immunity* **2011**, *79*, 4299–4307.
- [35] G. D. van Duyn, R. F. Standaert, P. A. Karplus, S. L. Schreiber, J. Clardy, *Science (New York, N.Y.)* **1991**, *252*, 839–842.

-
- [36] G. D. van Duyne, R. F. Standaert, P. A. Karplus, S. L. Schreiber, J. Clardy, *Journal of molecular biology* **1993**, *229*, 105–124.
- [37] G. D. van Duyne, R. F. Standaert, S. L. Schreiber, J. Clardy, *Journal of the American Chemical Society* **1991**, *113*, 7433–7434.
- [38] B. E. Bierer, P. S. Mattila, R. F. Standaert, L. A. Herzenberg, S. J. Burakoff, G. Crabtree, S. L. Schreiber, *Proceedings of the National Academy of Sciences of the United States of America* **1990**, *87*, 9231–9235.
- [39] a) F. J. Dumont, M. J. Staruch, S. L. Koprak, J. J. Siekierka, C. S. Lin, R. Harrison, T. Sewell, V. M. Kindt, T. R. Beattie, M. Wyvratt, *The Journal of experimental medicine* **1992**, *176*, 751–760; b) J. I. Luengo, D. S. Yamashita, D. Dunnington, A. K. Beck, L. W. Rozamus, H.-K. Yen, M. J. Bossard, M. A. Levy, A. Hand, T. Newman-Tarr et al., *Chemistry & Biology* **1995**, *2*, 471–481; c) M. Nambu, J. A. Covell, M. Kapoor, X. Li, M. K. Moloney, M. M. Numa, Q. A. Soltow, M. Trzoss, P. Webb, R. R. Webb et al., *Bioorganic & Medicinal Chemistry Letters* **2017**, *27*, 2465–2471; d) H. M. Organ, M. A. Holmes, J. M. Pisano, M. J. Staruch, M. J. Wyvratt, F. J. Dumont, P. J. Sinclair, *Bioorganic & Medicinal Chemistry Letters* **1993**, *3*, 657–662;
- [40] D. A. Holt, A. L. Konialian-Beck, H.-J. Oh, H.-K. Yen, L. W. Rozamus, A. J. Krog, K. F. Erhard, E. Ortiz, M. A. Levy, M. Brandt et al., *Bioorganic & Medicinal Chemistry Letters* **1994**, *4*, 315–320.
- [41] D. M. Armistead, M. C. Badia, D. D. Deininger, J. P. Duffy, J. O. Saunders, R. D. Tung, J. A. Thomson, M. T. DeCenzo, O. Futer, D. J. Livingston et al., *Acta crystallographica. Section D, Biological crystallography* **1995**, *51*, 522–528.
- [42] D. A. Holt, J. I. Luengo, D. S. Yamashita, H. J. Oh, A. L. Konialian, H. K. Yen, L. W. Rozamus, M. Brandt, M. J. Bossard, M. A. Levy et al., *Journal of the American Chemical Society* **1993**, *115*, 9925–9938.
- [43] W. Yang, L. W. Rozamus, S. Narula, C. T. Rollins, R. Yuan, L. J. Andrade, M. K. Ram, T. B. Phillips, M. R. van Schravendijk, D. Dalgarno et al., *Journal of medicinal chemistry* **2000**, *43*, 1135–1142.
- [44] T. Clackson, W. Yang, L. W. Rozamus, M. Hatada, J. F. Amara, C. T. Rollins, L. F. Stevenson, S. R. Magari, S. A. Wood, N. L. Courage et al., *Proceedings of the National Academy of Sciences of the United States of America* **1998**, *95*, 10437–10442.
- [45] C. Kozany, A. März, C. Kress, F. Hausch, *Chembiochem : a European journal of chemical biology* **2009**, *10*, 1402–1410.
- [46] S. Gaali, A. Kirschner, S. Cuboni, J. Hartmann, C. Kozany, G. Balsevich, C. Namendorf, P. Fernandez-Vizorra, C. Sippel, A. S. Zannas et al., *Nature chemical biology* **2015**, *11*, 33–37.
- [47] M. Bauder, C. Meyners, P. L. Purder, S. Merz, W. O. Sugiarto, A. M. Voll, T. Heymann, F. Hausch, *Journal of medicinal chemistry* **2021**, *64*, 3320–3349.

- [48] A. M. Voll, C. Meyners, M. C. Taubert, T. Bajaj, T. Heymann, S. Merz, A. Charalampidou, J. Kolos, P. L. Purder, T. M. Geiger et al., *Angew. Chem. Int. Ed. Engl.* **2021**, *60*, 13257–13263.
- [49] R. Gopalakrishnan, C. Kozany, Y. Wang, S. Schneider, B. Hoogeland, A. Bracher, F. Hausch, *Journal of medicinal chemistry* **2012**, *55*, 4123–4131.
- [50] F. Seufert, M. Kuhn, M. Hein, M. Weiwad, M. Vivoli, I. H. Norville, M. Sarkar-Tyson, L. E. Marshall, K. Schweimer, H. Bruhn et al., *Bioorganic & medicinal chemistry* **2016**, *24*, 5134–5147.
- [51] C. Guo, S. Reich, R. Showalter, E. Villafranca, L. Dong, *Tetrahedron Letters* **2000**, *41*, 5307–5311.
- [52] D. C. Limburg, B. E. Thomas, J.-H. Li, M. Fuller, D. Spicer, Y. Chen, H. Guo, J. P. Steiner, G. S. Hamilton, Y.-Q. Wu, *Bioorganic & Medicinal Chemistry Letters* **2003**, *13*, 3867–3870.
- [53] R. A. Hudack, N. S. Barta, C. Guo, J. Deal, L. Dong, L. K. Fay, B. Caprathe, A. Chatterjee, D. Vanderpool, C. Bigge et al., *Journal of medicinal chemistry* **2006**, *49*, 1202–1206.
- [54] Y. Wang, A. Kirschner, A.-K. Fabian, R. Gopalakrishnan, C. Kress, B. Hoogeland, U. Koch, C. Kozany, A. Bracher, F. Hausch, *Journal of medicinal chemistry* **2013**, *56*, 3922–3935.
- [55] M. Bischoff, C. Sippel, A. Bracher, F. Hausch, *Organic letters* **2014**, *16*, 5254–5257.
- [56] S. Pomplun, Y. Wang, A. Kirschner, C. Kozany, A. Bracher, F. Hausch, *Angewandte Chemie (International ed. in English)* **2015**, *54*, 345–348.
- [57] S. Pomplun, C. Sippel, A. Hähle, D. Tay, K. Shima, A. Klages, C. M. Ünal, B. Rieß, H. T. Toh, G. Hansen et al., *Journal of medicinal chemistry* **2018**, *61*, 3660–3673.
- [58] a) S. W. Brusilow, R. C. Koehler, R. J. Traystman, A. J. L. Cooper, *Neurotherapeutics : the journal of the American Society for Experimental NeuroTherapeutics* **2010**, *7*, 452–470; b) I. Suárez, G. Bodega, B. Fernández, *Neurochemistry International* **2002**, *41*, 123–142; c) M. P. Wilkie, J. A. W. Stecyk, C. S. Couturier, S. Sidhu, G. K. Sandvik, G. E. Nilsson, *Comparative biochemistry and physiology. Part A, Molecular & integrative physiology* **2015**, *184*, 65–75;
- [59] M. J. Pawlik, M. Obara-Michlewska, M. P. Popek, A. M. Czarnecka, S. J. Czuczwar, J. Łuszczki, M. Kołodziej, A. Acewicz, T. Wierzba-Bobrowicz, J. Albrecht, *Brain research* **2021**, *1753*, 147253.
- [60] H. Son, S. Kim, D.-H. Jung, J. H. Baek, D. H. Lee, G. S. Roh, S. S. Kang, G. J. Cho, W. S. Choi, D. K. Lee et al., *Scientific reports* **2019**, *9*, 252.
- [61] K. Velickovic, H. A. Lugo Leija, A. Surrati, D.-H. Kim, H. Sacks, M. E. Symonds, V. Sottile, *Cellular physiology and biochemistry : international journal of experimental cellular physiology, biochemistry, and pharmacology* **2020**, *54*, 917–927.
- [62] G. W. Kim, D. H. Lee, Y. H. Jeon, J. Yoo, S. Y. Kim, S. W. Lee, H. Y. Cho, S. H. Kwon, *IJMS* **2021**, *22*.
- [63] G. Harth, M. A. Horwitz, *Journal of Biological Chemistry* **1997**, *272*, 22728–22735.
- [64] G. Harth, M. A. Horwitz, *The Journal of experimental medicine* **1999**, *189*, 1425–1436.

-
- [65] W. W. Krajewski, R. Collins, L. Holmberg-Schiavone, T. A. Jones, T. Karlberg, S. L. Mowbray, *Journal of molecular biology* **2008**, 375, 217–228.
- [66] a) W. W. Krajewski, T. A. Jones, S. L. Mowbray, *Proceedings of the National Academy of Sciences of the United States of America* **2005**, 102, 10499–10504; b) H. Unno, T. Uchida, H. Sugawara, G. Kurisu, T. Sugiyama, T. Yamaya, H. Sakakibara, T. Hase, M. Kusunoki, *Journal of Biological Chemistry* **2006**, 281, 29287–29296;
- [67] C. D. dos Santos Moreira, M. J. R. N. Ramos, P. M. A. A. Fernandes, *WIREs Comput Mol Sci* **2019**, 9.
- [68] D. Eisenberg, H. S. Gill, G. M. Pfluegl, S. H. Rotstein, *Biochimica et Biophysica Acta (BBA) - Protein Structure and Molecular Enzymology* **2000**, 1477, 122–145.
- [69] a) R. Mehta, J. T. Pearson, S. Mahajan, A. Nath, M. J. Hickey, D. R. Sherman, W. M. Atkins, *Journal of Biological Chemistry* **2004**, 279, 22477–22482; b) A. Theron, R. L. Roth, H. Hoppe, C. Parkinson, C. W. van der Westhuyzen, S. Stoychev, I. Wiid, R. D. Pietersen, B. Baker, C. P. Kenyon, *PloS one* **2017**, 12, e0185068;
- [70] C. Moreira, M. J. Ramos, P. A. Fernandes, *The journal of physical chemistry. B* **2017**, 121, 6313–6320.
- [71] G. Harth, S. Maslesa-Galić, M. V. Tullius, M. A. Horwitz, *Molecular microbiology* **2005**, 58, 1157–1172.
- [72] S. Krysenko, N. Okoniewski, A. Kulik, A. Matthews, J. Grimpo, W. Wohlleben, A. Bera, *Frontiers in microbiology* **2017**, 8, 726.
- [73] X. Yao, W. He, C.-D. Lu, *Journal of bacteriology* **2011**, 193, 3923–3930.
- [74] V. Rodríguez-Herrero, A. Peris, M. Camacho, V. Bautista, J. Esclapez, M.-J. Bonete, *Biomolecules* **2021**, 11.
- [75] S. Krysenko, N. Okoniewski, M. Nentwich, A. Matthews, M. Bäuerle, A. Zinser, T. Busche, A. Kulik, S. Gursch, A. Kemeny et al., *IJMS* **2022**, 23, 3752.
- [76] S. Krysenko, A. Matthews, N. Okoniewski, A. Kulik, M. G. Girbas, O. Tsypik, C. S. Meyners, F. Hausch, W. Wohlleben, A. Bera, *mBio* **2019**, 10.
- [77] G. Ferguson, W. Bridge, *Archives of biochemistry and biophysics* **2016**, 593, 12–23.
- [78] H. R. BENTLEY, E. E. McDERMOTT, *Nature* **1949**, 164, 438.
- [79] J. PACE, E. E. McDERMOTT, *Nature* **1952**, 169, 415–416.
- [80] T. M. Jeitner, A. J. L. Cooper, *Metabolic brain disease* **2014**, 29, 983–989.
- [81] S. L. Mowbray, M. K. Kathiravan, A. A. Pandey, L. R. Odell, *Molecules (Basel, Switzerland)* **2014**, 19, 13161–13176.
- [82] W. B. Rowe, A. Meister, *Proceedings of the National Academy of Sciences of the United States of America* **1970**, 66, 500–506.

- [83] G. Harth, M. A. Horwitz, *Infection and immunity* **2003**, *71*, 2297–2298.
- [84] G. Harth, O. W. Griffith, M. A. Horwitz (UNIV CALIFORNIA [US]; HARTH GUNTER [US]; GRIFFITH OWEN W [US]; HORWITZ MARCUS A [US]), WO2004045539 (A2), **2003**.
- [85] E. Bayer, K. H. Gugel, K. Hägele, H. Hagenmaier, S. Jessipow, W. A. König, H. Zähler, *Helvetica chimica acta* **1972**, *55*, 224–239.
- [86] a) Ł. Berlicki, A. Obojska, G. Forlani, P. Kafarski, *Journal of medicinal chemistry* **2005**, *48*, 6340–6349; b) G. Forlani, A. Obojska, Ł. Berlicki, P. Kafarski, *Journal of agricultural and food chemistry* **2006**, *54*, 796–802; c) A. Nordqvist, M. T. Nilsson, S. Röttger, L. R. Odell, W. W. Krajewski, C. Evalena Andersson, M. Larhed, S. L. Mowbray, A. Karlén, *Bioorganic & medicinal chemistry* **2008**, *16*, 5501–5513;
- [87] C. Couturier, S. Silve, R. Morales, B. Pessegue, S. Llopart, A. Nair, A. Bauer, B. Scheiper, C. Pöverlein, A. Ganzhorn et al., *Bioorganic & Medicinal Chemistry Letters* **2015**, *25*, 1455–1459.
- [88] J. Gising, M. T. Nilsson, L. R. Odell, S. Yahiaoui, M. Lindh, H. Iyer, A. M. Sinha, B. R. Srinivasa, M. Larhed, S. L. Mowbray et al., *Journal of medicinal chemistry* **2012**, *55*, 2894–2898.
- [89] a) M. T. Nilsson, W. W. Krajewski, S. Yellagunda, S. Prabhurthy, G. N. Chamarahally, C. Siddamadappa, B. R. Srinivasa, S. Yahiaoui, M. Larhed, A. Karlén et al., *Journal of molecular biology* **2009**, *393*, 504–513; b) A. Occhipinti, Ł. Berlicki, S. Giberti, G. Dziedziola, P. Kafarski, G. Forlani, *Pest management science* **2010**, *66*, 51–58; c) L. R. Odell, M. T. Nilsson, J. Gising, O. Lagerlund, D. Muthas, A. Nordqvist, A. Karlén, M. Larhed, *Bioorganic & Medicinal Chemistry Letters* **2009**, *19*, 4790–4793;
- [90] J. M. Kolos, S. Pomplun, S. Jung, B. Rieß, P. L. Purder, A. M. Voll, S. Merz, M. Gnatzy, T. M. Geiger, I. Quist-Løkken et al., *Chemical science* **2021**, *12*, 14758–14765.
- [91] L. D. Field, B. W. Skelton, S. Sternhell, A. H. White, *Aust. J. Chem.* **1985**, *38*, 391.
- [92] F. Hausch, J. Kolos (UNIV DARMSTADT TECH [DE]), EP3875151 (A1), **2020**.
- [93] G. C. Nandi, P. I. Arvidsson, *Advanced synthesis & catalysis* **2018**, *360*, 2976–3001.
- [94] P. K. Chinthakindi, A. Benediksdottir, A. Ibrahim, A. Wared, C.-J. Aurell, A. Pettersen, E. Zamaratski, P. I. Arvidsson, Y. Chen, A. Sandström, *Eur. J. Org. Chem.* **2019**, *2019*, 1045–1057.
- [95] T. Martzel, J.-F. Lohier, A.-C. Gaumont, J.-F. Brière, S. Perrio, *Eur. J. Org. Chem.* **2018**, *2018*, 5069–5073.
- [96] M. Datta, A. J. Buglass, *Synthetic Communications* **2012**, *42*, 1760–1769.
- [97] M. Zenzola, R. Doran, L. Degennaro, R. Luisi, J. A. Bull, *Angewandte Chemie (International ed. in English)* **2016**, *55*, 7203–7207.
- [98] S. Battula, G. V. Subbareddy, I. E. Chakravarthy, *Tetrahedron Letters* **2014**, *55*, 517–520.
- [99] a) J. Feng, H. Liu, Y. Yao, C.-D. Lu, *J. Org. Chem.* **2022**, *87*, 5005–5016; b) G. Proietti, J. Kuzmin, A. Z. Temerdashev, P. Dinér, *J. Org. Chem.* **2021**, *86*, 17119–17128;

-
- [100] X. Du, Y. Li, Y.-L. Xia, S.-M. Ai, J. Liang, P. Sang, X.-L. Ji, S.-Q. Liu, *IJMS* **2016**, *17*.
- [101] A. Flood, C. Trujillo, G. Sanchez-Sanz, B. Kelly, C. Muguruza, L. F. Callado, I. Rozas, *European journal of medicinal chemistry* **2017**, *138*, 38–50.
- [102] Ł. Berlicki, *Mini reviews in medicinal chemistry* **2008**, *8*, 869–878.
- [103] a) A. C. Dodds, A. Sutherland, *The Journal of organic chemistry* **2021**, *86*, 5922–5932; b) Q. Jiang, H. Li, X. Zhao, *Organic letters* **2021**, *23*, 8777–8782;
- [104] A. Armstrong, L. Challinor, J. H. Moir, *Angewandte Chemie (International ed. in English)* **2007**, *46*, 5369–5372.
- [105] H. H. Jung, A. W. Buesking, J. A. Ellman, *The Journal of organic chemistry* **2012**, *77*, 9593–9600.
- [106] S. Sohrabnezhad, K. Bahrami, F. Hakimpoor, *Journal of Sulfur Chemistry* **2019**, *40*, 256–264.
- [107] Y. Meyer, J.-A. Richard, M. Massonneau, P.-Y. Renard, A. Romieu, *Organic letters* **2008**, *10*, 1517–1520.
- [108] W. J. Moree, G. A. van der Marel, R. J. Liskamp, *J. Org. Chem.* **1995**, *60*, 5157–5169.
- [109] Y. Chen, J. Gibson, *RSC Adv.* **2015**, *5*, 4171–4174.
- [110] K. Okuma, T. Koike, H. Ohta, *J. Org. Chem.* **1988**, *53*, 4190–4193.
- [111] L. He, M. Wanunu, H.-S. Byun, R. Bittman, *J. Org. Chem.* **1999**, *64*, 6049–6055.
- [112] C. R. Lohani, J. Soley, B. Kralt, M. Palmer, S. D. Taylor, *J. Org. Chem.* **2016**, *81*, 11831–11840.
- [113] U. Lücking, *Angew. Chem. Int. Ed. Engl.* **2013**, *52*, 9399–9408.
- [114] M. T. Gnatzy, T. M. Geiger, A. Kuehn, N. Gutfreund, M. Walz, J. M. Kolos, F. Hausch, *Chembiochem : a European journal of chemical biology* **2021**, *22*, 2257–2261.
- [115] L. Scheithauer, M. Steinert, *Methods in molecular biology (Clifton, N.J.)* **2019**, *1921*, 323–331.
- [116] J. D. Gawronski, D. R. Benson, *Analytical biochemistry* **2004**, *327*, 114–118.
- [117] C. Evans, D. Herbert, D. W. Tempest in *Methods in Microbiology*, Elsevier, **1970**.